NANYANG TECHNOLOGICAL UNIVERSITY

CIVIL ENGINEERING RESEARCH

ISSN 0219-0370

No. 22, 2009

http://www.ntu.edu.sg/cee/research/bulletin/index.asp

WATER RECLAMATION AND MANAGEMENT

Nowadays, water is becoming the strategic resource for sustainable societal and economic development. There will be a significant increase in the worldwide demand for potable water due to rapid industrial and population growth. This will inevitably result in an increase in the generation and subsequent discharge of used water. The solution of the water problem is not just about purification technology, but also depends on resource management and planning. It is obvious that poor planning and management would lead to a diminution in the availability and accessibility of water resources arising from the impact of various water pollution from industrial and domestic sources. Furthermore, pollution, such as the emission of greenhouse gases, contributes to global climate change that will further affect the accessibility and availability of water resources in different locations across the world. Owing to the rapid technological development and advanced water management, water resources for potable water production have been extended from traditional surface and ground water to used water and seawater. As a result, water life cycle can and has been prolonged by using water more than once.

The conventional water treatment processes have been developed and successfully applied with the focus on purification of well managed surface and ground waters, but have no capability of producing potable water from used water and seawater. It has been realized that on the earth where we are living, there will not be enough natural fresh surface and ground water on a one-use and throw-away basis. The optimal use and management of diminishing natural water resources are becoming more and more important, and there is also a strong demand on novel ideas beyond the classical solutions.

Evidence shows that water scarcity and water stress endanger the water resources as well as social stability in both developed and developing countries. Solutions to global water problems are thus urgently needed, and they must be sustainable, economically viable and safe. The utilization of extended water sources, like used water and seawater, is one of the most promising options. In this aspect, membrane technology is becoming a core for the reclamation of used water and desalination of seawater. Meanwhile the knowledge and modelling of natural water processes are also becoming essential for advanced water resources planning and management towards sustainable water use.

The School of Civil and Environmental Engineering is a front runner in water reclamation and management in terms of education, science, technology and applications. The recent establishment of two research centres co-funded by Singapore's Environment and Water Industry Development Council (EWI) and Nanyang Technological University (NTU) further aid the effort. They are the Singapore Membrane Technology Centre (SMTC) and DHI-NTU Water & Environment Research Centre and Education Hub (DHI-NTU Centre). Multi-faceted technological and management approaches are investigated in depth by inter-disciplinary team members of these two research centres for high-performance water reclamation as well as for high-efficiency water resources management. The School believes that such synergies amongst researchers with the expertise in different fields is crucial in ensuring a better understanding of the complexity of the fast changing local and global water environment. This article thus aims to highlight the mission, features, core research capability and some on-going research projects of SMTC and DHI-NTU Centre.

SINGAPORE MEMBRANE TECHNOLOGY CENTRE

INTRODUCTION

Membrane technology is an emerging technology and has found numerous industrial applications. Today, membranes are widely accepted as the best available technology for water and wastewater treatments. Membrane technology also offers a viable alternative to conventional separations and purifications in chemicals and pharmaceutical processing, energy production, environmental monitoring and quality control, food and beverage processing, as well as fuel cells and bioseparation systems. The scope of the applications of membrane technology is still extending, stimulated by the developments of novel or improved membrane materials and membranes with better chemical, thermal and mechanical properties or better permeability and selectivity

characteristics, as well as by the decrease of capital and operation costs. In the 21st century, the world is facing great challenges in the areas of energy, water and the environment. Membrane technology is predicted to play an increasingly significant role in addressing these issues through extensive R&D on the membranes and process improvements.

The Singapore Membrane Technology Centre (SMTC), headed by Professor A.G. Fane, has been established to do fundamental and applied research in membrane technology. In particular, it has a mission to be a world class research centre in membranes for the environment and water technology (EWT) industries. The SMTC is part of the Nanyang Environment & Water Research Institute (NEWRI) 'ecosystem', and is supported by NTU, EWI and industry.

CORE FEATURES OF SMTC

The SMTC's objectives are:

- Education & Training ~ to produce PhDs and Researchers in membranes for EWT;
- Research & Development ~ research with links to industry and international community;
- Industry & Application ~ act as incubator for novel membrane technology in EWT.

Membrane research is multidisciplinary involving scientists and engineers in experimental and theoretical works (e.g. Figure 1). More than 30 researchers will be recruited over the 5-year period, including 22 PhD students and 8 Post-doctoral Fellows and supporting staff. At least, 12 academic staff will be involved in research and supervision. In addition, the SMTC expects to host several international specialists for collaborative research.

Figure 1. Goniometer for membrane contact angle measurement

A wide range of projects of interest to the water industry are being studied in the SMTC including:

- Improved and novel desalination
- Solar driven membrane distillation
- Carbon neutral membrane bioreactors
- Trace pollutant removal with membranes
- NEWater for water reclamation
- Novel membranes for water/wastewater
- Sensors for smart membrane systems
- Decentralized membranes for water/wastewater

The SMTC is also a key partner in the following projects:

(i) Solar driven membrane distillation and bioreactor for water production funded by Singapore's National Research Foundation;

(ii) Demonstration trials of Integrity Sensor for Membrane Plant under Singapore's Environment & Water Research Programme (EWRP) scheme;

(iii) Demonstration of waste heat driven membrane distillation bioreactor for industrial wastewater supported by The Enterprise Challenge (TEC) from the Prime Minister Office, Singapore.

The SMTC is currently in active discussion with a wide range of companies for potential collaboration.

PROJECT HIGHLIGHTS

Project 1: Integration of Novel Forward Osmosis Membranes and Optimized Bioprocess for Water Reclamation

The integration of the Forward Osmosis (FO) membrane and the activated sludge bioprocess is a new variant of the membrane bioreactor (MBR) technology known as the forward osmotic membrane bioreactor (FOMBR) as illustrated in Figure 2. By using dense FO membranes, the FOMBR offers potential advantages such as lower energy requirement and high quality purified water for water reclamation. This is because the dense FO membrane retains recalcitrant organics and increases their biodegradation. However, a number of technical barriers impede FOMBR industrial applications. Two major challenges are the lack of an ideal membrane that can produce a high water flux and poor optimization of bioprocess performance in the bioreactor.

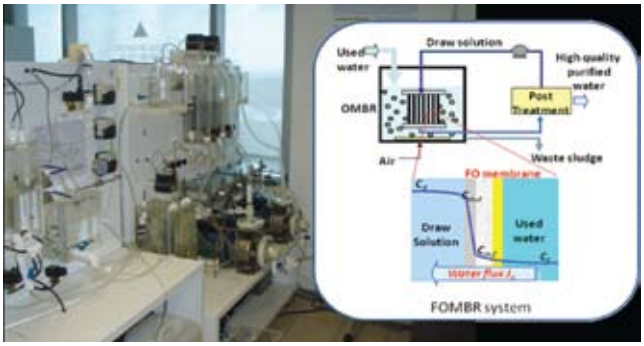

Figure 2. FOMBR system and principle of operation.

With the financial support from the Environmental and Water Industry (EWI) Development Council of Singapore, (EWI RFP 08/01), Professor A.G. Fane and his team are developing novel FO membranes suitable for use in the FOMBR systems for water reclamation. The membranes will be integrated with a biological process enhanced by system optimization. The multidisciplinary team includes Assoc Prof Wang Rong, Asst Prof Tang Chuyang, Assoc Prof Liu Yu and collaborators from the Centre for Advanced Water Technology (CAWT), DHI-NTU centre (e.g. Dr Qin Jianjun, Mr Kiran Kekre) and Imperial College (Prof Li Kang). The expertise encompasses membrane fabrication and characterisation, membrane separation/fouling, biological reaction/modelling, and system operation/optimization.

The aim of this project is to further develop the FOMBR technology and translate it from bench scale into practical application. It will have direct benefits for the water industry in terms of better water quality and lower production cost as well as more options for various types of used water treatment. It will also provide strategic benefits for Singapore by meeting the national goals in sustainability through water reclamation.

Project 2: A Novel Integrity Sensor for Membrane Processes

Membranes are used for both water treatment and wastewater treatment where the quality of the filtered output is important for human health. Membrane integrity needs to be checked on a regular basis to ensure that membranes are intact for membrane processes. A wide range of techniques such as particle counting, particle monitoring, turbidity monitoring, sonic leak testing, air pressure testing, bubble pressure testing, and routine microbial analysis have been applied to membrane integrity tests. The disadvantages of the available monitoring techniques are mainly cost, sensitivity, and reliance on high-technology sensors such as lasers and sonic instruments.

This project is developing a novel technique for membrane integrity testing which is simple to operate, low cost, and easy to install. Membranes are suitable for both large-scale and small-scale (decentralized) systems and this sensor could be applied at any scale. It is particularly suited to small, decentralized systems where reliable, sensitive, and low cost integrity monitors are required. It is also suited for online multi-channel monitoring of large plant where individual sensors could be applied to relatively small subunits of the larger plant.

The key feature of the patented concept is to apply a relative trans-membrane pressure monitoring technique for integrity testing of membrane processes via a multi-membrane device located downstream incorporating small-area membranes connected in series. The sensor unit features double membranes in series together with two digital pressure transducers that monitor changes of pressures above both membranes in the sensor. The signals from the pressure transducers are collected and analyzed to characterize the integrity of the membranes in the membrane process. It should be noted that the sensor can also be used to indicate the fouling propensity of a feed stream and is being considered as an alternative to the Silt Density Index. Figure 3 shows the typical response of the sensor to feeds of low turbidity.

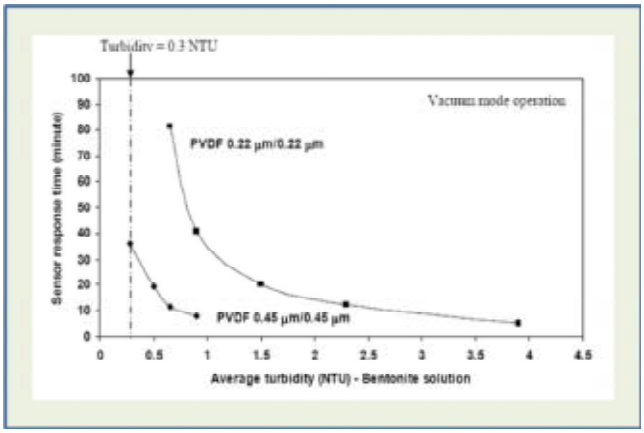

Figure 3. Response times for the membrane sensor vs. feed turbidity.

The sensor was originally developed in the A*STAR-funded Temasek Professor programme led by Professor A.G. Fane and its further development is now funded by EWI. This project has been in collaboration with iESE. Plans to commercialize the concept are in hand.

Project 3: UV Pre-treatment for the Control of Biofilm Formation on RO Membranes

Biofouling has long been recognized as one of the most problematic types of fouling in the reverse osmosis (RO) process. The removal of bacteria by micro/ultra-filtration as a pre-treatment step is not sufficient to eliminate biofilm formation on the surface of RO membranes. This is because the microorganism inventory is dominated by 'viable but not culturable' (VBNC) bacteria. These bacteria are of the order of 0.1 µm size compared with the 1 µm size of typical heterotrophes that can be removed by MF. The bacteria that escape the MF/UF and enter the RO system are transported to the membrane surface due to the permeation flux and can be resuscitated in the RO process by the new environment. For example, the organic (TOC) level in the feed is substantially increased by passage through the RO plant due to recovery (typical concentration increase is 2x) and concentration polarization at the membrane surface (concentration increase by a factor of 1.2 to perhaps 1.5x); thus TOC could rise by 2.4 to 3.0x in the process. This raised nutrient level combined with the extensive surface for adsorption provides a favourable environment for some of the VBNC bacteria to colonize and form biofilms. Control of biofouling by chlorination (and dechlorination prior to the membrane) has been shown not to be particularly effective for VBNC bacteria. Clearly, an alternative means of removal or inactivation of VBNC bacteria is required.

This project will assess the efficacy of UV pre-treatment for the control of biofilm formation on RO membrane. It is a 'proof of concept' study and aims to confirm the approach by means of well-controlled laboratory trials. It also involves pilot study at a NEWater plant to allow process optimization (Figure 4).

Figure 4. Experimental rig of reverse osmosis system

The research will be in collaboration with Professor Harvey Winters (FDU, USA) who is an expert in RO biofouling with experience on large-scale facilities as well as laboratory techniques. Financial support will be coming from Public Utilities Board of Singapore and an industrial partner, Trojan UV.

DHI-NTU WATER & ENVIRONMENT RESEARCH CENTRE AND EDUCATION HUB

INTRODUCTION

With the support from the Environment & Water Industry (EWI) Development Council and under the banner of the Nanyang Environment and Water Research Institute (NEWRI), DHI-NTU Water & Environment Research Centre and Education Hub (DHI-NTU Centre) was set up by DHI Water & Environment (S) Pte Ltd (DHI Singapore) and Nanyang Technological University (NTU) in October 2007. Adopting an industry-oriented approach, NTU plays the role of the collaborator and DHI Water and Environment (S) Pte Ltd plays the leading role in this R&D endeavour.

DHI-NTU Centre is an interdisciplinary research and training centre for water and environment. The centre strives to generate innovative solutions and new water technologies to strengthen the water and environment industry in their efforts to cope with existing problems and to meet future demands in Singapore. With extensive knowledge and advanced technological know-how in the various fields related to water and environment, as well as support of a team of dedicated professional, DHI-NTU Centre is well on track to deliver more than 200 man-years in research efforts, in addition to 10 PhDs, scientific papers and new products during its first phase of 5 years from 2007-2012.

MISSION

DHI-NTU Centre's objectives are to advance technological development and competence in the fields of hydraulic engineering, oceanography and marine environment, water resources, aquatic ecology, environmental chemistry, health and environment, water in industry and urban planning, as well as various fields related thereto with a view to strengthening the abilities of industry in the most effective manner, technically, economically and environmentally. In addition, DHI-NTU Centre aims to transform knowledge of water into value for customers and welfare for the global community through the technological links between applied research and development of problem-solution methodologies related to water, environment and health.

DHI and NTU are working as a team and jointly carrying out cutting-edge research projects. Through DHI's extensive technological development in the main thematic research areas, and leveraging on NTU's strength in science and engineering capabilities, DHI-NTU Centre endeavours to contribute to better understanding of the physical, biological, and chemical phenomena that affect the water environment, as well as provide integrated technologies and solutions for the economic benefits of water and environmental industry in Singapore. The synergetic collaboration would also bring forth environmental benefit from an improved understanding of an environmentally friendly water and waste management in the context of Singapore.

The activities of DHI-NTU Water & Environment Research Centre include the following key research and technology development areas:

- Industrial Water Management
- Urban Planning and Water Management
- Solid Waste Management
- Environmental Impact Assessment
- Decision Support System

On the training side, the DHI-NTU Education Hub provides training of water and environment research personnel and engineers in Singapore and neighboring countries to strengthen the manpower development of the water and environment industry.

ACTIVITIES SINCE ITS FORMATION

The key activities of the DHI-NTU Centre are based on relevant research projects with impacts. Although DHI-NTU Centre has only been in operation for one year, it has developed and established 28 R&D projects including 10 PhD projects, 6 industry R&D projects, and more than 12 future projects at various stages of developments. Several key projects are briefly described as follows:

- Detailed flow and aeration processes in controlled water courses (Figure 5)

Figure 5. Overall set up

- Comparison study of regional hydrology – water quality runoff model (Figure 6)

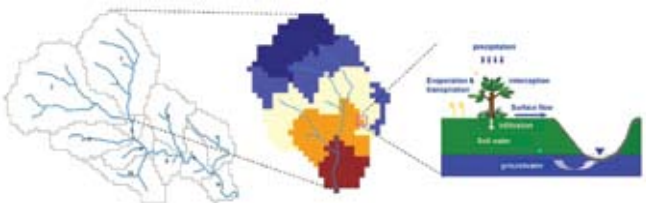

Figure 6. Schematic of geomorphology-based hydrologic model (GBHM)

- Nutrient removal from reservoir inflows using floating vegetation mats (Figure 7)

Figure 7. Experimental setup - The Perspex tank

- Local scour around submarine pipelines (Figure 8)

Figure 8. Scour under pipelines in current

- Wetland hydrodynamics: laboratory study of vegetated open channel flows with simulated vegetation (Figure 9)

Figure 9. Vegetated channel

- Estuarine transport of fine suspended sediments
- Role of carbon financing in developing nations to mitigate GHG emissions

- Assembling of multifunctional TiO_2 nanofiber member for water treatment
- Water for energy, energy for water, research analysis of policy implication for Singapore
- Characterization and modelling of sediment transport in the presence of silt screens
- Granular-liquid flows in a turbulent stream down a steep slope
- Characterization and modelling of storm runoff from a tropical catchment with diverse land use (Figure 10).

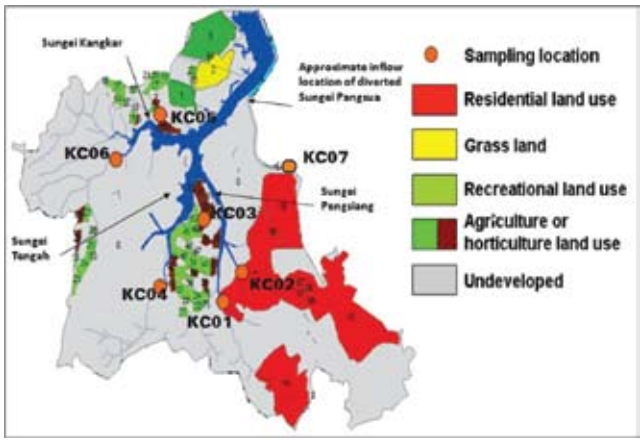

Figure 10. Kranji catchment

Since October 2007, the centre has the support of various faculty members and 8 PhD candidates, in addition to 3 EWT Scholarship holders/PhD students. The Centre is also supporting 3 MSc students through various student-assistance schemes. On the professional training/education, the Centre has organized more than 10 in-house and public workshops and symposia. With extensive knowledge and advanced technological know-how in the various fields related to water and environment, as well as support of a team of dedicated professional, DHI-NTU Centre is well on track to becoming a major industry-oriented R&D and training centre for water and environment.

ACHIEVEMENTS AND COMMENDATIONS

AWARDS

The Tan Chin Tuan Centennial Professorship in the field of engineering was set up by NTU and Tan Chin Tuan Foundation (TCTF) to catalyze a high standard of research for the benefit of industry and the community. For his contributions and merits to the discipline of engineering and research, the inaugural professorship is awarded to **Professor Ng Wun Jern**, Executive Director, Nanyang Environment and Water Research Institute (NEWRI), NTU.

Professor Anthony Gordon Fane was selected as the (American) Association of Environmental Engineering and Science Professors Distinguished Lecturer for 2008/9. This involves visiting over a dozen Universities in the US and presenting a public lecture on "Membranes and Water: Achievements and Challenges". He was also awarded a Royal Academy of Engineering Distinguished Visiting Fellowship to visit Oxford University in June 2008.

The research team led by **Assoc Prof Darren Sun** won the Innovation Award 2008 from the International Water Association (IWA) and the IES Prestigious Engineering Achievement Award 2008 from the Institution of Engineers, Singapore (IES). This is in recognition of their outstanding contributions to the TiO_2 nanostructured microsphere photocatalyst for membrane water purification.

From left: Darren Sun, James Leckie, Alan Du, Swee Loong Khor, Peifung Lee, Xiwang Zhang, Jiawei Ng and Jiahong Pan

Assoc Prof Tommy Wong has authored two articles which are within the Top-Ten Article Downloads for 2008 in the Journal of Professional Issues in Engineering Education and Practice, American Society of Civil Engineers (ASCE). The two articles are entitled (1) How to write an award-winning paper (ranked 5th), and (2) How to review or not to review a paper (ranked 6th).

Asst Prof Chen Po-Han received the Best Paper Award at the 24th International Symposium on Automation and Robotics in Construction (ISARC 2007), 19-21 September 2007, Kochi, India. His paper title is *"Simulated Annealing Algorithm for Optimizing Multi-Project Linear Scheduling with Multiple Resource Constraints"*.

Asst Prof Chen Po-Han receiving the Best Paper Award in Kochi, India

EDITORSHIPS

Professor Pan Tso-Chien was appointed as a Member of Editorial Board to the International Journal of Smart Structures and Systems and Institution of Engineers Singapore, Journal A: Civil and Structural Engineering.

Professor Chiew Yee Meng was appointed as an Associate Editor in the Journal of Hydraulic Engineering, ASCE. He was appointed as a Member of Editorial Board to IES Journal and in Recent Patents on Mechanical Engineering.

Professor Henry Fan was appointed as the Editorial Board member in the IES journals and Journal of Aviation Management.

Professor Harianto Rahardjo was appointed as a Member of Editorial Panel in Geotechnical Engineering, Journals of the Southeast Asian Geotechnical Society and Geomechanics & Engineering, Techno-Press.

Professor Anthony Gordon Fane was appointed as the Editorial Board member in the Journals of Membrane Science and Desalination.

Assoc Prof Chu Jian was appointed as:

- Co-editor to Geotechnical Engineering, Journal of Southeast Asian Geotechnical Society.

- Member of Editorial Board in *Acta Geotechnica*, Springer, Germany.
- Member of Editorial Board in *Geomechanics and Geoengineering, An International Journal*, Taylor & Francis, UK.
- Member of the 10th Editorial Board of the Chinese Journal of Geotechnical Engineering, Journal of the Chinese Institution of Geotechnical Engineering, China.
- Member of Editorial Board in *Geomechanics and Engineering, An International Journal*, Techno-Press, South Korea.
- Member of International Editorial Advisory Board in *Central Asian University Herald – Natural and Engineering Science Series,* Kazakhstan.

Assoc Prof Cheng Nian Sheng was appointed as a member of Editorial board in International Journal of Sediment Research (published by Elsevier)

Assoc Prof Chiew Sing-Ping was appointed as a Member in International Journal for Advanced Steel Construction and IES Journal Part A: Civil and Structural Engineering.

Assoc Prof Adrian Law Wing-Keung was appointed as an Associate Editor for the Journal of Hydro-Environment Research.

Assoc Prof Lo Yat-Man, Edmond was appointed as an Associate Editor for the Journal of Hydro-Environment Research, published by IAHR.

Assoc Prof Li Bing was appointed as an Associate Editor in the ASCE Journal of Structural Engineering.

Assoc Prof Liu Yu was appointed as an Editorial Board Member to Open Biotechnology Journal and in Recent Patents on Biotechnology. He was also appointed as a Guest Editor in the International Journal of Environment and Waste Management.

Assoc Prof Darren Sun was appointed as an Associate Editor for Water Science and Technology. He has been elected as Chair for International Water Associate (IWA) Chemical Specialist Group.

Assoc Prof Tan Soon Keat was appointed as an Associate Editor to the International Journal of Ocean and Climate Systems.

Assoc Prof Tommy Sai Wai Wong was appointed as

- Associate Editor to Journal of Hydrologic Engineering, ASCE
- Corresponding Editor in Journal of Professional Issues in Engineering Education and Practice, ASCE
- Member in Advances in Water Resources, Elsevier

Asst Prof Chen Po-Han was appointed as an Editorial Advisory Board Member to the Open Construction and Building Technology Journal.

INVITED LECTURES

Professor Pan Tso-Chien was invited to deliver a keynote lecture entitled "Seismic risk of the region surrounding Singapore" at the 11th *East Asia-Pacific Conference on Structural Engineering and Construction (EASEC-11)*, 19-21 November 2008, Taipei, TAIWAN.

Professor Henry Fan was invited to deliver a lecture entitled "Reducing Aircraft Emissions on the Ground" at the *International Forum on Shipping, Ports and Airports 2008*, Hong Kong SAR, May 2008.

Professor Anthony Gordon Fane was invited to serve as a Keynote speaker to the International Membrane Science & Technology Conference, Sydney, November 2007 and in IWA Leading Edge Technology Conference, Zurich, June 2008.

Professor Harianto Rahardjo was invited by School of Civil and Environmental Engineering, Yonsei University, Seoul, South Korea to teach "Unsaturated Soil Mechanics" to Graduate Students from several universities in South Korea from 26 to 29 February 2008 under the Brain Korea 21 program. He was also invited to deliver lectures at the following conferences:

- *Keynote Lecture:* "Monitoring and modeling of slope response to climate changes". *Proceedings of the 10th International Symposium on Landslides and Engineered Slopes. Chinese Institution of Soil Mechanics and Geotechnical Engineering – China Civil Engineering Society, Chinese National Commission on Engineering Geology, Chinese Society of Rock Mechanics and Engineering, Geotechnical Division of the Hong Kong Institution of Engineers,* Xi'an, China, 30 June – 4 July 2007.
- *Invited Lecture*: "Unsaturated Soil Mechanics for Slope Stability." *Proceedings of 2007 National Conference of Korean Geotechnical Society (KGS). Busan, Korea, 14-15 September 2007*, pp. 1-21.
- *Keynote Lecture:* "Unsaturated soil mechanics for solving seepage and slope stability problems." *Proceedings of the 12th International Colloquium on Structural and Geotechnical Engineering.* Ain Shams University, Cairo, Egypt, 10-12 December 2007.
- *Keynote Lecture*: "Role of antecedent rainfall in slope stability." *Proceedings of the GEOTROPIKA 2008*. Kuala Lumpur, Malaysia, 26-27 May 2008.
- *Keynote Lecture:* "Role of real time monitoring in slope stability". *Proceedings of the International*

Seminar on Civil and Infrastructure Engineering 2008 for Environmental Sustainability. Shah Alam, Malaysia, 11-12 June 2008.

Assoc Prof Chu Jian was invited to deliver lectures at the following conferences:

- *Invited Lecture:* 2nd International Conference on Geotechnical Engineering for Disaster Mitigation and Rehabilitation, 16-19 May 2008, Nanjing, China.
- *Invited Lecture*, International Symposium on Disaster Mitigation and Community Based Reconstruction, 9 August 2007, Yogyakarta, Indonesia.
- *Keynote Lecture:* "Geotechnical considerations of access road construction for disaster rehabilitation." *Proceedings of the 4th International Conference on Disaster Prevention and Rehabilitation,* 10-11 September 2007, Semarang.
- *Invited Special Session Lecture:* ISSMGE TC39 Session, 13th Asian Regional Conference on Soil Mechanics and Foundation Engineering, 10-14 December 2007, Kolkata, India.
- *Invited Panelist Presentation:* 13th Asian Regional Conference on Soil Mechanics and Foundation Engineering, 10-14 December 2007, Kolkata, India.

Assoc Prof Lie Seng Tjhen was invited to deliver a lecture at the Department of Engineering Mechanics, Tsinghua University on 19 December 2008.

Assoc Prof Darren Sun was invited to deliver a lecture at Keppel Technology Annular Panel (KTAP) Corporation Board Council Meeting, November 2007, Singapore.

RESEARCH CENTRES

Activities of Centre for Infrastructure Systems (CIS) from July 2007 to June 2008

RESEARCH AND DEVELOPMENT

1. **Singapore-ETH Centre (SEC) for Global Environmental Sustainability**

   During the reporting period, Prof Henry Fan was part of the NTU team involved in coordinating with researchers at the Swiss Federal Institute of Technology Zurich for the proposed Future Cities Research Program within the SEC initiative.

2. **Study to update Speed-Flow Models for Expressways & Arterial Road**

   In April 2008, CIS completed a study for the Land Transport Authority (LTA) to update a set of traffic speed-flow models for expressways and arterial roads in Singapore. The faculty members involved in the project included Prof Henry Fan, Assoc Prof Lum Kit Meng and Assoc Prof Tan Yan Weng.

EDUCATION AND TRAINING

Short Courses

1. **Singapore Cooperation Programme – Urban Transport Planning & Design Short Course**

   20 Transport officials from Riau, Indonesia attended the short course on Urban Transport Planning and Design. Organised by CIS from 12 to 23 November 2007, the course was conducted on behalf of the Ministry of Foreign Affairs under its Small Island Developing States Technical Cooperation Programme (SIDSTEC) and the Singapore Cooperation Programme Training Awards (SCPTA).

   The instructors for the course were Prof Henry Fan, Assoc Prof Lum Kit Meng, Assoc Prof Tan Yan Weng and Assoc Prof Wong Yiik Diew.

2. **Short Course on Urban Transport Planning & Design**

   CIS organized a 3.5-day short course on Urban Transport Planning. Conducted in Abu Dhabi from 25-28 June 2008, the course was attended by staff from the Bus Transport Office, Department of Transport of Abu Dhabi. Prof Henry Fan was the instructor for this course.

Workshop

In April 2008, Assoc Prof Lum Kit Meng conducted a workshop for officers from the Land Transport Authority on the development of updated speed-flow relationships for Singapore roads. Prof Henry Fan and Assoc Prof Tan Yan Weng also participated in this workshop.

SEMINARS AND CONFERENCES

SMRT Professor in Transportation Studies

Professor Anthony D. May from the University of Leeds in United Kingdom visited the School from 9 October to 7 November 2007. He was appointed the 2007 SMRT Professor in Transportation Studies at NTU. During his four-week stay with the School, Professor May delivered 3 public presentations as follows:

- Public Lecture on **How Feasible is it to Make Urban Transport Sustainable?** held on 19 October 2007
- Public Seminar on **Designing Effective Urban Transport Strategies** held on 25 October 2007
- Public Seminar on **Developing Successful Road Pricing Schemes** held on 1 November 2007

The presentations were attended by government officials, industry professionals, public transport operators as well as by faculty and students.

International Conference Participation

International Forum on Shipping, Ports and Airports (IFSPA) 2008, Hong Kong SAR, 25-28 May 2008

Prof Henry Fan was an invited Honorary Guest Speaker. He presented a paper entitled "Reducing Aircraft Emissions on the Ground" at the conference.

Activities of Environmental Engineering Research Centre (EERC) from July 2007 to June 2008

CENTRE ACTIVITIES

Seminars

1. **Bioenergy as a renewable green and clean energy** (Energy forum)

   Assoc Prof Wang Jing-Yuan, Nanyang Technological University
   6 June 2007
   Venue: Institute of Southeast Asian Studies
   ** A/P Wang was invited to speak at the Institute of Southeast Asian Studies (Energy Forum) with 70 attendees in total; Lianhe Zaobao (LHZB) featured an interview and story on 7 June.

2. **Urban environmental management & sustainability** (guest lecture series)

   Assoc Prof Wang Jing-Yuan, Nanyang Technological University
   21 August 2007
   Venue: Department of Architecture, School of Design and Environment, National University of Singapore

3. **New directions in desalination**

   Professor Raphael Semiat
   Director of Grand Water Research Institute
   Head of GWRI Rabin Desalination Laboratory
   The Chemical Engineering Department
   Technion - Israel Institute of Technology
   24 August 2007

4. **Stability of *Pseudomonas putida* Cultures during the Off-Gas Treatment of Toluene and Benzene**

   Dr Raul Muñoz
   Senior Researcher
   Dept of Chemical Engineering and Environmental Technology
   Valladolid University, Spain
   13 September 2007

5. **Off-gas treatment of *VOC*S in two-phase partitioning bioreactors: potential and limitations**

   Dr Raul Muñoz
   Senior Researcher
   Dept of Chemical Engineering and Environmental Technology
   Valladolid University, Spain
   20 September 2007

6. **Free nitric acid inhibition on nitrous oxide reduction in denitrification and could polyphosphate-accumulating organisms be glycogen-accumulating organisms?**

   Dr Raymond J Zeng
   Advanced Water Management Centre
   University of Queensland, Australia
   7 December 2007

7. **Waste as a Resource – New Challenges for the Future**

   Prof Dr-Ing. R. Stegmann
   Hamburg University of Technology Institute of Waste Resource Management Germany
   19 March 2008

Workshops

- **Project Atmospheric Brown Clouds (ABC) – Water Impact Study Group meeting @ Nanyang Executive Centre, NTU;** 15-16 September 2007

  Jointly hosted by EERC and MRC, this was the second Water Impact Study Group meeting held in Singapore.

- **Training Workshops for Chongqing Water Authority Group;** 26 December 2007 – 3 January 2008

  EERC conducted a series of lectures and site visits for the delegates from the Chongqing Water Authority, China.

- **NEA-Industry-NEWRI Waste Management Workshop;** 11 April 2008

  The workshop cum discussion is for NEA, Industry and NEWRI to seek collaboration opportunities so as to address not only Singapore's waste management issues, but also pursue R&D directions which can lead to business opportunities for the Singapore industry in the global market.

International Conferences

- **4th IWA Leading Edge Conference on Water and Wastewater Technologies (LET) @ Swissotel The Stamford, Singapore;** 3-6 June 2007

  NTU Participants: Assoc Prof Edmond Lo Yat-Man, Assoc Prof Wang Jing-Yuan, Assoc Prof Darren Sun and EERC researchers.

- **Science team meeting and workshop on Impact Assessment - Project Atmospheric Brown Clouds (ABC) @ Imperial Palace Hotel, Seoul, Korea;** 27-29 August 2007

  NTU Team: Assoc Prof Tan Soon Keat, Assoc Prof Wang Jing-Yuan, Asst Prof Victor Chang and Dr Wang XiKun.

- **RUC meeting @ Tongji University, Shanghai, China;** 19-22 September 2007

  Assoc Prof Wang (Director-EERC) was invited to present on environmental research in NTU at the RUC meeting.

- **11th World Congress on Anaerobic Digestion (AD11) - Bioenergy for our future @ Brisbane, Australia;** 24-27 September 2007

  Assoc Prof Wang (Director-EERC) and his graduate student, Ding HongBo attended the conference.

Colloquium

- **EERC hosted a joint colloquium for the delegation from the department of environmental engineering (DEE) of National Cheng Kung University (NCKU) of Taiwan** on 2 November 2007.

  The NCKU team comprised 8 professors and 6 graduate students. Several of the CEE Faculty and researchers attended the colloquium to interact with the NCKU visitors. A number of our faculty members had also given presentation on topics related to their research interests. The joint colloquium has achieved its main objective to let the colleagues from 2 institutions discuss their common interests and possible collaboration. An MOU was signed between NTU and NCKU on the same day.

- **Joint colloquium with Tungnan University** (Taiwan); 24-26 March 2008.

  A delegate of 21 members consisting of professors and researchers visited EERC and shared research interests with EERC researchers.

Community Involvement

National Science Challenge 2007

- The annual National Science Challenge, jointly organised by the Agency for Science, Technology and Research, Singapore Science Centre and the MOE, is a major Science competition for Secondary Schools.

  EERC was invited by the Singapore Science Centre to host an Outdoor Challenge (on 12 September 2007) for the National Science Challenge grand final. The challenge proposed and coordinated by EERC, "Making Nanyang Lake a Sustainable Eco-Lake" was a full day program which comprised site investigation at the lake followed by laboratory analysis, presentation of findings and proposals on a conceptual master plan by the competing teams. A number of the EWRE faculty staff was invited to be lecturers and judges for the competition.

International Conference Participation

- **Regional Forum on Bioenergy Sector Development: Challenges, Opportunities, and The Way Forward. Bangkok, Thailand;** 23-25 January 2008
  Attendee: Assoc Prof Wang Jing-Yuan, Director-EERC

- **2008 Jade Mountain Forum on Sustainable Environment;** 19-20 April 2008
  Tainan City, Taiwan
  Attendee: Assoc Prof Wang Jing-Yuan, Director-EERC

- **RUC Research Colloquium & the RUC 7th Board Meeting**; 24-26 April 2008
  Asian Institute of Technology (AIT) Bangkok, Thailand
  Attendee: Assoc Prof Wang Jing-Yuan, Director-EERC

Oversea Visits

- **CII Centres of Excellence Visit: Delhi, Hyderabad and Bangalore, India;**
  16-18 January 2008
  Director-EERC, Assoc Prof Wang Jing-Yuan was among the NTU delegates who visited Indian companies/ industries to seek collaboration opportunities in Delhi, Hyderabad and Bangalore, India.

Activities of Maritime Research Centre (MRC) from July 2007 to June 2008

CENTRE ACTIVITIES

Seminars

- Introduction to Current Research on Hydrology and Water Resources in Tsinghua University by Prof Yang Dawen (24 January 2008, NTU)
- Singapore Chemical Industry Council (SCIC) Meeting to introduce DHI-NTU Centre Seminar, 30 January 2008, Public Seminar.

International Conference

- International Symposium on Fatigue and Fracture of Steel Structures (4 December 2007, NTU)

Colloquium

- 2nd United Nations Environment Programme – Atmospheric Brown Clouds (UNEP-ABC) Water Impact Study Group Meeting (15-16 September 2007, NTU)

Community involvement

- Special Interest Lecture at Nanyang Girls' High School (15 April 2008, Nanyang Girls' High School)

International Conference Participation

- Hao, Z., Lim, A.T.B., Wang, X.K. and Tan, S.K. "Simulation of regular waves and their impact on a semi-submerged cylinder". *MTEC 2007 - International Maritime – Port Technology and Development Conference*, 26-28 September 2007, Singapore.
- Lie, S.T., Zhang, B.F. and Shao, Y.B., 2007. "Residual Strength of Cracked Circular Hollow Section (CHS) Tubular K-joints". *Proceedings of the 9th International Conference on Steel Space & Composite Structures, 10-15 October 2007, Yantai and Beijing, P.R. China,* pp. 461-467.
- Zhang, B.F., Teng, Y., Qu, S.Y., Lie, S.T. and Shao, Y.B., 2007. "Experimental Study of Stress Concentration Factors (SCFs) of a Completely Overlapped CHS K-joint". *Proceedings of the 9th International Conference on Steel Space & Composite Structures, 10-15 October 2007, Yantai and Beijing, P.R. China,* pp. 501-508.
- Lie, S.T. and Yang, Z.M., 2007. "BS7910:2005 Failure Assessment Diagram (FAD) on Cracked Circular Hollow Section (CHS) Welded Joints". *Fifth International Conference on Advances in Steel Structures – ICASS 2007, Singapore, 5-7 December 2007, pp*. 535-540.

Oversea Visits

- China, Nanjing – Hohai University, September 2007
- China, Shanghai - Shanghai Maritime University, Shanghai Jiaotong University, Tongji University – October 2007
- Vietnam, Hanoi – Water Resources University, University of Civil Engineering, University of Science and Technology, November 2007
- Denmark – DHI, DANTEK and Technical University of Denmark, March 2008

Activities of Protective Technology Research Centre (PTRC) from July 2007 to June 2008

OUTREACH PROGRAMMES

At PTRC, we have the privilege of organizing outreach programmes for visiting professors, our NTU faculty members and researchers. These programmes provide a platform for sharing knowledge and expertise, as well as establishing collaborations with local and foreign agencies in the area of protective technology and homeland security.

International Conference

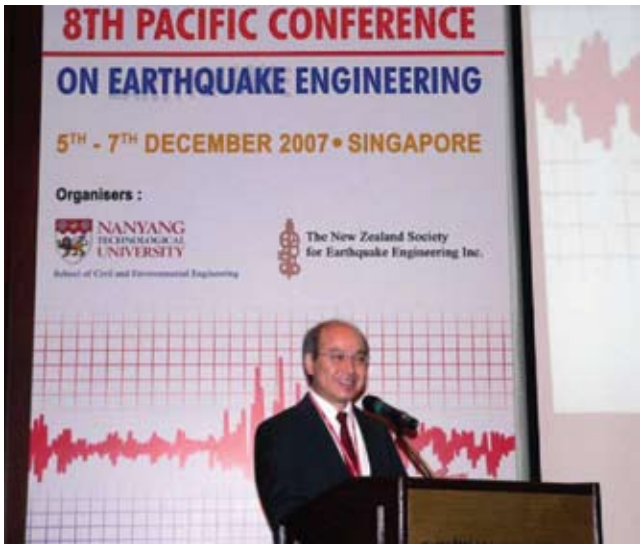

PTRC has initiated and been involved in the initial planning and coordination of the 8th Pacific Conference on Earthquake Engineering (8PCEE). It was jointly organized by School of CEE and New Zealand National Society for Earthquake Engineering, and received an overwhelming response of more than 200 papers and 239 participants. Speakers from over 36 countries participated in the conference, which provided an invaluable forum for designers and researchers to share ideas on the state-of-the-art earthquake resistant designs. During the 3-day conference held from 5 to 7 December 2007 at Swissotel Merchant Court, there were 9 Keynote Speakers and 108 presentation sessions.

The Keynote Speakers were:

- Professor Michael N. Fardis, University of Patras, Greece
- Professor Chin-Hsiung Loh, National Taiwan University, Taiwan
- Professor Jack P. Moehle, U.C. Berkeley, USA
- Professor Tso-Chien Pan, NTU, Singapore
- Professor (Emeritus) Haresh Shah, Stanford University, USA
- Dr Richard Sharpe, Beca Applied Technologies Ltd, New Zealand
- Professor Kerry Sieh, California Institute of Technology, USA
- Professor Lai Susumu, Kyoto University, Japan
- Professor Zhou Xi-Yuan, Beijing University of Technology, China

Public Seminars

1. An Introduction to the Norwegian Tunnelling Techniques

Professor Lu Ming, Chief Scientist, SINTEF Building and Infrastructure, Norway; Adjunct Professor, Norwegian University of Science and Technology, 25 July 2007

The seminar started with a brief introduction of Norway and SINTEF, and a short description of Norwegian tunnelling and use of underground space, followed by three technical presentations on Tunnel Support Design in Norway, Subsea Tunnelling, and Underground Oil and Gas Storage.

2. Earthquake Risk Modelling in Australia

Mr David Robinson, Geophysicist, Natural Hazards Impacts Project, Geoscience Australia, 29 November 2007

National strategies, as well as international events such as the Great Indian Ocean Tsunami, have emphasised the need to understand risks posed by natural hazards. Geoscience Australia's earthquake risk model (EQRM) combines physical models of earth processes and economic and social models of vulnerability to forecast the probability and possible impacts of future events. The EQRM provides Geoscience Australia with the ability to undertake city and national scale earthquake risk assessments as well as model catastrophic scenarios for emergency management planning. These tools can also be used to assess the major sources of uncertainties in earthquake risk, guiding and prioritising earthquake risk research in Australia.

3. Modelling Tsunami Hazards from Manila Trench to Singapore

Dr Wu Tso-Ren, Assistant Professor, Graduate Institute of Hydrological and Oceanic Sciences, National Central University, Taiwan, 27 March 2008

Recently, the U.S. Geological Survey issued a report

assessing the potential risk from tsunami sources along the entire Pacific subduction zones. One high-risk zone is identified along the Manila (Luzon) trench, where the Eurasian plate is subducting eastward underneath the Luzon volcanic arc on the Philippine Sea plate. This subduction zone may rupture and generate large tsunamis in the future that will have significant impact on countries bordering the South China Sea. This presentation focused on the numerical simulation on the tsunami waves excited by the hypothetical earthquake events and the effect to the coastal area of Singapore.

4. Catastrophe Risk Management – History, Modelling & Implementation

Dr Dong Weimin, Chief Risk Officer, Risk Management Solutions, Inc., USA, 1 April 2008

Unexpected nature and severe consequences characterize catastrophe risk, from natural disasters to man-made calamities. In order to manage these kinds of risk, the first priority is to quantify them, both in frequency and severity domain. This lecture described how the modern science and technology can be utilized to model catastrophic disasters. It also discussed how insurance mechanism can alleviate such disasters and provide a win-win situation for individual, government as well as the insurance industry.

5. Catastrophe Risk Modelling for Asia – Status and Challenges

Dr Pane Stojanovski, Vice President, Risk Management Solutions, Inc., Model Development Operations, USA, 1 April 2008

Catastrophe (CAT) modelling faces global challenges, but some of these challenges are very specific to Asia (e.g. very low insurance penetration rate). This talk looked at the 2007 CAT loss Asia experience, covering the status of CAT modeling in Asia for various perils, and identifying some of the challenges that need to be addressed in order to effectively manage and reduce the catastrophe risk in Asia.

6. The World Seismic Safety Initiative – Its Past, Present and Future

Dr Tsuneo Katayama, Professor of Tokyo Denki University; Professor Emeritus of the University of Tokyo; President of the International Association for Earthquake Engineering, 3 April 2008

The World Seismic Safety Initiative (WSSI) is a non-profit corporation registered in Singapore at CEE, NTU, working in the field of earthquake disaster mitigation in developing countries. It was established in 1993 to support the UN's International Decade for Natural Disaster Reduction (IDNDR). As one of its founding members, Dr Katayama summarized how IDNDR and WSSI originated, what activities they have been engaged in, what problems they have faced, and what its future may be.

Short Course

1. Block Theory and its Applications to Rock Engineering

Dr Shi Genhua, Chairman and Numerical Analyst & Consulting Engineer of DDA Company, 21-22 February 2008

Dr Shi Genhua has developed several engineering numerical methods and computer codes such as the Discontinuous Deformation Analysis (DDA) of Deformable Dynamic and Static Block Systems. His DDA and manifold method have been recognized as among the newest numerical methods on discontinuous and continuous arithmetic tools in the 21st century. Block theory has been studied and applied widely in rock engineering from its initiation. In the short course, Dr Shi explained that with the determination of the key-block types, the theory provides a description of the locations around the excavation whether the key block is a potential hazard. The next step will be either to provide timely support to prevent the movement of this block, or to analyze further if friction on the faces will hold it safely.

Workshops

1. Tsunami Generation and Modelling

Professor Kerry Sieh, Robert P. Sharp Professor of Geology, California Institute of Technology, who is also NTU Visiting Professor, conducted a training session on 13 September 2007 together with Dr Jose Borrero, Manager of ASR Marine Consulting and Research, New Zealand. This training session presented participants with several possible sources that may generate tsunamis, the process of tsunami generation, the characteristics of tsunami waves, and the impact to coastal environment. The modelling of tsunami wave propagation and assumptions, and simplifications

usually made in modelling were discussed during the workshop.

2. **Risk Assessment in Geotechnical Engineering and Underground Construction**

Risk assessment in all human activities and particularly in engineering is becoming increasingly important. In geotechnical engineering, given the uncertainties involved, risk assessment and analysis is a must. This course introduced the problem with emphasis on rock engineering and expanded to a treatment of natural hazards. A large portion of the course then dealt specifically with creating the basis for risk assessment in underground construction through an introduction of the Decision Aids for Tunnelling and using tunnel exploration. Professor Herbert H. Einstein, Department of Civil and Environmental Engineering, Massachusetts Institute of Technology, USA and Mr Jean-Paul Dudt, Rock Mechanics Laboratory, Swiss Federal Institute of Technology, Lausanne, Switzerland, were invited by CEE Asst Prof Ma Guowei to conduct the 2-day workshop.

Forum

In April 2008, PTRC organized the 2nd Micro-Insurance Round Table Forum, together with Risk Management Solutions, Inc., California, USA, which is one of the initiatives that underscores our commitment to the community. Foreign delegates, industry practitioners and professors shared their expertise in this field, examining how micro-insurance can be made available to victims of natural disasters. The objective is to help the less privileged protect themselves against catastrophic risks such as earthquakes, major floods and tsunamis. The group will be developing pertinent financial products and implementing various initiatives to further promote micro-insurance. The 3rd Forum will be a 2-day event in April 2009.

INTERNATIONAL AND LOCAL VISITORS

The investment of the shake table in the Protective Engineering Laboratory and Split Hopkinson Bar in the Construction Technology Laboratory of CEE is largely for the purpose of facilitating research carried out by PTRC. Both the shake table and Split Hopkinson Bar have attracted many visitors locally and from different parts of the world.

Visit by Professor Ted Krauthammer and Dr Van Romero, 14 December 2007

i) Professor Ted Krauthammer, University of Florida, USA

ii) Dr Van Romero, Vice President for Research of New Mexico Tech, USA

Visit by Shiraz University, Iran, 11 April 2008

i) Professor Nematollah Riazi, Vice Chancellor for Research

ii) Dr Ali Reza Khayatian, Chair, School of Engineering

iii) Dr Mohammad Reza Rahimpour, Chair, College of Oil and Gas

iv) Professor Mohammad Ali Alishahi, Department of Mechanical Engineering

Visit by participants of the Ministry of Home Affairs (MHA) Building Security Course

PTRC hosted the visit for the participants of the MHA Building Security Course on 3 October 2007, which was a success. Participants of the 2nd and 3rd run also visited the Protective Engineering and Construction Technology Laboratories on 6 November 2007 and 9 May 2008, respectively.

R&D PROJECTS AND PROGRAMME

One of the notable on-going research developments is the work with Defence Science and Technology Agency (DSTA) on progressive collapse of structures due to extreme loads. This work was sponsored by Ministry of Home Affairs (MHA) and Building and Construction Authority (BCA), and administered by DSTA. It is known as Explosion Consequence Assessment Model (ECAM).

The objective of this study is to understand the structural response in large deformation and develop numerical software capable of large deformations to simulate the response of a structure when subjected to extreme loads such as blast and post-blast fire event. The predictive software is to incorporate both steel and reinforced concrete material characteristics. For this phase of development, software predictions will be calibrated with published component tests on reinforced concrete beams, columns and slabs.

To further investigate the collapse behaviour of structural components, reinforced concrete columns and beam-column joints are currently being tested at PTRC. Leveraging on this work, DSTA has teamed up with Defense Threat Reduction Agency (DTRA), USA, to develop an extensive testing programme to simulate the blast effects on a reinforced concrete structure. NTU team comprising Professor Pan Tso-Chien, Assoc Prof Tan Kang Hai and Assoc Prof Li Bing will advise DSTA on the details and implementations of the testing programme.

On-going Projects

The table below shows the on-going projects during the reporting period.

No	Project Title	Principal Investigator(s)	External Funds (S$)	Collaborating Partners
1	Underground Technology and Rock Engineering (UTRE) Programme, Phase I	Asst Prof Ma Guowei Assoc Prof Zhao Zhiye Asst Prof Yang Yaowen Assoc Prof Tor Yam Khoon Assoc Prof Tan Kang Hai	2,398,000	DSTA
2	Study on Debris Modelling and Prediction II	Prof Fan Sau Cheong	764,500	DSTA
3	Integrated Explosion Modelling	Asst Prof Ma Guowei	398,750	DSTA
4	Dynamic Properties of Singapore Soils	Assoc Prof Leong Eng Choon	164,800	DSTA
5	Development of Analytical Tools for Progressive Collapse due to Terrorist Bombing	Assoc Prof Li Bing Assoc Prof Tan Kang Hai	1,060,000	DSTA
6	Research and Development of Operational Tsunami Prediction and Assessment System	Asst Prof Kusnowidjaja Megawati	447,352	National Environment Agency (NEA)

RESEARCH PROJECTS

A list of approved research projects is summarized below. Readers are welcome to email the respective investigators for more information regarding their work.

PROJECT TITLES	PRINCIPAL INVESTIGATOR
Internal Project	
Failure modes and ultimate strength of tubular joints under elevated temperatures	Tan Kang Hai ckhtan@ntu.edu.sg
Estuarine transport of fine suspended sediments from urban tropical catchments	Lloyd Chua Hock Chye chchua@ntu.edu.sg
Dynamics of floating breakwater in nonlinear shallow water waves	Huang Zhenhua zhhuang@ntu.edu.sg
Fouling of reverse osmosis and nanofiltration membranes by biological macromolecules - probing the foulant-membrane and foulant-foulant interactions	Tang Chuyang cytang@ntu.edu.sg
Fatigue life of steel catenary risers at the touchdown point	Low Ying Min ymlow@ntu.edu.sg
High performance computational simulations of multi-scale and multiphase flows in membrane filtration	Jim Chen jimchen@ntu.edu.sg
Retention of perfluorochemical surfactants by reverse osmosis and nanofiltration membranes	Tang Chuyang cytang@ntu.edu.sg
Local nonlinear wave forces on oscillating cylinders	Huang Zhenhua zhhuang@ntu.edu.sg
Innovative arsenic removal from waters using a new breed of layered double hydroxide as a thermally stable and regenerable adsorbent	Lim Teik Thye cttlim@ntu.edu.sg
Microfluidic bacterial cell separation for environmental monitoring	Volodymyr Ivanov cvivanov@ntu.edu.sg
External	
Underground Technology and Rock Engineering (UTRE) Program - Behaviour of rock cavern under dynamic loads. (This project is a continuation from previous project by Zhao Jian who resigned in 2005). The new PI is ZhaoZY	Zhao Zhiye czzhao@ntu.edu.sg
Atmospheric brown clouds (water budget) – water impact study	Wang Jing-Yuan jywang@ntu.edu.sg Tan Soon Keat ctansk@ntu.edu.sg
Experimental and theoretical studies of vortex shedding of side-by-side multiple cylinders	Cheng Nian Sheng cnscheng@ntu.edu.sg
Emerging organic contaminants in catchment surface waters of the marina bay	Karina Gin Yew-Hoong cyhgin@ntu.edu.sg
Development of an online pathogen detection system	Karina Gin Yew-Hoong cyhgin@ntu.edu.sg

PROJECT TITLES	PRINCIPAL INVESTIGATOR
The Jurong rock cavern project at Banyan Basin, Jurong Island (JTC C05502007)	Low Bak Kong cbklow@ntu.edu.sg Ma Guowei cgwma@ntu.edu.sg Zhao Zhiye czzhao@ntu.edu.sg Yang Yaowen cywyang@ntu.edu.sg Tor Yam Khoon cyktor@ntu.edu.sg
Modelling of wave run-up, air-gap and hydrodynamic loads of semisubmersible structures	Huang Zhenhua zhhuang@ntu.edu.sg
TiO_2 based solar panel for maritime and port applications	Darren Sun Delai ddsun@ntu.edu.sg
Development of specialized container technology for growing of street trees in Singapore	Harianto Rahardjo chrahardjo@ntu.edu.sg
Innovative design of civil defence shelters	Ma Guowei cgwma@ntu.edu.sg
Slope repair and technology in Singapore	Harianto Rahardjo chrahardjo@ntu.edu.sg
Development of a high performance submerged aerobic granular sludge MBR	Liu Yu cyliu@ntu.edu.sg
Development and evaluation of novel TiO_2 nanofiber membrane for the removal of marine micro-organisms	Darren Sun Delai ddsun@ntu.edu.sg
Dynamic fracturing mechanism of rock	Zhao Zhiye czzhao@ntu.edu.sg
Novel bending stiffeners for easy transportation and installation in flexible risers of offshore floating structures	Low Ying Min ymlow@ntu.edu.sg
Nitrogen-Doped TiO_2-Activated Carbon (AC) composite for adsorptive photocatalytic oxidation-reduction of refractory organic substances under solar irradiation in water purification	Lim Teik Thye cttlim@ntu.edu.sg
Development of flexible dye sensitized solar cells for commercial applications	Darren Sun Delai ddsun@ntu.edu.sg
Sediment plume in waves (smart subward agreement No.02)	Law Wing-Keung cwklaw@ntu.edu.sg

ACTIVE OXYGEN AS AN ALTERNATIVE OIL DISPERSANT AND OIL SPILL COMBAT AGENT

Tan Soon Keat (ctansk@ntu.edu.sg)
Dai Ying (daiying@ntu.edu.sg)
Nguyen Manh Tuan (NHUTNGUYEN@ntu.edu.sg)

INTRODUCTION

Oil pollution from major disasters at sea has aroused extensive public attention. Chemical oil dispersant is one of the methods to combat oil spill, but past research findings and experience have shown that the use of oil dispersant in the combat of oil spill has many limitations, including the window of effective application as well as the introduction of potential, undesirable by-products in the environment. However, past research findings, market practices and applications demonstrated that ozone (O_3) has been successful in its application in the agricultural industry as a bio-degrading agent for removing high levels of hydrocarbon content in soil. Based on this information and precedence of success, this article is a study on using ozone as an alternative dispersant to chemical oil dispersant in the biodegradation of hydrocarbon contents in crude oil for maritime applications. Experiments on treating crude oil with ozone were performed to establish the optimum concentration and rate of dispensing ozone in the various applications, windows of effectiveness of ozone on the different types of oil and qualitative assessment of the potential side effects or undesirable products, if any, from the application.

EXPERIMENTS ON DISPERSING CRUDE OIL WITH OZONE

Laboratory experiments are conducted to test the effectiveness of ozone (vapour) on dispersing three different types of oil (cSt180, cSt380 and cSt580) on the surface of water column and sand column. The main steps are: first, pour a certain amount of crude oil on to the surface of the water/sand column to form an oil layer which can cover the full surface of the water/sand column; second**,** the ozone spray is applied onto the oil layer for a certain period of time; finally, visual observation and photographs were taken at selected interval during the experiments.

The results and some photos are shown below:

Type of oil	Time needed to get clear water surface (hours)	
	15 Engines	30 Engines
cSt180	7	4
cSt380	15	more than 10
cSt580	much more than 15	more than 13

Thickness of oil layer: 1mm;
Ozone spraying intensity: 15,000 mg/hr spray (15Engines) and 30,000 mg/hr spray (30Engines)

Table 1. Results for Water Column Test

Type of oil	Time needed to get clear sand surface (hours)	
	Respond time 1 hour	Respond time 3 hours
cSt180	30mins~1	30mins~1
cSt380	1~2	1~2
cSt580	more than 1	more than 3

Single oil layer; Ozone spraying intensity: 15,000 mg/hr spray (15Engines)

Table 2. Results for Sand Column - Single Oil Layer Test

Type of oil	Time needed to get clear sand surface (hours)
cSt180	30 mins
cSt380	2
cSt580	more than 2

Multiple oil layers (six layers); Ozone spraying intensity: 15,000 mg/hr spray (15Engines)

Table 3. Results for Sand Column - Multiple Oil Layers (six layers) Test

Oil cSt180, oil layer thickness 1mm, Ozone 15 Engines:

oil cSt180, treated 0 hour

cSt180, treated 5 hours

Oil cSt180, single oil layer, respond time 1 hour, Ozone 15 Engines:

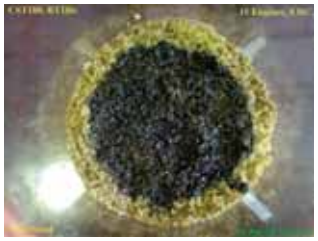

cSt180, treated 0 hour

cSt180, treated 1 hour

CONCLUSIONS

Through the findings from the experiments and qualitative assessment (visual inspection) of the treatment process, ozone is found to be efficient for dispersing crude oil both on water surface and on sand surface. It was also found from the investigations that the higher the ozone spraying intensity the more efficient is O_3 in dispersing oil. Treatment /dispersing of oil appears to be longer with the viscosity of oil treated. Based on the findings of the experiments, it was also found that there appears no distinct time window longer than which, the treatment using ozone becomes ineffective. In fact, all oil could be dispersed if ozone is applied for a sufficiently long duration. This study also found, through visual observation, that there appears to be no side effect or undesirable products arising from the use of ozone, at least for the duration and the sets of experiments carried out.

REFERENCES

[1] Committee on Understanding Oil Spill Dispersants: Efficacy and Effects Ocean Studies Board, Division on Earth and Life Studies, National Research Council of the National Academies. (2005). *Oil Spill Dispersants: Efficacy and Effects.* The United States of America: The National Academies Press, Washington, DC.

[2] Francis, A.W., 1997. Ozone. In *McGraw-Hill Encyclopedia of Science and Technology 8th Edition*, McGraw-Hill, NY, Vol. 12, pp. 683-686.

[3] Khurana, A., Chynoweth, D.P. and Teixeira, 2003. Ozone treatment for prevention of microbial growth in air conditioning systems. Masters theses, University of Florida.

[4] (n.a.), (1998). *Hazards of ozone generating air-cleaning devices*. Consumers' Research Magazine, Vol. 81, No. 7, pp. 23-25.

[5] Laurence Franken, M.S., 2005. *White Paper, The Application of Ozone Technology for Public Health and Industry.* Retrieved 16 November 2007, from http://www.webbwiz.com/WhitePaperFranken20051103.pdf

RESPIRATION PROFILES OF AEROBIC GRANULES WITH DIFFERENT SIZES

Li Yong (liyo0002@ntu.edu.sg)
Liu Yu (cyliu@ntu.edu.sg)

INTRODUCTION

Aerobic granules are dense bacterial spheres formed through cell-to-cell self-immobilization which is driven by selection pressure[1], and their superiorities over conventional activated sludge flocs suggest that aerobic granules would be a promising alterative form of microorganisms for advanced wastewater treatment. So far, little information is currently available about the metabolic behaviors of aerobic granules with different sizes. Therefore, this study looked into respiration profiles of aerobic granules with different mean sizes.

MATERIALS AND METHODS

A respirometer (MicroOxymax, Columbus, USA) was used to study metabolism of aerobic granules with different mean sizes. It was equipped with online oxygen and carbon dioxide probes, which allow simultaneous determination of the oxygen utilization and carbon dioxide production. The sorted aerobic granules were put into four chambers of the respirometer with 50 ml of substrate solution in which dissolved organic carbon (DOC) concentration was kept at 240 mg L^{-1}.

The initial biomass concentrations in the four chambers of the respirometer were controlled at the same level of 2.0 g L^{-1}. The DOC concentration was analyzed by TOC analyzer (Shimadzu, TOC-Vcsh, USA). The other measurements were all done according to standard methods[2].

RESULTS AND DISCUSSION

Figure 1 showed the profiles of oxygen utilization rate (OUR) and carbon dioxide production rate (CPR) for aerobic granules with two different sizes, meanwhile utilization of external DOC was also presented in the same figure. Regardless of the granule size, three metabolic phases can be differentiated in Figure 1: (I) a rapid utilization of the external DOC was observed, and this DOC reduction resulted in a maximum OUR as well as a maximum CPR. In this phase, external organic carbon would likely be converted to storage materials first; (II) after depletion of the external DOC, aerobic granules further grew on the stored materials derived from Phase I. As the result, a low OUR and CPR were recorded; (III) by the end of Phase II, most stored materials were likely consumed, and microbial metabolism came into the endogenous respiration leading to a constant and minimum OUR and CPR. In fact, Ekama et al.[3] also observed a nearly constant OUR in the endogenous respiration phase of activated sludge.

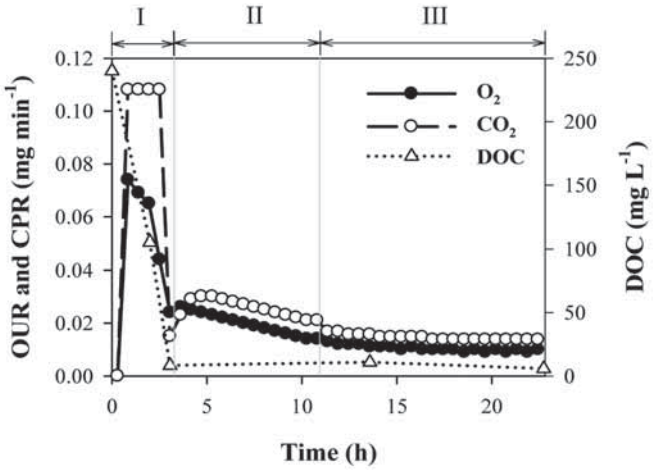

(a)

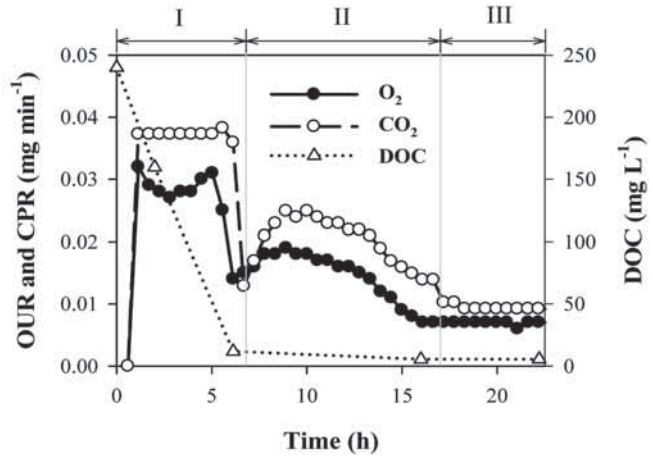

(b)

Figure 1. Changes in OUR, CPR and DOC concentration during respirometric tests of aerobic granules with different sizes. a: 0.75 mm; b: 2.4 mm.

In Figure 1, Phase I represents the feast period in which the external acetate-DOC was available, and Phase II is the famine phase where the external DOC was no longer present. It can be seen that the respiration activity of aerobic granules was high during the feast period, however after the external acetate-DOC was depleted, the degradation rate of storage materials in terms of OUR was 1.5 to 4 times lower than that of the external acetate-DOC observed in the feast phase (Phase I). The slow degradation of storage substance may allow aggregated bacteria in aerobic granules to have sufficient time for growth. In a study of potential role of PHB in simultaneous nitrification and denitrification, Third et al.[4] also found that the oxidation rate of PHB was up to 6 times slower than that of soluble acetate in the famine period of the activated sludge culture.

The OURs of smaller aerobic granules were found to be higher than those of bigger granules in all the three phases. For instance, in Phase I, the OUR of aerobic granules with the size of 0.75 mm was almost three times higher than that of aerobic granules with the size of 3.4 mm. This can be explained by the diffusion limitation in bigger granules. Previous study showed that diffusion of organic substrate and oxygen in aerobic granules smaller than 0.9 mm would not be a limiting factor of the biodegradation of external DOC[5]. The less diffusion limitation would be expected in smaller aerobic granules, leading to a higher microbial activity of smaller aerobic granules in terms of OUR and CPR as observed in Figure 1.

CONCLUSIONS

Metabolisms of aerobic granule were found to comprise three phases: (i) a quick reduction in the external DOC concentration associated with a maximum OUR as well as a maximum CPR. In this phase, external organic carbon would likely be converted to the PHB-like materials first; (ii) after depletion of the external DOC, aerobic granules further grew on the stored materials derived from Phase I; (iii) by the end of Phase II, most stored materials were consumed, and microbial metabolism came into the endogenous respiration leading to a minimum OUR.

REFERENCES

[1] Liu, Y. and Tay, J.H., 2004. State of the art of biogranulation technology for wastewater treatment. *Biotechnol Adv*. Vol. 22, pp. 533-563.

2] APHA 1998. Standard methods for the examination of water and wastewater. *20th edition, American Health Association, USA*.

[3] Ekama, G.A., Doid, P.L. and Marais, G.V.R., 1986. Procedures for determining influent COD fractions and the maximum specific growth rate of heterotrophs in activated sludge systems. *Water Sci. Technol.* Vol. 18, pp. 91-114.

[4] Third, K.A., Newland, M. and Cord-Ruwisch, R., 2003. The effect of dissolved oxygen on PHB accumulation in activated sludge cultures. *Biotechnol. Bioeng*. Vol. 82, pp. 238-250.

[5] Li, Y. and Liu, Y., 2005. Diffusion of substrate and dissolved oxygen in aerobic granule. *Biochem. Eng. J.,* Vol. 27, pp. 45-52.

COMPARISON BETWEEN KINEMATIC WAVE AND ARTIFICIAL NEURAL NETWORK MODELS IN EVENT-BASED RUNOFF SIMULATION FOR AN OVERLAND PLANE

Lloyd H. C. Chua (chcchua@ntu.edu.sg)
Tommy S. W. Wong (cswwong@ntu.edu.sg)
Sriramula L.K. (leela_Krishna_sriramula@pub.gov.sg)

INTRODUCTION

Artificial neural networks (ANNs) are being used extensively in rainfall-runoff modelling and forecasting. However, there appears to be a general lack of information on the comparison between the ANN and kinematic wave models (Dawson and Wilby, 2001), in spite of the fact that the kinematic wave model is a widely accepted physically-based approach and the ANN has gained popularity and has proven to be accurate. In addition, even when a comparison between these two methods is made, the comparisons are usually not made on an equitable basis. One of the difficulties encountered in trying to carry out a comparative study is in the choice of inputs. Input to the kinematic wave model is fixed by the requirements of the differential equations describing momentum and mass conservation. The ANN however learns by association and inputs to the ANN are not fixed and may include measured flow and rainfall from previous time steps in order to predict the flow at the current time step. The motivation for this study is therefore to carry out an objective assessment on the relative performance of these two modelling paradigms. The data for ten rainfall-runoff events obtained from an outdoor experimental station comprising a 25m long by 1m wide asphalt plane was analysed using Artificial Neural Network (ANN) and the Kinematic Wave (KWM) methods. The Nash-Sutcliffe coefficient (*NS*) was used as the goodness-of-fit parameter.

KINEMATIC WAVE AND ARTIFICIAL NEURAL NETWORK MODELS

The discretised form of the kinematic wave equations for flow on an overland plane are:

$$y_j^t = y_j^{t-1} + \Delta t[i_n - \frac{(q_j^{t-1} - q_{j-1}^{t-1})}{\Delta x}] \quad \ldots (1)$$

$$q_j^t = \alpha(y_j^t)^\beta \quad \ldots (2)$$

where y is the flow depth, t is time, q is the discharge, x is distance along the plane in the direction of flow, i_n is the net rainfall, $\alpha = \sqrt{S}/n$, $\beta = 5/3$, S is the overland slope, and n is the Manning's roughness coefficient of the overland surface. The kinematic wave model takes the net rainfall, i_n, as input, and predicts q (or y). As such, it also requires losses as input for the hydrographs to be simulated. Since it is not possible to determine the losses *a priori*, the net rainfall for the simulation event is determined based on the loss rate of the calibration event.

The class of ANNs employed in this study is the multi-layered feed forward neural network, also known as the multilayer perceptron. This class of ANNs is popular and is well suited for time series prediction and modelling applications. Two categories of ANN models, based on the choice of inputs, are considered:

(1) using measured rainfall only, and using measured rainfall with calculated discharge, and
(2) using both measured rainfall and measured discharge as input to the ANN.

For (1) the three input configurations for the ANN model considered were:

(i) Type 1 (5R) - The input consists of R_t, R_{t-1}, R_{t-2}, R_{t-3} and R_{t-4} where R is the total (measured) rain.
(ii) Type 2 (5R1Q_K) – The input is same as Type 1 plus a calculated total flow, $q_{k,t-1}$. and
(iii) Type 3 (1R1Q_A) - The input consists of R_t and $q_{a,t-1}$ where $q_{a,t-1}$ is the discharge predicted by the ANN at the previous time step.

For (2) the three input configurations for the ANN model considered were:

(i) Type 4 (5R3Q) - The input consists of R_t, R_{t-1}, R_{t-2}, R_{t-3}, R_{t-4}, $q_{m,t-1}$, $q_{m,t-2}$ and $q_{m,t-3}$.
(ii) Type 5 (5R1Q) - The input consists of R_t, R_{t-1}, R_{t-2}, R_{t-3}, R_{t-4} and $q_{m,t-1}$ and
(iii) Type 6 (1R1Q) - The input consists of R_t and $q_{m,t-1}$.

RESULTS AND DISCUSSION

Kinematic Wave Model

The strength in kinematic wave modelling is that the values of the parameters can be determined *a priori*. In this study, the physical dimensions of the overland plane are known. A Manning $n = 0.011$ was adopted for the asphalt surface. The process of model calibration is reduced to the determination of the loss rate (Φ-index was used in this study) for each

event. The Φ-index was then determined for each event by equating the net rainfall depth to the runoff depth, and this is considered as the calibrated Φ-index. The calibrated Φ-index was then used to simulate the other nine events. This was done successively for all the ten events. It is expected that *NS* is highest when the Φ-index of the calibration event is the same or close to that of the simulated event. The storm events can thus be grouped according to their calibrated Φ-index, as shown in Figure 1.

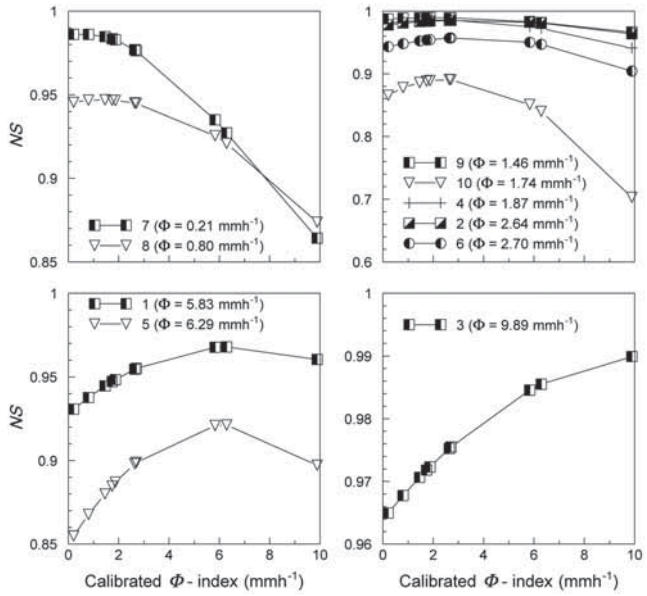

Figure 1. NS for each of the events simulated by the KWM, based on various calibration events with Φ-index equal to: (a.) 0.21 and 0.80 (mm·hr^{-1}), (b.) 1.46, 1.74, 1.87, 2.64 and 2.70 (mm·hr^{-1}), (c.) 5.83 and 6.29 (mm·hr^{-1}) and (d.) 9.89 (mm·hr^{-1}).

Event 3 with the highest Φ (= 9.89 mm·h^{-1}) produced a high *NS* when it is used to predict Event 3, but consistently lower *NS* for the other events where the calibrated Φ-index were significantly smaller. As shown in the figure, since the Φ-index for Events 7 and 8 are small, *NS* is highest for the events with small calibrated Φ-index and *NS* becomes lower for the events with large calibrated Φ-index.

For the *NS* to be a universal measure of goodness-of-fit, the curves in Figures 1(a) - 1(c) should be close to one another, meaning that the *NS* should be independent of event, so long as the calibrated Φ-index are similar. However, this is obviously not the case since even if the physical parameters of the catchment are known precisely, the disadvantage of the KWM is that it requires an accurate specification of the loss rate as the KWM accounts for direct runoff through the prescription of the effective rain. The ANN, on the other hand, does not have this shortcoming, as total rain is used as input. However, the use of total rainfall is not ideal from a physical viewpoint because it is the net rain that contributes to runoff.

Comparison of ANN and Kinematic Wave Models (Without measured discharge)

The *NS* values for the Type 1 to Type 3 ANNs, trained using six selected training events are shown in Figure 2. The figure also shows the *NS* values for the KWM. The Type 1 (5R) ANN, with a few exceptions, generally gives worse performance than the KWM, for all the training events. In fact, the KWM can out-perform the Type 1 (5R) ANN even when the ANN was used to predict the event that was used in training. This highlights the shortcoming of using only the total rainfall as input to the ANN.

A comparison of *NS* between the Type 1 (5R) ANN and the Type 2 (5R1Q$_K$) ANN [Figures 2(a) - 2(f)] shows that there are major improvements when q_k was added to the input. For example, as shown in Figure 2(c) where Event 5 was the training event, the *NS* for simulation Event 1 improved from 0.766 to 0.978. The *NS* for the Type 2 (5R1Q$_K$) ANN is also generally higher than those for the KWM. However, it can be argued that the Type 2 (5R1Q$_K$) ANN has the benefit of using two models.

The most direct comparison that can be made between the KWM and ANN models is by comparing the *NS* between the KWM and the Type 3 (1R1Q$_A$) ANN model (Figure 2). The comparison shows that the *NS* for the ANN are generally lower. Looping the output from the ANN into the input layer leads to an accumulation of errors as simulation progresses. The results obtained from the Type 3 (1R1Q$_A$) ANN are also unpredictable. Thus, the Type 3 (1R1Q$_A$) ANN is an unreliable method for runoff prediction and should be used with caution.

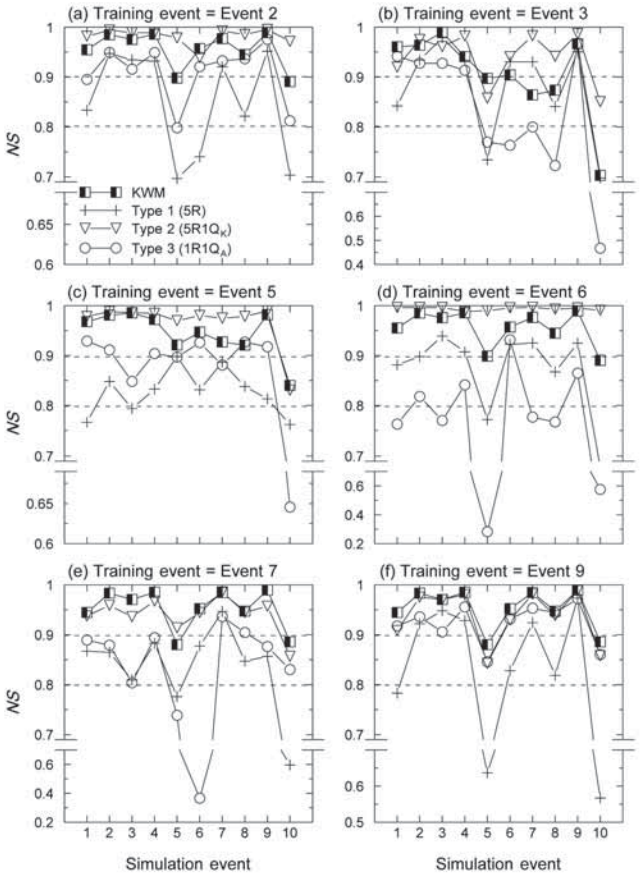

Figure 2. Comparison of NS values obtained from ANN (without discharge) trained on selected storm events with the KWM.

Comparison of ANN and Kinematic Wave Models (With measured discharge)

The *NS* values for the Type 4 to Type 6 ANNs for the six training events are shown in Figure 3. The figure also shows the *NS* values for the KWM. It is apparent that the *NS*, for the Type 4 (5R3Q) and the Type 5 (5R1Q) ANNs are similar, meaning that there is no advantage to include q beyond $q_{m,t-1}$ in the input. However, the *NS* for Type 6 (1R1Q) ANN are generally lower, suggesting that the ANN is more sensitive to the inclusion of antecedent rainfall than discharge in the input. The *NS* obtained by the KWM in Figures 3(a) - 3(f) are identical as the KWM predictions are based on the actual Φ-index.

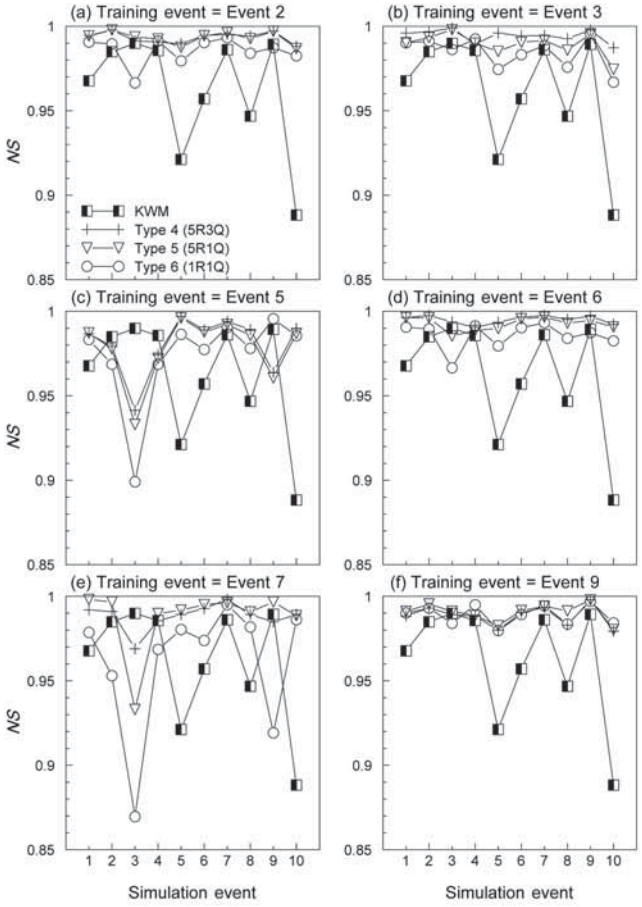

Figure 3. Comparison of NS values obtained from ANN (with discharge) trained on selected storm events with the KWM.

With the exception of simulations based on the Training Events 5 and 7 [Figures 3(c) and 3(e)], the *NS* values for the ANN models are generally very high (*NS* > 0.95). The low *NS* for Event 5 and Event 7 is very likely due to the lower peak flow as Event 5 and Event 7 have the lowest peak flows (for Event 7, rainfall intensity is also the lowest). Comparing the *NS* values between the ANNs and KWM, it is apparent that the *NS* values for the ANNs are generally higher than those for the KWM. However, the KWM did not have the benefit using measured discharge as a basis for predictions.

The inability for ANN to extrapolate is again highlighted in Figure 3(e), where Event 7 (which has a low measured peak discharge) was used in training. The *NS* values are significantly lower. Observations of the simulated hydrographs show that the peak discharges are consistently under-predicted, even though the *NS* for the ANN can be higher than that for the KWM. Conversely, it can be observed that the ANN does an excellent job when it is used to predict events that are within the range of the training dataset. This can be observed by the high *NS* values in Figures 3(a), 3(b), 3(d) and 3(f) where the training events had high peak discharge.

CONCLUSIONS

Based on the rainfall and runoff data on the asphalt plane for ten natural storm events at 0.25-min interval, the Type 1 (5R) ANN generally gives worse performance than the KWM. The KWM was found to out-perform the ANN even when the ANN was used to predict the event that was used in training. This highlights the shortcoming of using only the total rainfall as input to the ANN. A comparison between the Type 1 (5R) ANN and the Type 2 ($5R1Q_K$) ANN results shows that there are major improvements when a calculated discharge by the KWM was added to the input. The Type 2 ($5R1Q_K$) ANN also generally performed better than the KWM. However, this ANN has the benefit of using two models. Being the most direct comparison between KWM and ANN, a comparison between the KWM and the Type 3 ($1R1Q_A$) ANN shows that the ANN performed poorer. Looping the output from the ANN into the input layer led to accumulation of errors, and was found to be an unreliable method for runoff prediction.

For the Type 4 to Type 6 ANNs which included measured discharge as input, they generally out-performed the KWM. However, the predictions by the KWM were based on the calculated discharge and not the measured discharge. Further, the performance of Type 4 (5R3Q) and Type 5 (5R1Q) ANNs are similar, meaning that there is no advantage to include measured discharge beyond the previous time step in the input. The performance of Type 6 (1R1Q) ANN is generally poorer than that of Type 4 and Type 5 ANNs, suggesting that ANN is more sensitive to the inclusion of antecedent rainfall than discharge in the input.

Finally, ANN performance was poor when it was used to make predictions beyond the range of its training data. The KWM does not have this limitation, and the inability of the ANN to extrapolate is an obvious disadvantage of the ANN. On the other hand, when measured discharge is included in its input, the ANN can be expected to perform well when it is used within the range of its training data.

DEVELOPMENT OF ACTIVE OXYGEN PROCESSING SYSTEM FOR FREIGHT DECONTAMINATION (THE PART OF SMALL SET UP)

Tan Soon Keat (ctansk@ntu.edu.sg)
Dai Ying (daiying@ntu.edu.sg)
Nguyen Manh Tuan (NHUTNGUYEN@ntu.edu.sg)

INTRODUCTION

When meeting today's global challenges, it is imperative for market players to ensure speed, efficacy and competitiveness in their operations. The decontamination, eradication and maintenance of key facilities are important services and deliverables for the transportation, freight forwarding and shipping industry. To date, freight infestation by fungi, mold, mildew, and Invasive Alien Species (IAS) is common and remains an unresolved issue in the industry. The industry standards ISPM 15 requires freight and other solid wood packing material (SWPM), including furniture component, to undergo heat treatment which kills pests during treatment but does not provide a lasting effect after treatment. Prior to shipping, end-users often fumigate the container together with its contents using Methyl Bromide. However, Methyl Bromide is classified as a Class 1 ozone depleting substance, recognized as highly toxic, and is being phased out by most countries in response to international lobbying under the Montreal Protocol. The issue of re-infestation remains a problem even with heat treatment certification. Shock ozone (O_3) treatment has been used in certain industries to remove and retard fungi, mold and mildew growth in buildings. This shock O_3 treatment involves the production of high quantities of O_3 to reach a required O_3 concentration level to kill/retard fungi, mold and mildew growth. Past research and studies also reveal that disease bearing pests such as cockroaches, beetles, rats, insects etc. are adverse to an oxygen-rich environment and may stay away from O_3-treated areas. Therefore, with the strong oxidation and disinfection capability, ozone appears to be the alternatives that hold promise to revolutionize the decontamination process and industry practice.

EXPERIMENTS ON SMALL SET UP

Small set-up experiments are conducted for establishing optimum active oxygen concentration and dosing duration for treating small sample wooden pieces. The main steps are: firstly, small sample wooden pieces were treated with the following dosages (see Table 1). Secondly, put both 3 pieces of samples which were treated with each of the parameters above and 3 pieces of untreated samples with the same size (for comparison) into three different kinds of environment (near water, in a shelter, and in a dark and humid area) were tested and the performance of the O_3-treated samples were established in terms of time to see the first sign of algae/fungal/mildew growth, i.e. to test how long the samples can remain clean without any algae/fungal/mildew growth, so that we can see the effectiveness of ozone. Thirdly, observations were done every day during the first month. Records were kept and photographs were taken for the samples. Finally, the analysis and calculation were done for the next phase of experiment.

Table 1: Ozone Dosages

Determining optimum results
2000 mg/hr for 1 hr
1000 mg/hr for 2 hrs
500 mg/hr for 4 hrs
Determining optimum treatment duration
1000 mg/hr for 1 hr
1000 mg/hr for 2 hrs
1000 mg/hr for 5 hrs
Determining optimum concentration
2000 mg/hr for 2 hrs
1000 mg/hr for 2 hrs
500 mg/hr for 2 hrs

Figure 1. Experimental set-up for small set up

Dark & Humid | Near Water | In A Shelter

Figure 2. Samples in the Three Kinds of Environment

RESULTS AND CONCLUSIONS

The small set-up experiments lasted three months in all. Here we will only focus on the extreme condition --- dark and humid environment.

In summary, through three months of visual inspection, we noted that:

Firstly, ozone is effective on retarding mildew growth on wood. It is very obvious that the untreated samples have mildew growing much earlier and spreading faster than the treated samples.

In the dark and humid environment, the untreated samples could last 19 days without infection of algae/fungal/mildew; meanwhile, the samples treated with parameter 500 mg/hr for 4 hrs remained clean for 38 days; for the samples treated with other parameters, their results have no big difference --- they could last at least 80 days without infection of algae/fungal/mildew. After 80 days of treatment, if time is long enough, mildew will develop in all samples gradually, one after another, but the order is stochastic / random.

Secondly, based on the observation result, since almost all of the treated samples do not have any mildew within 80 days, no matter with which parameter above they were treated, we could anticipate that there is no optimum O_3 concentration and dosing duration. It will be that the higher the ozone spraying intensity and the longer the treatment duration, the better is the treatment result, i.e. the longer the samples can remain clean without infection of algae/ fungal/mildew.

Thirdly, the first sign of the mildew growth is affected by many factors. Not only the treatment parameters, but the samples' own condition, e.g. its own humidity, and the original bacteria situation, etc. can also affect the result.

REFERENCES

[1] US Department of Agriculture, Animal and Plant Health Inspection Service, 1991. An efficacy review of control measures for potential pests of imported Soviet timber. Misc. Pub. 1496, September 1991, Riverdale, MD.

[2] US Department of Agriculture, Animal and Plant Health Inspection Service, and US Department of Agriculture, Forest Service, 2000. Pest risk assessment for importation of solid wood packing materials into the United States. Draft assessment-August 2000, Riverdale, MD.

[3] Plant Protection and Quarantine, Animal and Plant Health Inspection Service, US Department of Agriculture. (October 2002). *Importation of solid wood packing material, Draft Environmental Impact Statement.* Retrieved 5 January, 2008, from http://www.aphis.usda.gov/ppd/es/pdf%20files/swpmdeis.pdf

[4] Secretariat of the International Plant Protection Convention, Food and Agriculture Organization of the United Nations. (March 2002). *International Standards for Phytosanitary Measures, Guidelines for Regulating Wood Packaging material in International Trade. Publication No. 15.* Retrieved 5 January, 2008, from http://www.tis-gdv.de/tis_e/verpack/holz/export/ispm15.pdf

EXPERIMENTAL STUDY ON 3-DIMENSIONAL SCOUR AT SUBMARINE PIPELINES

Wu Yushi (wuyu0006@ntu.edu.sg)
Chiew Yee Meng (CYMCHIEW@ntu.edu.sg)

INTRODUCTION

As the offshore oil industry develops rapidly, thousands of kilometres of pipelines are laid annually on the sea bed in offshore regions. The presence of the pipelines changes the local flow field, often resulting in the formation of scour holes on the erodible bed. An increasing attention is drawn to this topic because scouring may bring about failure of the pipeline if its free span becomes large enough to cause flow-induced vibration under certain conditions.

Although the scour hole is actually 3-dimensional in the offshore environment, most of the published laboratory studies and numerical modelling of scour were done with a 2-dimensional model[1]. This is because of the difficulty associated with experimental study and high demand on computational capacity related to numerical simulations. To better understand the development of a scour hole at submarine pipelines in the offshore environment, this study aims to examine the 3-dimensional characteristics of pipeline scour experimentally.

The development of a 3-dimensional scour may include the following behaviours:
(1) lateral propagation of scour hole;
(2) free span behaviour;
(3) sinking at the span shoulders; and
(4) deposition or self-burial of the pipeline.

The objective of this article focuses on studying the first process, i.e., lateral propagation of the scour hole, which is governed by the scour hole dimensions at different time stages and the propagation velocity, $V_L = \frac{dL}{dt}$, in which L is the length of the scour hole as shown in Figure 1 and t is time.

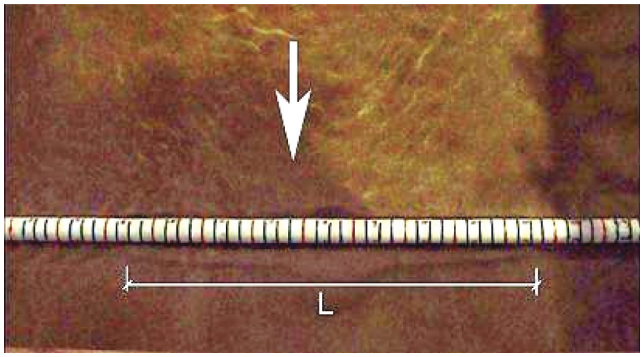

Figure 1. Top view of a propagating scour hole

EXPERIMENT SET-UP

The experiments were conducted in a glass-sided flume that is 20.0 m long, 1.6 m wide and 0.6 m deep, as shown in Figure 2. Seven pieces of Perspex plates with the same sand as the test material glued on their top were fixed to the bottom of the flume as the false floors. Five of them (total length = 6 m) were located upstream of, and two (total length = 2.4 m) located downstream of the test section. The total length of the test section was 1.8 m. Additionally, two sets of dowel pegs with a height of 100 mm were installed at the location 4 m downstream from the flume inlet. The purpose of the dowel pegs was to assist in the formation of a fully developed boundary layer. The test material of the study was uniform sand with median grain size = 0.56 mm and the slope of the flume was set at 1:1000. Four model pipelines with diameters = 26 mm, 35 mm, 49 mm and 116 mm were used in the study. The pipeline was placed on top of the sand bed in the test section with its ends fixed to the flume walls. It was either partially buried or placed above the sand bed. The water depth and flow velocity can be controlled by adjusting the tail gate and discharge rate.

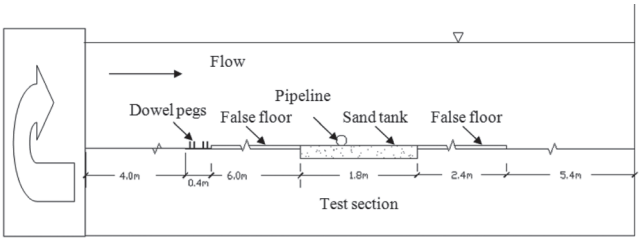

Figure 2. Experiment set-up

RESULTS AND DISCUSSION

Three series of experiments viz. Series A, B and C, which are defined in Table 1, were conducted to examine how flow velocity, water depth, pipeline diameter and pipeline embedment ratio affect the propagation velocity of the scour hole. A dimensional analysis had been carried out and four parameters identified for further investigation in this study. They are: (1) flow Froude number $F = \frac{V}{\sqrt{gy}}$ (V = mean flow velocity, g = acceleration due to gravity and y = normal flow depth); (2) the undisturbed applied Shield's parameter $\theta = \frac{U_*^2}{g(s\text{-}1)d_{50}}$ (U_* = friction velocity, s = specific gravity of

sediment grains and d_{50} = median grain size); (3) embedment ratio e/D (e = embedment depth and D = diameter of pipeline model), which had been proven to be important in determining the propagation velocity[2]; and (4) water depth to pipeline diameter ratio y/D, which reflects the blockage effect.

Only part of Experiment Series A had been completed at the time of preparing this article. Figure 3 shows the temporal development of the free span length with different pipeline embedment ratio, e/D. In all these experiments, the same water depth of 200 mm, mean flow velocity of 0.24 m/s and pipe diameter of 49 mm were used. The gradient of each curve represents the propagation velocity of the free span length at the corresponding time of scour.

Table 1. Experiment plan

Test number	D (mm)	V (m/s)	y (mm)	e/D	y/D	F	θ
Experiments Series A							
D2e1a	49	0.240	200	0.1	4.08	4.082	0.171
D2e0	49	0.240	200	0	4.08	4.082	0.171
D2e1	49	0.240	200	-0.1	4.08	4.082	0.171
D2e2	49	0.240	200	-0.2	4.08	4.082	0.171
D2e3	49	0.240	200	-0.3	4.08	4.082	0.171
Experiments Series B							
D4	116	0.240	200	-0.1	1.72	0.171	0.018
D3	49	0.240	200	-0.1	4.08	0.171	0.018
D2	35	0.240	200	-0.1	5.71	0.171	0.018
D1	26	0.240	200	-0.1	7.69	0.171	0.018
Experiments Series C							
D2F1S1	49	0.260	200	-0.1	4.08	0.186	0.021
D2F2S2	49	0.240	200	-0.1	4.08	0.171	0.018
D2F3S3	49	0.217	200	-0.1	4.08	0.155	0.014
D2F4S4	49	0.195	200	-0.1	4.08	0.139	0.012
D2F5S5	49	0.174	200	-0.1	4.08	0.124	0.009
D1F1S01	26	0.189	106	-0.1	4.08	0.186	0.013
D1F2S01	26	0.175	106	-0.1	4.08	0.171	0.011
D1F3S01	26	0.158	106	-0.1	4.08	0.155	0.009
D1F4S01	26	0.142	106	-0.1	4.08	0.139	0.007
D1F5S01	26	0.126	106	-0.1	4.08	0.124	0.006
D1F01S1	26	0.238	106	-0.1	4.08	0.234	0.021
D1F01S2	26	0.220	106	-0.1	4.08	0.216	0.018
D1F01S3	26	0.199	106	-0.1	4.08	0.195	0.014
D1F01S4	26	0.179	106	-0.1	4.08	0.176	0.012
D1F01S5	26	0.159	106	-0.1	4.08	0.156	0.009
D1F1S02	35	0.220	143	-0.1	4.08	0.186	0.016
D1F2S02	35	0.203	143	-0.1	4.08	0.171	0.014
D1F3S02	35	0.183	143	-0.1	4.08	0.155	0.011
D1F4S02	35	0.165	143	-0.1	4.08	0.139	0.009
D1F5S02	35	0.147	143	-0.1	4.08	0.124	0.007
D1F02S1	35	0.238	143	-0.1	4.08	0.201	0.021
D1F02S2	35	0.220	143	-0.1	4.08	0.186	0.018
D1F02S3	35	0.199	143	-0.1	4.08	0.168	0.014
D1F02S4	35	0.179	143	-0.1	4.08	0.151	0.012
D1F02S5	35	0.159	143	-0.1	4.08	0.134	0.009

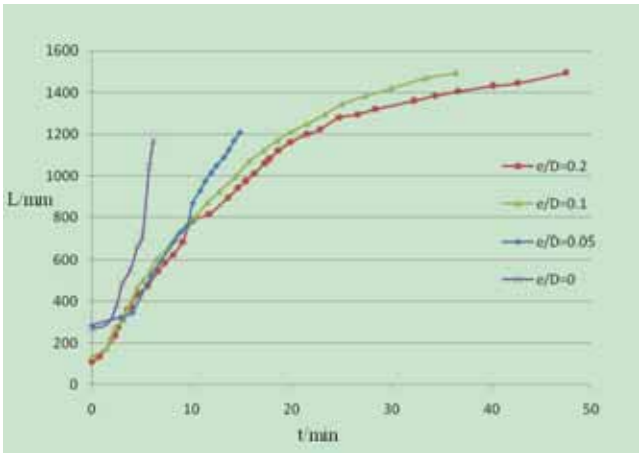

Figure 3. Scour hole propagation with different pipeline embedment ratio

The curve corresponding to the embedment ratio = 0.2 shows the typical development of scour hole length. The first five minutes were the adjustment stage, in which the flow velocity and water depth are adjusted to the expected value gradually in order not to cause disturbance to the test section. In the next stage of development, the free span develops linearly with time, from which the propagation velocity can be easily calculated from the gradient. Finally when a certain point is reached, the propagation velocity starts to decrease with time. The reason is probably due to the variation of flow velocity profile caused by wall effect. Table 2 shows the propagation velocity calculated using the data of the linear developing stage of free span. The result clearly shows that the propagation velocity reduces exponentially with decreasing embedment ratios. It may also be surmised from the data as shown in Figure 4 that a critical embedment ratio existed under which the scour hole does not propagate at all. Further experiments, however, are needed to determine this value, which is likely not only related to the embedment ratio, but also the flow conditions and sediment properties.

Table 2. Free span propagation velocity with different pipe embedment ratio

embedment ratio e/D	$V_L = \frac{dL}{dt}$ (cm/min)
0	28.85
-0.05	7.00
-0.1	5.29
-0.2	4.84

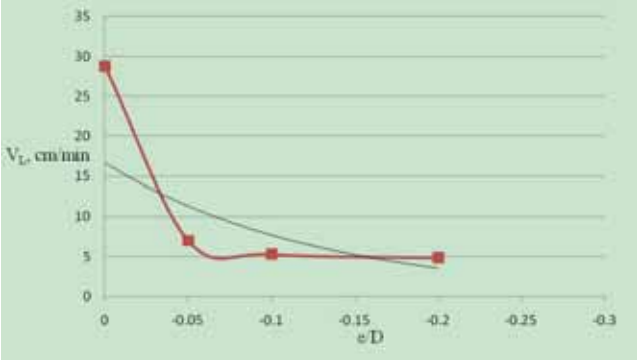

Figure 4. Free span propagation velocity with different pipe embedment ratio

Another objective of the study is to obtain a description of the temporal development of the 3-dimensional scour hole, which means that the dimensions of the scour hole at different time stages must be measured. To this end, the flow needs to be stopped when the scour hole has developed to a certain stage, and water drained slowly under surveillance to ensure that the actual dimensions of the scour hole are not disturbed. Figure 5 shows the bathymetric contour of the scour hole 3.3 minutes after the commencement of the test. In this test, the diameter of the pipeline = 116 mm, the water depth = 200 mm and the mean flow velocity = 0.24 m/s are adopted. The bed elevation was measured with a point gauge. Information of the 3-dimensional scour hole development is crucial to the understanding of the scour mechanism at the span shoulder.

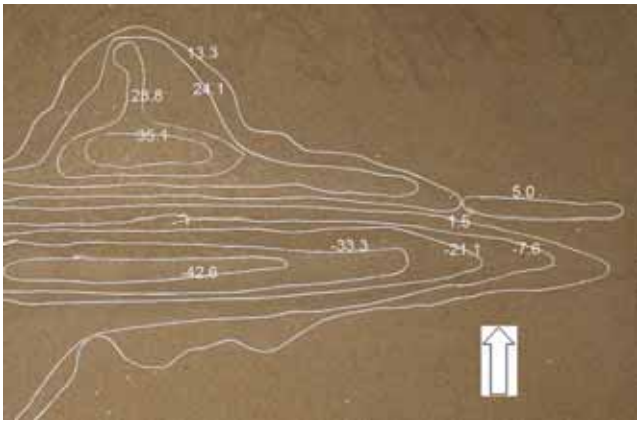

Figure 5. Contour of a 3.3 min scour hole

CONCLUDING REMARKS

Preliminary results from this study confirm that all the four parameters deduced from dimensional analysis exert important influences on the development of scour hole and free span. Free span propagation velocity increases with an increasing pipeline embedment ratio and decreasing water depth to pipeline diameter ratio. Further efforts will be made to examine the mechanism associated with this observation.

REFERENCES

[1] Sumer, M., B., Fredsøe, J., 2002. The Mechanics of Scour in the Marine Environment. *World Scientific, Singapore, xiv,* 24 p

[2] Hansen, E.A., et al., 1991. Time-development of scour induced free spans of pipelines. *OMAE 1991,* Vol. 5, pp. 25-31.

LINEAR ANALYSIS OF AIR-GAP FOR SEMI-SUBMERSIBLES

Li Jing (jingli@ntu.edu.sg)
Huang Zhenhua (ZHHuang@ntu.edu.sg)
Adi Kurniawan (kurniawan@ntu.edu.sg)
Liu Chunrong (LIUCR@ntu.edu.sg)
Wang Xikun (CXKWang@ntu.edu.sg)
Hao Zhiyong (HaoZhiyong@ntu.edu.sg)
Tan Soon Keat (CTANSK@ntu.edu.sg)

INTRODUCTION

One of the key factors in the design of ocean platform is the wave run-up and associated air gap that may occur under the deck. Since the deck height is limited by weight and stability considerations, the air-gap demand is a substantial cost driver for the platform. The purpose of this study is to investigate the linear air-gap behavior of a semi submersible under specified wave environments.

METHOD FOR AIR GAP ANALYSIS

A schematic view of a typical semi-submersible is shown in Figure 1, where the responses of the semi-submersible to waves are also depicted. In the presence of waves, the instantaneous air gap at any position along the structure will be:

$$a(t) = a_0(t) - [\eta(t) - \xi_{netz}(t)] \quad \ldots (1)$$

where $a_0(t)$ is the air gap in the absence of waves, $\eta(t)$ the wave surface elevation at a particular location, and $\xi_{netz}(t)$ the corresponding vertical motion of the platform. Large impact force on deck will occur if the air gap $a(t)<0$.

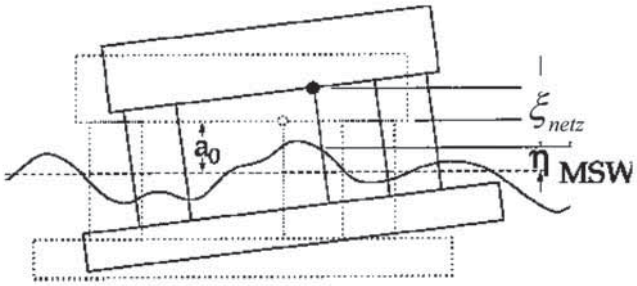

Figure 1. Air gap variable definitions

The time series of surface displacement $\eta_i(t)$ can be simulated by equation (2) for a specified target sea-state (power spectrum), where we have taken the time series of the incident random waves as a Gaussian process,

$$\eta_i(t) = \sum_{k=1}^{N} A_k \cos(\omega_k t + \theta_k) = \mathrm{Re} \sum_{k=1}^{N} |A_k| e^{i(\omega_k t + \theta_k)} \quad \ldots (2)$$

In equation (2), $|A_k| = \sqrt{2S(\omega_k)\Delta\omega}$ is the amplitude of the wave component with the frequency ω_k. From the RAOs ($\overline{\xi_k}$) of the platform and the surface elevation values ($\overline{\eta_k}$) computed by WAMIT (WAMIT, 2006) in frequency domain, the body motion and local wave elevation in time domain can be simulated by,

$$\xi(t) = \sum_{k=1}^{N} |A_k| \overline{\xi_k} \cos(\omega_k t + \phi_k + \theta_k)$$

$$\eta(t) = \sum_{k=1}^{N} |A_k| \overline{\eta_k} \cos(\omega_k t + \varphi_k + \theta_k) \quad \ldots (3)$$

For a linear analysis, the net displacement ($\xi_{net}(t)$) of the platform at any location of interest can be calculated by

$$\xi_{netz} = \xi_3 + \xi_4 y - \xi_5 x \quad \ldots (4)$$

In view of equation (3), and equation (4), the time series of the air-gap $a(t)$ can be calculated by equation (1), and the values of the minimum air gap can be obtained by a wave-by-wave analysis. After ranking the minimum air gaps in order, we can calculate cumulative probability P_c.

Pearson type III distribution (IMSL, 1987) is adopted here to perform the extreme distribution of air gap. Let x be any air-gap, its probability density function is expressed as

$$f(x) = \frac{\beta^{\alpha}}{\Gamma(\alpha)} (x-\gamma)^{\alpha-1} e^{-\beta(x-\gamma)} \quad \ldots (5)$$

where α, β, γ are related to the expectation $\overline{x}$, the variance coefficient Cv and the skewness coefficient Cs

$$\alpha = \frac{4}{C_s^2}, \beta = \frac{2}{\overline{x} C_v C_s}, \gamma = \overline{x}\left(1 - \frac{2C_v}{C_s}\right) \quad \ldots (6)$$

It then follows that Pearson type III distribution of extreme air gap values is

$$P(x_{\min} < x < x_{\max}) = \int_{x_{\min}}^{x_{\max}} f(x)dx, \quad \ldots (7)$$

where the extreme air gap demands at any given location can be predicted by the derived distribution in terms of the expected fractal.

RESULTS AND DISCUSSIONS

Here we report a case study to illustrate the linear air-gap analysis outlined in the previous section. The semi-submersible with large diameter columns and pontoons has significant diffraction-radiation effects on both the air-gap under the deck and the wave run-up columns. We have identified six locations at the sides of columns where large wave run-ups and small air-gaps are likely to occur (see Figure 2). At these locations, WAMIT diffraction analysis was performed for different wave headings. As an example, we examined a JONSWAP spectrum with the significant wave height H_s = 5.1m, the peak period T_p = 9.7s and the peak factor γ = 1.4. The computation was performed for three wave headings (head seas, quartering seas, and Beam seas). Figure 3 lists the extreme air-gap distribution at the chosen 6 given locations for head seas. The probability of the simulated air–gap agrees quite well with Pearson type III distribution. As is shown in Figure 3, the air-gap at the point 1 is the smallest while the air-gap at the point 6 is the largest in general. Moreover, the duration of wave record and the random phase used in simulating the random waves also have significant effects on air gap analysis. Figure 4 and Figure 5 show the significant air-gaps (a_s) and the minimum air-gaps (a_{min}) at different locations for 4 durations of wave record and 6 series of random phase, respectively. It can be observed that the significant air-gap is affected significantly by the duration of wave record and the random phase used. However, the minimum air-gap is strongly affected by the duration of wave record and the random phase; the minimum air gap has more chance to achieve the large value with increasing duration.

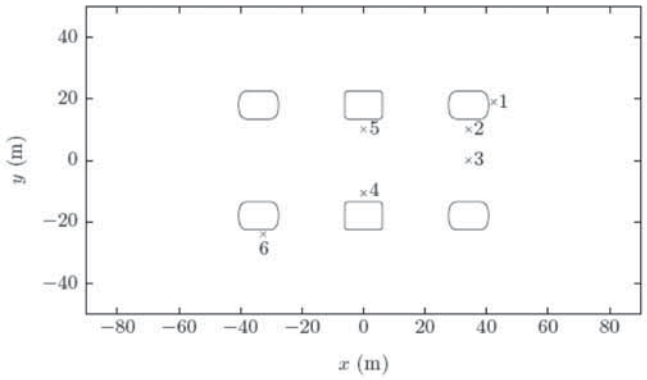

Figure 2. Plan view of locations of possible extreme air gap

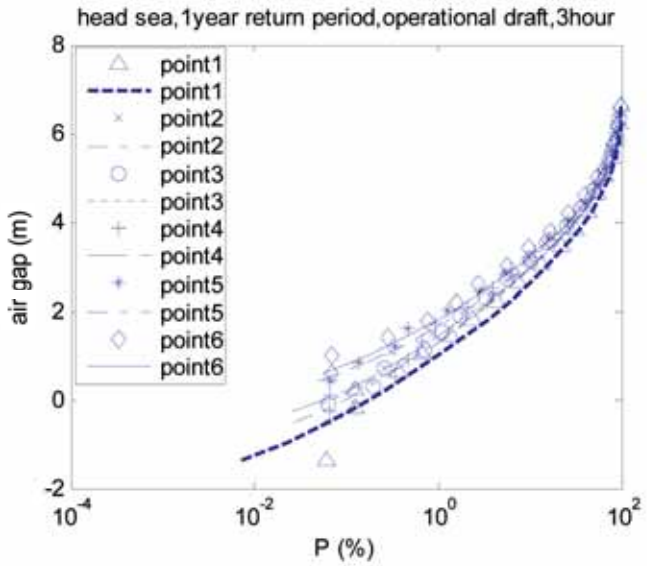

Figure 3. Extreme distribution of air gap in head sea with record of 3 hours

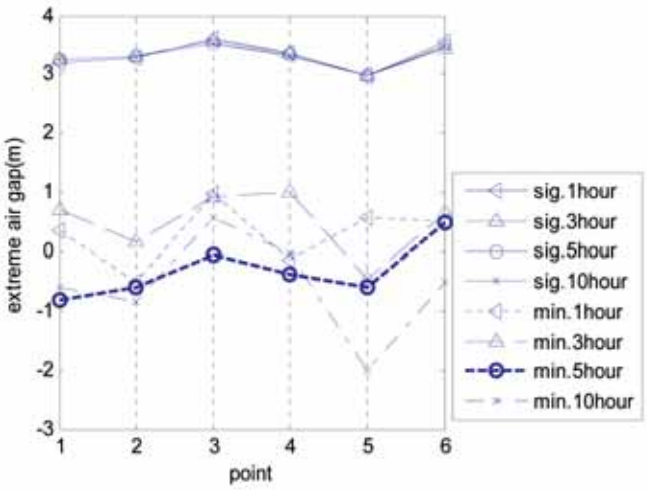

Figure 4. Comparison of a_s and a_{min} for various durations of wave record at different locations for quartering seas

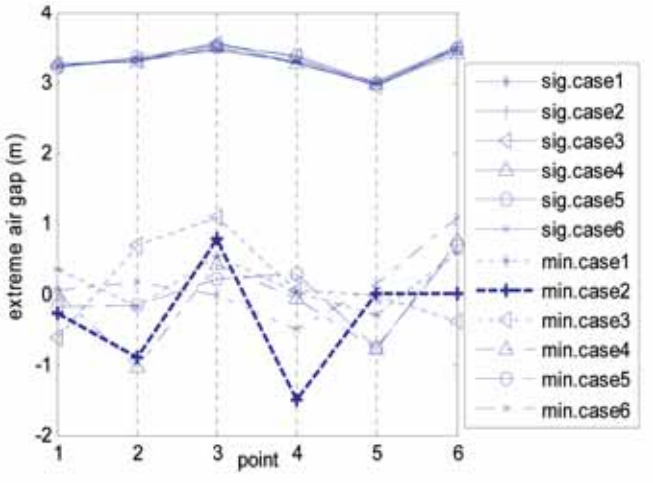

Figure 5. Comparison of a_s and a_{min} for various random phases at different locations for quartering seas

CONCLUSIONS

In this study, we present a method of analyzing the linear air-gap for semi submersibles. With proposed method, extreme distributions of air-gap at chosen locations are discussed for a JONSWAP spectrum. It is shown that the duration of the wave record and the random phase used in simulating the random waves can significantly affect the predicted minimum air-gap, but have fewer effects on the predicted significant air-gap. The method discussed here can be easily expanded to nonlinear air-gap analysis.

REFERENCES

[1] Chakrabarti, Subrata K., 1987. "Hydrodynamics of Offshore Structures". Springer-Verlag.

[2] Hasselmann, K., Barnett, T.P. and Bouws, E., et al., 1973. "Measurements of wind wave growth and swell decay during the Joint North Sea Wave Project (JONSWAP)". *Erganzungsheft Zeit Deut Hydr Zeit,* 12:95.

[3] IMSL (International Mathematical and Statistical Libraries), 1987. STAT/LIBRARY User's Manual, Version 1.

[4] Sweetman, B. and Winterstein, S.R., 2003. "Non-Gaussian air gap response models for floating structures". *ASCE Journal of Engineering Mechanics,* Vol. 129, No. 3, pp. 302-309.

[5] WAMIT User Manual, 2006. WAMIT, Inc. (available from the website www.wamit.com).

MODIFICATION AND DESIGN OF GREASE TRAP TO MEET OIL & GREASE DISCHARGE LIMIT

Victor Chang Wei Chung (wcchang@ntu.edu.sg)
Tang Chu Yang (CYTang@ntu.edu.sg)
Dai Ying (daiying@ntu.edu.sg)
Nguyen Manh Tuan (NHUTNGUYEN@ntu.edu.sg)

INTRODUCTION

Grease traps are required for food and beverage establishments to capture the grease present in culinary wastewater prior to discharge into the public sewer. A conventional design developed decades ago is provided in PUB's Code of Practice for current industry practices. In conjunction with Singapore's efforts to improve water quality and reduce the loading to wastewater treatment facilities, this study aims to review and study possible modification of the current design as well as to explore creative design for higher grease removal efficiency.

EXPERIMENTS

Grease trap monitoring is conducted to know the current efficiency of current grease traps. Grease trap design via relevant physical modifications to existing designs is conducted to improve the efficiency.

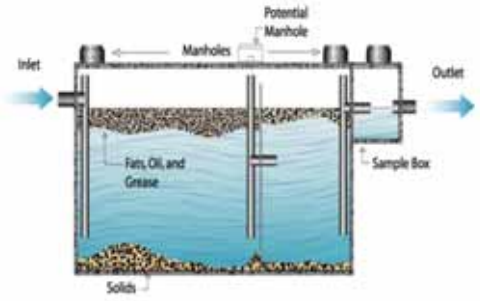

Conventional Grease Trap

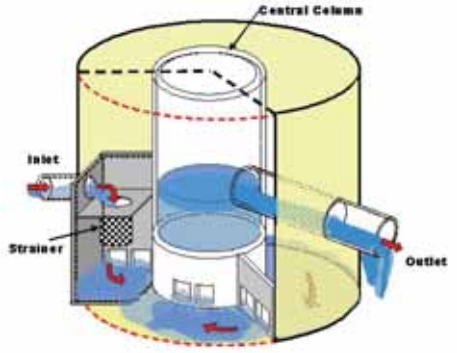

Schematics of current grease trap design in Singapore

GREASE TRAP MONITORING

Procedures

(a) Sampling

According to the vacuuming plan, the last vacuuming for (1) fast food, (2) food court was on 9 September 2008 and the next vacuuming was scheduled on 23 September 2008; meanwhile, the last vacuuming for (3) café was on 14 August 2008 and the next vacuuming was scheduled on 18 September 2008.

Figure 1. Outside view of grease trap

Figure 2. Screen bar

Figure 3. First chamber

Figure 4. Centre chamber

Eight samples were taken at 12:00 on 17 September 2008. Grease trap no.1 refers to the fast food canteen (1st floor); Grease trap no.2 refers to the food court canteen which is on the 2nd floor; and grease trap no.3 refers to the café. The food court canteen is the busiest canteen.

Table 1. Vacuuming plan

Items	Grease trap No.1	Grease trap No.2	Grease trap No.3
Vacuuming frequency	2 times/month	2 times/month	1 time/month
Last vacuuming day	09-Sep-08	16-Sep-08	14-Aug-08
Measurement day	17-Sep-08	17-Sep-08	17-Sep-08
Next vacuuming day	23-Sep-08	23-Sep-08	18-Sep-08

The sampling locations include (1) before the screen bars; (2) at the inlet of each grease trap; and (3) at the grease trap outlet. Three sample points of each grease trap were taken as shown in the below diagram. The first point is taken for measuring the influent quantity and quality of waste water. The second and third points are used for evaluating the efficiency or effectiveness of grease trap.

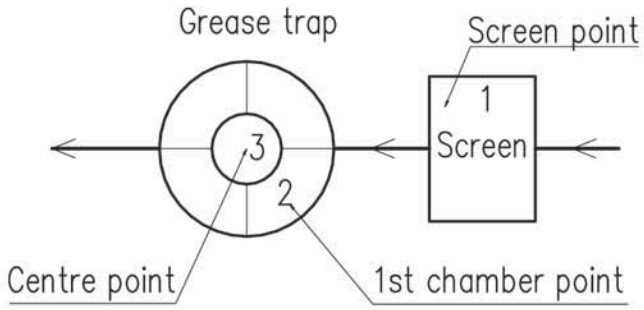

Figure 5. Sample points

Figure 6. Grease layer in the trap

Figure 7. Fine screen in first chamber

(b) Sample Test

The sample tests include FOG content, TSS (total suspended solid), VSS (volatile suspended solid), and TOC (total organic carbon). In addition, pH, temperature, and flow rate are measured on site.

Result data

- *Onsite measured parameters*

  pH value, temperature (^{0}C), flow rate (L/s), grease thickness (cm).

Table 2. Onsite data

Items		Grease trap No.1	Grease trap No.2	Grease trap No.3
Vacuuming frequency		2 times/month	2 times/month	1 time/month
Last vacuuming day		09-Sep-08	16-Sep-08	14-Aug-08
Measurement day		17-Sep-08	17-Sep-08	17-Sep-08
Screen point	pH	6.33	5.52	-
	T (^{0}C)	30.7	30.5	-
1st Chamber point	pH	5.42	5.16	5.19
	T (^{0}C)	30.2	30.6	30.5
Centre point	pH	5.49	5.66	5.18
	T (^{0}C)	30.6	30.2	30.5
Flow rate, L/s		2.4L/8s=0.3L/s	6.5L/10s=0.65L/s	Very small
Thickness, cm		2~3	0.5~1	4~5

- *TOC parameters*

Table 3. TOC data

Items		Grease trap No.1	Grease trap No.2	Grease trap No.3
Screen point	TOC (mg/L)	148.1	480.2	-
1st Chamber point	TOC (mg/L)	194	338.7	254.6
Centre point	TOC (mg/L)	261.4	370.1	531

- *TSS parameters*

Table 4. TSS data

Items		Grease trap No.1	Grease trap No.2	Grease trap No.3
Screen point	TSS (mg/L)	370.67	440.00	-
1st Chamber point	TSS (mg/L)	318.00	1362.00	2074.77
Centre point	TSS (mg/L)	306.00	440	226

- *VSS parameters*

Table 5. VSS data

Items		Grease trap No.1	Grease trap No.2	Grease trap No.3
Screen point	VSS (mg/L)	286.67	394.00	-
1st Chamber point	VSS (mg/L)	280.00	1296.00	1925.23
Centre point	VSS (mg/L)	260.00	338.95	150

- *FOG parameters*

Table 6. FOG content data

Items		Grease trap No.1	Grease trap No.2	Grease trap No.3
Screen point	FOG (mg/L)	88.50	32.50	-
1st Chamber point	FOG (mg/L)	78.80	35.00	14.50
Centre point	FOG (mg/L)	12.10	8.70	4.5

Analysis and Conclusions

(a) Water quality standards for Trade Effluent discharge into public sewer

The physical and chemical characteristics of the trade effluent to be discharged into the public sewer shall not exceed the following limits:

- The temperature of the trade effluent shall not exceed 45° Celsius at the point of its entry into any public sewer.
- The pH value of the trade effluent shall not be less than 6 nor more than 9 at the point of its entry into any public sewer.
- The caustic alkalinity of the trade effluent shall not be more than 2,000 milligrams of calcium carbonate per liter at the point of its entry into any public sewer.
- Maximum concentrations of certain substances in trade effluent:

Table 7. Limit data

S/No	List of Substances	Limit in milligrams per litre of trade effluent
1	Total Suspended Solids	400
2	Grease and Oil (Hydrocarbon)	60
3	Grease and Oil (Non-hydrocarbon)	100

(b) Analysis

Comparing the measured parameters with Water quality standards for Trade Effluent discharge into public sewer, we find that:

(i) pH discharges are slightly lower than that of pH standard range which is from 6 to 9. The pH discharges are 5.49, 5.66, and 5.18, respectively.

(ii) The temperature of the trade effluent meets the requirement which is less than 45^{0}C.

(iii) TSSs of grease trap no.1 and no.3 are 306.00 mg/L, and 226 mg/L; therefore they can meet the requirement. Meanwhile, TSS of grease trap no.2 (440mg/L) is slightly higher than that of requirement (400 mg/L).

(iv) FOGs of three grease traps which are 12.10, 8.70, and 4.5 are lower than that of effluent discharge standards.

From the result datas, we can find the effectiveness of the three grease traps in term of TOC, TSS, and FOG removals as shown in following table.

Table 8. Analysis and calculation

Items		Grease trap No.1		Grease trap No.2		Grease trap No.3	
		Effectiveness		Effectiveness		Effectiveness	
TOC, mg/L	1st Chamber point	194	-	338	-	254	-
	Centre point	261.4		370		531	
TSS, mg/L	1st Chamber point	318	3.4%	1362	67.7%	2074.8	89.1%
	Centre point	306		440		226	
FOG, mg/L	1st Chamber point	78.80	84.6%	35.00	75.1%	14.40	68.8%
	Centre point	12.10		8.70		4.5	

From the above table, some comments can be obtained:

(i) The FOG removal effectiveness of the three grease traps are quite high. Therefore, most of the grease is trapped in the grease trap before discharging to the sewer.

(ii) The TSS removal effectiveness of grease trap no.2 and no.3 is evident. In contrast, the efficiency of grease trap no.1 is very low.

(iii) In terms of TOC removal, the efficiency is poor. This is due to the accumulation of TOC in the centre point.

REFERENCES

[1] APHA, 1992. Standard methods for the examination of water and wastewater. *American Public Health Association, American Water Works Association (AWWA) and Water Environment Association (WEA), Washington D.C.: 18th Edition.*

[2] Ecotec Grease Extractor of Berry Café North Sydney, 1996. Grease-Traps Studies on Total Suspended Solids and Oil & Grease in Sydney, Australia.

[3] Eddy, N., 1998. Restaurants and commercial facilities present specific problems for onsite systems. *Small Flow J.,* Vol. 12, No. 2, pp. 1-5.

[4] Stoll, U. and Gupta, H., 1993. Management strategies for oil and grease residues. *Waste Management Res.,* Vol. 15, No. 1, pp. 23-32.

[5] Interagency Resource for Achieving Cooperation (IRAC), September 2004. *A Guide to Restaurant Grease Management (A Regulator's Desk Reference).* Retrieved 20 June, 2008, from http://www.govlink.org/hazwaste/publications/irac_grease.pdf

HYBRID COAGULATION-NANOFILTRATION: EFFECTS OF HUMIC ACID, CALCIUM, ALUM COAGULANT AND THEIR COMBINATIONS ON THE SPECIFIC CAKE RESISTANCE

Karina Listiarini (ka0001ni@ntu.edu.sg)
Darren Delai Sun (ddsun@ntu.edu.sg)
James O Leckie (leckie@stanford.edu)

INTRODUCTION

Nanofiltration (NF) has been gaining attention as the polishing step in water treatment technology since 20 years ago. One of the major drawbacks in this technology is organic fouling, which causes a decline in permeate flux quality and quantity[1]. In addition, divalent cations such as calcium (Ca^{2+}), which are naturally present in raw water, are responsible for neutralizing the negatively-charged organic matter and capable of forming bridges between membrane surface and organic matter, resulting in more severe flux decline[2-4]. In drinking water treatment train, organic matter is commonly removed via coagulation/flocculation process using coagulating agents such as aluminum. By combining coagulation and filtration ("Hybrid Coagulation-Filtration"), a smaller footprint can be achieved. We have found that the use of hybrid coagulation-nanofiltration in a dead-end setup to remove organic foulant may alleviate flux decline, decrease cake resistance, and improve permeate quality[5].

The objectives of this study are to systematically investigate the flux decline trends in systems containing humic

acid, calcium ions, aluminum-based coagulant and their combinations, and subsequently evaluate the specific cake resistance and fouling mechanism of these systems based on the findings. These results could give insights to the possibilities of employing hybrid coagulation-nanofiltration technology in drinking water treatment.

MATERIALS AND METHODS

Fouling experiments were conducted in a bench-scale dead-end nanofiltration system which comprised of a reservoir tank connected to a stainless steel stirred cell and housed a 47 mm diameter membrane sample. Pressure was provided by a compressed nitrogen gas tank which was applied to the reservoir tank. Permeate flux was collected and the mass was monitored continuously over time using a weighing scale connected to a data logger. NF 270 membrane coupons were soaked in DI water at least for 24 hours prior to fouling experiments. Before each test, membrane coupon inside the cell was compacted with DI water for at least 2 hours, followed by conditioning with background electrolyte (10 mM NaCl at pH 7) for at least 3 hours. Fouling experiments were conducted for 16 hours or stopped when it had filtered 450 ± 100 mL of feed solution. Accumulated humic materials on the membrane surface were extracted and analyzed at the end of each fouling experiment. Characterization of membrane and foulant was conducted through zeta potential analysis, atomic force microscopy (AFM), particle size analysis and jar test. Humic acid accumulation on membrane surface was measured, and corresponding resistance analyses were performed.

RESULTS AND DISCUSSION

As shown in Figure 1, the least flux decline occurs in system containing PAHA, calcium, alum. The severity increases in the following order: (PAHA, calcium, alum) < (PAHA, alum) < PAHA < (PAHA, calcium), which implies that the addition of alum coagulant will alleviate flux decline despite the presence of calcium.

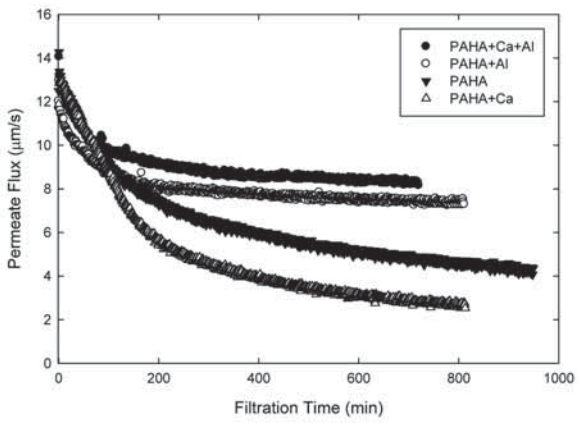

Figure 1. Permeate flux as a function of time of the investigated systems. Concentrations of humic acid, calcium and alum are 30mg/l, 1 mM and 30mg/l respectively. Other test conditions: 25°C, ionic strength 10mM NaCl, and pH 7.

Specific cake resistance was calculated based on two methods: experimental (MFI) and empirical, and both results were compared in order to observe whether there existed a significant difference between the two methods as shown in Table 1. The experimental specific cake resistance values of the three combined systems (PAHA, calcium, alum; PAHA and alum; PAHA and calcium) are relatively close to the empirical ones. As for the system containing only PAHA, the empirical value is more than 30 times larger than the experimental. By visual observation, the addition of alum and/or calcium improves the attachment of PAHA on the membrane surface. This attachment efficiency has a direct impact on the empirical value of the specific cake resistance since it is calculated by dividing the cake resistance with the accumulated mass normalized by the membrane surface area. On the other hand, the experimental specific cake resistance, α, is calculated from the fouling index, I, and the bulk concentration of foulants, C_b, which implies that all the mass added into the feed as the bulk concentration will attach on the membrane surface. This suggests that a correction factor in the MFI equation that accounts for foulant attachment should be considered.

Zeta potential measurements of the investigated systems were conducted to further understand this behavior. Figure 2 shows the zeta (ζ) potential values of the four investigated systems. As seen in this figure, the addition of calcium or alum to solutions containing humic acid will result in more positive ζ potential values and increase the attachment of foulant. The addition of only alum will increase the attachment of foulant to the membrane surface similar to that of only calcium despite the more negative charge. This indicates that in addition to charge screening and complex formation as occurred when calcium is present, there exists other mechanism that promotes the attachment when alum is present, possibly sweep flocculation. Since the addition of alum lowers the cake resistance whether calcium is present or not, this shows that the cake formed when alum is present is less compact compared to that when only calcium is present. Similar findings were reported by [2,6]. They found that the cake formed when calcium was present seemed to be denser and thicker and resulted in severe fouling, whereas coagulated foulant in dead-end filtration system resulted in higher membrane permeability. These findings confirm that the cake layer formed in the presence of calcium will be more compact, and the addition of alum will result in less compact cake layer.

Table 1. Specific cake resistance values and humic attachments of the investigated systems.

System	α_{MFI} x 10^{12} (m/g)	α_{emp} x 10^{12} (m/g)	α_{MFI} / α_{emp} (-)	Attachment (%)
PAHA+Al+Ca	0.22 (±0.001)	1.10 (±0.0004)	0.20	93
PAHA+Al	0.65 (±0.003)	1.70 (±0.0006)	0.38	79
PAHA	5.82 (±0.02)	186 (±0.4)	0.03	1
PAHA+Ca	3.35 (±0.01)	10.6 (±0.02)	0.32	68
No Alum	5.82 (±0.02)	186 (±0.4)	0.03	1
Alum 10	2.62 (±0.008)	136 (±0.38)	0.02	1
Alum 20	0.65 (±0.002)	2.1 (±0.0002)	0.31	76
Alum 30	0.65 (±0.003)	1.70 (±0.0006)	0.38	79
Alum 50	0.27 (±0.001)	1.99 (±0.001)	0.13	71
Alum 100	0.19 (±0.0006)	2.65 (±0.003)	0.07	74

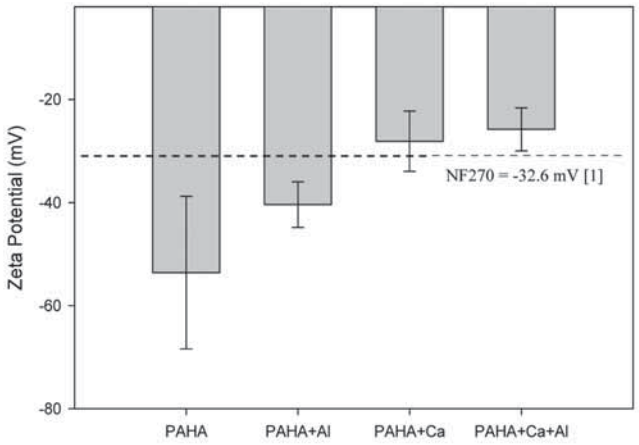

Figure 2. ζ potential values of the investigated systems.

CONCLUSIONS

The severity of flux decline of dead-end nanofiltration of systems containing humic acid, calcium, alum, and their combinations is in the following order: (PAHA+alum+calcium) < (PAHA+alum) < (PAHA) < (PAHA+calcium), indicating that the addition of alum will alleviate the flux decline regardless the presence of calcium. In addition to charge screening and complex formation as occurred when calcium is present, there exists other mechanism that promotes the attachment when alum is present, possibly sweep flocculation. This mechanism results in less compact fouling layer compared to when only PAHA and calcium are added into the system. Based on these findings, hybrid coagulation-nanofiltration for removal of NOM is potential to be applied in drinking water treatment.

REFERENCES

[1] Tang, C.Y., Kwon, Y.-N. and Leckie, J.O., 2007. Fouling of reverse osmosis and nanofiltration membranes by humic acid-Effects of solution composition and hydrodynamic conditions. *Journal of Membrane Science,* Vol. 290, pp. 86-94.

[2] Tang, C.Y., Kwon, Y.-N. and Leckie, J.O., 2007. Characterization of humic acid fouled reverse osmosis and nanofiltration membranes by transmission electron microscopy and streaming potential measurements. *Environmental Science and Technology,* Vol. 41, pp. 942-949.

[3] Li, Q. and Elimelech, M., 2004. Organic fouling and chemical cleaning of nanofiltration membranes: Measurements and mechanisms. *Environmental Science and Technology,* Vol. 38, pp. 4683-4693.

[4] Lee, S. and Elimelech, M., 2006. Relating organic fouling of reverse osmosis membranes to intermolecular adhesion forces. *Environmental Science and Technology,* Vol. 40, pp. 980-987.

[5] Listiarini, K., Sadreddini, S., Sun, D.D. and Leckie, J.O., 2008. Organic fouling of nanofiltration membranes: Resistance calculations of systems containing organic foulants, coagulant and divalent cations. *IWA 6th World Water Congress, Vienna*.

[6] Lee, J.-D., Lee, S.-H., Jo, M.-H., Park, P.-K., Lee, C.-H. and Kwak, J.-W., 2000. Effect of coagulation conditions on membrane filtration characteristics in coagulation-microfiltration process for water treatment. *Environmental Science and Technology,* Vol. 34, pp. 3780-3788.

THE RESPONSES OF METHANOGENIC REACTOR TREATING DIFFERENT EFFLUENT FRACTIONS OF FERMENTATIVE H_2 PRODUCTION IN TWO-PHASE ANAEROBIC DIGESTION SYSTEMS

Ding Hong-Bo (ding0012@ntu.edu.sg)
Wang Jing-Yuan (jywang@ntu.edu.sg)

INTRODUCTION

Dark fermentation (DF) is one of the biological H_2 producing processes. It was found that due to the intrinsic fast-growth and high-biomass-yield nature of H_2 producing acidogens, the effluents from fermentative H_2 production, not only contained different types of soluble byproducts such as acids and solvents, but also comprised of a significant amount of colloidal matters and suspended biomass[1]. The biomass carried a big portion of the influent carbohydrate / COD, e.g., 0.22 g VSS g^{-1} glucose in Fang and Liu's study[2] and 6.6-11.6% of influent glucose COD in Lin and Chang's study[3]. Furthermore, the H_2 biomass residues in many studies possessed high contents of EPS[4] and may cause sludge bulking and poor settling later on in the subsequent waste treatment processes. The colloidal matters were considered to be originated from the EPS peeled off from active cells and intracellular matters released from the lysis of dead cells. In this study, a two-phase anaerobic digestion system for co-production of H_2 and CH_4, consisting of a H_2-producing reactor (RH) and a CH_4-producing reactor (RM) was set up to investigate the corresponding RM performance by treating different fractions of H_2 production effluent from RH.

MATERIALS AND METHODS

The H_2-producing reactor RH was a fixed-bed reactor (10 cm in diameter and 25 cm in height) with a working volume of 0.8 L. The CH_4-producing reactor RM was a modified UASB reactor (10 cm in diameter and 70 cm in height) with a working volume of 4.5 L. A detailed diagram of the whole set-up is shown in Figure 1. All the reactors were operated at 30±1°C. The pretreatments used on RH effluent are listed in Table 1. The slightly settled effluent was collected overnight and centrifuged at 3000 rpm for 20 min the next day. The supernatant containing soluble, colloidal matters, and a small amount of suspended solids (< 50 mg L^{-1}) were collected to simulate the extremely well settled effluent (EFF2). The soluble portion of the effluent (EFF1) was obtained by filtrating EFF2 through 0.45 µm membrane filter papers to remove most of the colloidal solids and some residual suspended solids. The slightly settled RH effluent was used as poorly settled raw effluent (EFF3). The pretreated effluents were stored at 4°C before use.

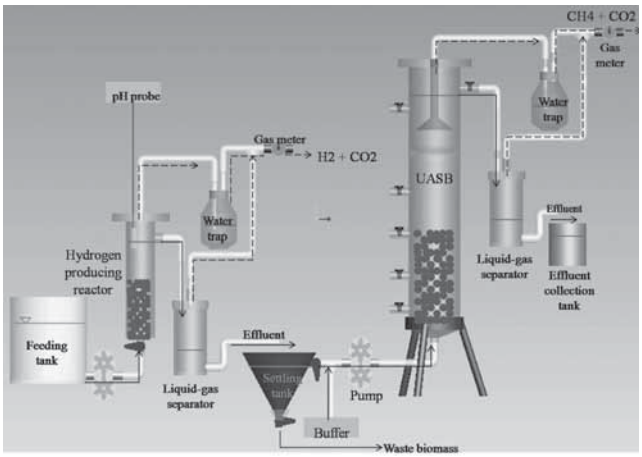

Figure 1. Two-phase anaerobic digestion system for co-production of H_2 and CH_4

Table 1. Outline of the procedure in preparing the various effluent fractions

Effluent RH fractions	*Separation and collection procedure*	*Size limits of fraction removed*
Raw effluent		
⇩	Collected overnight in a big container	Flocculated sludge
EFF3 = Suspended Solids (SS) + Colloidal + Soluble Fraction		
⇩	Centrifuged at 3000 rpm and only supernatant collected	Most of SS
EFF2 = Colloidal +Soluble fraction + Small amount of SS		
⇩	(Supernatant) filtered through 0.45 µm membrane filter	Most colloidal of 7.4 to 0.45 µm
EFF1 = Soluble fraction	Stored at 4°C	

Throughout the whole experiment, the HRT of RM was maintained at 20 h. In stage 1 (day 0 to day 28) or the startup stage, RM was fed with the synthetic glucose wastewater of 2.5 g-COD L^{-1}. In stage 2 (day 29 to day 38), glucose was replaced by diluted EFF1 of the same COD concentration (COD-equivalent) and the concentrations of other nutrients were unchanged so the substrate influent still had a COD of 2.5 g L^{-1}. In stage 3 (day 38 to day 52), from day 38, the concentration of EFF1 was increased to such a level that the COD concentration of RM influent reached 5.0 g L^{-1} on day 52 whereas the concentrations of other nutrients were also increased proportionally. In stage 4 (day 53 to day 70), the centrifuged EFF2 was used and the feeding substrate contained not only a soluble COD (SCOD) of 4.0 g L^{-1} but also a colloidal COD (CCOD) of 0.2 g L^{-1}. In stage 5 (day 71 to day 82), from day 71, the concentrates of all the components in the RM substrate were proportionally increased and reached an SCOD of 7.0 g L^{-1} and CCOD of 0.2-0.3 g L^{-1} on day 82. In stage 6, from day 82 onwards, with others unchanged, untreated EFF3 was used and the RM substrate contained an SCOD of 7.0±1.0 g L^{-1}, a CCOD of 0.3±0.1 g L^{-1}, and a suspended solid COD of 1.0±0.2 g L^{-1}. In stages 1-3, the total COD (TCOD) = SCOD = COD since all substrates were in soluble form; in stages 4-5, TCOD = SCOD + CCOD; in stage 6, TCOD = SCOD + CCOD + VSS COD.

RESULTS AND DISCUSSION

Characteristics of RH effluent used as RM substrate

The major soluble organic compounds of RH effluent, in terms of percentage of SCOD were glucose, ethanol, acetate, butyrate, and caproate. Propionate only contributed less than 1% of SCOD. Due to incomplete glucose utilization, the residue glucose contributed significant COD, which however decreased from 45-50% to 15-17%. In the early RM stages, SCOD contributions of ethanol, acetate, and butyrate were similar and were around 9% and 11% for stage 2 and stage 3, respectively, while caproate contribution was 1-5%. In the later stages, the contributions of butyrate and caproate increased significantly above 20%, while those of ethanol and acetate dropped to below 10%. When RH influent contained around 20 g L^{-1} glucose, RH effluent had an SCOD of 17-19 g L^{-1}. The RH effluent CCOD was approximately 5% of the SCOD. The biomass in the slightly settled RH effluent contributed 1 g COD L^{-1}.

Comparison of CH_4 production of different fractions of RH effluent

Figure 2 demonstrates the CH_4 production performance of RM fed with different types of RH effluent under different OLRs. The membrane-filtered RH effluent (EFF1) and centrifuged RH effluent (EFF2) were used as major COD substrates in stages 2-3 and stages 4-5, respectively. The OLRs for all stages were calculated based on the SCOD for easy comparison. The corresponding VMPRs were linearly and positively correlated with SCOD OLRs (both R^2>0.95 and $p < 0.001$) when RM treated EFF1 and EFF2. The VMPR of RM treating EFF2 of SCOD OLRs of 2-6 g-COD $L^{-1}d^{-1}$ with additional CCOD OLR of 0.1-0.3 g-COD $L^{-1}d^{-1}$ was much higher than that treating EFF1. However, with the increase of SCOD OLR to 6-10 g-COD $L^{-1}d^{-1}$, which corresponded to additional CCOD OLR of 0.3-0.5 g-COD $L^{-1}d^{-1}$, there was an insignificant difference between the amount of CH_4 produced from EFF2 and EFF1. In other words, colloidal matters started to exhibit inhibition on the RM CH_4 production performance. The performance of RM treating raw effluent of RH (EFF3) was much worse.

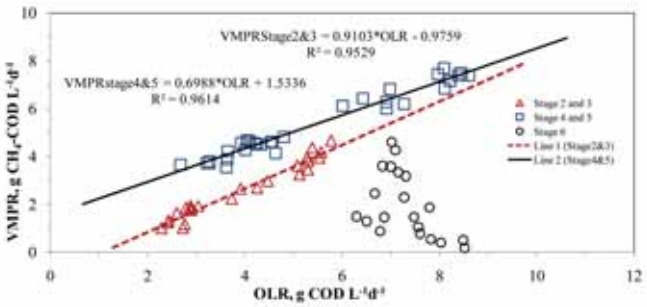

Figure 2. Volumetric methane production rate of RM

CONCLUSIONS

The results demonstrated that the RM easily converted soluble byproducts under various OLRs, but it had difficulties when treating colloidal organic matters under high loadings. The colloidal matters were thought to be absorbed onto the surface of granular sludge and formed a film of increasing thickness which retarded substrate supply into the inner acetogens and methanogens. This study found that the RM performance treating centrifuged RH effluent was satisfactory under a combined OLR of an SCOD OLR of 2-6 g-COD $L^{-1}d^{-1}$ with a CCOD OLR of 0.1-0.3 g-COD $L^{-1}d^{-1}$ but deteriorated under a combined OLR of an SCOD OLR of 6-10 g-COD $L^{-1}d^{-1}$ with a CCOD OLR of 0.3-0.5 g-COD $L^{-1}d^{-1}$. The degradation of the suspended solid was slow under the tested RM HRT of 20 h. The suspended solids in RH effluent fed to RM reactor was either trapped in the RM causing the expansion of sludge bed or washed out with the RM effluent. The washed out VSS may become carrier for in-growing methanogenic organisms and negatively affect the growth of granular sludge. This study recommended the suspended solid in the RH effluent to be removed before RM to treat elsewhere or recycled such as inoculum for H_2-producing solid-fermentation from organic waste. Additional care should be taken to finetune the RM to facilitate the degradation of colloidal matters by increasing HRT and dilution of influent by internal recirculation.

REFERENCES

[1] Ding, H.-B. and Wang, J.-Y., 2008. "Responses of the methanogenic reactor to different effluent fractions of fermentative hydrogen production in a phase-separated anaerobic digestion system." *International Journal of Hydrog. Energy* doi:10.1016/j.ijhydene.2008.09.021.

[2] Fang, H.H.P. and Liu, H. 2002. "Effect of pH on hydrogen production from glucose by a mixed culture". *Bioresour. Technology*, Vol. 82, No. 1, pp. 87-93.

[3] Lin, C.-Y. and Chang, R.-C., 1999. "Hydrogen production during the anaerobic acidogenic conversion of glucose". *Journal of Chem. Tech. Biotechnol.*, Vol. 74, No. 6, pp. 498-500.

[4] Zhang, Z.-P., Show, K.-Y., Tay, J.-H., Liang, D.-T., Lee, D.-J. and Jiang, W.-J., 2007. "Rapid formation of hydrogen-producing granules in an anaerobic continuous stirred tank reactor induced by acid incubation". *Biotechnol. Bioeng.*, Vol. 96, No. 6, pp. 1040-1050.

BRINE DISCHARGES INTO SHALLOW COASTAL WATERS

Dongdong Shao (shao0004@ntu.edu.sg)
Adrian Wing-Keung Law (cwklaw@ntu.edu.sg)

INTRODUCTION

Desalination is now an increasingly viable option to supplement the water supply for many coastal cities due to the significant advancement of membrane technologies in recent years and the reduction of cost. The operation of a desalination plant generates a continuous discharge of brine, which is a highly concentrated saline water, as a by-product into the surrounding sea water. Although the presence of salinity seems natural to the seawater, an excessive input of salinity for an extended period can adversely affect exposed marine organisms, particularly if the exposure lasts an extended period of time for continuous brine discharges (Iso et al, 1994). Therefore, the design and placement of the brine outfall is critical as it has a direct effect on the magnitude of the salinity buildup in the ambient waters. In this study, we investigate the relationship between the salinity buildup and the brine outfall location, and also examine the salinity fluctuations in the presence of the oscillatory tidal currents, as well as the effects of other relevant parameters including the anisotropy and time dependency of the turbulent dispersivity.

DEVELOPMENT OF MATHEMATICAL MODEL

For shallow coastal waters, the dispersion in the vertical direction occurs much faster than the horizontal directions. Hence, the transient salinity advection-diffusion equation can be derived in the following two-dimensional form,

$$\frac{\partial C}{\partial t} = D_x \frac{\partial^2 C}{\partial x^2} + D_y \frac{\partial^2 C}{\partial y^2} - U(t)\frac{\partial C}{\partial y}$$

$$0 \le x < \infty \qquad -\infty < y < \infty \qquad \ldots (1)$$

where C denotes the salinity excess above the ambient level, and D_x and D_y the eddy dispersivities in the x and y directions, respectively. The alongshore tidal current, U(t), typically consists of a small residual current, V, plus a periodic component, $U_0 \sin\omega t$, i.e., $U(t)=V+U_0\sin\omega t$, where U_0 is the amplitude of the oscillatory current which is usually much larger than V, $\omega = 2\pi/T$ (T is the tidal period) is the angular frequency of the oscillatory current, and t denotes time. The brine outfall is deployed at a distance of x_0 offshore, and acts like a point source of concentrated brine injection. For brevity, the boundary conditions applied herein are neglected.

The solution can be written in the form of a convolution integral in dimensionless form (Holley, 1969) as,

$$C_c^*(\xi,\eta,\tau) = \int_0^\tau \frac{d\tau_0}{\tau_0}\left\{\exp\left[-\lambda\alpha^2\frac{(\xi-\xi_0)^2}{\tau_0}\right] + \exp\left[-\lambda\alpha^2\frac{(\xi+\xi_0)^2}{\tau_0}\right]\right\}$$

$$\cdot\exp\left[-\lambda\frac{[\eta-\nu\tau_0+\cos\tau-\cos(\tau-\tau_0)]^2}{\tau_0}\right]$$

The dimensionless variables and parameters are defined as follows,

$$\tau = \omega t,\ \tau_0 = \omega(t-t_0),\ \xi = \frac{\omega x}{U_0},\ \xi_0 = \frac{\omega x_0}{U_0},\ \eta = \frac{\omega y}{U_0}$$

$$C^* = C/\left(C_0 Q/4\pi h_0\sqrt{D_x D_y}\right)$$

$$\alpha = \left(\frac{D_y}{D_x}\right)^{1/2},\quad \nu = \frac{V}{U_0},\quad \lambda = \frac{U_0^2}{4\omega D_y}$$

It is noted that the solution is usually amenable only by means of numerical integration.

EFFECTS OF VARYING N

To examine the effects of varying ν, the shoreline salinity excess profiles are plotted in Fig. 1 for both HWS (at $\tau=20\pi$) and LWS (at $\tau=21\pi$) over a wide range of ν values from 0.05 to 1.0. Comparing the different profiles, it is evident that the general effect of increasing ν and thus the intensity of the residual current would be to decrease the magnitude of the maximum salinity excess at the shore. The resulting series of peaks demands special considerations when assessing local salinity excess. As ν is decreased gradually, the adjacent peaks overlap each other and become less discernable, and also increase the overall magnitude of the salinity excess as a result. As shown in Figure 1, the numbers of distinct peaks decrease from 5 for ν=0.5 to 3 for ν=0.4. When ν is further decreased to 0.2, there is only one clearly visible peak within one tidal excursion downstream from the source, and the profile appears fairly smooth beyond about η=4, i.e., twofold tidal excursion distance.

COMPARISON OF TIME-DEPENDENT DISPERSIVITY AND CONSTANT DISPERSIVITY

In turbulent coastal flows, the shear dispersivity typically scales as the product of seawater depth and friction velocity, while the friction velocity is widely assumed to be proportional to the mean flow speed. Therefore, the dispersivity varies in proportion to the absolute value of the velocity as,

$$D_{x,y}(t) = D_{x,y}\frac{|U|}{\overline{U}} = D_{x,y}\frac{|V+U_0\sin\omega t|}{V} \qquad \text{... (2)}$$

in which the vertical bars indicate the absolute value and the over-bar indicates the average during a tidal cycle, i.e., the residual current.

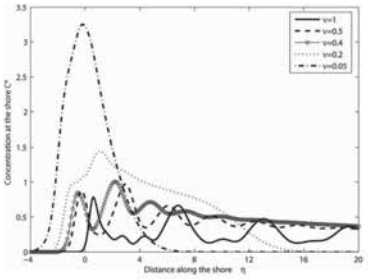

(a) $\tau = 20\pi$

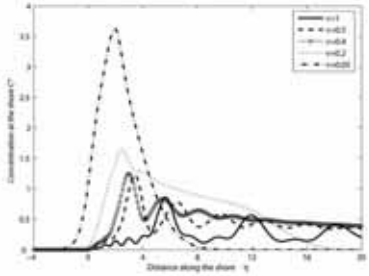

(b) $\tau = 21\pi$

Figure 1. Salinity along the shoreline

In engineering practice, tidally-averaged dispersivities are often assumed to approximate the overall transport over a tidal cycle, and the tidally-averaged dispersivity is defined as,

$$\overline{D_{x,y}} = D_{x,y}\frac{1}{T/2}\int_0^{T/2}\frac{(V+U_0\sin(2\pi t/T))}{V}dt = D_{x,y}(1+\frac{2}{\pi}U_0/V)$$

For $\nu=V/U_0=0.4$, the tidally-averaged dispersivity would thus be roughly 2.59 times of the assumed constant dispersivity.

A comparison of the shoreline salinity corresponding to the constant dispersivity, $D_{x,y}$, the time-varying dispersivity proportional to the flow speed, $D_{x,y}(t)$ and the tidally-averaged dispersivity, is performed. Compared to the constant dispersivity, the effect of the tidally-averaged dispersivity that accounts for both the residual and oscillatory currents is enhanced considerably. At the same time, the salinity profiles are similar between the time-varying and tidally-averaged dispersivity particularly near the source, which indicates that both approximations are valid for the range of the model parameters.

PRACTICAL APPLICATIONS

In disposal practices, the salinity level at the shore can be reduced by an offshore placement of the outfall. At the same time, the operator typically desires a shortest distance based on cost considerations. It is therefore necessary to have a quantitative assessment on the relationship between the salinity build-up and the offshore placement location. First, we consider how the shoreline salinity varies with different offshore locations of the outfall. As an illustration, we adopt the dimensionless parameters in Purnama and Al-Barwani (2006) with a tidal excursion approximately equal to 4.8km. The shoreline salinity corresponding to the different outfall locations at $\tau = 20\pi$ and 21π are plotted in Figure 2. They reveal how the salinity at the shore is reduced as the outfall is placed further offshore. More details from the model results can be found in Shao et al. (2008).

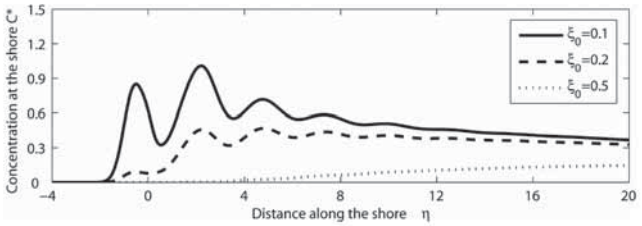

(a) $\tau = 20\pi$

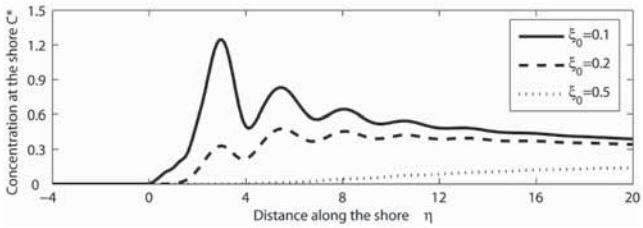

(b) $\tau = 21\pi$

Figure 2. Shoreline salinity with various outfall locations

REFERENCES

[1] Iso, S., Suizu, S. and Maejima, A., 1994. "The lethal effect of hypertonic solutions and avoidance of marine organisms in relation to discharged brine from a desalination plant". *Desalination*, Vol. 97, pp. 389-399.

[2] Purnama, A. and Al-Barwani, H.H., 2006. "Spreading of brine waste discharges into the Gulf of Oman". *Desalination*, Vol. 195, pp. 26-31.

[3] Holley, E.R., 1969. Discussion on "Difference modeling of stream pollution". *Proceedings of Sanitary Engineering Division ASCE*, Vol. 95, pp. 968-972.

[4] Shao, D.D., Law, A.W.K. and Li, H.Y., 2008. "Brine discharges into shallow coastal waters with mean and oscillatory tidal currents." *Journal of Hydro-environment Research,* Vol. 2, No. 2, pp. 91-97.

WAVELET ANALYSIS OF FLOW IMAGES OBTAINED BY PIV (PARTICLE IMAGE VELOCIMETRY)

Wang Xikun (cxkwang@ntu.edu.sg)
Hao Zhiyong (haozhiyong@ntu.edu.sg)
Tan Soon Keat (ctansk@ntu.edu.sg)

INTRODUCTION

Flow past a cylinder in an unbound medium gives rise to self-sustained, limit cycle oscillations involving formation of a regular, periodically alternating Karman vortex street. However, little attention has been paid to the effect of an adjacent free surface on the development of the Karman vortices and possible generation of new classes of the near-wake structure[1], see Figure 1. The technique of Particle Image Velocimetry (PIV) is a useful tool to this flow, considering that it is unsteady and multi-scale in nature.

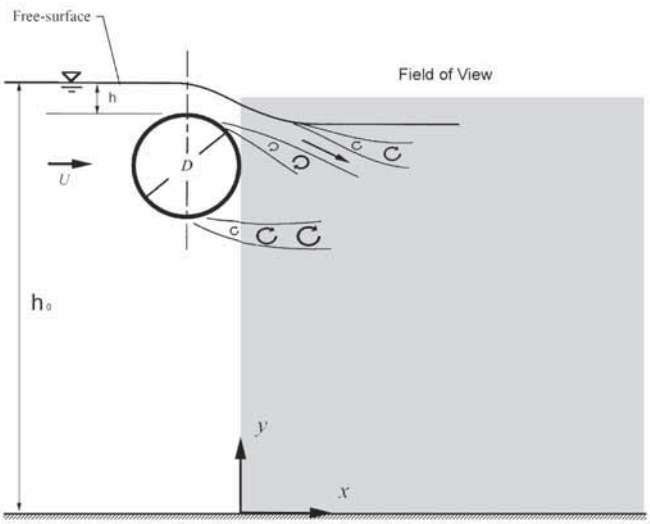

Figure 1. Flow schematic.

Wavelet analysis is positioned to be a promising tool for studying complex nonlinear systems (such as turbulence), see [2] for a review. Mathematically, wavelets are sets of L^2 functions derived from a single function (called a mother function) using 2 basic operations: translation and dilation. An important feature is the wavelet multi-resolution (or multi-scale) analysis. So far, the use of wavelets for analysis of PIV data is still limited. Camussi[3] used the 1D wavelet transform to analyze the PIV velocity fields. Schram and co-workers ([4, 5]) used 2D wavelet method to analyze the vorticity field obtained using PIV. However, these above papers used the continuous wavelet transform (CWT) method, which is suitable for identifying the coherent structures, but not for reconstruction. In present study, the discrete wavelet transform (DWT) method is used instead, because this approach is non-redundant and all orthogonal coefficients are de-correlated thus allowing for perfect reconstruction.

The aim of this paper is to apply the DWT method to analyze the PIV data obtained in the near wake of a circular cylinder beneath the free surface, in order to derive some understanding of the multi-scale vortical structures.

EXPERIMENTAL SETUP

The experiments were performed in a 12 m long, re-circulating open water channel with a rectangular cross section of 0.3 m (W) × 0.45 m (H). In the present study, the water depth (h_o) was maintained at about 100 mm, and the velocity in the potential region was maintained at U_∞ = 0.35 m/s. A circular cylinder with diameter D = 25 mm was mounted horizontally and adjusted to desired positions beneath the free surface (the submerged distance h was 15 mm in the present study). The coordinates x and y denote

the streamwise and vertical directions, respectively, with the origin specified at the intersection between the cylinder base face and the channel bottom wall, see Figure 1.

Measurements were conducted using a PIV system (LaVision model) in the mid-plane of the channel. The viewing area of the PIV measurements was 110 mm × 110 mm. A Quantel System double cavity Nd:YAG laser (power ~ 120 mJ per pulse, duration ~ 5 ns) was used to illuminate the flow field. The particle images were recorded using an 8-bit charge-coupled device (CCD) camera, with a resolution of 1024 × 1008 pixels and a frame rate of 15 Hz.

The particle displacement was calculated using the cross-correlation algorithm. The processing procedure included two passes, starting with a grid size of 64 × 64 pixels, stepping down to 32 × 32 pixels overlapping by 50%. This interrogation and evaluation procedure yielded the spatial resolution for the present set-up to be about 1.7 mm × 1.7 mm. A more detailed discussion of the processing procedure and the measurement uncertainty level is given[6].

RESULTS AND DISCUSSION

A snapshot of the instantaneous velocity vector (u, v) plot obtained by PIV is shown in Figure 2a. Figure 2b is the calculated vorticity ($\omega = \partial v/\partial y - \partial u/\partial x$) using the least operations extrapolation scheme. The vortices can be identified by either circular pattern of streamlines or concentrated region of vorticity. It can be seen that an upper row of clockwise vortices and a lower row of anti-clockwise vortices propagate into the downstream flow from the two sides of the cylinder. In addition, a jet-like flow is evident between the upper surface of the cylinder and the free surface. Between the jet-like flow and the free surface, several large-scale vortices (mainly anti-clockwise) are visible, indicating occurrence of reverse flow in this region.

The vorticity field is a good quantitative indicator of the presence of vortices in that their swirling strength is represented by the vorticity magnitude and their scale by the shape of the vorticity patches. Therefore, it is selected as an example to be post-processed by wavelet method. The instantaneous vorticity field $\omega(x, y)$ is decomposed at dyadically decreasing scales from the largest scale $l_{max} = 2^0$ to the smallest scale $l_{min} = 2^{J-1}$ (N = 2^{2J}):

$$\omega(x,y) = \overline{\omega}_{0,0,0}\phi_{0,0,0}(x,y) + \sum_{l=0}^{J-1}\sum_{k_x=0}^{2^l-1}\sum_{k_y=0}^{2^l-1}\sum_{\mu=1}^{3}\tilde{\omega}^{\mu}_{l,k_x,k_y}\psi^{\mu}_{l,k_x,k_y}$$

where l is the index of scale; k_x and k_y are the indices of translation; and $\mu = 1$, 2 and 3 are the three spatial directions (horizontal, vertical and diagonal, respectively).

The 2D scaling functions are $\phi_{l,k_x,k_y}(x,y) = \phi_{l,k_x}(x)\phi_{l,k_y}(y)$, and the corresponding wavelets are:

$$\psi^{\mu}_{l,k_x,k_y} = \begin{cases} \psi_{l,k_x}(x)\phi_{l,k_y}(y) & \text{for } \mu = 1 \\ \psi_{l,k_y}(x)\phi_{l,k_y}(y) & \text{for } \mu = 2 \\ \psi_{l,k_x}(x)\psi_{l,k_y}(y) & \text{for } \mu = 3 \end{cases}$$

where $\phi_{l,k}$ and $\psi_{l,k}$ are respectively the 1D scaling function and the corresponding wavelet. In the present study, the Biorthogonal (Bior 3.7) wavelet, which is approximately orthogonal while maintaining symmetry, is used. The scaling coefficients are given by $\phi_{0,0,0} = \langle \omega, \hat{\phi}_{0,0,0} \rangle$ and the wavelet coefficients are given by $\tilde{\omega}^{\mu}_{l,k_x,k_y} = \langle \omega, \hat{\psi}^{\mu}_{l,k_x,k_y} \rangle$, where $\langle \cdot,\cdot \rangle$ denotes the L^2-inner product and, $\hat{\phi}$ and $\hat{\psi}$ respectively denote the dual scaling function and the dual wavelet.

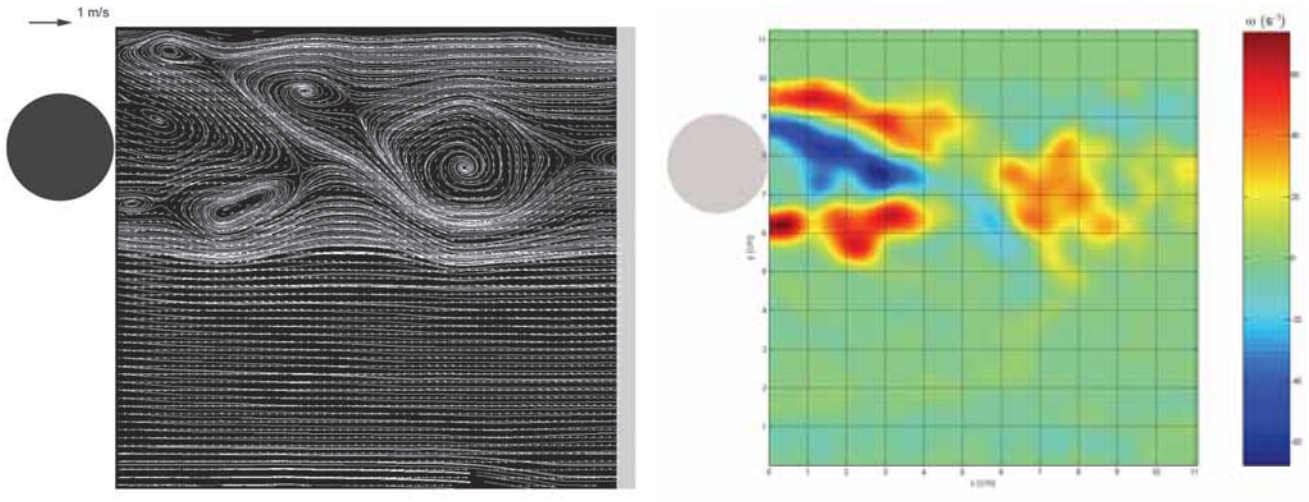

(a) (b)

Figure 2. An example of PIV data: (a) velocity vector field; (b) vorticity field.

Due to the orthogonality of the transform, the decomposition ensures a separation of the flow field at different scales. Figures 3(a), (b) and (c) are the results at three typical scales of l = 3, 4 and 5, corresponding to the resolution of 8 grid size (scale ≈ 13.6 mm), 4 grid size (≈ 6.8 mm), and 2 grid size (≈ 3.4 mm), respectively. Figure 3(a) displays only the large-scale (scale ≈ 13.6 mm) structures, whereas details of the structures have been smeared. When the scale is decreased to about 6.8 mm (Figure 3(b)), the detailed structures are more distinct, and the size, shape and peak values (both positive and negative) of decomposed vorticity field become more approximately similar to the original field in Figure 2(b). Figure 3(c), at a further smaller scale, achieves almost full recovery of the original field.

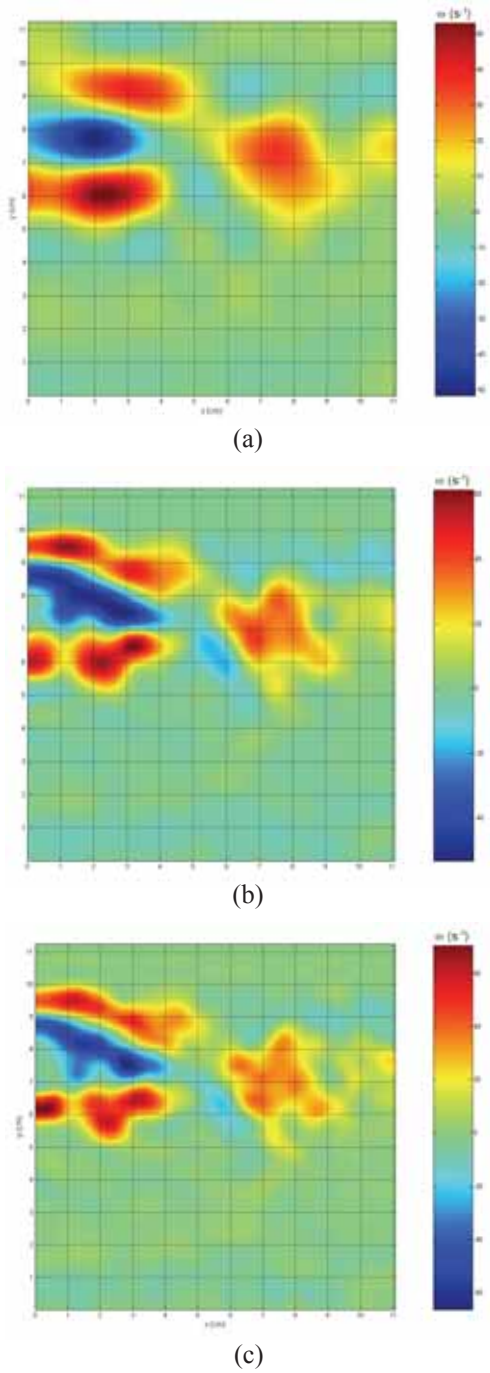

(a)

(b)

(c)

Figure 3. Vorticity field approximated at three different scales: (a) l = 3; (b) l = 4; and l = 5.

The selectivity property of wavelets permits visualization of the vortical structures at specific scale, as shown in Figure 4. It can be seen that different structures might indeed be visualized or hidden, depending on the selected scale. For example, at the largest scale (Figure 4(a)), three strong vortices are evident in the near wake region: two vortices (with alternative signs) behind the cylinder, and another vortex (negative) adjacent to the free surface. In contrast, at smaller scales (as shown in either Figure 4(b) or 4(c), multiple vortices are apparent; moreover, the small-scale vortices are loosely distributed over the wake region. Due to the multi-scale nature of turbulent flows, the scale-specific property of the decomposition provides a great advantage, and reveals a diversity of the vortical structures.

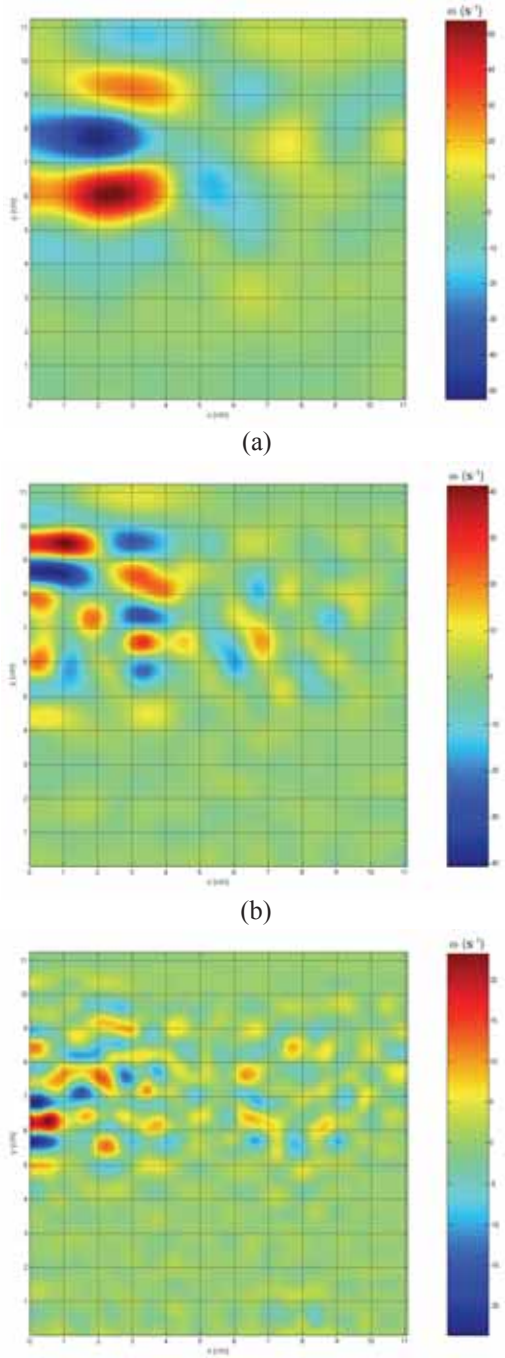

(a)

(b)

(c)

Figure 4. Decomposition of the vorticity field at three different scales: (a) l = 3; (b) l = 4; and l = 5.

CONCLUSIONS

PIV (Particle Image Velocimetry) and wavelet analysis using DWT (discrete wavelet transform) scheme are combined in this work in order to investigate the flow characteristics in the wake of a circular cylinder beneath a free surface. The selectivity property of wavelets permits decomposition of the vortical structures at different scales and visualization of their corresponding spatial localization. The wavelet-based multi-resolution technique will be applied to process sufficiently large amount of PIV images (several hundred velocity fields have been obtained for this type of flow), in order to achieve a statistical characterization of the vortical structures.

REFERENCES

[1] Sheridan, J., Lin, J.C. and Rockwell, D., 1997. "Flow past a cylinder close to a free surface." *Journal of Fluid Mechanics,* Vol. 330, pp. 1-30.
[2] Farge, M., 1992. "Wavelet transforms and their applications to turbulence." *Annual Review of Fluid Mechanics*, Vol. 24, pp. 395-457.
[3] Camussi, R., 2002. "Coherent structure identification from wavelet analysis of particle image velocimetry data." *Experiments in Fluids*, Vol. 32, pp. 76-86.
[4] Schram, C. and Riethmuller, M.L., 2001. "Vortex ring evolution in an impulsively started jet using digital particle image velocimetry and continuous wavelet analysis." *Measurement Science and Technology*, Vol. 12, pp. 1413-1421.
[5] Schram, C., Rambaud, P. and Riethmuller, M.L., 2004. "Wavelet based eddy structure deduction from a backward facing step flow investigated using particle image velocimetry". *Experiments in Fluids,* Vol. 36, pp. 233-245.
[6] Wang, X.K. and Tan, S.K., 2008. "Near-wake flow characteristics of a circular cylinder close to a wall." *Journal of Fluids and Structures*, Vol. 24, pp. 605-627.

TREATMENT AND UTILISATION OF INCINERATOR BOTTOM ASH (IBA) FOR ROAD CONSTRUCTION

Tan Soon Keat (ctansk@ntu.edu.sg)
Le Tuyet Minh (LTMinh@ntu.edu.sg)
Nguyen Anh Tuan (ATNGUYEN@ntu.edu.sg)

INTRODUCTION

More than 90% of municipal solid waste (MSW) in Singapore is incinerated and the residues (bottom ash and fly ash/air pollution control residues) are subsequently disposed of and landfilled. Once the facility is full, new space has to be found instead. At the same time, Singapore imports raw materials such as aggregates (sand/gravel) to be used as the sub-base in road construction. In several European countries which also rely strongly on incineration for MSW management, incinerator bottom ash (IBA) has been used as sub-base in road construction, subject to certain functional and environmental quality requirements.

This study will characterise representative IBA samples from Singapore in terms of chemical composition, leaching behaviour and geotechnical properties, and examine the feasibility of utilising IBA as a road base material.

OBJECTIVES

In order to utilise IBA for construction work in a sustainable and environmentally safe manner, the project objective will include the following:

1) To update the information on the functional and environmental properties of Singapore's IBA based on tests and analyses as well as existing information;
2) To compare the situation in Singapore with that in other countries (UK, USA, Netherlands, Denmark, Germany, Sweden, Japan, Taiwan, Bermudas, etc) in terms of the IBA quality, functional and environmental criteria for utilisation (road construction) as well as the needs and likely possibilities for IBA treatment;
3) To recommend options for treating IBA in the local context; and
4) To recommend environmental protection criteria suitable to Singapore conditions in order to obtain better IBA quality management.

EXPERIMENTS

Three experiments will be conducted in the CEE Environmental Lab to investigate the leaching behavior, applying the following conditions:

- pH dependence test;
- leaching behavior in terms of liquid-to-solid ratio
- leaching of non-volatile organic component

Results of these experiments will be used for modelling to predict the trends of leaching behaviour in the next 20 – 50 years.

Figure 1. pH dependence test

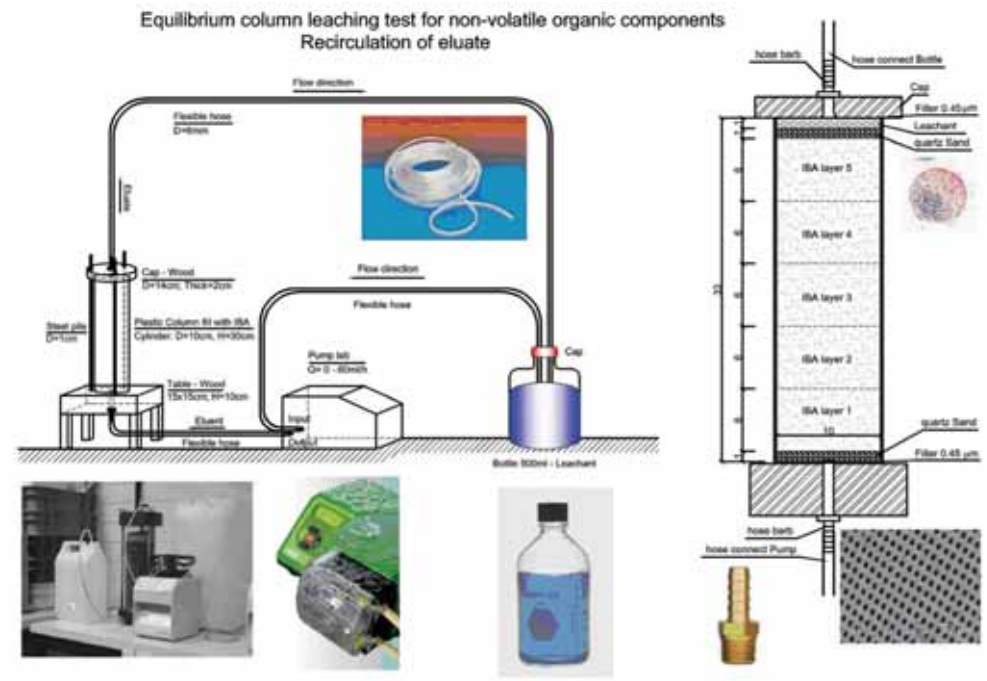

Figure 2. Leaching behaviour tests

THE REMOVAL OF PHOSPHATE FROM REJECT WATER OF A MUNICIPAL WASTEWATER TREATMENT PLANT USING IRON ORE IN THE STATIC AND ROTATING REACTORS

Guo Chenghong (GUOC0002@ntu.edu.sg)
Kuang Shengli (KUAN0010@ntu.edu.sg)
Volodymyr Ivanov (cvivanov@ntu.edu.sg)

INTRODUCTION

Reject water (RW) is the liquid fraction produced after dewatering of anaerobically digested activated sludge. The concentration of phosphorus in municipal wastewater is from 5 to 20 mg/L, however; the concentration of phosphorus in RW is up to 130 mg/L. RW contributes from 10% to 80% of phosphorous load on the activated sludge tank[1]. Therefore, the removal of phosphorus from reject water can significantly reduce the phosphorus load to the main stream. Ferric chloride and ferrous sulfate are commonly used in the phosphorus chemical removal; however, the disadvantage of the chemical precipitation is the high cost of the chemical iron salt. An alternative method for the removal of phosphate by BioIronTech process using cheap iron ore[2,3] reduced by iron reducing bacteria (IRB) under anaerobic conditions has been demonstrated. However, the study was performed in static reactors where diffusion was the major mechanism of mass transfer. The production of ferrous from iron ore and the removal of phosphorus from reject water under higher mass transfer rate have not been studied yet. The aim of the present research is to compare the production of ferrous and removal of phosphorus from reject water using bioreduction of iron ore by iron reducing bacteria in the static and rotating reactors.

MATERIALS AND METHODS

The reject water and anaerobic sludge (a source of IRB) were collected from a local municipal wastewater treatment plant. The characteristics of the reject water and anaerobic sludge are given in the Table 1. The iron ore, with iron content 60% (w/w), was supplied from China. The major mineral was hematite (Fe_2O_3). Three sets of iron ore particles with the sizes of 7.6 ± 1.9 mm, 2.4 ± 0.4 mm and 0.6 ± 0.1 mm were used in the experiments.

Table 1. Characteristics of reject water and anaerobic sludge

Concentration (mg/L)	Reject water	Anaerobic sludge
Dissolved TOC	450-600	1900
TSS	430-670	5240
VSS	380-560	4000
Dissolved PO_4^{3-}	64-110	80
Total Fe(II)	4-7	167

The experiment on the removal of phosphorus under static conditions was performed in batch culture. Iron ore, 1 kg, reject water, 4.5 L, and anaerobic sludge, 0.5 L, were added into each 5 L bioreactor. No iron ore or anaerobic sludge were added in the control reactor. The bioreactors were maintained at 35°C for 28 days.

The experiment on the removal of phosphorus under continuous mechanical mixing was performed also in batch culture. Iron ore, 400 g, reject water, 1.8 L, and anaerobic sludge, 200 mL, were added in each 2 L bioreactor. The bioreactors were rotated on VELP® OVERHEAD MIXER rotax 6.8 (Velp Scientifica) (5 rpm/min) for 18 days of continuous mixing at 35°C. Each bioreactor was purged with nitrogen gas for 5 minutes and sealed up to ensure anaerobic conditions.

The total suspended solids (TSS) and volatile suspended solids (VSS) were determined in the well-mixed sample by standard methods. pH, the concentrations of total ferrous ions, dissolved phosphate, and dissolved total organic carbon (TOC) were measured in the samples in triplicates. The concentration of total ferrous ions was measured according to a modified phenanthroline method. The modified vanadomolybdophosphoric acid colorimetric method was used to determine the concentration of dissolved orthophosphate[2,3].

RESULTS AND DISCUSSION

The ferrous production was in both reactors (Figure 1).

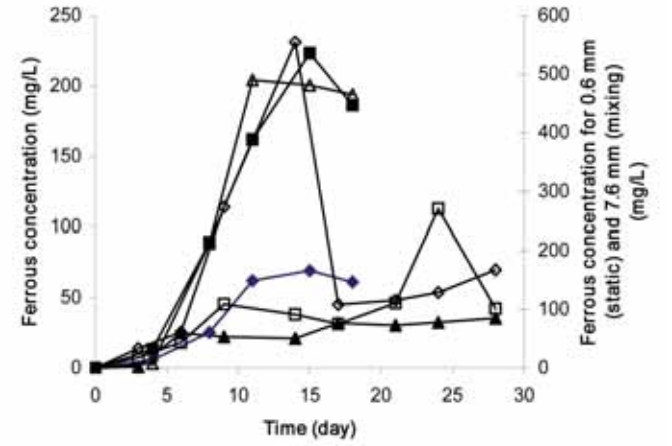

Figure 1. The production of ferrous in static (S) and rotating (R) reactors. The sizes of iron ore particles were: ♦ 0.6 mm (R); ◊ 0.6 mm (S); ■ 2.4 mm (R); □ 2.4 mm (S); Δ 7.6 mm (S); ▲ 7.6 mm (R).

In the static reactors, the highest ferrous production rate was with the smallest iron ore particle size of 0.6 mm, and the highest ferrous concentration was 550 mg/L. However, in the process with the mechanical mixing, the highest ferrous production rate was in the reactor with the biggest iron ore particle size of 7.6 mm. The highest ferrous production rate in the rotating bioreactor with the biggest iron ore particles can be hypothetically explained by the strong mechanical impulses and friction between large iron ore particles, which produced fine and fast reduced iron ore powder.

The concentration of dissolved phosphorus decreased during both cultivation processes (Figure 2).

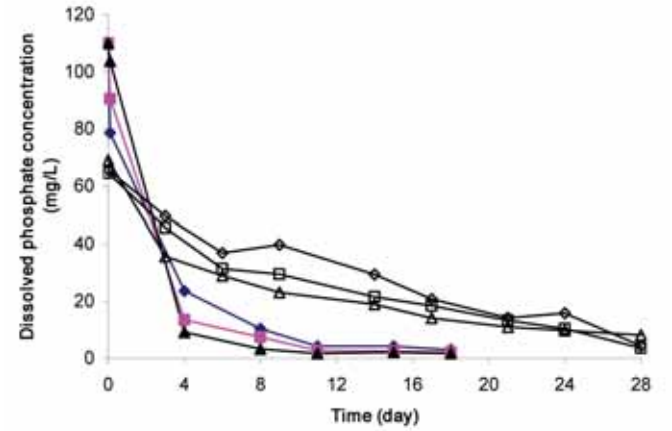

Figure 2. Concentration of dissolved phosphorus in static (S) and rotating (R) reactors. The sizes of iron ore particles were: ♦ 0.6 mm (S); ◊ 0.6 mm (R); ■ 2.4 mm (S); □ 2.4 mm(R); Δ 7.6 mm (S); .▲ 7.6 mm (R).

In the static cultivation, removal efficiency was about 90% and the similar mean phosphorus removal rates (2.17 mg P/L/day) were in all three reactors with iron ore sizes of 0.6 mm, 2.4 mm, and 7.6 mm. The maximum phosphorus removal rate was 11 mg P/L/day. The concentration of dissolved orthophosphate in the control without iron ore remained the same during the cultivation process. During the cultivation with the mechanical mixing, the phosphorus was removed by 79%, 88% and 92% within 4 days and by 91%, 93%, and 97% within 8 days for iron ore particles with mean sizes of 0.6mm, 2.4 mm, and 7.6 mm, respectively. In contrast to the static cultivation, the process with largest iron ore particles in rotating reactor had highest phosphorus removal rate, which was in accordance with the highest ferrous production rate. The highest phosphorus removal rate in rotating reactor was 25 mg P/L/day for the particles of iron ore with mean size of 7.6 mm.

The changes of TOC concentration in both cultivation processes are shown in Figure 3. The removal efficiency of TOC in the static cultivation was 71%, 86% and 89% for iron ore mean sizes of 0.6 mm, 2.4 mm and 7.6 mm, respectively. However, the removal efficiency of TOC was only 31%, 41% and 63% for iron ore mean size of 0.6 mm, 2.4 mm and 7.6 mm in the rotating bioreactors.

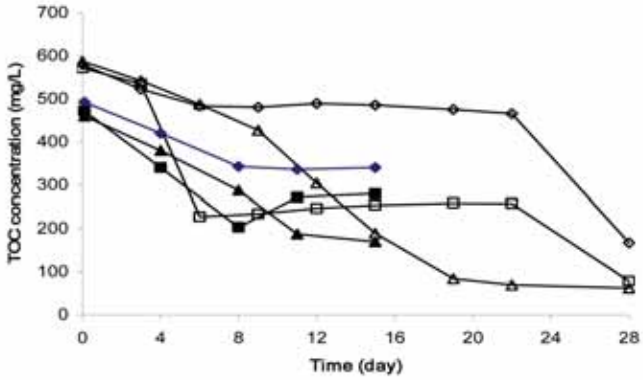

Figure 3. Concentrations of TOC in the static and rotating bioreactors. The sizes of iron ore particles were: ♦ 0.6 mm (R); ◊ 0.6 mm (S); ■ 2.4 mm (R); □ 2.4 mm (S); ▲ 7.6 mm (R); Δ 7.6mm (S).

The results of the experiments are summarized in the Table 2.

Table 2. TOC removal and ferrous production during static and mechanically mixing cultivation processes

Parameters (mg/L)	Static reactors			Rotating reactors		
	with iron ore particles, mm					
	0.6	2.4	7.6	0.6	2.4	7.6
TOC removal	413	493	525	152	191	290
Fe^{2+} production	168	42	36	61	186	465

CONCLUSIONS

The removal of phosphorus from reject water of municipal wastewater treatment plant using bioreduction of iron ore by iron-reducing bacteria under anaerobic conditions was best in the bioreactor with the mechanical mixing. These data will be used for the design of the biofilter for the removal of phosphorus from reject water of municipal wastewater treatment plants.

REFERENCES

[1] Van Loosdrecht M.C.M. and Salem, S., 2006. Biological treatment of sludge digester liquids. *Water Sci Technol.,* Vol. 53, pp. 11-20.

[2] Ivanov, V., Stabnikov, V., Zhuang, W.Q., Tay, J.H. and Tay, S.T.L., 2005. Phosphate removal from the returned liquor of municipal wastewater treatment plant using iron-reducing bacteria. *Journal of Applied Microbiol.,* Vol. 98, pp. 1152-1161.

[3] Ivanov, V., Guo, C.-H., Stabnikov, V. and Kuang, S.-L., 2008. The removal of phosphorus from reject water in a municipal wastewater treatment plant using iron ore. *Journal of Chem. Technol. Biotechnol.,* Vol. 84, pp. 78-82.

PHYSIOLOGICAL HETEROGENEITY OF MICROBIAL POPULATIONS AND COMMUNITIES IN THE ENVIRONMENTAL BIOTECHNOLOGICAL PROCESSES

Saeid Rezaei Nejad (SAEI0001@ntu.edu.sg)
Ivanov Volodymyr (CVIvanov@ntu.edu.sg)

INTRODUCTION

Microbial population is physiologically heterogeneous in terms cell enzymatic activities, including respiration activity reflecting biodegradation activity of cells. New methods are needed in order to study the physiological properties of individual microbial cells in environmental engineering systems. Alcohol dehydrogenase (ADH) activity, respiratory activity and membrane potential of individual cells can be useful parameters to monitor biodegradation activity of individual cells in microbial populations and communities. The aim of this research was to examine this idea.

MATERIALS AND METHODS

Strain of yeast *Saccharomyces cerevisiae* 70449 (DSMZ, Germany) was used as eukaryotic model and strain of bacteria *Escherichia coli* 1329 (DSMZ, Germany) was used as prokaryotic model. Yeasts were grown aerobically in YMPG broth (DifcoTM, Becton Dickinson, Sparks, MD, USA) in flasks placed in the shaker at 200 rpm for 16 hrs at 30ºC. The samples were treated by 1% (v/v) allyl alcohol and incubated for 10 minutes at 30ºC. LIVE/DEAD BacLight™ Viability kit (Molecular Probes, Eugene, OR, USA) contains SYTO 9 and propidium iodide (PI) was used in the study[2]. To determine respiration activity, cells were stained with 5-cyano-2, 3-ditolyl tetrazolium chloride (CTC) (Polyscience, Inc., Warrington, PA, USA)[3]. To determine membrane potential, cells were stained with bis-(1,3-dibutylbarbituric acid) trimethine oxo (DiBAC4) (Molecular Probes, Eugene, OR, USA)[1]. Stained cells were viewed using an Olympus Fluoview FV300 confocal laser scanning microscope (CLSM) (Olympus Optical, Tokyo, Japan) with a 100× objective. The flow cytometry measurements were performed using Becton Dickinson (BD) FACSCaliburTM flow cytometer with CELLQuest TM software.

RESULTS AND DISCUSSION

There were two subpopulations, with low and high ADH activity in populations of *S. cerevisiae* (Figures 1, 2) and *E. coli* (Figure 3). Cells with higher level of ADH and, respectively, higher level of respiration activity were intoxicated with the product of allyl alcohol oxidation. The portion of cells population, which has been shifted from the R2 to R1 region in panel C was about 17% (Figure 1).

The cells subpopulations of *E.coli* with high and low activity of ADH were 10% and 90% of total cell number, respectively.

94% of E. coli cells reduced CTC to fluorescent formazan (CTF) in mid- exponential growth phase, whereas 84% of cells were CTC-positive during late stationary growth phase (Figure 4).

4% of E. coli cells were depolarized (or having negative charge outside cytoplasmic membrane) in mid- exponential growth phase, whereas 26% of cells were depolarized (or having negative charge outside cytoplasmic membrane) during late stationary growth phase by using membrane potential dyes (Figure 5).

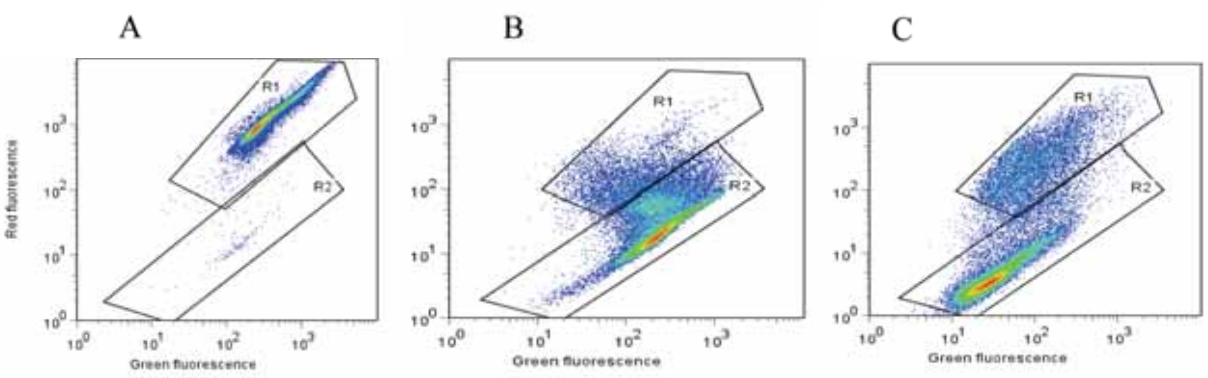

Figure 1. Flow cytometry detection of S. cerevisiae subpopulations with low and high ADH activity using the Live/Dead BacLight™ viability kit. A, dead cells treated with 20% (v/v) of allyl alcohol solution for 30 min; B, sample of intact cells; C, sample treated with 1% (v/v) of allyl alcohol solution for 10 min.

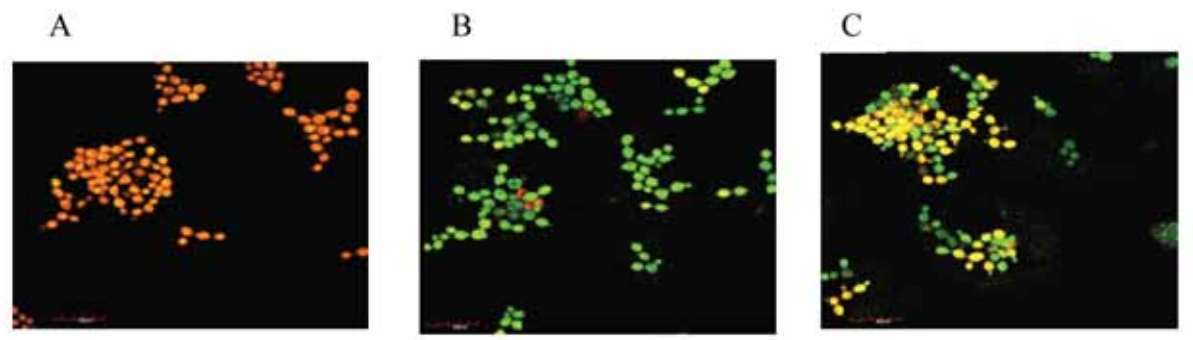

Figure 2. Cells S. cerevisiae stained by Live/Dead Baclight observed by CLSM; A, dead cells treated with 20% (v/v) of allyl alcohol for 30 min; B, sample of intact cells; C, sample treated with 1% (v/v) allyl alcohol for 10 min. The dead cells are differentiated by yellow colour due to staining by PI and Syto9 in panel C, whereas the live cells are green colour due to staining by Syto9 fluorescent dye.

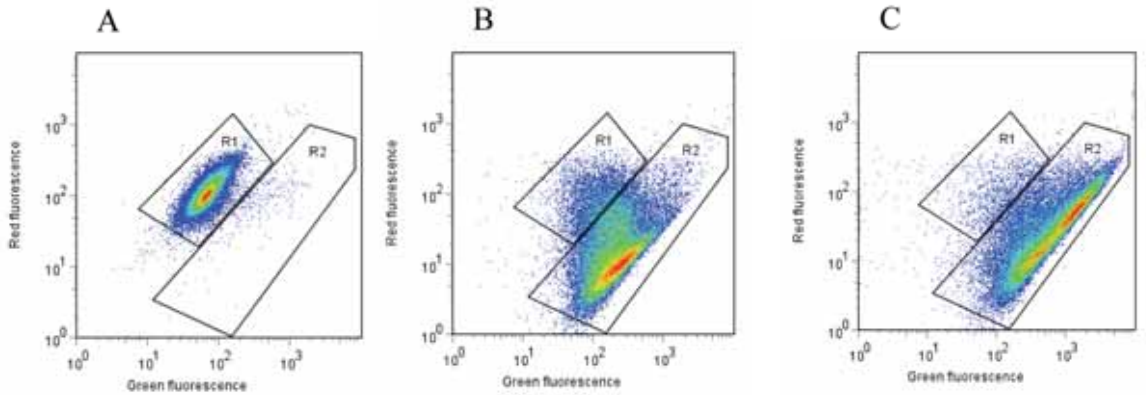

Figure 3. Flow cytometry analysis of E.coli, using the Live/Dead Baclight stain. A, dead cells treated with 20% (v/v) of allyl alcohol for 30 min; B, sample of intact cells; C, sample treated with 1% (v/v) allyl alcohol for 10 min.

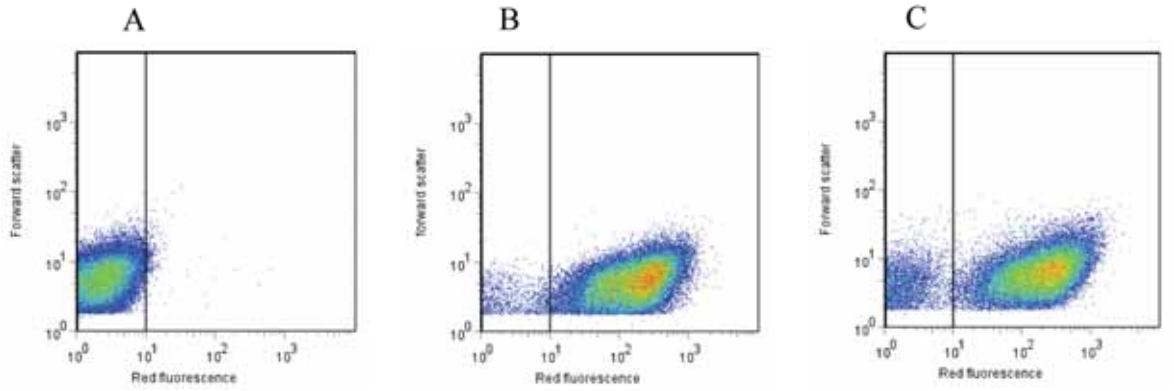

Figure 4. Flow cytometry analysis of E. coli cells. A, dead cells treated with 20% v/v of allyl alcohol for 30 min; B, sample of mid-exponential growth phase; C, sample of late stationary growth phase.

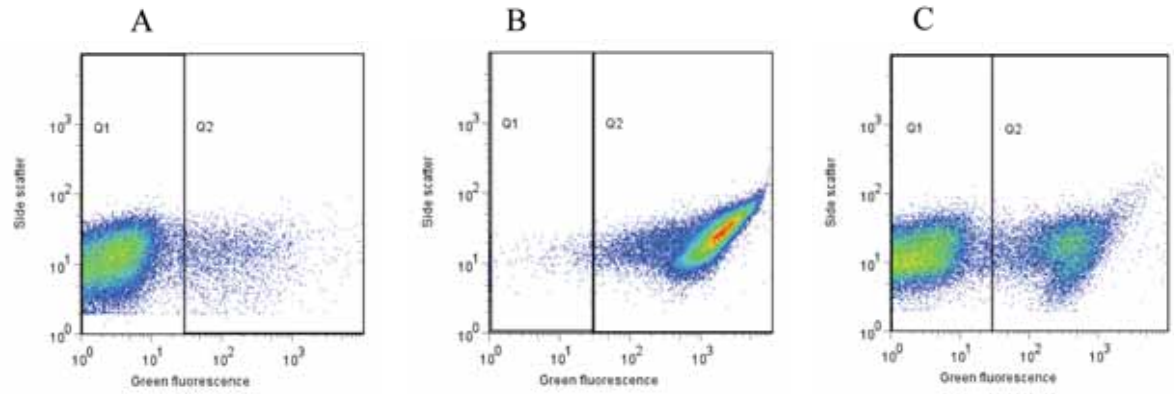

Figure 5. Flow cytometry analysis of E. coli cells, using DiBAC4 stain. A, dead cells treated with 20% v/v of allyl alcohol for 30 min; B and C, samples of mid-exponential and late stationary growth phases.

REFERENCES

[1] Anderson, A.Z., Poulsen, A.K., Brasen, J.C. and Olsen, L.F., 2007. On-line measurements of oscillating mitochondrial membrane potential in glucose-fermenting *Saccharomyces cerevisiae*. Yeast, Vol. 24, pp. 731-739.

[2] Berney, M., Hammes, F., Bosshard, F., Weilnmann, H.U. and Eglii, T., 2007. Assessment and interpretation of bacterial viability by using the LIVE/DEAD BacLight kit in combination flow cytometry. *Appl. Environ. Microbiol.,* Vol. 73, pp. 3283-3290.

[3] Creach, V., Baudoux, A.C., Bertru, G. and Rouzic, B.L., 2003. Direct estimate of active bacteria: and CTC use and limitation. *Journal of Microbiol. Methods.,* Vol. 52, pp. 19-28.

BIOCEMENT – A NEW SUSTAINABLE AND ENERGY SAVING MATERIAL FOR CONSTRUCTION AND WASTE TREATMENT

Chu Jian (cjchu@ntu.edu.sg)
Volodymyr Ivanov (cvivanov@ntu.edu.sg)

INTRODUCTION

Using bacteria for soil improvement? It sounds like a strange idea, but it has become a reality and this new method should be ready to be used in practice in the near future (Ivanov and Chu, 2008). At present, cement or chemicals are commonly used for treating soils and wastes for civil and environmental engineering applications. However, the production of cement is energy intensive and environmentally unfriendly. The use of cement for soil improvement or waste treatment is also expensive and time consuming. Using the latest microbial biotechnology, a new type of construction material, *biocement*, can be developed as an alternative to cement. Biocement is made of naturally occurring microorganisms at ambient temperature and thus requires much less energy to produce. It is sustainable as microorganisms are abundant in nature and can be reproduced easily at low cost. The microorganisms that are suitable for making biocement are non-pathogenic and environmentally friendly. Furthermore, unlike the use of cement, soils or contaminated land can even be treated or improved without disturbing the ground or environment as microorganisms can penetrate and reproduce themselves in soil. Harnessing this natural, unexhausted resource may result in an entirely new approach to geotechnical or environmental engineering problems and bring in enormous economical benefit to construction industries. The application of microbial biotechnology to construction may also simplify some of the existing construction processes and revolutionize the ways soils and wastes are treated.

A study at the School of Civil and Environmental Engineering, NTU, is being carried out to invent biocement as a new and economical construction material and develop cost-effective and environmentally friendly microbiological methods to use biocement for geotechnical or environmental engineering problems. The study also intends to establish the fundamental principles, microbiological and biochemical mechanisms that govern the formation of biocement. The study may also lead to the establishment of a new discipline, *Microbial Geotechnology*, which deals with the merging of knowledge of microbiology and geomechanics and the new knowledge generated from the existing and future studies. The impact of this study has been highlighted by a recent report published by the National Research Council (NRC) of USA (NRC, 2006) in which Biological Processes in Geotechnical Engineering has been identified as a "high priority" research area and cited as "a critical research thrust and the opportunity for the future".

Biocement will have two major areas of applications: *bioclogging* and *biocementation*. Bioclogging refers to a process in which pore-filling materials are produced through microbial activities so that the porosity and hydraulic conductivity of soil can be reduced. Biocementation refers to a process in which particle-binding materials are generated through microbial activities so that the shear strength of soil can be increased. Bioclogging is used to reduce drain channel erosion, form grout curtains to reduce the migration of heavy metals and organic pollutants, control ground water flow, and prevent piping of earth dams and dikes. Biocementation is used to prevent soil avalanching, reduce the swelling potential of clayey soil, mitigate the liquefaction potential of sand, enhance stability of slopes and dams, and compact soil on reclaimed land sites.

LABORATORY STUDY

A method for the screening of the suitable physiological groups of prokaryotes has been suggested by (Ivanov and Chu, 2008). Physiological state of microbial cells used in biocementation could be monitored using flow cytometry or confocal laser ascanning microscopy (Ivanov et al., 2009). Biocement made of the following types of microorganisms and related materials have been developed and used to treat beach sand in the study:

1) Anaerobic ferrous-containing solution produced by iron-reducing bacteria from iron ore (Ivanov et al., 2005; Stabnikov and Ivanov, 2006; Ivanov et al., 2008; Lee and Oh, 2007) separately from sand or inside the sand sample;
2) Oligotrophic bacteria producing exopolysaccharides strongly binding sand grains (Lee and Oh, 2007; Ivanov and Chu, 2008);
3) Nitrifying bacteria producing exopolysaccharides binding sand grains (Lee and Oh, 2007; Ivanov and Chu, 2008; Ong and Hong, 2008);
4) Microbial polysaccharide xanthan (Lee and Oh, 2007);
5) Conventional biogrout containing $CaCl_2$, urea, and urease-hydrolysing bacteria (Mitchell and Santamarina, 2005; Ivanov and Chu, 2008; Ong and Hong, 2008).

Sand specimens were prepared by depositing sand into a plastic cylinder. Biocement solutions, or *biogrouts*, were poured on top of the specimens. Dry sand columns treated by three different types of biocement: (a) microbial polysaccharide xanthan; (b) cultivation of oligotrophic

bacteria; and (c) iron-reducing bacteria are shown in Figure 1. It should be noted that dry sand cannot even stand as a column, obviously it is not able to sustain weight. Therefore, the effect of the microbial treatment is obvious. Under suitable conditions, the unconfined compressive strength of the biocement treated sand can be as high as 1500 kPa, as shown in Figure 2. Such a compressive strength is comparable to cement or chemical treated soil.

(a) (b) (c)

Figure 1. Sand columns produced by sand treated by (a) microbial polysaccharide xanthan; (b) cultivation of oligotrophic bacteria; and (c) iron-reducing bacteria.

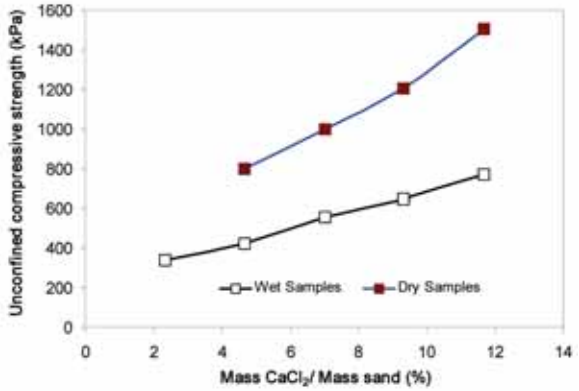

Figure 2. Unconfined compressive strength as a function of mass ratio of $CaCl_2$ to sand

The mechanisms of bioclogging and biocementation can be explained using the SEM image shown in Figure 3. In this case, exocellular biopolymers produced by microorganisms fill in the voids between sand grains and thus reduce the permeability of the soil. This biopolymer also bonds sand grains together to produce a cementation effect similar to the use of cement and thus increase the shear strength of the soil. Another mechanism of bioclogging and biocementation is bacteria-mediated precipitation of ferric and calcium compounds in the voids.

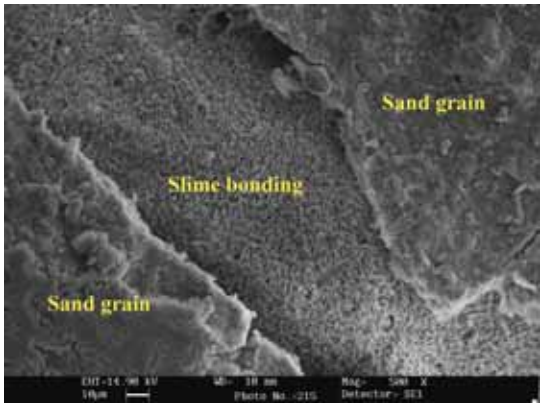

Figure 3. Bonding of sand grains by slime produced by microorganisms

CONCLUSIONS

Biocement – a new sustainable and energy saving material can be produced using naturally occurring microorganisms and used for soil improvement in a way similar to the use of cement. The production of biocement is more energy saving and environmentally friendly. It is also sustainable as microorganisms are abundant in nature and can be reproduced easily at low cost. Harnessing this natural, unexhausted resource may result in an entirely new approach to geotechnical or environmental engineering problems and bring in enormous economical benefits to construction industries. The study made so far has shown that soil treated by biocement can have desirable engineering properties as that treated by ordinary cement.

REFERENCES

[1] Ivanov, V., Stabnikov, V., Zhuang, W.-Q., Tay, S.T.-L. and Tay, J.-H., 2005. "Phosphate removal from return liquor of municipal wastewater treatment plant using iron-reducing bacteria". *Journal of Applied Microbiology,* Vol. 98, pp. 1152-1161.

[2] Ivanov, V. and Chu, J., 2008. "Applications of microorganisms to geotechnical engineering for bioclogging and biocementation of soil in situ". *Reviews in Environmental Science and Biotechnology*, Vol. 7, pp. 139-153.

[3] Ivanov, V., Kuang, S.-L., Guo, C.-H. and Stabnikov, V., 2008. "The removal of phosphorus from reject water in a municipal wastewater treatment plant using iron ore". *Journal of Chemical Technology and Biotechnology* (in press).

[4] Ivanov, V., Rezaei, Nejad S., Yi, S. and Wang, X.-H., 2009. "Physiological heterogeneity of suspended microbial aggregates". *Water Science and Technology* (in press).

[5] Lee, M.F. and Oh, X.M., 2007. "Improvement of Geotechnical Properties of Sand Fill using Biotechnological/Chemical Methods". *Final Year Project Report*, Nanyang Technological University.

[6] Mitchell, J.K. and Santamarina, J.C., 2005. "Biological Considerations in Geotechnical Engineering". *Journal of Geotech. Geoenvir. Eng., ASCE,* Vol. 131, pp. 1222-1233.

[7] Ong, F.S. and Hong, Y.S., 2008. "Improvement of Geotechnical Properties of Sandy Soil using Biotechnological Approaches". *Final Year Project Report*, Nanyang Technological University.

[8] Stabnikov, V.P. and Ivanov, V.N., 2006. "The effect of various iron hydroxide concentrations on the anaerobic fermentation of sulfate-containing model wastewater". *Applied Biochemistry and Microbiology,* Vol. 42, No. 3, pp. 284-288.

CATASTROPHIC RISK ANALYSIS OF INFRASTRUCTURE SYSTEMS

Robert, TIONG Lee Kong (CLKTIONG@ntu.edu.sg)
Qi-Yu QIAN (QIAN0012@ntu.edu.sg)

Globally, there is an increasing trend in adopting a Public-Private partnership (PPP) scheme to develop large-scale infrastructure systems. (Shen, Lee et al 1996) At the same time, the losses from catastrophes such as hurricanes, earthquakes, tsunamis and terrorism have increased dramatically in the past 15 years. (Munich 2007) Evidence indicates that, apart from the weather-related events associated with global warming and geopolitical issues related to terrorism, the frequency of catastrophes has not increased, but the scope of social and financial impact has increased dramatically. This is mostly attributable to growing vulnerabilities, which often expand without any progress in risk mitigation or management behavior. Loss growth is largely, if not exclusively, a function of vulnerability growth. Unsustainable urbanization is increasing the city's vulnerability because most of new growth has been generated by its urban economies. (Ryrie 2007)

Infrastructure facilities and systems are pillars supporting economic growth and sustaining the daily life of human being, however, the evaluation and risk assessment of many infrastructure projects focus mainly on "traditional" risk factors, such as construction, technology, law and regulations, demand, interest rate, foreign exchange, inflation and operation. There are little efforts paid to assess the impact of catastrophic risk on the economics (i.e. cash flows) of infrastructure projects and risk management under the PPP schemes.

Nowadays, the risk analysis and management process during the course of infrastructure project development typically does not include catastrophic risks. One reason for this is the assumption that catastrophic risks, as a form of force majeure risks, can be readily transferred to the insurance industry. However, this should not be taken lightly as a default option, since insurance cover: may not be available for certain types of catastrophes (e.g. terrorism) in some countries; available only at a very high cost, particularly during the aftermath of an event; or available but subject to various exclusions, thus rendering the purchase of such coverage economically inefficient. What's more, insurance density/ penetration is low particularly in lower-income or less developed countries (Mechler 2004). As a consequence, the financing of recovery in developing countries often relies on government and multilateral agencies' initiatives. Incidentally, with a lack of public funds in these countries, infrastructure systems are sometimes financed using a PPP scheme (e.g. the BOT mode). In a typical PPP/BOT setting, both public and private sectors are locked into a long-term contractual relationship. The implications of catastrophic events leading to potential loss of functionality of these systems would therefore become even more complex.

To promote better economic efficiency and make the project sustainable, there is a need to re-examine whether project stakeholders can manage such risks in a more involved manner. Catastrophe risk management as one necessary component of risk management must be taken into consideration. A pro forma cash flow model would form a useful basis for quantifying catastrophic risks and measuring the financial vulnerability of the project.

Catastrophic risks may be superimposed onto a set of pro forma cash flows and represented as a potential disruption to the annual cash flows for a specified duration. Resumption of annual cash flows would depend on the expected recovery period. Subsequently, adjustments can be made according to different severities of catastrophes and associated duration of cash flow disruptions and recovery periods. The various degree of severities, timing of catastrophes, duration of disruptions and recovery period would then lead to the generation of different loss financing options. Figure 1 shows the catastrophic risk management framework.

Contractual arrangement of PPP infrastructure projects should be the first step of risk management. Public private partnerships are increasingly viewed necessary as concerted effort to respond to catastrophic risks. For a BOT project, such initiatives can be structured inherently as part of the concession contract, instead of transferring the risks to the insurance sector as a default solution. This may turn out to be more cost effective, since design can be customarily modified to mitigate the risks at the early stage of the project lifecycle. Depending on the insurance loading, the subjective loss of the insured and other insurance contractual details, it is sometimes more effective to absorb rather than transfer the risks to the insurance sector. (Hoshiya et al. 2004)

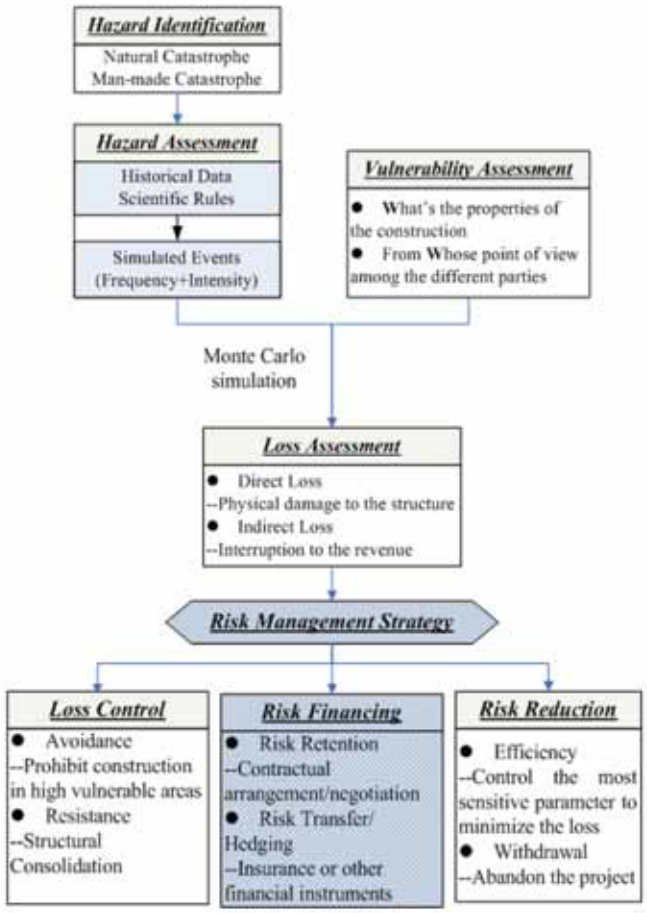

Figure 1. Catastrophic risk management framework

Financing using a combination of ex-ante risk financing instruments and ex post vehicles will fill the relevant liquidity gap after the occurrence of catastrophe events. Catastrophe risk financing instruments can ensure availability of funds during the aftermath of catastrophic events and sustain the operations of the facility or system. However, their costs may greatly exceed expected losses, so it is important to closely examine their benefits and alternatives. To minimize the costs/risks and maximize the benefits from these instruments, an optimal catastrophe risk financing strategy including catastrophe insurance and catastrophe bond, etc should be developed a priori.

This research starts with an introduction of catastrophic risks and special properties of PPP infrastructure projects before drawing the connection to risk quantification and risk management of infrastructure projects under a conceptual framework. The objective of this research is to develop a methodology for assessing the financial impact of catastrophic risks of PPP infrastructure projects and to structure respective catastrophe risk management strategies.

REFERENCES

[1] Hoshiya, M., Nakamura, T. and Mochizuki, T., 2004. "Transfer of Financial Implications of Seismic Risk to Insurance". *Natural Hazards Review,* Vol. 5, No. 3, pp. 141-146.
[2] Munich Re, 2007. 2006 Risk Management Report. pp. 5-12.
[3] Mechler, R., 2004. "Financing disaster risks in developing and emerging economy countries". *Proceedings of the OECD Conference on Catastrophic Risk and Insurance,* Organisation for economic co-operation and development Paris, France.
[4] Ryrie, S., 2007. "Asian Megacities & Catastrophes". *6th Conference on Catastrophe Insurance in Asia, Beijing.*
[5] Shen, L., R.K.H. Lee, et al., 1996. "Application of BOT system for infrastructure projects in China". *Journal of construction engineering and management*, Vol. 122, No. 4, pp. 319-324.

COMPETITION AMONG MAJOR PORTS IN SOUTHEAST ASIA: SLOT CAPACITY ANALYSIS

LAM Siu Lee Jasmine (sllam@ntu.edu.sg)

INTRODUCTION

Container ports in Southeast Asia account for an estimated 30% of the world's transhipment traffic. This large and expanding market has encouraged major container terminal operators in Singapore, Port Klang and Tanjung Pelepas to compete intensively for this business. The study aims to shed light on port competition in Southeast Asia for transhipment containers by an in-depth and quantitative analysis.

SLOT CAPACITY ANALYSIS

The method of analysing slot capacity connected to the ports can generate insightful information on market dynamics. Computation of annualised slot capacity (ASC) for *k* shipping services calling at a port can be obtained with the formula:

$$\sum_{i=1}^{k} ASC_i = \sum_{i=1}^{k} V_i F_i$$

where V denotes average vessel capacity and F denotes the frequency of call in a year.

This research method of analysing ASC can reveal the connectivity of the ports, and the presence, extent and development of port competition in a systematic and quantifiable manner.

MAJOR RESULTS ON SINGAPORE'S MARKET SHARE

By slot capacity analysis, we are able to compute the volumes for parallel calls and exclusive calls at the respective ports. Evidence shows that competition from Port Klang in Selangor and Tanjung Pelepas in Johor – two ports in the most developed states in peninsular Malaysia -- have a negative impact on Singapore's transhipment performance. Although Singapore continues to enjoy a dominant position as the premier transhipment hub in the region in terms of market share by both transhipment throughput and slot capacity, the evidence suggests that its hold on the market appears to be slipping, albeit gradually.

The decline in Singapore's market share is a result of Port Klang and Tanjung Pelepas emerging as credible alternatives for transhipment operations. This has encouraged some shipping lines to relocate their transhipment hubs to these ports from Singapore. Some shipping services drop Singapore and call at Port Klang and/ or Tanjung Pelepas instead. As a result, the two Malaysian ports are able to increase their share of exclusive calls.

Slot capacity analysis can reveal port competition at the trade route level. The establishment of transhipment hubs at Port Klang by some of the world's largest carriers, such as CMA-CGM and China Shipping, results in significant gains of slot capacity calling exclusively at the port on the Europe-Far East, Mediterranean-Far East and Far East-Africa trade routes. The decisions by Maersk and Evergreen to hub their transhipment operations at Tanjung Pelepas result in notable gains of exclusive slot capacity calling at the port on the Europe-Far East, Transpacific, Mediterranean-Far East, Southeast Asia-Australasia and Far East-Middle East trade routes.

MANAGERIAL AND POLICY IMPLICATIONS FOR THE PORTS

Tanjung Pelepas has become the second largest transhipment centre in Southeast Asia within a span of three years. The port has also become the strongest competitor to Singapore for the transhipment pie in the region. Apart from pulling over many mainline services that used to call at Singapore by Maersk and Evergreen, the effort to create a feeder network also eroded, to a certain extent, Singapore's traditional grip on the intra-Southeast Asia, Southeast Asia-Indian subcontinent and Southeast Asia-Australasia trade routes.

Importantly, Tanjung Pelepas and Port Klang are increasingly competitive in narrowing the gap with PSA Singapore in the overall costs of using their terminal services. This has taken those intangible costs such as efficiency and reliability into account. As a whole, good connectivity in terms of shipping network is essential for transhipment ports. We notice the interrelationship between mainline services and the availability of feeder services at a port. Mainline services attract feeders but a perceived insufficiency of feeder services offered by a port will deter mainline services calling at the port.

When the acquisition of P&O Nedlloyd by Maersk was announced in May 2005, Singapore looked set to lose an estimated 1.5 million TEUs to Tanjung Pelepas. However, limited container terminal capacity at the port prevented such a move. Capacity utilisation of Tanjung Pelepas reached 92.7% with 4.2 million TEUs handled in 2005. Nonetheless, the port is trying to expedite capacity expansion to accommodate increasing container traffic.

Furthermore, Tanjung Pelepas also recognises that a sufficient local cargo base is essential as this could achieve two goals: First, it will reduce dependence on foot-loose transhipment cargo; and second, it will attract more shipping lines to call at the port. As such, the port is putting in much effort to grow the share of local containers. Attracting more lines to call at the port is also in line with APM Terminals' strategy to transform Tanjung Pelepas into a common user port.

Nonetheless, Singapore is able to adjust to the new competition by moving away from its traditional stance on common user terminal to one that allows for dedicated facilities by shipping lines. However, the key to Singapore's success in winning the transhipment battle would depend on two developments: One, entrenching existing and winning back major customer lines to Singapore; and two, ensuring adequate capacity to accommodate growing transhipment traffic in an increasingly congested land and sea environment. The challenge is the limited space for both the land side and the sea side. Land reclamation will reduce the available sea space for navigation, while the navigation channels are also increasingly congested.

While Port Klang was able to attract CMA-CGM and China Shipping to hub their transhipment activities at the port, continued success in expanding the share of transhipment containers vis-à-vis Singapore and Tanjung Pelepas would depend on the port's ability to succeed in two tasks. The first is to create and sustain a viable and independent feeder network to support its transhipment hub. The second is to attract other lines to hub their transhipment activities at the port.

The first task is challenging as most common and dedicated feeder operators continue to rely on Singapore as the major source of local and transhipment cargo, in particular, on the smaller trade routes, despite attempts to develop Port Klang as the national load centre by the Malaysian government. Marketing programmes, citing lower costs as compared to Singapore, also have limited success. This suggests that such advantages of hubbing at the port could be outweighed by other disadvantages such as network diseconomies.

As for the second task, events over the past five years have spurred PSA to act to anchor major container shipping lines in Singapore. Hence, persuading lines to hub their transhipment operations at Port Klang would require greater efforts and resources. This would become critical should growth in Port Klang's transhipment demand fail to match up to the supply of new container terminal capacity.

CONCLUSIONS

Overall, there is fiercer competition among Singapore, Port Klang and Tanjung Pelepas. The major container terminal operators in the three ports compete intensively for transhipment. They do so by attracting major container shipping lines that operate along key east-west sailing routes to hub at their terminals. The knock-on effect is to attract other carriers, in particular, common feeder operators to call at the ports. In the long run, the key to success is to sustain a port's connectivity in terms of shipping network.

CONSTRUCTION INDUSTRIAL COMPETITIVENESS: AN ANALYSIS FRAMEWORK FOR THE CHINESE CONSTRUCTION INDUSTRY

Chew Ah Seng David (caschew@ntu.edu.sg)
Li Xianguang (lixianguang@tom.com)

INTRODUCTION

The Construction industry is a major component of an integrated economy, making up a substantial part of every country's GDP and up to 10% national employment (Rezgui et. al 2002). Traditionally, the construction industry in every country has established its unique advantage of competitiveness due to its local conditions. However, with the globalization of the world economy and formalization of international construction market, a country's construction industry faces the double pressure of internal industry structure consolidation and the international competition from the external sources. To understand how well the industry policies are working and the challenges facing the industry, it is important for the government and industry stakeholders to understand the construction industry competitiveness in the context of the globalization. This research aims to explore an applicable framework to analyze the formation mechanism of China's construction industry and its evaluation approach based on multi-industrial competitiveness theory and analysis. A framework based on improved Porter's Diamond model (Porter 1990) is proposed.

DEFINING CONSTRUCTION INDUSTRIAL COMPETITIVENESS (CIC)

Industrial competitiveness is a definition extended from competitiveness, and is generally viewed as an industry's ability to produce or export its goods and services effectively (Reinaud 2005). Although construction industry is often heterogeneous in what it produces, it always employs very similar technologies, equipment and labour to produce the products and services. Since industrial competitiveness is an aggregate subject of firms' competitiveness, and is also a component of national competitiveness, it is important to understand the nature of CIC and its relationships with national competitiveness, firm competitiveness and construction product competitiveness. Fundamentally, construction product and service are the objectives of achieving construction firm competitiveness. A reasonably competitive firm hails from a construction industry with strong competitiveness, which sustains and promotes national competitiveness. From this analysis, the following framework synthesizes the competitiveness system at the product, firm industry and national levels, from simple to complex, as well as from micro to macro, as shown in Figure 1.

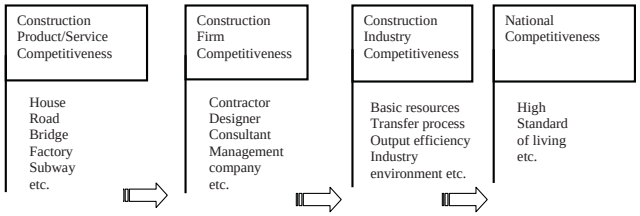

Figure 1. Construction competitiveness at product, firm and industry levels

THEORETICAL FOUNDATION FOR ANALYZING CIC

The modern construction industry has surpassed the elementary stage of competition on production capacity and technical equipment. The competition has been extended in scope to the financing, procurement and operation services, and emphasizes the ability of strategic management and adaptability to new changes. It is suggested that the nature and sources of CIC could be analyzed through application of absolute advantage theory, comparative advantage theory, and new trade theory and competitiveness concept of Porter (1990).

Absolute advantage theory proposes that all nations should produce and export goods for which they possess an absolute advantage and import others which other nations possess an absolute advantage. Applying this idea in construction industry, advanced countries such as the US, Japan and European region have transferred their profitable areas from traditional housing construction to petrochemical, environmental and infrastructure construction, all of which entail high requirement for capital and technology investment. In contrast, China's international construction market share is focused on housing, traditional industrial and irrigation construction works, which reflect China's absolute advantage in cheap human resources.

Comparative advantage theory indicates that each country should choose one or more kinds of construction services with comparative advantage and expand it rather than provide all kinds of construction services. If one country focuses on a specific specialty in construction industry, it may improve its efficiency and finally its competitiveness through economy of scale and better service. However, since the construction industry does not involve many high technologies, it is easy to achieve similar competitiveness by imitating the production and organizational processes. Thus it is difficult for a construction company or nation to maintain its comparative advantage in a special service for the long term.

From the new trade theory perspective, CIC should come from the scale economy and product differentiation. However, the basic characteristic of construction industry is project-oriented and the project location is always changing. It rarely happens that a company has many projects in the same location which could result in economies of scale. More often than not, construction companies improve their competitiveness through product differentiation, such as providing financing or training services, proposing BOT, DBO and other PPP arrangements.

The competitiveness theory of Porter (1990) called the "Diamond" model analyses the competitive strengths of nations and by implication their industries. This theory incorporates four kinds of conditions that determine the competitiveness of construction industry: factor endowment, demand conditions, support industries, and firm strategy, structure and rivalry.

It is generally viewed that the CIC is influenced by both external and internal factors, with the internal factors being more crucial. The internal factors indicate influences which reflect the importance of human resources, industry structure, business process and innovation; the external factors indicate influences which are beyond the control of the construction industry such as government policy and chance events.

FRAMEWORK FOR ANALYZING CIC

As identified earlier, competitiveness includes both the ends and the means towards those ends. The approaches to analyze and measure competitiveness should address not only the performance but also the potentials and process which lead to that performance. This research proposed an improved framework of Porter's Diamond model to analyze CIC through lifecycle factors based on a process view, that is: raw material input ➔ production process ➔ promotion and distribution ➔ adding value and self-improving. The influence factors were classified into four related clusters: resources conditions, production process, output efficiency and industry environment, as shown in Figure 2. This framework empowers the industry's internal factors and performance indicators by respectively enhancing the production process factors and output efficiency indicators, while demand conditions and related industries are incorporated as industry environment.

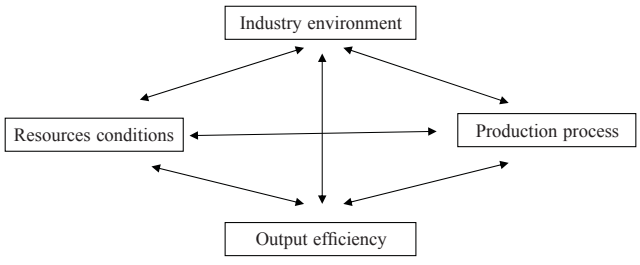

Figure 2. Modified construction competitiveness diamond model

Through analysis of the above four clusters of factors influencing construction competitiveness, this research analyzes and evaluates construction competitiveness along the pathway of "environment ➔ resources ➔ production ➔ output", the nature and relationship of which are shown in Table 1.

Table 1. Analysis hierarchy of CIC

Hierarchy	Object	Content example	Nature
Fourth level	Output efficiency	Production value, added value, tax, profit, etc.	Performance
Third level	Production process	Technology, management, market promotion, etc.	Main body
Second level	Resources conditions	Human resource, capital, equipment, etc.	Precondition
First level	Industry environment	Government role, relative industries, domestic demand, etc.	External factors

Among the four clusters of factors, resources conditions and production process are the main internal factors that directly determine the CIC; industry environment affects the construction industry from the external; output efficiency measures the industry performance that also acts as an enabler for the other factors.

THE CASE OF CHINESE CONSTRUCTION INDUSTRY

Based on theory analysis, a preparatory evaluation indicator system of CIC was proposed and translated into a questionnaire. Interviews with 22 industry practitioners and experts were conducted. A workshop with multidisciplinary expertise was held to improve the system. The final robust sub-factors system including the four clusters of factors (outlined in Figure 2) is shown in Table 2. Although this system is meant for analyzing and diagnosing the development of Chinese CIC, it can also be adapted and used to suit other country's CIC assessment.

The series value of Chinese CIC from 1996 to 2005 evaluated by the system reflects the development of the Chinese construction industry. Overall, weightiness interview results showed that resource conditions are the most important factors influencing the construction, followed by production process factors. Most of the experts interviewed emphasized on the importance of human resources and the industry environment since they determine the technical and management levels of an industry. The results of the evaluated scores for resource conditions and industry environment are shown in Figures 3 and 4 respectively. Figure 5 shows the Chinese CIC from 1996 to 2005.

Table 2. Evaluation indicator system and weightiness

Factors	**1. Resources Conditions**	**2. Production Process**
Indicators	**Human resources** • Amount of employment • Education level of works • Wage level **Equipment resources** • Amount of machines • Per capital machinery • Machinery capacity **Capital resources** • Amount of fixed asserts • Current asserts • Industry liability **Industry structure** • Enterprise amount • Assets amount per enterprise • Industry concentrative ratio	**Technology ability** • R&D investment • Patent amount • Technology innovation **Construction management** • Percentage of eligible projects • Safety management ability • Resources consumption per output • Energy consumption per output **Market promotion** • Domestic market share • International market share • Industry globalization level **Sustainability** • Environment protection practice • Energy efficiency building • Sustainability code
Factors	**3. Output Efficiency**	**4. Industry Environment**
Indicators	**Production scale** • Total production value • Added value • Construction area **Economic return** • Rate of taxes to output value • Rate of gross profits to asserts • Productivity • Average profits **Social benefits** • Amount of taxes • Contribution to GDP • Total social contribution • Environment protection investment	**Government roles** • Industry policy • Free market competition **Domestic economic environment** • GDP • Construction legal system **Domestic demand** • Fixed asserts investment • Ratio of asserts investment to GDP **Support industries** • Main material supply • Status of equipment industry • Total finance for construction industry

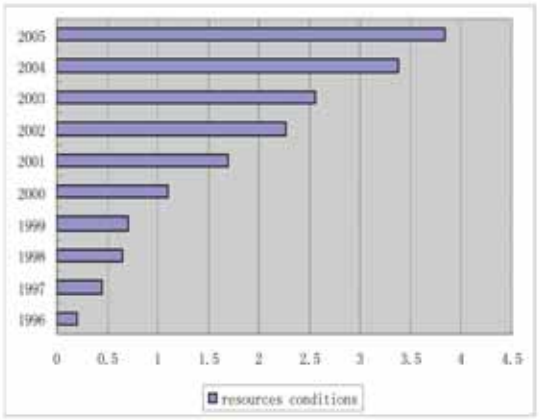

Figure 3. Resource condition score

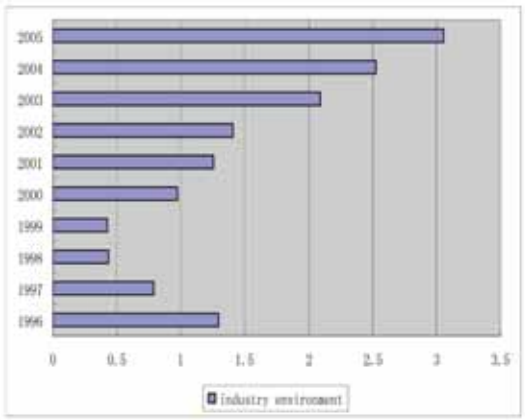

Figure 4. Industry environment score

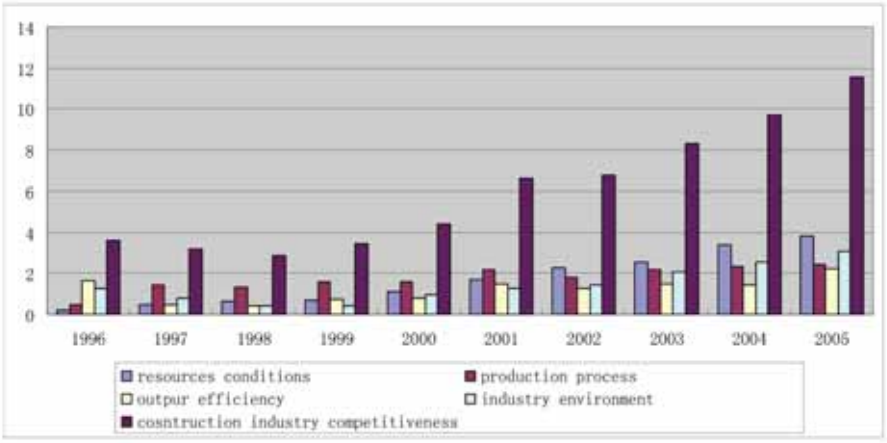

Figure 5. Chinese CIC comparison from 1996 to 2005

Overall, as most of the indicators increased or improved, it is concluded that the Chinese CIC has continually increased since 1998, albeit occasional small fluctuations. Figure 6 shows the historical development trend of Chinese CIC through the spider chart of the key indicators. It is found that most of the indicators decreased in 1998 and the polygon area enclosed by the indicator points in 1998 was smaller than that of 1996, indicating that Chinese CIC has descended during the two years. Figure 6 also shows that Chinese CIC in 2005 is ranked highly since all the secondary indicators has improved respectively.

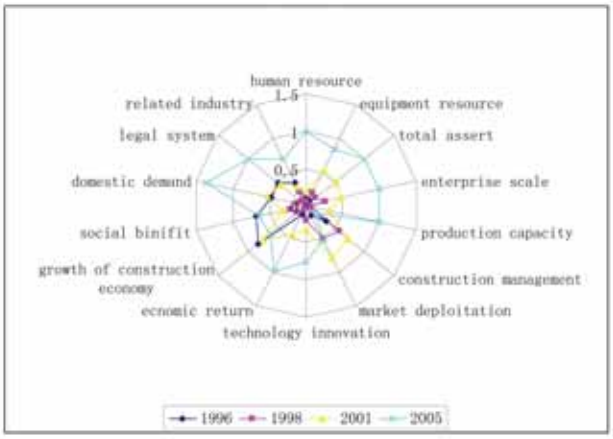

Figure 6. Historical development trend of Chinese CIC

CONCLUSIONS

CIC is the ability of a country's construction industry to utilize the relative resources and transfer them into better market performance, higher client satisfaction and competitive return for industry investors through better construction services. This research suggests a process-oriented, improved construction competitiveness diamond model to analyze the Chinese CIC, using a list of evaluation indicator system to facilitate its assessment. The results show that Chinese construction industry experienced two phases during 1996 to 2005: a descending phase (1996-1998) and an ascending phase (1998-2005). Historical data and interviews show that the evaluation system can reflect the performance and potential construction competitiveness in the real world. It could be used to determine the strengths and weaknesses of a construction industry and help to sustain competitiveness.

REFERENCES

[1] Porter, M.E., 1990. "The Competitive Advantage of Nations". *Macmillan, London*.

[2] Reinaud, J., 2005. "Industrial Competitiveness under the European Union Emissions Trading Scheme". *IEA Information Paper, International Energy Agency Report*.

[3] Rezgui, Y. et. al., 2002. "Enhancing the Competitiveness of the European Construction Industry in the Digital Economy". *ECIS Proceedings 2002, Gdansk, Poland,* pp. 1477-1486.

DETERMINATION OF PERMEABILITY OF UNSATURATED SOIL USING DISK INFILTROMETER

T.T. Nyunt (TH0002NT@ntu.edu.sg)
E.C. Leong (cecleong@ntu.edu.sg)
H. Rahardjo (chrahardjo@ntu.edu.sg)

INTRODUCTION

Permeability function of unsaturated soil is an important property in many geotechnical engineering problems involving unsaturated soils. As direct methods of measuring permeability of unsaturated soils are tedious and time consuming, a number of indirect methods have been developed to determine the permeability function of unsaturated soils (Leong and Rahardjo, 1997a). One of the more rigorous indirect methods is the statistical method which makes use of the saturated permeability and the soil-water characteristic curve (SWCC) of the soil to derive the permeability function (Mualem, 1986). In the statistical method, the saturated permeability is the key parameter in determining the range of the entire permeability function. A more reliable permeability function can be obtained if several values of permeability near saturation can be measured. Permeability of unsaturated soils near saturation is difficult to measure in the laboratory as it is difficult to impose low matric suctions (2 to 5 kPa) on a soil specimen. However, the disk infiltrometer can be used to determine the permeability of unsaturated soil near saturation either in the field or in the laboratory. There are many ways of determining the permeability of unsaturated soils using data from the disk infiltrometer test. The objective of this paper is to critically examine the use of one such method.

PRINCIPLE OF DISK INFILTROMETER

The disk infiltrometer consists of two Mariotte tubes arrangement as shown in Figure 1. One of the Mariotte tubes acts as a water reservoir and also as a means of measuring the rate of water flow through the disk into the soil. The second Mariotte tube with a moveable air tube, known as the bubbling tube, is used to apply the tension on the disk. Tension of 0 to several tens of centimetres of water head can be applied to the disk.

There are generally two methods to analyse the disk infiltrometer tests:
(1) Steady-state flow method, and
(2) Transient flow method.

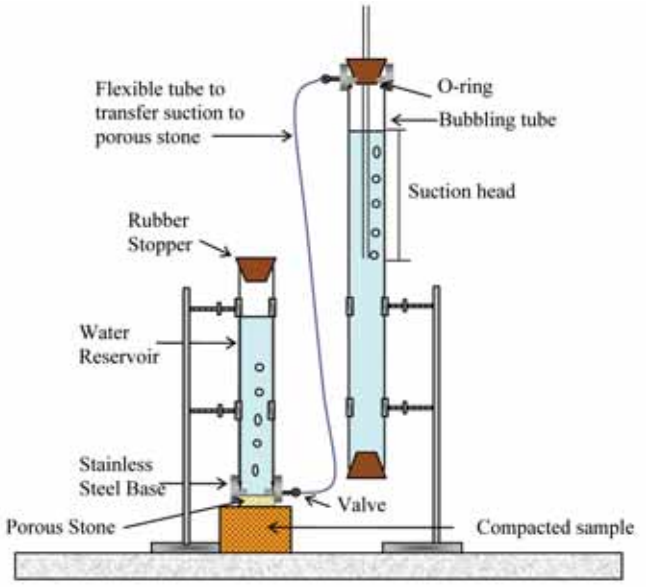

Figure 1. Disk infiltrometer test set-up

In the steady-state flow method, the soil is assumed to be homogenous and isotropic. The initial water content is assumed to be uniform and the permeability at the initial pressure head is much lower than the permeability at the wetting pressure head. The widely used steady-state flux expression is from Wooding (1968):

$$q_{\infty} = k + \frac{4\phi}{\pi R} \quad \ldots (1)$$

where k is permeability, R is the radius of the infiltrometer disk and ϕ can be defined as

$$\phi = \int_{h_n}^{h_0} k(h)dh \quad \ldots (2)$$

and permeability k is expressed as a function of suction head, $h_o \leq 0$ and subscripts 0 and n denote the initial and surface boundary conditions respectively. There are several shortcomings of the steady-state method (Vandervaere et al. 2000):
(1) Assumptions that the soil is homogeneous and isotropic, and the initial water content is uniform do not normally occur, and
(2) The time required to reach steady-state condition may be very long especially for low permeability soils.

For the above reasons, the transient flow method, the subject of this paper, has several advantages over the steady-state flow method. Several expressions were proposed for the transient flow method. Starting from Philip's (1957) equation for one dimensional infiltrated depth, I_{1D}:

$$I_{1D} = S\sqrt{t} + At \quad \text{... (3)}$$

where S is capillary sorptivity, t is time and A is a constant, the equation for three dimensional infiltrated depth, I_{3D}, is modified to:

$$I_{3D} = S\sqrt{t} + (A+B)t \quad \text{... (4)}$$

where B is a term accounting for the side effect due to the axisymmetic flow geometry. Using the work of Turner and Parlange (1974), Smetten et al. (1994) showed that

$$I_{3D} - I_{1D} = \frac{\gamma S^2}{R(\theta_o - \theta_n)}t \quad \text{... (5)}$$

where θ is the initial volumetric water content, subscripts 0 and n denotes initial and surface boundary conditions respectively, γ is a constant and theoretically equal to $\sqrt{0.3}$ when the effects of gravity are neglected at the perimeter of the disk. Based on Equation 3, Haverkamp et al. (1994) developed a physically based infiltration equation for disk infiltrometers that is valid for short to medium test duration:

$$I_{3D} = S\sqrt{t} + \left[\frac{2-\beta}{3}K + \frac{\gamma S^2}{R(\theta_o - \theta_n)}\right]t \quad \text{... (6)}$$

where β is a constant having a value between 0 and 1. Equation 6 can be simplified as follows (Vandervaere et al., 2000):

$$I_{3D} = C_1 t^{1/2} + C_2 t \quad \text{... (7)}$$

where C_1 and C_2 can be expressed as

$$C_1 = S \quad \text{... (8)}$$

$$C_2 = \frac{2-\beta}{3}K + \frac{\gamma S^2}{R(\theta_o - \theta_n)} \quad \text{... (9)}$$

Warrick (1992) and Zhang (1997) also proposed equations similar to Equation 7, but expressions for coefficients C_1 and C_2 were obtained by fitting the non-linear cumulative infiltration-time curve. These parameters are related to sorptivity S and permeability K as follows,

$$C_1(h_0) = A_1 S(h_0) \quad \text{... (10)}$$

$$C_2(h_0) = A_2 K(h_0) \quad \text{... (11)}$$

where A_1 and A_2 are dimensionless coefficients and h_o is the tension value of the disk infiltrometer used during the infiltration process. Soil sorptivity $S(h_0)$ and permeability $k(h_0)$ can be calculated from:

$$S(h_0) = C_1 / A_1 \quad \text{... (12)}$$

$$k(h_0) = C_2 / A_2 \quad \text{... (13)}$$

Using numerical experimental data, Zhang (1997) obtained different empirical equations for coefficients A_1 and A_2 for three SWCC functions: van Genuchten (1980), Gardner (1958) and Zhang and van Genuchten (1994). Leong and Rahardjo (1997b) evaluated the more popular SWCC equations and found that Fredlund and Xing (1994) SWCC equation with the correction factor of unity fits well the experimental SWCC of most soil types. Therefore, only three SWCC functions will be examined: van Genuchten (1980), Gardner (1958) and Fredlund and Xing (1994) with the correction factor of unity. As the focus of this paper is on permeability, only coefficient A_2 will be discussed. The van Genuchten (1980) SWCC equation is given as:

$$\Theta = \frac{\theta_w - \theta_r}{\theta_s - \theta_r} = \left[\frac{1}{1+(\alpha h)^n}\right]^m \quad \text{... (14)}$$

where Θ is the normalised volumetric water content, θ_w is the volumetric water content, θ_s is the saturated volumetric water content, θ_r is the residual volumetric water content, h is the suction head, and α, n and m are constants. Gardner (1958) SWCC function is given by:

$$\Theta = \frac{1}{1+\alpha h^n} \quad \text{... (15)}$$

where α and n are constants. The Fredlund and Xing (1994) SWCC function with the correction factor of unity is given as:

$$\Theta = \frac{1}{\left\{\ln\left[e + \left(\frac{h}{a}\right)^n\right]\right\}^m} \quad \text{... (16)}$$

where e is the natural logarithm number, a, n, and m are constants.

For van Genuchten (1980) SWCC, Zhang (1997) obtained the following expression for coefficient A_2 assuming that $m = 1\text{-}1/n$ and $n > 1$:

$$A_2 = \frac{11.65(n^{0.1}-1)\exp[2.92(n-1.9)\alpha h_o]}{(\alpha r_o)^{0.91}} \quad n \geq 1.9 \quad \text{... (17a)}$$

$$A_2 = \frac{11.65(n^{0.1}-1)\exp[7.5(n-1.9)\alpha h_o]}{(\alpha r_o)^{0.91}} \quad n < 1.9 \quad \text{... (17b)}$$

where h_o (≤ 0) is the pressure head of the infiltrometer and r_o is the radius of the infiltrometer disk.

For Gardner (1958) SWCC, Zhang (1997) obtained the following expression for A_2:

$$A_2 = 1 + \frac{1.388}{\alpha r_0} \quad \text{... (18)}$$

Investigation using permeability data obtained from inverse analyses of disk infiltrometer data by Šimůnek et al. (1998a, b) and Šimůnek (1999) showed that while Equations 17 and 18 gave good agreement with most of the data, the

permeability value may vary greatly for higher applied suction heads for soil types with high air entry value. A typical case for the A_2 value from the van Genuchten (1980) SWCC (Equation 17) is shown in Figure 2. Using the same data, modifications were made to the expressions for coefficient A_2. The modified expressions for coefficient A_2 for the van Genuchten (1980) SWCC and Gardner (1958) SWCC are given in the following equations respectively:

$$A_2 = \frac{(n-1)\exp(0.1n\alpha h_o)}{(\alpha r_o)} \quad \ldots (19)$$

$$A_2 = \frac{(n-1)\exp\left(\alpha^{1/n} h_o\right)}{\left(\alpha^{1/n} r_o\right)} \quad \ldots (20)$$

An expression for coefficient A_2 based on Fredlund and Xing (1994) SWCC was also obtained as follows:

$$A_2 = \frac{(n-1)\exp(0.5h_o / a)}{(r_o / a)} \quad \ldots (21)$$

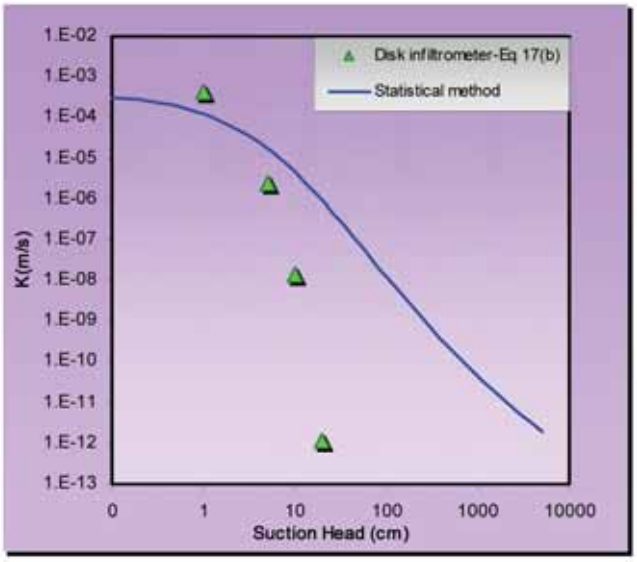

Figure 2. Comparison of permeability of loam (data from Šimůnek 1999)

EXPERIMENTAL VERIFICATION

Saturated permeability tests, pressure plate tests to obtain SWCC and disk infiltrometer tests were conducted on two soils (sandy silt and residual soil). The basic properties of the soils are summarised in Table 1. The soil samples were prepared by static compaction (ASTM D698, 2007) at the same compaction condition (see Table 1). Firstly, for each soil, three compacted soil samples (each 100 mm diameter by 100mm height) were used for the disk infiltrometer test under three different applied suctions from 2 to 20 cm water head. The disk infiltrometer, shown in Figure 1, consists of two acrylic tubes with an internal diameter of 25 mm. The height of the water reservoir is 0.5 m and that of the bubbling tube is 1 m. The water reservoir has a steel base in which a porous disk (25 mm diameter) is fixed. The water reservoir and bubbling tube are connected by a flexible tube from the top of the bubbling tube to the steel base of the

Table 1. Basic properties of soils

Properties	Sandy silt	Residual soil
Specific Gravity, G_s	2.62	2.62
Liquid Limit	56	38
Plastic Limit	32	22
Plasticity Index	24	16
Grain size distribution:		
Clay (%)	11	15
Silt (%)	64	50
Sand (%)	25	35
Optimum water content (%)	26	16
Maximum dry density (Mg/m^3)	1.52	1.77
Compaction condition:		
Water content (%)	21.5	12.2
Dry density (Mg/m^3)	1.47	1.75

water reservoir. The disk infiltrometer was placed on the compacted sample and it was ensured that there was good contact between the porous disk and the soil. The water reservoir and bubbling tube were held in place by retort stands. The disk infiltrometer test results are shown in Figure 3. After the disk infiltrometer test, the samples were trimmed to 50 mm diameter and 50 mm height specimens for the saturated permeability test using a flexible wall permeameter and 50 mm diameter and 25 mm height specimens for the pressure plate tests. The constant head method was applied in the measurement of saturated permeability. Water outflow was collected in a beaker which was placed on a weighing machine. The weighing machine was connected to a personal computer and the changes in weight with time were recorded by the computer. The saturated permeability values of the sandy silt and residual soil are 5 x 10^{-8} m/s and 9 x 10^{-9} m/s respectively. A pressure plate apparatus was used to obtain the SWCC. Five matric suctions of 50, 100, 200, 300 and 400 kPa were applied in order to determine the SWCC. The SWCCs of the sandy silt and residual soil are shown in Figure 4.

The saturated permeability and the SWCC were used to determine the permeability functions of the compacted sandy silt and residual soil via the statistical method. The values of permeability determined from the disk infiltrometer tests using Equations 13, 19, 20 and 21 were compared with the permeability function as shown in Figure 5. Good agreement was found between the values of permeability determined from the disk infiltrometer tests and the permeability functions.

CONCLUSIONS

The disk infiltrometer provides a reliable means of determining the coefficients of permeability near saturation. Modifications were made to the Zhang (1997) equations which were then verified with experimental data on compacted sandy silt and residual soil specimens. The modified equations gave good agreement between the permeability from the disk infiltrometer test and the permeability function from the statistical method.

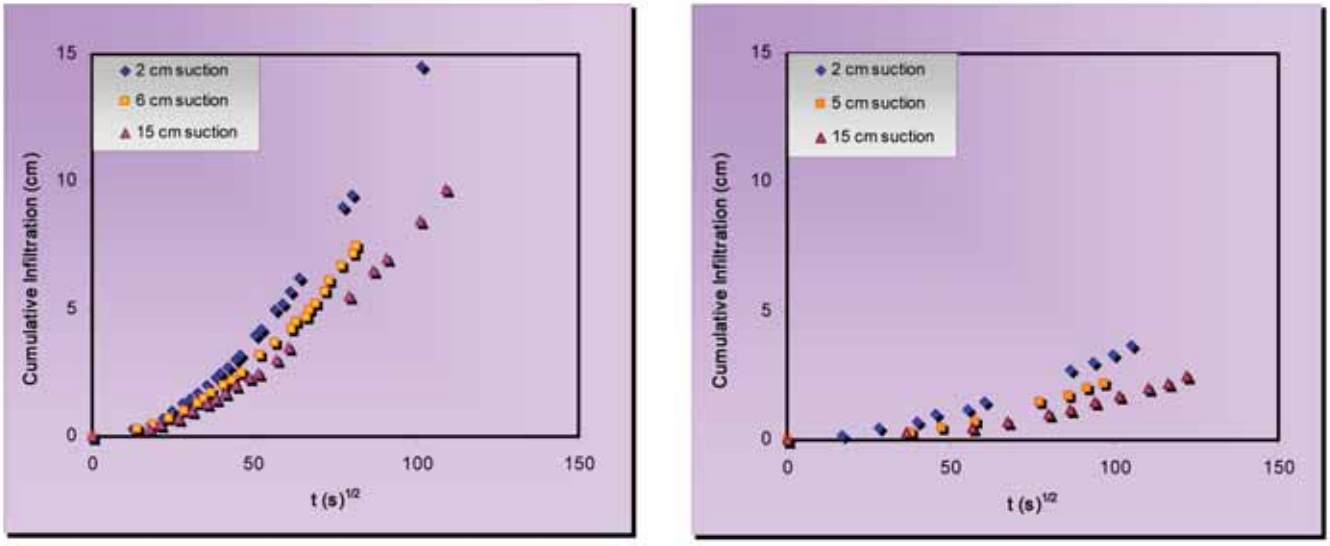

(a) Sandy silt (b) Residual soil

Figure 3. Disk infiltrometer test results

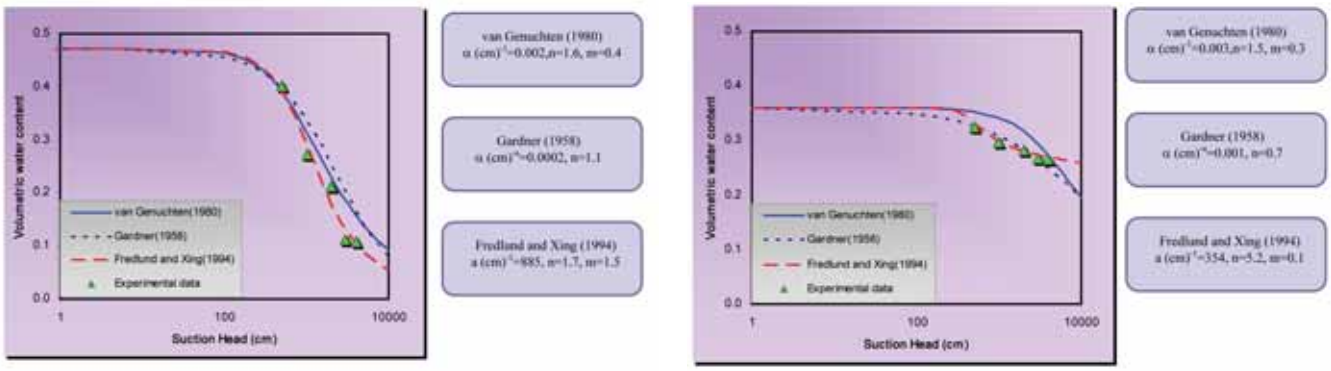

(a) Sandy silt (b) Residual soil

Figure 4. SWCC of Sandy silt and Residual soil

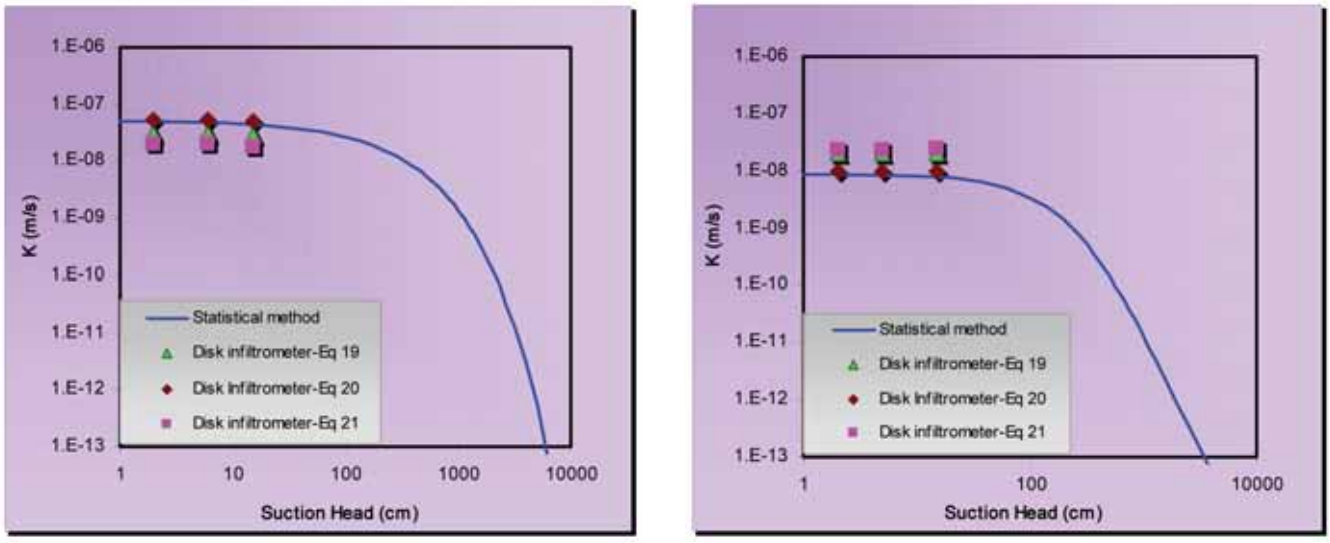

(a) Sandy silt (b) Residual soil

Figure 5. Comparison of permeability results

REFERENCES

[1] ASTM, 2007. "D698 Standard test method for laboratory compaction characteristics of soil using standard effort (12400 ft-lbf/ft^3 (600 kN-m/m^3))." *ASTM Volume 04.08 Soil and Rock (I): D 420 - D 5611, West Conshohocken, PA: American Society for Testing and Materials.*

[2] Fredlund, D.G. and Xing, A., 1994. "Equations for the Soil-water Characteristic Curve." *Canadian Geotechnical Journal,* Vol. 31, pp. 533-546.

[3] Gardner, W.R., 1958. "Some Steady-state Solutions of the Unsaturated Moisture Flow Equation with Application to Evaporation from a Water Table." *Soil Science,* Vol. 85, pp. 228-232.

[4] Haverkamp, R., Ross, P.J., Smetten, K.R.J. and Parlange, J.Y., 1994. "Three-dimensional analysis of infiltration from the disc infiltrometer: 2. Physically based infiltration equation." *Water Resources Research,* Vol. 30, pp. 2931-2935.

[5] Leong, E.C. and Rahardjo, H., 1997a. "Permeability Functions for Unsaturated Soils." *Journal of Geotechnical and Geoenvironmental Engineering,* Vol. 123, pp. 1118-1126.

[6] Leong, E.C. and Rahardjo, H., 1997b. "Review of Soil Water Characteristic Curve Equations." *Journal of Geotechnical and Geoenvironmental Engineering,* Vol. 123, pp. 1106-1117.

[7] Mualem, Y., 1986. "Hydraulic conductivity of unsaturated soils: prediction and formulas." *Methods of soil analysis. Part 1, Physical and mineralogical methods. 2nd Ed., Agronomy, A. Klute, ed. Am. Soc. of Agronomy, Inc., and Soil Sci. Soc. of Am., Inc., Madison, Wis.*, pp. 799-823.

[8] Philip, J.R., 1957. "The theory of infiltration: sortivity and algebraic infiltration equations." *Soil Science,* Vol. 84, pp. 9-703.

[9] Šimůnek, J., Wang, D., Shouse, P.J. and van Genuchten, M.Th., 1998a. "Analysis of field tension disc infiltrometer data by parameter estimation." *International Agrophysics,* Vol. 12, No. 3, pp. 167-180.

[10] Šimůnek, J., Angulo-Jaramillo, R., Schaap, M.G., Vandervaere, J.P. and van Genuchten, M.Th., 1998b. "Using an inverse method to estimate the hydraulic properties of crusted soils from tension-disc infiltrometer data." *GEODERMA,* Vol. 86, No. 1-2, pp. 61-81.

[11] Šimůnek, J., 1999. "Estimating unsaturated soil hydraulic properties from laboratory tension disc infiltrometer experiments." *Water Resources Research,* Vol. 35, pp. 2965-2979.

[12] Smetten, K.R.J., Parlange, J.-Y., Ross, P.J, and Haverkamp, R., 1994. "Three dimensional analysis of infiltration from the disc infiltrometer: A Capillary-based theory." *Water Resources Research,* Vol. 30, pp. 2925-2929.

[13] Turner, N.C. and Parlange, J.-Y., 1974. "Lateral movement at the periphery of a one-dimensional flow of water." *Soil Science,* Vol. 118, pp. 70-77.

[14] van Genuchten, M.Th., 1980. "A closed form equation for predicting the hydraulic conductivity of unsaturated Soils." *Soil Science Society of America Journal,* Vol. 44, pp. 892-898.

[15] Vandervaere, J.P., Vauclin, M. and Elrick, D.E., 2000. "Transient flow from tension infiltrometers: I. The two parameter equation." *Soil Science Society of America Journal,* Vol. 64, No. 12, pp. 1263-1272.

[16] Warrick, A.W., 1992. "Models for disc infiltrometers." *Water Resources Research,* Vol. 28, pp. 1319-1327.

[17] Wooding, R.A., 1968. "Steady Infiltration from a Shallow Circular Pond." *Water Resource Research,* Vol. 4, pp. 1259-1273.

[18] Zhang, R., 1997. "Determination of soil sorptivity and hydraulic conductivity from the disk infiltrometer." *Soil Science Society of America Journal,* Vol. 61, pp. 1024-1030.

[19] Zhang, R. and van Genuchten, M.Th., 1994. "New models for unsaturated soil hydraulic properties." *Soil Science*, Vol. 158, pp. 77-85.

INDOOR 3D MODELLING AND VISUALIZING BASED ON 3D TERRESTRIAL LASER SCANNER

Jia Dongzhen (jiadongzhen@hhu.edu.cn)
Tor Yam Khoon (cyktor@ntu.edu.sg)
Zhong Zheng (zhongz_78@263.net)
Zhou Qi (sevenlaand@hotmail.com)

INTRODUCTION

The 3D Terrestrial Laser Scanner (3DTLS) uses non-contact high-speed laser pulse for measurement of the surface profile of objects and directly acquires their distance and reflection intensity and stores this data in its database. The advanced terrestrial laser scanner can capture 500,000 points per second with point accuracy of 6 mm or better; it is therefore able to acquire high accuracy 3D points within a short period of time.

An entire scan results in collections of these 3D points which are called "point clouds". These point clouds provide the basis for surface reconstruction or modelling. The objectives of this study were to harness the point clouds and extract information from them, and use points, polygons, curves,

surfaces and other graphical primitives to model the real world and visualize it in an virtual environment.

Position and Wireless Technology Centre (PWTC) of NTU was used as the test site. It is about 550-600 square metres. There are about 10 rooms, 100 fluorescent lamps, 80 fire sprinklers and 20 tables. In this paper we present the laser scanning, modelling and visualisation of the 3D structure of the centre.

ACCURACY AND RESOLUTION OF SCANNING

Generally, without taking into account the inherent measuring signal error of the instrument, accuracy of scanning depends mainly on the size of the laser spot and the distance between successive points. The smaller the laser spot and the shorter the scanning distance, the higher will be the accuracy of the scanned point. The 3DTLS used in this study has a point accuracy of 6 mm at 1 sigma as per specification. The accuracy of the modelled object was specified as 2 mm at 1 sigma. The size of the laser spot was 4 mm from 0 – 50 m and the point spacing was fully selectable both horizontally and vertically with less than 1 mm minimum spacing through the full range of 300 m.

The resolution of the scanning, i.e. the distance between the adjacent scanned points, on the other hand, depends on the incident angle and the range of the laser beam. For instance, the resolution of the scanned points on the ceiling and the floor of a room is a function of the incident angle between the laser beam and the plane of the ceiling and the floor. The desired maximum resolution can be achieved by limiting the radius of scanning. As shown in Figure 1, where θ is the angle between two successive incident lasers beam; L & S are the preset range & resolution; h is the distance between horizontal axis of the instrument and ceiling or the floor; R is the limiting scanning radius; r is the maximum resolution of model; the distances between laser scanner and two scanned points are x and y respectively, and $x \approx y$. So, θ can be performed as follows:

$$\theta = r / y \quad \ldots (1)$$

and,

$$\theta = S / L \quad \ldots (2)$$

so,

$$x \approx y = L \cdot r / S \quad \ldots (3)$$

According to the relationship of the right-angle triangle:

$$R = \sqrt{y^2 - h^2} = \sqrt{\left(\frac{L \cdot r}{S}\right)^2 - h^2} \quad \ldots (4)$$

Since L, S, h, r are known or preset/desired values, the maximum value of scanning radius R could be computed. The number of instrument stations for an indoor scanning could thus be planned.

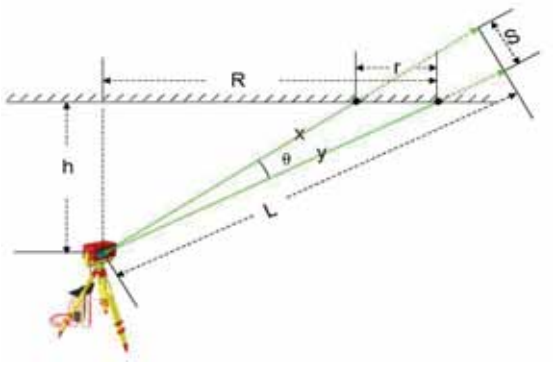

Figure 1. Calculation of scanning radius

DATA ACQUISITION

In order to combine the different scanning scenes into a single coordinate system, it is necessary to acquire some common points, defined by either targets or distinct features, between two adjacent scanner stations.

Although scanning the whole PWTC in high resolution with more scanning stations is feasible, it will consume more time and also acquire superfluous point clouds of little use for modelling. Level of detail (LOD) is a group of models at different scales, which are used to describe one scene or its object. Adopting the same concept as LOD, an initial scanning was done at low resolution of 5 mm to acquire panoramic data, followed by higher resolution of 1 mm to scan key parts, such as the fluorescent lamps and fire sprinklers. This not only meets the accuracy, but also substantially reduces redundant data. Ten sets of point clouds, one from each scanning station, were obtained and stored into a single database. The scanning process lasted one and a half days.

DATA PROCESSING

The ten sets of point clouds, each with its own coordinate system, were required to be aligned into one common coordinate system in a registration process. This process is depicted in Figure 2.

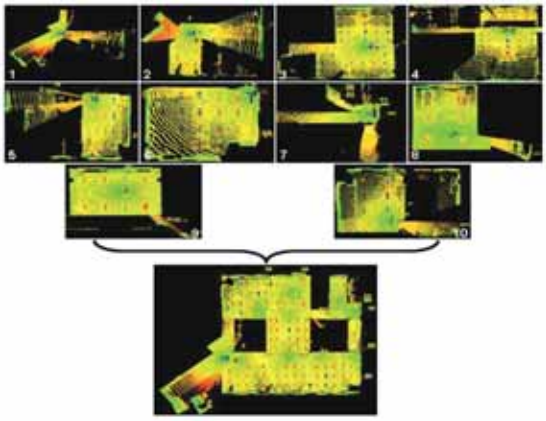

Figure 2. Result of point clouds registration

Point clouds are composed of a number of data including some noise components which comes from surface quality and laser dispersion. Noise removal and smoothing should be done after registration.

Modelling

Point clouds acquired by 3DTLS constitute discrete vector points and this data contains rich characteristic information, but the points do not include any shape and topological relationship. Thus, modelling is usually performed by experienced operators and it requires a skilled technique to get the resultant surface of high quality and precision.

The 3D object model comprises geometric and texture models. Since the most common representations of these objects in 3D models are lines, surfaces and volumes, we used these basic geometric elements as the smallest unit in our model. From the point clouds, these geometric elements are interactively constructed and integrated to complete the model. The work consisted of six main steps:

1. Noises, i.e. spurious point clouds, were removed from the whole scene;
2. The point clouds defining an object were segregated from the whole scene and the object was modelled as line, surface or volume;
3. The modelled object was merged into the original scene;
4. Step 2 and step 3 were repeated till the whole model was completed;
5. The whole model was fine tuned, for instance by intersecting and trimming surfaces, replicating objects etc;
6. The surfaces of the model were textually mapped.

There are five basic models in the modelling of PWTC: wall model, floor and ceiling model, desk model, fire sprinkler and fluorescent lamp model. The entire model is shown in Figure 3. The modelling took about two days.

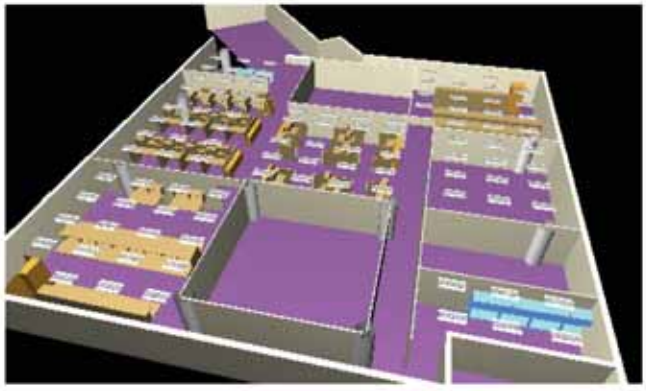

Figure 3. 3D model of PWTC

3D VIEW VISUALIZATION AND INTERACTIVE PLATFORM

Visualization is the basis of human-machine interaction. For the user, it provides the window and the tool to feel the real environment. It can make the user immerse in a 3D scene and to interact with the model.

The work flow of the visualization process consists of three parts: data preparation and preprocessing; establishment of 3D model; and 3D model management and display. The architecture of the system is shown in Figure 4.

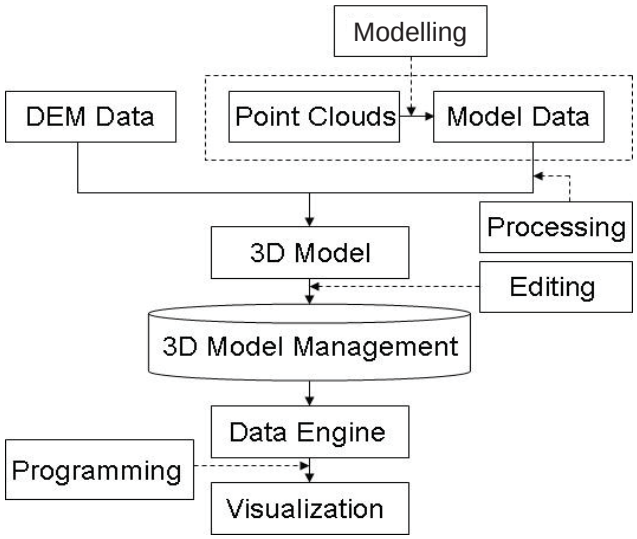

Figure 4. Flowchart of the visualization

A data conversion system was developed with VC++ for 3D model creation, attribute data edition, management and so on. The 3D model of PWTC was converted to 3D geography object library by the conversion system and was applied in the later stage.

The visualization is achieved using the VC++ and OpenGL platform. The platform has features such as multi-angle viewing, walkthrough, spatial query and distance measuring. A 2D navigation map was provided for an intuitive browsing and aid in orientation. An interactive display of the 2D map and the associated 3D scene was implemented. The interfaces are as shown in Figures 5 and 6. Crosses in Figure 6 are the accurate positions of the fire sprinkler.

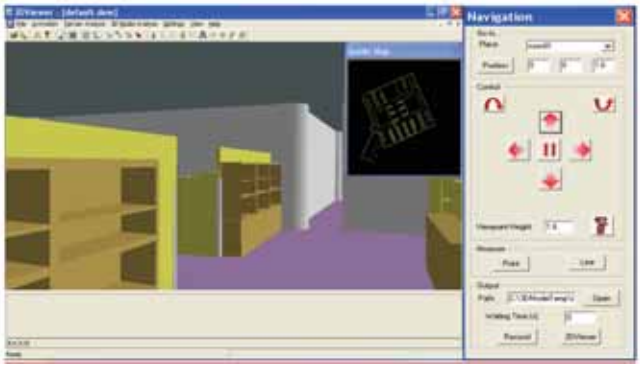

Figure 5. Navigation of 2D map and 3D scene

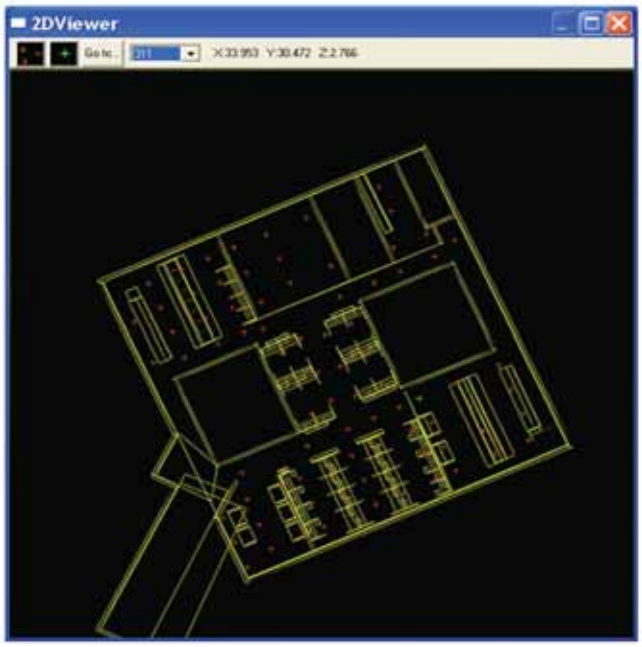

Figure 6. Interface of 2D view

CONCLUSIONS

This paper introduced 3D data acquisition, processing, modelling and visualization using 3D Terrestrial Laser Scanner. For optimum scanning resolution of 3D point clouds, a detailed calculation method of laser scanning radius was presented and applied in this study. Due to different complexity of indoor objects and different accuracy requirements, various scanning resolutions were used to scan the indoor objects. This helped to reduce time and cost to meet the stipulated accuracy. A 3D application platform was developed for the 3D model of PWTC, in which dynamic display of 3D model and an interactive operation were realized.

STATIC COMPACTION OF CLAY MIXTURE

Budi Wibawa (cwibawa@ntu.edu.sg)
Lim Melvin (melvin_lim@singnet.com.sg)

ABSTRACT

Static Compaction of clay mixtures were carried out and compared with that of standard compaction focusing on the energy efficiency. In addition, a null type axis translation testing method was used to measure the initial matric suction of the statically compacted clay mixtures in order to observe the effect of water content on the matric suction. It was observed that the static compaction curve shows only the 'rising' portion and indicates more energy efficiency than that of the standard compaction at relatively high bentonite content of the clay mixture. The effect of water content and bentonite in the clay mixtures on the initial matric suction was also studied.

INTRODUCTION

Waste is buried in landfills that are built into the ground and isolated from the surrounding environment. The isolation of landfills is accomplished with bottom liners and covers of soil to prevent pollution. Compacted clay mixtures are used as the liners and covers for landfills to prevent the infiltration of water to the waste material and evaporation of gases to the atmosphere. Without a good impermeable interface between the waste material and environment, leachate and biogases will be released into the surrounding and atmosphere.

Sand and bentonite, as the clay mixtures, are usually used as the liners and covers of landfills. The sand is mixed with a certain percentage of bentonite which acts as the filler for the void spaces. The smaller bentonite particles are present in pores between the sand granules and when wetted, the bentonite swells and seals the pores, forming a 'tight' soil matrix. Kenny et al. (1992) found that many void spaces of the mixtures did not contain bentonite when the bentonite content was less than 7.4% leading to inadequate distribution of bentonite in the mixture.

The clay mixture needs to be compacted to ensure adequate strength under future loadings. As a standard to check the quality of the field compaction of the clay mixture, a standard laboratory compaction has been established. Although the laboratory compaction testing is often conducted using the standard compaction method, a simpler method, i.e. static compaction, will be introduced as an alternative testing method. The static compaction is done by confining the loose soil mixture in a container and the compaction is achieved by gradual compression of a piston. However, the efficiency of the static compaction of clay mixtures is still not clear.

Matric suction is one of the characteristics of the compacted clay mixture. Matric suction is related with the ability known as capillary action caused by the attraction between the molecules of the liquid by various intermolecular forces. Olsen and Langfelder (1965) found that as the dry density, ρ_d increases, the negative pore water pressure of the soil becomes more negative. In addition, they found that matric suction in the compacted state is related to water content, i.e. the lower the water content, the higher the matric suction. However, the matric suction of clay mixtures by the static compaction still needs to be clarified.

Therefore, the objectives of this paper are firstly, to investigate the energy efficiency of static compaction method compared to that of standard proctor; secondly, to observe the effect of water content on the energy of static compaction; and thirdly, to study the effect of water content on the initial matric suction of clay mixtures.

EXPERIMENTS AND RESULTS

Materials and Method

The clay mixtures consisting of sand and various bentonite contents were used for the experiments. The sand from Changi Beach, Singapore is predominantly fine sand with the effective diameter of 0.16 mm. The index properties of the bentonite from American Petroleum Institute (API) are: Liquid Limit of 247.5%, Plastic Limit of 80.1% and Shrinkage Limit of 47.2%.

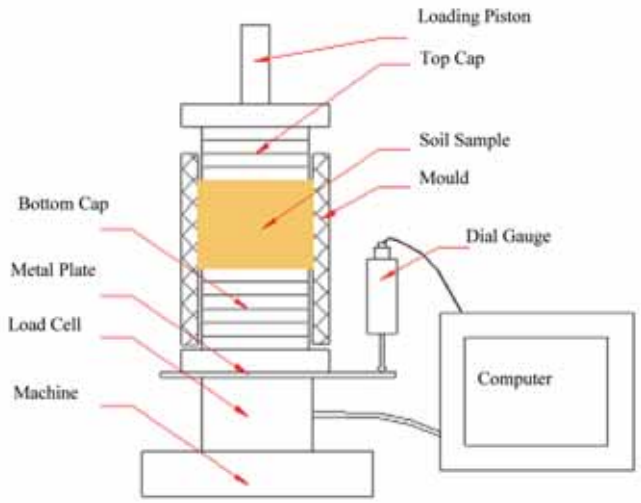

Figure 1. Typical Static Compaction Set-up

Figure 1 shows the experimental set-up using clay mixture as the soil specimen in the static compaction test. The standard compaction test was carried out in accordance with ASTM D698-00 for the clay mixtures. In addition, the static compaction tests under various molding water contents were carried out with 10%, 15% and 20% of bentonite content using the set-up above. Furthermore, the matric suction of the clay mixture specimens was measured by the null-type axis translation method.

Force vs. Displacement in the Static Compaction

Figure 2 shows a typical force versus displacement of the clay mixture with 90% sand and 10% bentonite mixture during a static compaction. Figure 2 indicates that the slope of the curve tends to be gentler initially, and the gradient becomes steeper as the displacement increases. This was as expected; as the clay mixture hardens it becomes more difficult to reduce the available voids for the compaction. The objective of obtaining the force vs. displacement curve is to obtain the energy required to compress the soil to a pre-determined dry density for particular water content. The curve also provides information that the necessary force to produce the same displacement is significantly higher than that of the pure bentonite (Wibawa and Chan, 2008).

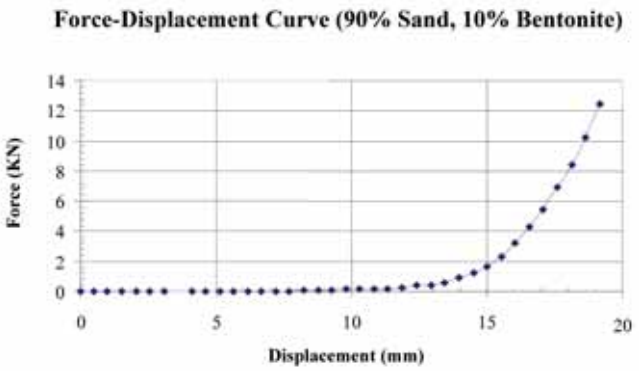

Figure 2. Typical Force vs. Displacement of 90% sand and 10% bentonite mixture

Maximum Dry Density in the Standard Compaction

Referring to the result of the standard compaction, the clay mixture with 20% bentonite content indicates the relatively high dry density $(\rho_d)_{max}$ and the lowest optimum moisture content than that of 10% and 15%. It was observed that the $(\rho_d)_{max}$ of the clay mixture increases with the bentonite content, which is similar to the findings by Kenny at al. (1992) and Howell et al. (1997). This is probably due to the more bentonite particles filling the void spaces between the sand particles with the increasing bentonite content.

DISCUSSION AND ANALYSIS

Static vs. Standard Compaction

The compaction curves of the static and laboratory standard compaction show different characteristics. Firstly, Reddy and Jagadish (1993) emphasized the difference between the compaction curves, especially beyond the optimum moisture content (OMC). As shown in Figure 3, they noticed that the static compaction curve showed only the 'rising' portion and the point at which it terminates was stated to be the maximum dry density $(\rho_d)_{max}$ that was reached for that particular compaction effort. The compaction curve of the clay mixture in the standard compaction, however, indicates a bell-shaped curve (see Figure 3). The soil does not go through any consolidation process in the standard compaction test; therefore, any increase in water content

above the OMC will not further compact the soil and hence, the 'dropping' portion of the curve.

On the other hand, the soil sample undergoes consolidation after the OMC in the static compaction test. As such, any dry density, ρ_d, beyond the OMC is ambiguous as it does not reflect the actual ρ_d, causing a halt to the compaction curve. In other words, the $(\rho_d)_{max}$ should be close to that of the 100% saturation for the static compaction.

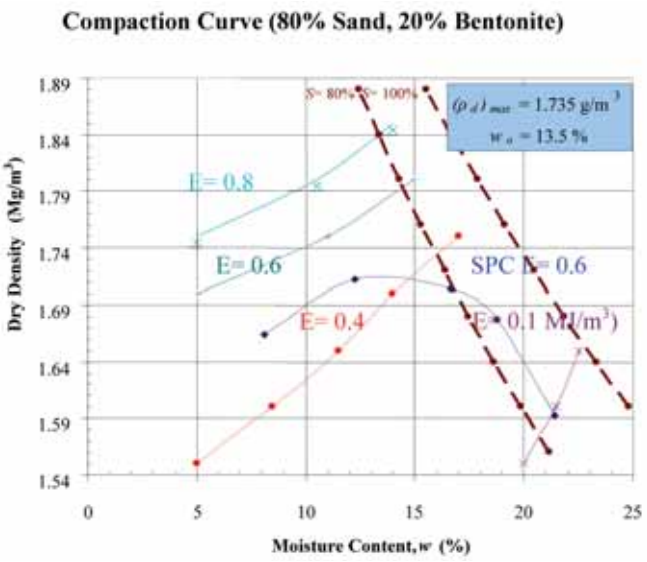

Figure 3. Static Compaction vs. Standard Compaction Tests for 80% sand and 20% bentonite mixture (E in MJ/m³)

Secondly, Figure 3 shows the dry density versus water content of 80% sand and 20% bentonite mixture for various compacting energy in the static compaction tests. Figure 3 indicates that the energy of the static compaction of this particular composition is a little more efficient than that of the standard compaction (0.6 MJ/m³) as the static compaction of the same energy produces the relatively higher dry density with the same water content. This is consistent with Reddy and Jagadish's findings (1993) where static compaction is relatively more efficient than standard compaction.

However, the above trend was not found to be consistent for the 10% and 15% bentonite content in the clay mixture. This is probably due to insufficient distribution of bentonite content in the static compaction test (Kenny et al, 1991). In short, the findings seem to point to the static compaction being more energy efficient than the standard one with a relatively higher bentonite content, i.e. 20%, thus revealing the influence of the bentonite content on the efficiency of the statically compacting energy.

Effect of Moisture Content on Compacting Energy

Figure 4 shows the relationship of the compacting energy of the static compaction and the water content for various dry densities of 90% sand and 10% bentonite. Firstly, it is obvious that the compacting energy increases as the dry density becomes higher as more energy is necessary to densify the soil. Secondly, all the curves indicate a downward trend with increasing water content, that is consistent with the findings of Reddy and Jagadish (1993) where the increase in static compaction energy leads to a reduction of the optimum moisture content for any target dry density. This is probably because the water serves as a lubricant, softening clay bonds and reducing surface tension forces within the clay mixture, thus making them easier to move about and reoriented into a denser configuration. In addition, the above trends also apply to 15% and 20% bentonite content in this research and the compacted pure bentonite (Wibawa and Chan, 2008).

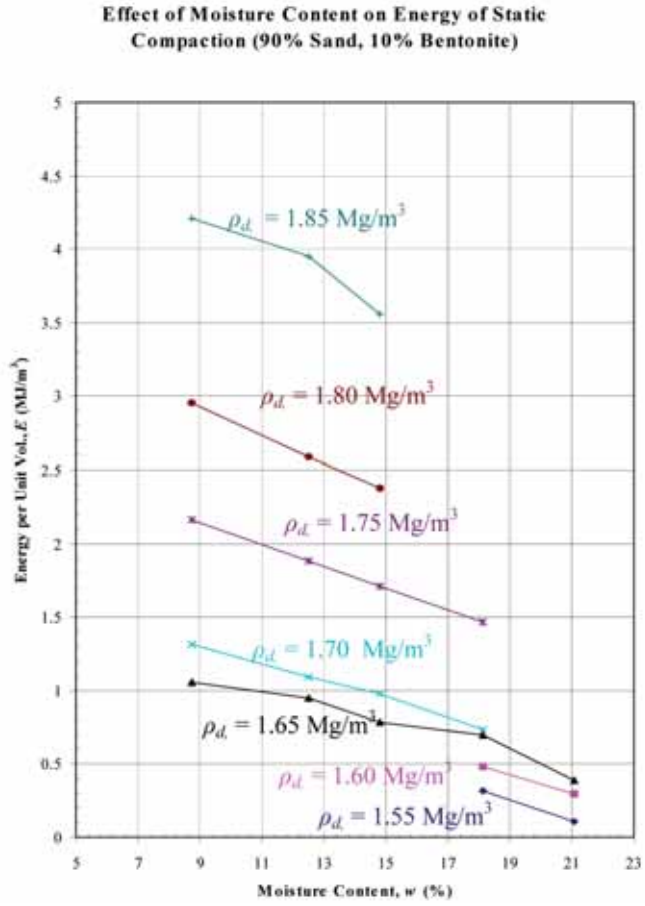

Figure 4. Compacting Energy vs. Water Content in a Static Compaction of 90% sand and 10% bentonite mixture

Effect of Moisture Content on Initial Matric Suction

Figure 5 shows the water content versus the initial matric suction of the clay mixtures with 10%, 15% and 20% bentonite content. Figure 5 indicates that a typical trend of the initial matric suction, decreasing with the increasing water content, is consistent with the results observed by Vatsala and Murthy (2002). According to Olson and Langfelder (1965), the voids in the mixture are nearly filled with water, making the meniscus relatively flat under higher water content. However, the meniscus starts to form under the lower water contents, thus implicating the reduction of the radius of the meniscus, and causing the pore-water pressure to become more and more negative.

Effect of Bentonite Content on Initial Matric Suction

Figure 5 also indicates that the higher bentonite content in the clay mixture will result in the higher initial matric suction for the same water content. With the increase in the bentonite content in the clay mixture, more voids between the sand particles can be filled with bentonite, thus resulting in a smaller pore radius and hence generating higher matric suction (Olsen and Langfelder, 1965). The significantly high initial matric suction was also found in statically compacted pure bentonite, thus confirming such an effect of bentonite content on the generation of the matric suction (Wibawa and Chan, 2008).

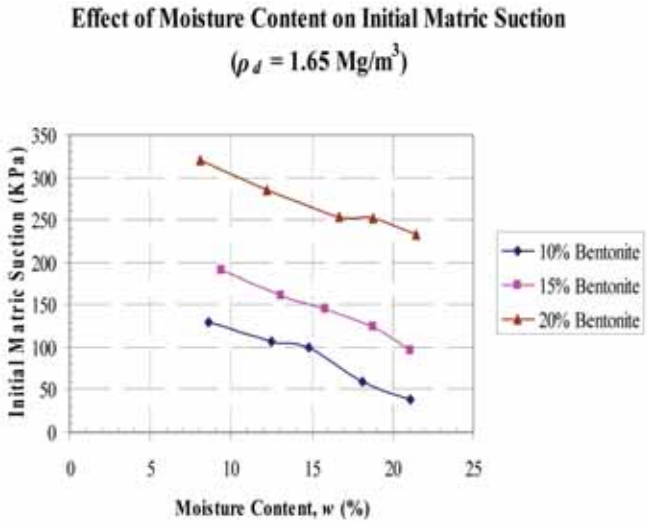

Figure 5. Initial Matric Suction vs. Moisture Content at ρ_d = 1.65Mg/m^3

CONCLUSIONS

1. The static compaction curve of the clay mixtures shows only the 'rising' portion, whereas the compaction curve in the standard compaction shows a bell-shaped curve.
2. The compacting energy of the static compaction for the same dry density indicates a downward trend with the increase in water content. The static compaction is probably more energy efficient than the standard one at higher bentonite content, e.g. 20% of the clay mixture, thus revealing the influence of the bentonite content on the efficiency of the compacting energy.
3. The higher bentonite content in the clay mixture will result in the higher initial matric suction and the initial matric suction decreases with the increase in water content.

REFERENCES

[1] Howell, J.L, Shackelford, C.D., Amer, N.H. and Stern, R.T., 1997. "Compaction of Sand-Processed Clay Soil Mixtures." *Geotechnical Testing Journal*, Vol. 20, No. 4, pp. 443-458.

[2] Kenny, T.C., van Veen, W.A., Swallow, M.A. and Sungalia, M.A., 1991. "Hydraulic Conductivity of Compacted Bentonite-Sand Mixtures." *Canadian Geotechnical Journal*, Vol. 19, No. 3, pp. 364- 374.

[3] Olson, R.E. and Langfelder, L.J., 1965. "Pore Water Pressures in Unsaturated Soils." *Journal of Soil Mechanics and Foundation Div., Proceedings of the American Society Civil Engineers*, Vol. 91, pp. 127-160.

[4] Reddy, B.V. and Jagadish, K.S., 1993. "The Static Compaction of Soil." *Geotechnique*, Vol. 43, No. 2, pp. 337-341.

[5] Wibawa, B. and Chan, W.M., 2008. "Static Compaction of Bentonite." *Civil Engineering Research, Nanyang Technological University. Singapore,* No. 21, pp. 54-56.

[6] Vatsala, A. and Murthy, B.R.S., 2002. "Suction in compacted states". *Geotechnique*, Vol. 52, pp. 279-283.

AIC BASED ENSEMBLE NEURAL NETWORK FOR MUDSTONE MODELLING

Zhang Yun (zh0002un@ntu.edu.sg)
Zhao Zhiye (czzhao@ntu.edu.sg)

INTRODUCTION

The artificial neural network (NN) is a computational model for information processing which is based on biological neural networks[1]. An ensemble NN usually includes several component networks in its structure, and each component network commonly uses a single feed-forward network. The design of the ensemble NN architectures is a challenging multi-criterion optimization problem, since the architecture of an ensemble NN has a significant impact on its generalization capability. In this paper, an ensemble NN, which combines the component networks by using the Akaike Information Criterion (AIC)[2,3], is proposed. The AIC based ensemble NN searches the best weight configuration of each component network first, and then uses the AIC as an automating design tool to search the best combining weights of the ensemble NN. A material modelling problem - the stress-strain-time relationship of the mudstone - is used to assess the accuracy of the proposed ensemble approach. The computational experiment has verified that the proposed AIC based ensemble NN outperforms both the simple averaging ensemble NN and the standalone single NN.

DESIGN ENSEMBLE NEURAL NETWORKS USING AIC

In an ensemble network, there are a finite number of component NNs. Each component network provides a solution to the same task, and better generalisation can be obtained by combining the component NNs[4]. A typical architecture of the ensemble NN is shown in Figure 1.

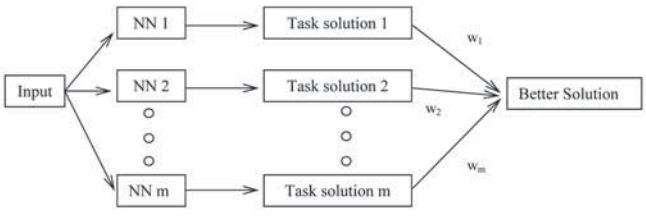

Figure 1. Architecture of the ensemble NN

In general, an ensemble NN is constructed in two parts: creating component networks and combining component networks in the ensemble NN. The major steps of the proposed AIC based ensemble NN are shown in Figure 2.

Creation of the component network can be divided into two steps. The first step is to create the training data and testing data, and the second step is to create the component networks. Since the AIC is adopted as a measurement of model accuracy, one should ensure that the same data set is used for each model to make the AIC comparison meaningful.

The back-propagation neural networks (BPNNs) are adopted in this research to create the component NNs making each component NN a BPNN. The BPNNs are multi-layer feed-forward networks combined with a back-propagation learning algorithm. It should be noted that the randomly assigned initial weights in each component NN may result in different performances. The criterion to choose the best

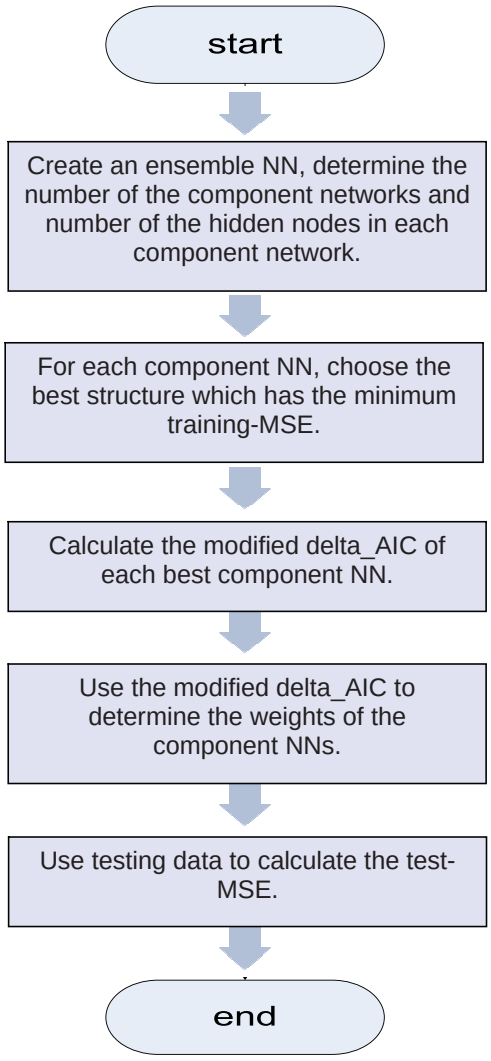

Figure 2. Flowchart of the AIC based ensemble NN

weight configuration of the individual component network is the one with the smallest training mean squared error (MSE). Since good regression ensemble members must be both accurate and diverse, different number of hidden nodes will be used in different component networks.

Considering the network's accuracy and the model's complexity, the AIC is used to combine these best component networks. The AIC is an information criterion for the identification of an optimal model from a class of competing models. The AIC belongs to the indirect approaches since it penalizes the model complexity [2].

The formula for the AIC calculation is given by

$$AIC = n\log(\hat{\sigma}^2) + 2K \quad \ldots (1)$$

where $\hat{\sigma}^2 = \sum \varepsilon_i^2 / n$; n is the sample size; ε_i is the estimated residual for a particular candidate model; and K is the number of estimated parameters in the model (i.e., number of variables and the intercept). In an ensemble NN, the K value can be directly determined by each component network structure, i.e., the number of weights and biases in the NN model plus one for $\hat{\sigma}^2$.

Since the model with the smallest AIC value is the optimal model, the weights should be inversely proportional to the AIC values. Due to the different complexity and accuracy of the component network, the AIC value of the component network may appear positive or negative in the same ensemble NN. To avoid negative values, the delta_AIC, which is a measure of each model relative to the best model, will be used to assess the performance of each component NN.

In a regression analysis, the range of Delta_AIC (Δ_i) in general is quite small due to the small variation of the number of parameters. For a typical regression model, a $\Delta_i < 2$ suggests substantial evidence for the model, $3 < \Delta_i < 7$ indicates that the model has considerably less support, whereas a $\Delta_i > 10$ indicates that the model is very unlikely. However, due to the large number of parameters, the range of Δ_i in the NN is usually very large, so the common rules used for the regression analysis can not be used directly. Otherwise, many component networks will have very small (approach to zero) weights, and will lose their networks' contributions to the ensemble NN. Therefore, a modified AIC measurement is proposed to determine the component network's weights in this paper.

To consider the contributions of all the component networks to the ensemble NN, a modified delta_AIC is proposed as follows:

$$(\Delta_m)_i = 1 + \frac{\Delta_i - \Delta_{\min}}{\Delta_{\max} - \Delta_{\min}} \cdot \beta \quad \ldots (2)$$

where $\Delta_{\min}$ and $\Delta_{\max}$ are the delta_AIC value of the best and worst component network respectively; $(\Delta_m)_i$ is the modified delta_AIC value of the ith component network; and β is a constant. The value of β determines the range of the modified delta_AIC. A small β represents a more uniform Δ_m distribution, whereas a large β value corresponds to a more diverse Δ_m distribution. Since β is a measure of diversity, it is proposed to be defined as the ratio of the maximum diversity value of the component network to the minimum diversity value of the component network. The diversity of the component network is calculated by training data. Given that all the weights sum to one, and each weight is not more than one, the AIC-based weights of the component networks can be found. More details on the determination of the weights for the ensemble NN can be found in [3].

COMPUTATIONAL EXPERIMENTS

To verify the performance of the ensemble NN proposed in this paper, a material modelling problem - the stress-strain-time relationship of the mudstone - was applied. For comparison purposes, a simple averaging ensemble NN that combine the component networks with the uniform weights and a single NN were also implemented.

The strain softening behaviour is an important aspect of soil properties. Many material models have been proposed to describe the stress-strain relationship after the peak strength of the soil-like materials. For mudstone (or soft rock), a modified Cam Clay model has been used to estimate the stress-strain-time relationship[4]. The nonlinear constitutive law of soft rock is very complex, especially when the strain rate effect is considered. Therefore, it is not convenient to build a mathematical expression of the stress-strain-time relationship. Being a flexible modelling tool, the artificial NN provides an excellent alternative to establish the material model based on the experimental data.

In general, there are four key parameters in the stress-strain-time relationship: strain ε, mean effective stress p'), deviator stress q and strain rate $\dot{\varepsilon}$. So the proposed ensemble NN model aims to build a functional relationship of $q = f(\varepsilon, \dot{\varepsilon}, p')$, namely three inputs and one output. In order to compare the performance of the proposed AIC based ensemble NN, the other two NNs (single NN and Ave-ENN) were also used for simulations.

Triaxial experiments were conducted on diatomaceous mudstones [5]. The mudstone samples have the following properties: specific gravity $2.183\ g/cm^3$, natural water contents 119.6%, liquid limit 172.7%, plastic limit 94.7 and compressive index 1.458. The cylindrical specimens have a diameter 5 cm and height of 10 cm. The specimens were completely saturated. The consolidated and undrained triaxial tests were carried out under strain rate from 0.0044%/min to 1.75%/min, and the consolidation pressure was 2.5MPa. In total, there are 204 sets of experimental data. Two third of the experimental data (i.e. 136) were chosen as the training data, and the remaining one third (i.e. 68) was used for NN testing. The maximum training epoch of each network was set to 30.

After a series of trail and error, it was found that 12 is the optimal hidden nodes for the single NN. In the other two ensemble NNs, there are 4 component networks. The numbers of hidden nodes in the component networks are 3, 6, 9 and 12 respectively. Each component network was trained 5 times randomly to find the best weight configuration. Then, the AIC value of each best component network was calculated to determine the component weights in the AIC based ensemble NN. The uniform weights were adopted to the simple averaging ensemble NN. The single NN uses the best result from the 5 random runs.

The statistical performance of the MSE on the training data set and the testing data set of 20 runs for these 3 different NNs are shown in Table 1. It can be observed that the proposed ensemble NN can provide better accuracy than that by the other two methods. Thus, the result of this example demonstrated that the AIC based weighted ensemble NN outperforms the single NN and simple averaging ensemble NN.

Table 1. Results of twenty runs on mudstone modelling

		Single	Ave-ENN	AIC-ENN
Test-MSE	Minimum	1896.0	1970.9	1782.4
	Mean	2774.9	2543.1	2266.0
	S.D.	564.8	586.9	432.7
Train-MSE	Minimum	556.4	277.7	449.0
	Mean	751.2	360.5	747.1
	S.D.	71.1	67.3	203.5

CONCLUSIONS

Determination of model complexity in an NN is crucial in NN design. This paper aimed to use AIC to balance the model complexity with model accuracy. Using AIC to combine these best component networks enabled us to balance the ensemble network's accuracy and penalize the model's complexity, and helped to create a simple, accurate and stable ensemble NN.

The material modelling example presented shows the potential of the proposed ensemble NN for practical applications. This study has shown some promising results, and a follow-up study is under way to further enhance the applicability of the proposed AIC based ensemble neural networks.

REFERENCES

[1] McCulloch, W.S. and Pitts, W., 1943. "A logical calculus of the ideas immanent in nervous activity". *Bulletin of Mathematical Biophysics,* Vol. 5, pp. 115-133. *Reprinted in Anderson & Rosenfeld [1988],* pp. 18-28.

[2] Akaike, H., 1973. "Information theory and an extension of the maximum likelihood principle". *2nd International Symposium on Information Theory*, pp. 267-281.

[3] Zhao, Z., Zhang, Y. and Liao, H., 2008. "Design of ensemble neural network using the Akaike information criterion". *Journal of Engineering applications of artificial intelligence,* Vol. 21, No. 8, pp. 1182-1188.

[4] Sharkey, A. (Ed.), 1999. "Combining Artificial Neural Nets: Ensemble and Modular Multi-Net Systems". *Springer, London.*

[5] Liao, H., Ning, C., Akaishi, M. and Zhou, L., 1998. "Effects of the time-dependent behavior on strain softening of diatomaceous soft rock". *Journal of Metals and Materials,* Vol. 4, No. 5, pp. 1093-1096.

AN OVERVIEW OF TUBULAR JOINT RESEARCH AT NTU IN THE PAST 10 YEARS

Chiew Sing Ping (cspchiew@ntu.edu.sg)
Lee Chi King (ccklee@ntu.edu.sg)
Lie Seng Tjhen (cstlie@ntu.edu.sg)

INTRODUCTION

This article summarizes the research works and the findings discovered by the authors' research group in the past ten years on the topic of fatigue performances of tubular connections. These projects embraced both experimental and numerical studies on a number of welded tubular connection types. Research efforts had been directed to study the fatigue performances of different tubular joint types and to develop research methodologies, modelling tools and assessment procedures that are applicable to different types of commonly used tubular joints. Based on the research outcomes of these studies, important findings and parameters that critically affect the fatigue performance of tubular connections are presented. In addition, some potential areas for further extensions of the presented works are suggested.

MAIN STUDY PROCEDURE AND SCOPE OF WORKS

The procedure for studying a given joint type consists of two main components, namely, the *experimental component* and *the numerical component* that complement each another. The experimental component could be divided into three phases, namely, the *planning phase*, the *testing phase* and the *analysis phase*. The planning phase mainly involves the selection of section geometry and connection type that could be handled by the dynamic testing frame (the "orange rig") in the construction technology laboratory of NTU (Figure 1). This orange rig which is equipped with three independent dynamic actuators allows tests on planar T/Y/K circular hollow section (CHS) and rectangular hollow section (RHS) joints to be conducted up to maximum section size and thickness of 400mm and 25mm respectively. In the test phase, both *static test* and *fatigue test* were conducted. The static test allows the researchers to obtain responses of the uncracked joint under different loading conditions. The fatigue test needs the longest time to complete as more than one million cycles of cyclic loading are often needed to fail a joint[1]. During the fatigue test, the alternating current potential drop (ACPD) technique was employed to monitor the crack growth rate along the weld profile and the penetration rate through the thickness of the section. In the *analysis phase*, the cracked joint is opened up along the cracked region for measurement of the length, depth and profile of the final crack. A simple clay moulding method[1] was used to capture the shapes of the crack surface and mouth for subsequent finite element (FE) modelling. In addition, by processing the ACPD results, the relationship between the crack depth a and the number of loading cycles applied, N was established and the Paris' law[2]

$$\frac{da}{dN} = C(\Delta K)^m \quad \ldots (1)$$

was employed for the estimation of the stress intensity factor (SIF) along the crack mouth. In Eqn. (1), C and m are two material parameters from the section supplier. ΔK is the range of the SIF in one loading cycle.

Figure 1. The "Orange" rig in NTU.

For the numerical components, two main parts, namely, the *modelling of uncracked and cracked joints*, and *development of analysis tools and assessment methods,* are involved. During the modelling of uncracked and cracked joints, the following procedures were employed:

(1) Construction of geometrical models for the uncracked and cracked joints.
(2) Implementation of FE model generation tools for large scale parametric FE study.
(3) Verification of the modelling results against experimental measurements.

In the development part, conclusions for the study are given and the following design aids were developed:

(1) Prediction tools of stress concentration factor (SCF) and hot spot stress (HSS) values for uncracked joint and SIF for cracked joint.
(2) Computation procedures for residual fatigue life prediction of a cracked joint.
(3) Assessment of failure for the cracked joint.

JOINT TYPES STUDIED

Table 1 lists out the research projects completed in the last ten years. Note that at least two full scale specimens were tested in all studies. The study period listed in Table 1 included the time for both experimental and numerical components. The projects are tabulated in chronological order so that the increase in complexity of the joint type studied and the overlapping of the study periods can be seen. Such overlapping schedule was to optimize the use of the test rig so that when the experimental component of one project was completed and the numerical component was started, the test rig could be continuously used for the next project.

Table 1. Projects completed from 1998-2008

S/N	Study period	Joint Type	No. of tests
1	1998-2002	CHS T joint	3
2	2000-2004	CHS Gapped K joint	2
3	2002-2006	RHS T joint	4
4	2004-2008	CHS Partially overlapped K joint	3

TOOLS AND PROCEDURES DEVELOPED

A consistent geometrical modelling procedure for weld profile

As stringent weld profile quality along the joint intersection curves is required in all tubular joints[3,4], careful investigations were carried out to construct a realistic model for the weld profile. The model developed was constructed by considering the welding specifications from the design codes and validated against many actual

measurements. It is designed in such a way that the weld thickness generated:

(i) is a continuous function along the weld intersection,
(ii) satisfies the minimum requirements, and
(iii) is less than the thickness for most actual joints constructed.

A consistent geometrical modelling procedure for the crack surface and front

The geometrical models for the crack surface and front were again developed based on the experimental measurements obtained from full scale tests. The shape of the crack surface is defined by its cross sections perpendicular to the tubular sections (Figure 2). After investigating the measurements obtained from full scale tests, it was found that the geometry of the crack surface could be defined implicitly by the angle ω which is almost constant for CHS joints and varies linearly with the crack depth for RHS joints. The crack front is constructed by first measuring the positions of the deepest point and the two tips of the crack and then linked to the crack surface model by a mapping procedure so that the crack front is described as an unsymmetrical bi-elliptical curve on a projected plane.

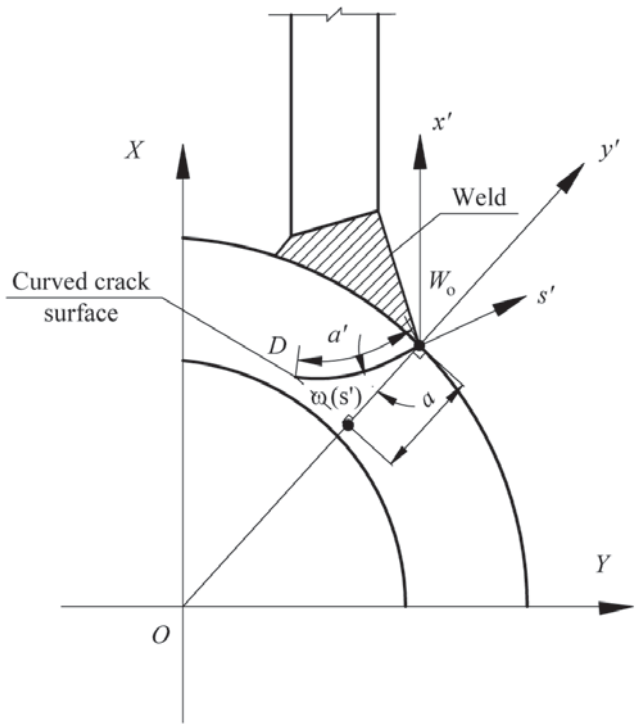

Figure 2. Definition of crack surface

Standardized procedures for measuring the weld profile and crack surface shape

In order to extract geometrical information of the weld profile and the crack surface from the test results, a simple measurement procedure using clay moulding technique was developed. The main step of the procedure was to apply mouldable clay around the interested area and leave the moulding material to set. The dried clay mould was then removed and cut into sections for scanning, and digital measurements were taken to obtain the values of the desired parameters. Note that this procedure is inexpensive and is non-destructive so that repeated measurements could be applied to the specimen.

A hierarchical mesh generation procedure

As large scale parametric studies are required in all projects, it was found that the use of automatic mesh generation procedure was mandatory and a *hierarchical* mesh generation procedure was eventually developed. This procedure allows a series of consistent meshes with increasing levels of geometrical details to be created automatically. An example of such a series of meshes for a partially overlapped CHS K-joint is shown in Figure 3. Starting from the simplest surface mesh (Figure 3a) for ultimate strength study, more details were added for the construction of solid meshes with or without welding detail (Figures 3b and 3c) for SCF analysis and eventually meshes with surface crack (Figure 4) for SIF computation. This automatic mesh generation procedure allows the modeller to create a large number of models in a short time for the parameter study and all the meshes generated are consistent regardless of the actual dimensions of the connections.

Interpolation method for prediction of responses of tubular connections

In most design codes, the variations of responses (e.g. SCF and SIF) with respect to the key parameters of the joint are usually described by some empirical equations which are obtained by applying regression analysis to a set of parametric studies results. However, for a complicated joint, as any response is often a complex function of many parameters, the regression approach would often result in lengthy equations that do not always give good predictions. To overcome this problem a new approach using the interpolation technique was proposed. In this method, the responses over the selected parametric ranges at some fixed intervals are pre-computed first. A good approximation of the predicted response is then constructed by using the standard Lagrangian interpolation functions used in FE analysis.

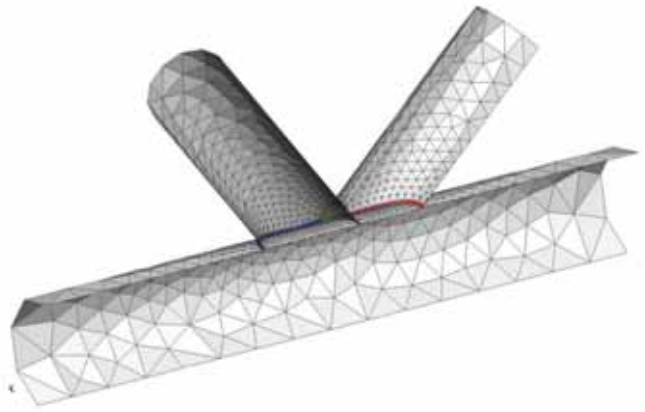

(a) Surface mesh

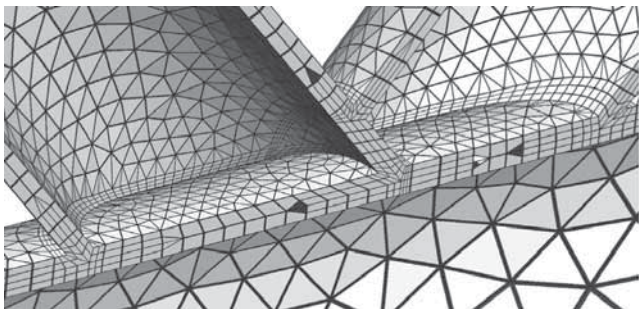

(b) Solid mesh without welding details

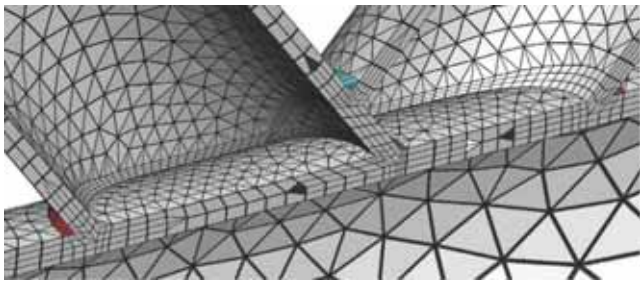

(c) Solid mesh with welding details

Figure 3. Mesh generated for uncracked joints

Figure 5 shows an example for the 2D case where the response Φ varies with two parameters ξ^1 and ξ^2. The i_1th interval along the ξ^1 axis and the i_2th interval along the ξ^2 axis which define four nodes enclosing the desired point $\left(\xi^1_{eval}, \xi^2_{eval}\right)$ are first identified. The approximated value $\tilde{\Phi}\left(\xi^1_{eval}, \xi^2_{eval}\right)$ at $\left(\xi^1_{eval}, \xi^2_{eval}\right)$ could then be written as

$$\tilde{\Phi}\left(\xi^1_{eval}, \xi^2_{eval}\right) = \sum_{\alpha_1,\alpha_2=1,2}^{\alpha_1+\alpha_2\le 4} L^1_{\alpha_1}\left(\xi^1_{eval}\right) L^2_{\alpha_2}\left(\xi^2_{eval}\right) \Phi_{i_1+\alpha_1-1, i_2+\alpha_2-1} \quad \ldots (2)$$

$$L^k_1\left(\xi^k\right) = \frac{\xi^k_{i_k+1} - \xi^k}{\xi^k_{i_k+1} - \xi^k_{i_k}}, \quad L^k_2\left(\xi^k\right) = \frac{\xi^k - \xi^k_{i_k+1}}{\xi^k_{i_k+1} - \xi^k_{i_k}}, k = 1,2 \quad \ldots (3)$$

In general, Eqns. (2) and (3) could be extended to the M-dimensional space involving a set of M parameters ξ^k, k = 1, …., M so that the point of evaluation $\xi_{eval} = \left(\xi^1_{eval}, \xi^2_{eval}, \ldots, \xi^M_{eval}\right)$ is enclosed by a hypercube with 2^M nodes and M intervals $[\xi^k_{i_k}, \xi^k_{i_{k+1}}]$ where

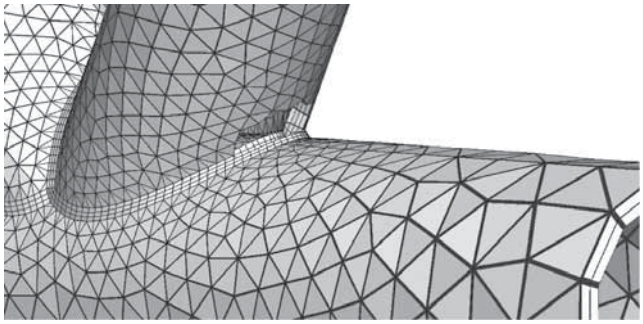

(a) Mesh with cracked region extracted

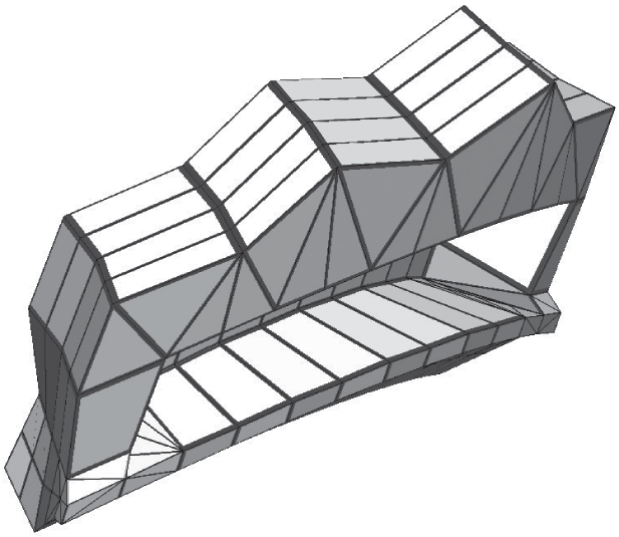

(b) Connection block for cracked region

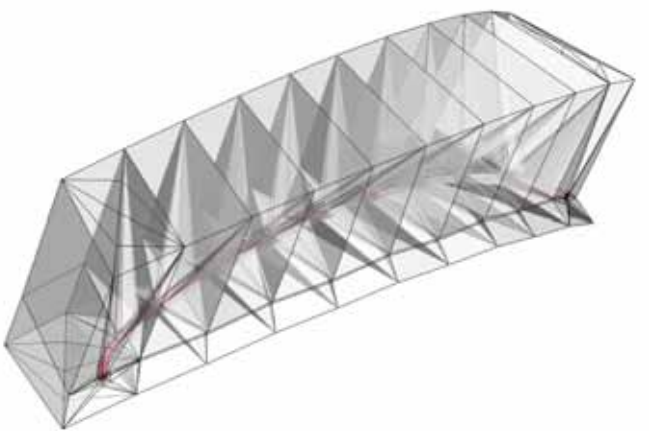

(c) Mesh near the crack mouth

Figure 4. Mesh generated for cracked joints

$\xi^k_{i_k} \le \xi^k_{eval} \le \xi^k_{i_{k+1}}$. The expression of the approximated value at $\xi_{eval}, \tilde{\Phi}\left(\xi_{eval}\right)$ is given by

$$\tilde{\Phi}\left(\boldsymbol{\xi}_{eval}\right) = \sum_{\alpha_k=1,2,k=1,..M}^{\sum \alpha_k \le 2M} \left(\prod_{k=1}^{M} L^k_{\alpha_k}\left(\xi^k_{eval}\right) \right) \Phi_{i_k+\alpha_k-1} \quad \ldots (4)$$

In Eqn. 4, $\Phi_{i_k+\alpha_k-1}$ denotes the known nodal value of Φ at the node ($\xi^1_{i_1+\alpha_1-1}, \xi^2_{i_2+\alpha_2-1}, \ldots, \xi^k_{i_M+\alpha_M-1}$). Extensive numerical studies verified that this approach could lead

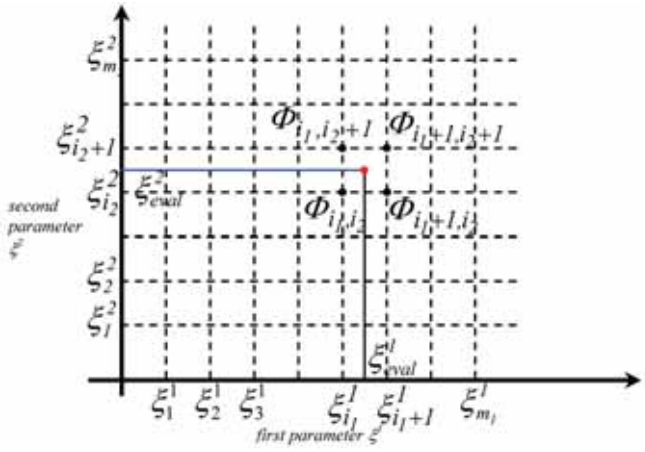

Figure 5. Computation of Φ by the interpolation method for the two parameters (2D) case

to more accurate and reliable response predictions with lower relative error when comparing with the regression analysis approach.

A procedure for the residual fatigue life prediction for cracked joints

A method to predict the residual fatigue life for a cracked joint is developed from Eqn. 1. By using a series of FE models with different maximum crack depths to obtain the values of ΔK, Eqn. 1 could now be integrated numerically so that the residual fatigue life, $N_{residual}$ for a cracked section with thickness t and current maximum crack depth a_c could be estimated as

$$N_{residual} = \int_{a_c}^{t} \frac{da}{C(\Delta K)^m} \approx \sum_{i=1}^{Q} w_i \left(\frac{1}{C(\Delta K_i)^m} \right) \quad \ldots (5)$$

where Q is the number of integration points (depths) used. w_i and ΔK_i are the weight and value of ΔK for the ith integration point respectively. It was found that first order Newton-Cotes quadrature with Q = 10-15 is sufficient to evaluate in Eqn. 5. Eqn. 5 also shows that estimation of residual fatigue life is a computational intensive process as at least $Q \geq 10$ FE models are required to be created and solved.

KEY RESEARCH FINDINGS

The effects of welding details on SCF prediction

From the experimental results obtained, it was found that the weld thickness employed in the FE model seriously affects the predicted SCF. Figure 6 shows the typical variations of the SCF for a CHS joint predicted by using different weld profile models using 3D solid FE models. It can be seen that while the numerical model constructed by the *ad hoc* weld thickness measurement gave the best prediction, the model without any welding detail overestimated the maximum SCF by 40%.

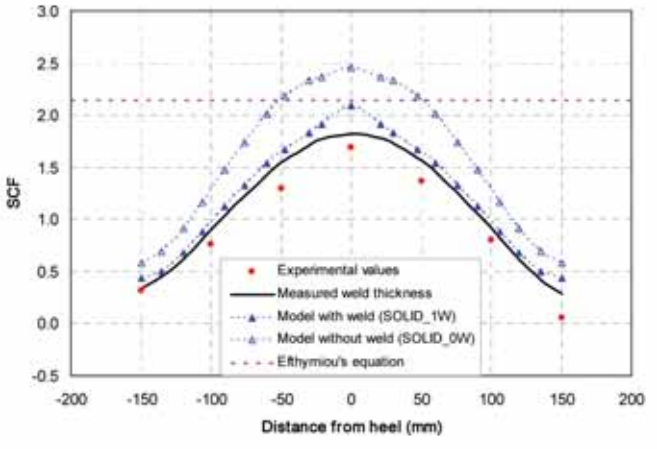

Figure 6. Effect of welding details on SCF prediction

The effects of the angle parameter ω in SIF computation

From the numerical experiments conducted, it was found that the angle ω (Figure 2) is the most critical geometrical parameter affecting the accuracy of the SIF prediction. Furthermore, for CHS joints, ω normally varies within the range of [0°-10°] and a constant value of ω = 0° could lead to good prediction of SIF. However, for RHS joints, ω could vary in the range [0°-75°] as a/t, the ratio between crack depth and the thickness of RHS section, increases. Therefore, for RHS joints a more complex geometrical model which allows variation of ω with the crack depth is needed. Figure 7 shows an example of the predicted SIF obtained by using different models of ω for a RHS joint.

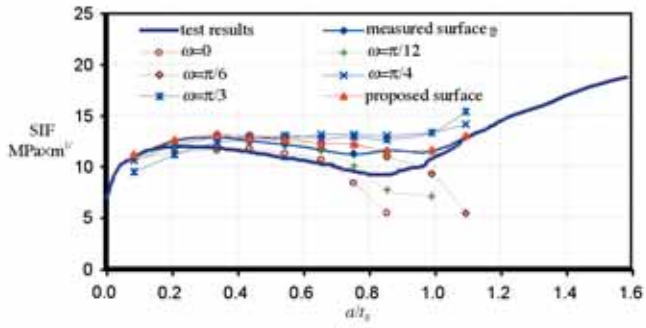

Figure 7. SIF Predictions a RHS joint using different models of ω

Accuracy of residual life estimation for cracked joints

Since Eqn. 4 involves the integration of the term $1/(\Delta K)^m$, it is more difficult to predict the residual life of a cracked joint than the SIF itself. In practice, it is found that even when the error of the SIF prediction is less than 5% for the whole crack growth history, the final error for fatigue life prediction could still be more than 30%. Figure 8 shows an example that demonstrates such error accumulation effect. It can be seen that even by adopting measured surface model, it is difficult to achieve a 10% error in fatigue life prediction during the initial phase of the crack growth.

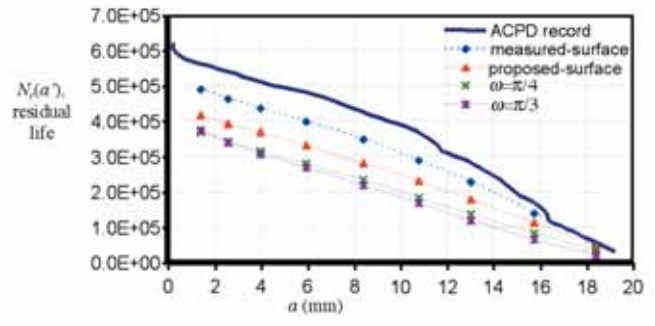

Figure 8. Prediction of residual fatigue life using different models of ω in Figure 7

CONCLUSIONS AND FURTHER WORKS

In this article, a review of research works done and findings obtained in the past ten years by the authors' research group on the fatigue performance of tubular joints was given. While the presented modelling procedures could lead to reasonable fatigue performance predictions, there is certainly room for improvement as listed below:

(1) **More efficient procedure for residual fatigue life estimation**
One possible method to reduce the computational cost for residual fatigue life prediction is to combine Eqn. 4 with Eqn. 5. By using Eqn. 4, approximated values of ΔK_i could be obtained without any FE analysis. However, further research is necessary to ensure that a conservative prediction could be obtained from the new method.

(2) **Studies on structural connections built from high strength steel**
All the summaries, tools and procedures reported in this paper are developed and could be extended to tubular connections constructed by high strength steel sections. Towards this end, some fundamental studies on the basic fatigue behaviour for high strength steel materials are needed.

(3) **Improvement of modelling technique for cracked joint**
While the presented modelling procedures for cracked joints could lead to good SIF predictions for surface cracks with depth greater than 10% of the thickness of the section, it could not always lead to good prediction for long and shallow cracks. Hence, a possible direction of future research is to employ a more advanced modelling procedure such as the extended finite element method to improve the modelling accuracy.

REFERENCES

[1] Chiew, S.P., Lee, C.K. and Lie, S.T. "An Overview of Tubular Joint Research at NTU". *To appear in IES Journal: Part A.*

[2] Paris, P. and Erdogan, F., 1963. "A critical analysis of crack propagation laws, Journal of Basic Engineering". *Transactions of the American Society of Mechanical Engineers,* December, pp. 528-534.

[3] Zhao, X.L., Herion, S., Packer, J.A., Puthli, R., Sedlacek, G., Wardenier, J., Weynand, K., van Wingerde, A. and Yeomans, N., 2000. "Design Guide for Circular and Rectangular hollow Section Joints under Fatigue Loading". CIDECT, TUV Germany.

[4] American Welding Society (AWS), 2008. AWS D1.1/1.1M-2008 Structural Welding Code-Steel, Miami, USA.

DAMAGE ASSESSMENT OF A CRACKED CIRCULAR HOLLOW SECTION K-JOINT USING BS7910: 2005

Lie Seng Tjhen (cstlie@ntu.edu.sg)
Zhang Baofeng (bfzhang@ntu.edu.sg)

INTRODUCTION

In practice, many offshore structures installed in the open seas are found to contain cracks caused by severe cyclic loads. As a result, the static joint capacity is reduced by these cracks, and therefore, these offshore structures with defects need to be assessed and checked periodically. The most widely used and accepted approach is the failure assessment diagram (FAD) method. Based on this approach, BS7910 (2005)[1] gives guidance for assessing the acceptability of defects in welded structures. In this code of practice, a specific assessment procedure for tubular joints in offshore structures has been proposed recently. In accordance with this procedure, a damaged tubular K-joint specimen, subjected under axial and in-plane loads, is analyzed and assessed illustrating the usage of this approach.

FAILURE ASSESSMENT DIAGRAM (FAD)

In BS7910 (2005)[1], for cases where the knowledge of a complete stress-strain curve is not available, the normal assessment route for general application Level 2A, which is expressed by Eqn. 1, is recommended for assessing a uni-planar cracked tubular CHS T, Y, K or KT-joint.

$$K_r = (1 - 0.14L_r^2)[0.3 + 0.7\exp(-0.65L_r^6)] \quad \ldots (1)$$

In this assessment curve, the vertical (fracture) axis K_r is defined as the ratio of the stress intensity factor K_I to the fracture toughness K_{IC}, and the horizontal (plasticity) axis L_r is defined as the ratio of the applied load P to the plastic collapse load P_c. If the assessment point falls inside the curve, the structure is considered safe, otherwise, it is deemed unsafe, as shown in Figure 1. The cut-off line which is set at the point L_r=L_{rmax} is to prevent localized plastic collapse.

FAILURE ASSESSMENT DIAGRAM OF A CRACKED K-JOINT SPECIMEN

A full-scale cracked tubular K-joint containing successive fatigue cracks was assessed in this study. In the fatigue test carried out earlier[2], the ACPD (alternating current potential drop) technique was used to capture the crack details, which are shown in Table 1.

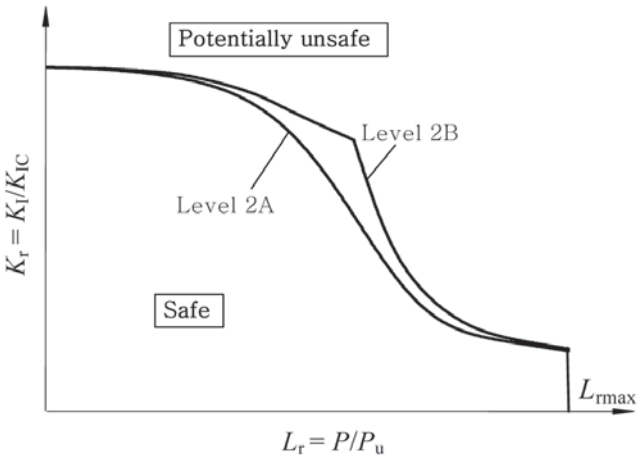

Figure 1. BS7910 (2005) [1] Levels 2A FAD curve

Table 1. Calculated K_r and L_r of different crack sizes

a	$2c$	K_I (tip)	K_I (depth)	K_r (tip)	K_r (depth)	L_r
(mm)	(mm)	(MPa.m$^{1/2}$)		(K_I/K_{IC})		(P/P_c)
3.30	70.40	25.12	14.34	0.171	0.098	0.210
5.33	89.64	25.51	21.27	0.173	0.145	0.390
8.13	117.96	26.39	25.73	0.180	0.175	1.335
10.41	132.24	28.21	29.66	0.192	0.202	2.988

To assess the safety and integrity of this cracked tubular K-joint, the assessment points need to be derived from two different calculations of fracture parameter K_r and plasticity parameter L_r, and then plotted on the diagram. The elastic stress intensity factors K_I along the 3D crack front of the K-joint specimen can be obtained from a finite element analysis [3]. The brace and chord members were fabricated from standard API 5L Grade B specifications pipes, and the fracture toughness measured at room temperature was approximately 147 MPa.m$^{1/2}$[4].

As it is very difficult to obtain the plastic collapse load of any offshore cracked tubular welded joint, BS7910 (2005) has recommended that the plastic collapse load of the cracked geometry P_c is determined by reducing the plastic collapse load for the corresponding uncracked geometry $P_{uncracked}$ using the correction factor F_{AR}. The plastic collapse load of an uncracked K-joint can be obtained from the Health and Safety Executive[5]. The correction factor F_{AR} for axial load is given by

$$F_{AR} = \left[1 - \frac{\text{cracked area}}{(\text{intersection length} \times T)}\right]\left(\frac{1}{Q_\beta}\right)^{m_q} \quad \ldots (2)$$

where T is the chord thickness, Q_β is 1 for $\beta \leq 0.6$ and m_q is 0 for the K-joints.

For in-plane bending moment, the correction factor F_{AR} is given by

$$F_{AR} = \cos\left(\frac{\varphi}{2}\right)\cdot\left(1-\sin\left(\frac{\varphi}{2}\right)\right) \quad \ldots (3)$$

where the angle φ is defined in Figure 2.

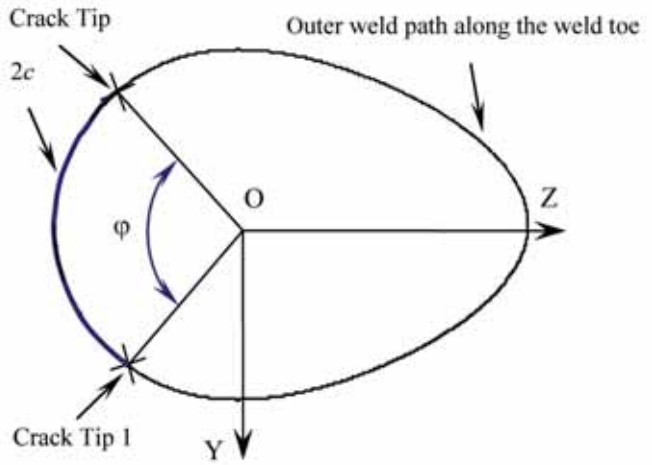

Figure 2. Definition of the angle φ in F_{AR}

In Annex B of BS7910 (2005), the L_r parameter for any tubular joint subjected under combined loads is given by the following equation:

$$L_r = \left(\frac{\sigma_F}{\sigma_Y}\right)\left\{\left|\frac{P_a}{P_c}\right| + \left(\frac{M_{ai}}{M_{ci}}\right)^2 + \left|\frac{M_{ao}}{M_{co}}\right|\right\} \quad \ldots (4)$$

where σ_F and σ_Y are the flow and yield stresses; P_a, M_{ai} and M_{ao} are the applied axial load, in-plane bending and out-of-plane bending; and P_c, M_{ci} and M_{co} are the plastic collapse load in the cracked condition for axial load, in-plane bending and out-of-plane bending respectively.

Using Eqns. (2), (3) and (4), the corresponding values of K_r and L_r for different crack sizes were computed (see Table 1). The assessment points of this cracked K-joint were plotted in the assessment curve as shown in Figures 3 and 4.

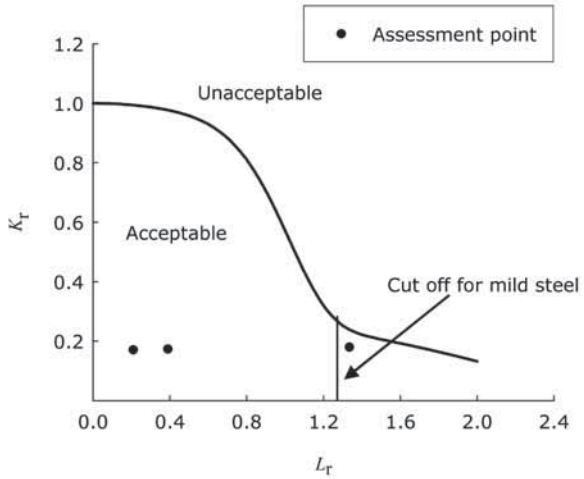

Figure 3. Plot of assessment points at the crack depth

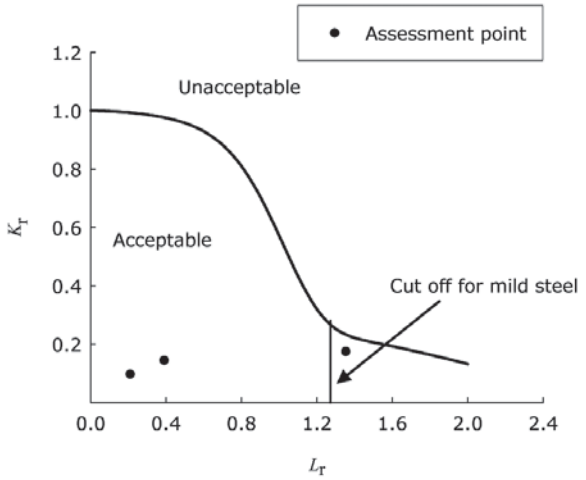

Figure 4. Plot of assessment points at the crack tips

From Figures 3 and 4, it can be seen that only three assessment points fall inside the standard Level 2A curve, i.e. when a/T is less than 0.4, hence, the crack K-joint is still safe. When a/T goes beyond 0.4, it was noted that the L_r values are substantially larger, and therefore the cracked K-joint is deemed to fail beyond this crack size.

CONCLUSIONS

This study demonstrated the usage of BS7910 (2005) [1] to assess the safety and integrity of a typical cracked tubular CHS K-joint where failure is characterized by two criteria, namely, crack tip failure where failure occurs when the applied load equals the LEFM failure load, and failure by plastic collapse of the ligament.

It enables the integrity of cracked CHS tubular K-joints to be assessed through two separate calculations based on the two extremes of fracture behaviour, linear elastic and fully plastic. A design curve was used to interpolate between the two failure criteria. The relative position of the assessment point on the diagram, derived from the two separate calculations, determines the integrity of the structure. If the assessment point falls inside the failure curve, the structure is deemed safe; if the assessment point is on or outside the curve, then failure is predicted to occur.

REFERENCES

[1] British Standard (BS) BS7910, 2005. Guide on Methods for Assessing the Acceptability of Flaws in Fusion Welded Structures. *British Standards Institution, London,* UK.

[2] Lie S.T., Chiew S.P., Lee C.K. and Shao, Y.B., 2005. "Validation of a Surface Crack Stress Intensity Factors of a Tubular K-joint". *International Journal of Pressure Vessels and Piping*, *Vol. 82, No. 8,* pp. 610-617.

[3] Lie, S.T., Lee, C.K., Chiew S.P. and Shao, Y.B. 2005. "Mesh Modelling and Analysis of Cracked Uni-planar Tubular K-joints". *Journal of Constructional Steel Research, Vol. 61, No. 2,* pp. 235-264.

[4] Somerday, B.P., 2007. "Technical Reference on Hydrogen Compatibility of Materials – Carbon Steel: C-Mn Alloys (Code 1100)". *Sandia National Laboratory, Livermore, California, USA.*

[5] Health and Safety Executive (HSE), 1995. "Offshore Installation: Guidance on Design, Construction and Certification". *4th Edition, 3rd Amendment, Her Majesty's Stationary Office, London, UK.*

ENERGY HARVESTING USING MICRO-FIBER COMPOSITES

Yang Yaowen (cywyang@ntu.edu.sg)
Tang Lihua (c070073@ntu.edu.sg)

INTRODUCTION

The decreasing energy consumption of MEMS, wireless sensors and portable electronics invokes the possibility to harvest energy from ambient vibrations for self power supply. One simple method for vibration energy harvesting is utilizing the direct piezoelectric effect. The macro-fiber composites (MFC)[1] are featured in their flexibility of large deformation, which enables them to harvest energy from vibrations with little brittle risk and to serve for an unlimited lifespan. However, the efficiency of MFC has not been well investigated. This article focuses on the efficiency of the energy harvesting system using MFC attached on a cantilever beam. The output voltage of the MFC harvester is tested and estimated using the finite element method (FEM). The procedures of energy storing to the capacitor are simulated using electronic design automation (EDA) software. By combining the FEM and EDA simulations, the efficiency of the MFC energy harvesting system is estimated.

EXPERIMENTAL STUDY

The energy harvesting system is composed of an aluminum cantilever beam, one piece of P1-type MFC as actuator and two pieces of P2-type MFCs as harvesters, an energy harvesting circuit EH300A, a small LED bulb and a power supply to the actuator, as shown in Figure 1.

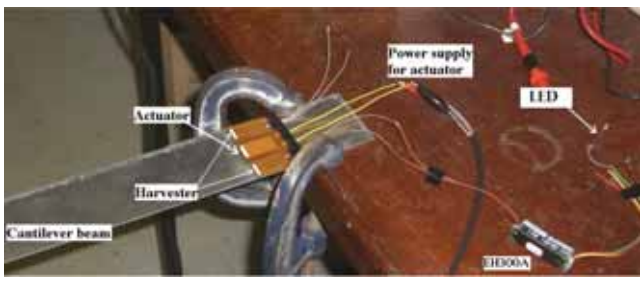

Figure 1. Energy harvesting system prototype

The harvesting circuit EH300A module is shown in Figure 2. When an energy source starts to inject energy into the inputs of the EH300A module, charge packets are collected and accumulated in an internal storage capacitor bank. Figure 3 shows the waveform of voltage across the capacitor bank in EH300A. Initially, the voltage across the capacitor bank, +V, starts at 0.0V. The internal circuit of the module monitors this +V. When +V reaches V_H, the module output (V_P) is triggered to supply power to the load, which is an LED bulb in this experiment. As the power is consumed by the LED, which gives a flash, during time duration t_3 (Figure 3), +V decreases. When it reaches V_L, output V_P switches to OFF and stops supplying any further power. The charging cycle restarts. During each charging cycle that +V increases from V_L to V_H or energy is delivered to the load, around 30mJ energy is accumulated or released. In the experiment, time t_2 in Figure 3 for different cases of energy harvesting is our concern.

Figure 2. EH300A

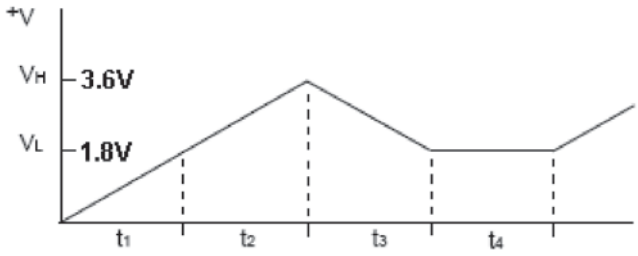

Figure 3. Voltage waveform across the capacitor bank in EH300A

FINITE ELEMENT MODELLING

To determine the ability of energy harvesting of MFC, a finite element model is developed using the commercial code ABAQUS6.6 to calculate the voltage output from MFC. The entire top and bottom surfaces of P2-type MFC are covered by electrode. In the finite element analysis (FEA), the equation constraint[2] should be imposed on the electrical potential degrees of the top and bottom surface nodes in order to ensure that the potential is uniform, which simulates the real electrodes. For the actuator P1-type MFC, it is quite difficult to directly model the inter-digital electrodes. For convenience in analysis, the P1-type MFC will be equivalently converted to P2-type MFC so that only the top and bottom surface electrodes are modelled. The equivalent conversion should ensure that the piezoelectric and electrical properties of the P1-type MFC remain unchanged. For the piezoelectric property, when applying the same voltage, the strain generated by MFC should remain the same:

$$d_{31}' \cdot \frac{V}{t_m} = d_{33} \cdot \frac{V}{e_m} \quad \ldots (1)$$

where t_m and e_m are the thickness and the distance between two neighbouring inter-digital electrodes of P1-type MFC, respectively. Besides, the dielectric constant should be changed to ensure that the capacitance of the converted MFC model is the same as the measurement.

Figure 4 shows the strain distribution of the cantilever beam and MFC harvesters at the 1st vibration mode. Figure 5 shows the root mean square (RMS) voltage distribution of MFC harvester. It is noted that the potential on the top surface is uniform with the real electrode, by using the equation constraint technique.

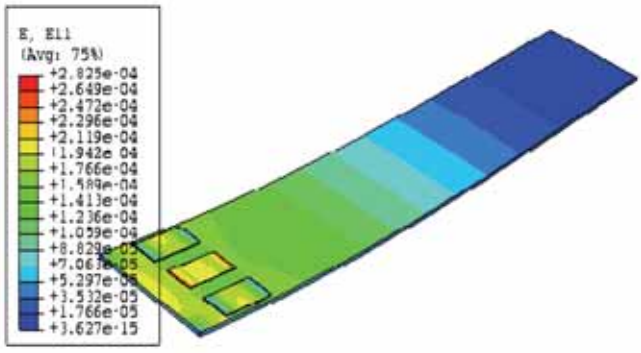

Figure 4. Strain distribution at the 1st natural frequency

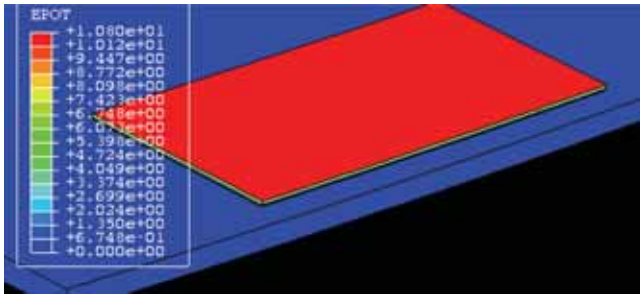

Figure 5. Electrical potential distribution at the 1st natural frequency

Figures 6 and 7 show the peak value of strain and RMS voltage output from one single MFC harvester, respectively. It is noted that the values of strain and voltage from FEA match well with the experimental results except for minor shifts on the frequency axis. This could be attributed to the fact that the cantilever beam is not perfectly clamped, as shown in Figure 1. For the 1st mode, the natural frequencies obtained from the experiment and simulation are 9.75Hz and 10.269Hz, respectively, and the RMS voltage output are 11.5V and 10.8V, respectively. The differences are around 5%. Therefore, the finite element model is able to accurately evaluate the voltage output of MFC harvester.

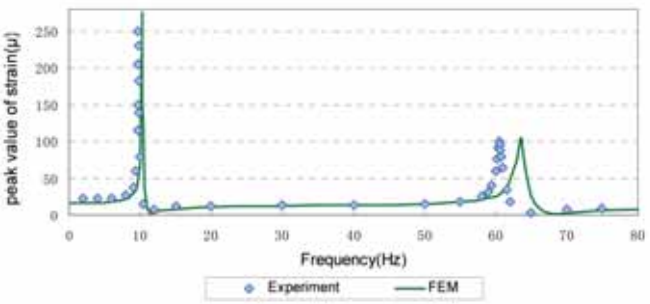

Figure 6. Peak value of strain versus frequency on the central top surface of MFC harvester

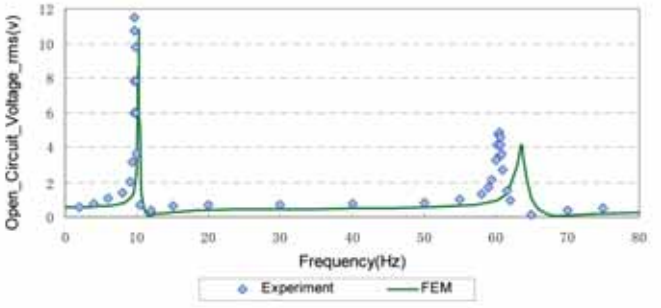

Figure 7. RMS voltage output of MFC harvester versus frequency

ELECTRONIC SIMULATION

The voltage output of MFC harvester can be obtained from the FEA. However, based on these results, we still cannot evaluate the power available to be extracted from the MFC harvester. Actually, because of the intrinsic capacitance, the power generated by the MFC harvester will be recovered back to the source. As a result, the efficiency of energy harvesting system depends on the amount of energy extracted and stored from the MFC. The EDA software Multisim10.0 by National Instrument is utilized to simulate the energy extraction and storing procedures from the MFC harvester. The entire energy harvesting circuit includes the equivalent circuit of MFC, the full-wave rectifier and the capacitor bank of the EH300A module, as shown in Figure 8. The ideal Norton's equivalent circuit[3] of the MFC harvester is employed, which is similar to that for the conventional piezoelectric material.

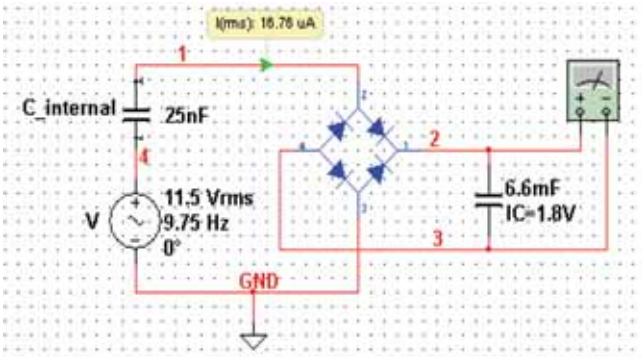

Figure 8. Circuit of energy harvesting system

The efficiency of the energy harvesting system at the 1st natural frequency is tested for 3 cases, namely, one single MFC, two MFCs electrically connected in series and in parallel. Figures 9 and 10 illustrate the history of charging current to the EH300A and the energy storing procedure in the capacitor bank in EH300A, respectively. Again, the simulation results match well with the experimental ones.

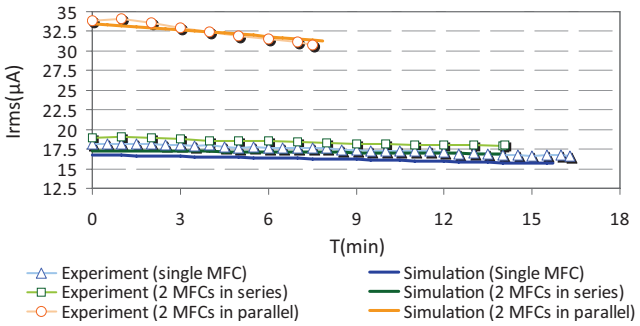

Figure 9. Charging curves for three cases—single MFC, 2 MFCs connected electrically in series and in parallel at the 1st natural frequency

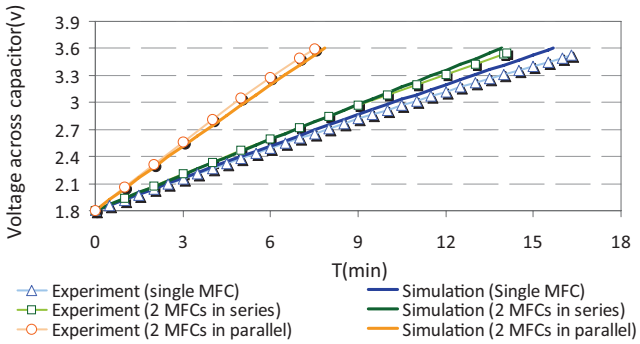

Figure 10. Energy storing procedures for three cases—single MFC, 2 MFCs connected electrically in series and in parallel at the 1st natural frequency

Table 1 lists the time t_2 (refer to Figure 3) for 30mJ accumulated in EH300A and the average power for energy storing from the experiment and electronic simulation for the three cases at the 1st natural frequency. It is noted that MFCs electrically connected in parallel generate the largest charging current to EH300A and hence are the most efficient in charging the energy storage capacitor with capacitance 6.6mF in EH300A.

Table 1. Energy harvesting performance for three cases

		Experiment		Simulation	
MFC connection	Open Circuit Vrms (v)	t_2 (sec)	P (μw)	t_2 (sec)	P (μw)
single	11.5	978	30.7	942	31.9
in series	21.5	845	35.5	835	35.9
in parallel	11.85	450	66.7	471	63.7

CONCLUSIONS

This study focuses on the efficiency of an energy harvesting system prototype with MFC patches bonded on a cantilever beam. A finite element model for the system is developed and verified by experiment. Subsequently, the procedure of energy extraction and storing to the capacitor in EH300A is simulated by using the EDA software. By combining the FEM and EDA simulations, the efficiency of energy harvesting is estimated. It is demonstrated that the combined FEM and EDA simulations are useful tools for evaluating the efficiency of MFC or other piezoelectric material based energy harvesting systems.

REFERENCES

[1] Werlink R.J., Bryant R.G. and Manos D., 2002. "Macro Fiber Piezocomposite Actuator Poling Study". NASA/TM-2002-211434.

[2] ABAQUS analysis User's manual version 6.6-1, Section 28.2.1: Linear constraint equations (2006)

[3] Park, C.H., 2001. "On the circuit Model of piezoceramics". *Journal of Intell. Mater. Syst. Struct.,* Vol. 12, pp. 515-522.

MONITORING VIBRATING STRUCTURES USING PZT IMPEDANCE TRANSDUCERS

Yang Yaowen (cywyang@ntu.edu.sg)
Miao Aiwei (miao0009@ntu.edu.sg)

INTRODUCTION

The electromechanical impedance (EMI) method has emerged as a widely recognized technique for dynamic identification and health monitoring of structural systems. The electromechanical admittance response of the smart system is derived from the dynamic interaction relation between the lead zirconate titanate (PZT) transducer and the host structure. For structural health monitoring (SHM) applications, these spectra may be compared at various times during the service lifespan of the structure, in which any change between the spectra is an indication of the presence of damage or material deterioration. However, the existing EMI method does not consider the structural vibration caused by the external excitation other than the PZT actuation, which means that the existing EMI method is only applicable to the static structures [1-3]. Unfortunately, many structures are subjected to vibrations in practice. The vibrations of the structures will influence the results of SHM by causing the changes in PZT signatures. The changes in PZT signatures caused by the external excitation and the structural damage must be differentiated such that the correct information of structural health state can be obtained. Therefore, this paper attempts to study the influence of the external excitation on the PZT impedance signature.

For this purpose, a new EMI model is developed for a simply supported beam structure with external excitations. Furthermore, an experimental test is carried out to verify the developed theoretical model.

THEORETICAL MODEL

This section presents the formulation of EMI model of beams with external excitations. Generally, for beam structures, the transverse vibration is much more critical compared to the extensional vibration. Therefore, only the transverse vibration is considered here.

The transverse displacement for the forced vibration of a simply supported beam is

$$w(x,t)=\sum_{k=1}^{\infty}\frac{G_k}{\rho_s A_s\left[\left(\frac{k\pi}{l_s}\right)^4\frac{E_S I_s}{\rho_s A_s}-\omega^2\right]}\sin\frac{k\pi}{l_s}x e^{i\omega t} \qquad \ldots (1)$$

where E_s is the elastic modulus; $A_s = b_s h_s$ is the cross-sectional area; ρ_s is the density of the material; $I_s = b_s h_s^3 / 12$ is the moment of inertia; ω is the frequency of external excitation; l_s, b_s and h_s are the length, width and height of the beam, respectively; $G_k = \frac{2}{l_s}\int_0^{l_s}\hat{g}(x)\sin\frac{k\pi}{l_s}xdx$; and $g(x,t) = \hat{g}(x)e^{i\omega t}$ is the harmonic distributed force.

The transverse displacement of the beam due to PZT actuation is

$$w_P(x,t)=\sum_{m=1}^{\infty}\frac{F_m\varphi_m(x)}{\rho_s A_s\left(\Omega_m^2-\omega_{PZT}{}^2\right)}e^{i\omega_{PZT}t} \qquad \ldots (2)$$

where $F_m = \frac{h_s}{l_s}\hat{F}_{PZT}\left[\varphi_m'(x_1)-\varphi_m'(x_2)\right]$; $\varphi_m(x)=\sin(m\pi x/l_s)$

$\Omega_m = \left(\frac{m\pi}{l_s}\right)^2\sqrt{\frac{E_s I_s}{\rho_s A_s}}$; ω_{PZT} is the angular frequency of PZT actuation; x_1 and x_2 are the coordinates of the two ends of the PZT transducer; and $\hat{F}_{PZT}$ is the magnitude of actuation force of the PZT.

The electromechanical admittance can be obtained as

$$Y=\frac{\tilde{Y}_{11}^E d^2 b}{h}\left\{\begin{array}{l}\dfrac{i\sin(\gamma l)\omega_{PZT}}{\psi}-il\omega_{PZT}\\ -i\wp\sum_{k=1}^{\infty}k\chi(k)\Delta\omega e^{i\Delta\omega t}\end{array}\right\}+\frac{ilb\tilde{\varepsilon}\omega_{PZT}}{h} \qquad \ldots (3)$$

where $\psi=\gamma\cos(\gamma l)+\frac{R}{l}\sin(\gamma l)$; $\wp=\frac{\sin^2(\gamma l)K_{str}{}^2 h_s\pi}{2l_s l\rho_s A_s\hat{F}_{PZT}\psi^2 K_{PZT}}$;

$\chi(k)=\frac{G_k}{\Omega_k^2-\omega^2}\left(\cos\frac{k\pi}{l_s}x_2-\cos\frac{k\pi}{l_s}x_1\right)$; $\Delta\omega = \omega - \omega_{PZT}$; $\tilde{Y}_{11}^E$ is the complex Young's modulus; d is the piezoelectric strain coefficient; γ is the wave number; $R = K_{str}K_{PZT}^{-1}$ is the stiffness ratio; K_{str} is the dynamic stiffness of the beam structure and $K_{PZT} = \tilde{Y}_{11}^E bhl^{-1}$ is the quasi-static stiffness of the PZT transducer; $\tilde{\varepsilon}$ is the complex permittivity of PZT; and l, b and h are the length, width and height of the PZT transducer, respectively.

EXPERIMENTAL INVESTIGATIONS

To verify the developed theoretical model, an experimental test is carried out on an aluminum beam boned with one PZT patch. The instruments and equipment used in this experiment are shown in Figure 1 and Figure 2. The model of the simply supported beam is shown in Figure 3. The beam is

stuck on the platforms by the blue tack and the mini-shaker generates vibration at the location of 6cm from the left end of the beam. The PZT patch with dimension 10mm x 10mm x 0.2mm is bonded to the beam at the central location. The properties of PZT patch and beam specimen are listed in Tables 1 and 2, respectively.

Figure 1. EMI measurement system

Figure 2. External excitation system

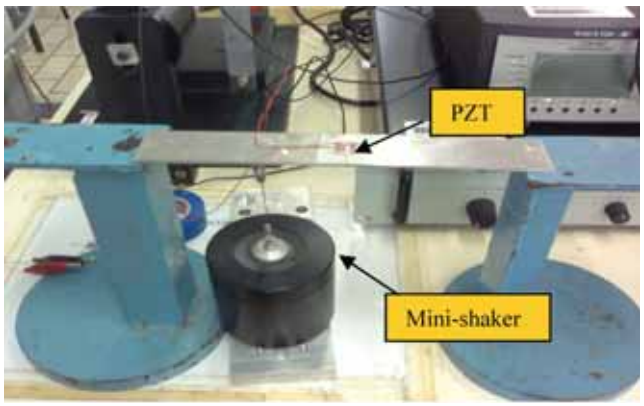

Figure 3. Beam specimen and mini-shaker

Table 1. Properties of PZT patch

Young's Modulus $Y(GPa)$	Loss Factor η	Mass Density $\rho(kg / m^3)$
68.9	0.001	7800
Strain Constant $d_{31}(m/volt)$	Permittivity $\varepsilon_{33}^{T}(farad/m)$	Dielectric Loss Factor δ
-2.10E-10	2.136E-08	1.47E-02

Table 2. Properties of beam specimen

Poisson's Ratio	Mass Density (kg / m^3)	Damping Ratio	Young's Modulus (GPa)
0.3	2700	0.005	67.8

In the experiment, the conductances for four cases (S1, S2, S3 and S4) are shown in Figure 4. S1 and S2 represent the signatures of the specimen without damage while S3 and S4 represent those with damage. The damage in the specimen is induced by drilling a hole of diameter 5mm with distance of 4cm from the right end of the beam. There is no external excitation applied to the specimen for S1 and S3 while the external excitation (generated by the mini-shaker) applies for S2 and S4. As expected, the shifts of the peaks are obvious. Comparison between S1 and S2 shows the effect of external excitation. From Figure 4 and Table 3 (the 5th column), this effect is apparent and there is no consistent shifting of peaks.

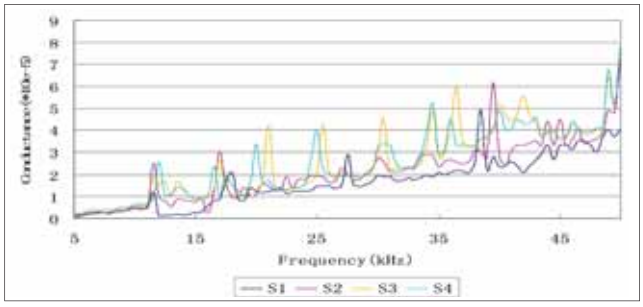

Figure 4. Signatures of experimental results of conductance

The peaks shifts between S1 and S3, and S2 and S4 represent the effect of damage on the signature. From Figure 4 and Table 3 (the last two columns), we can observe that the peak shifts due to damage are comparable for the specimen with or without external excitation. An important conclusion we can draw is that for damage assessment of a vibrating structure, the baseline should be obtained from the structure without damage and subjected to external excitation.

Table 3. Peak locations and shifts [unit: kHz]

S1	S2	S3	S4	S1-S2	S3-S1	S4-S2
11.5	11.5	12.5	12.3	0	+1	+0.8
18	17	17	16.2	-1	-1	-0.8
22	21.5	21	20.2	-0.5	-1	-1.3
27.5	27	25.5	25	-0.5	-2	-2
30	30	30.5	30.5	0	+0.5	+0.5
34	33.5	34.5	34.2	-0.5	+0.5	+0.7
35	35.5	36.3	36.3	+0.5	+1.3	+0.8
38.5	39.5	39.5	40.2	+1	+1	+0.7
41	42.5	42	43.5	+1.5	+1	+1

Figure 5 shows the theoretical prediction and the experimental recording of the PZT admittance signature. Table 4 compares the theoretical and experimental peaks. The results show that the theoretical model is able to accurately predict some of the electromechanical resonant peaks that can be found in the measured response. Nonetheless, discrepancies exist between the predicted response and the measured response. The most obvious discrepancy is found in the magnitude of the peaks in the predicted response and the measured response. This discrepancy may be attributable to the simplified one-dimensional nature of the PZT transducer, as well as, the assumptions made in the derivation of a closed-form solution for the dynamics of the structural substrate. As a whole, the accuracy of theoretical model is acceptable.

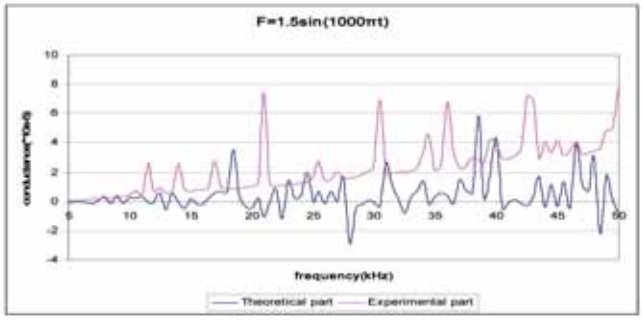

Figure 5. Signatures of conductance for F=1.5sin (1000πt)

Table 4. Theoretical and experimental peak values (F=1.5sin (1000πt))

Peak values [kHz]		
Theoretical	Experimental	Discrepancies
12.25	11.80	+0.45
13.75	14.25	-0.50
18.50	17.00	+1.50
21.30	20.50	+0.80
24.75	25.20	-0.45
27.25	27.00	+0.25
30.55	30.15	+0.40
34.55	34.75	-0.20
37.40	36.00	+1.40
38.50	38.30	+0.20
40.00	39.85	+0.15
43.40	42.50	+0.90
44.50	43.75	+0.75
45.55	45.00	+0.55
46.70	46.70	0

It is worth mentioning that we have focused on the peak shift because in the EMI technique, peak locations represent the natural frequencies of the host structure. Therefore peak shifts in admittance signature indicate the change of structural properties, which may be caused by damage. Other statistical method such as the RMSD can also be used to analyze the signatures[2].

CONCLUSIONS

This paper investigates the influence of external excitation of the main structure on the admittance signature of PZT transducers. The fundamental formulation of EMI method has been derived for a simply supported beam with external excitation. In the experiment, an aluminum beam specimen bonded with a PZT sensor has been tested. The experimental results for four different cases show the effects of excitation and damage on the admittance signature. Comparison between the theoretical and experimental results shows that the theoretical model is capable of predicting the resonant peaks in the admittance signature. An important conclusion is that for damage assessment of a vibrating structure, the baseline should be obtained from the structure without damage and subjected to external excitation.

REFERENCES

[1] Park, G., Cudney, H.H. and Inman, D.J., 2000. "Impedance-based health monitoring of civil structural components". *Journal of Infrastructure Systems,* Vol. 6, pp. 153-160.

[2] Xu, J.F., Yang, Y.W. and Soh, C.K., 2004. "Electromechanical impedance-based structural health monitoring with evolutionary programming". *Journal of Aerospace Engineering,* Vol. 17, pp. 182-193.

[3] Yang, Y.W., Xu, J.F. and Soh, C.K., 2005. "Generic impedance-based model for structure-piezoceramic interacting system". *Journal of Aerospace Engineering*, Vol. 18, pp. 93-101.

DAMAGE DETECTION USING MULTIPLE PIEZO-IMPEDANCE TRANSDUCERS

Yang Yaowen (cywyang@ntu.edu.sg)
Liu Hui (liuh0019@ntu.edu.sg)

INTRODUCTION

Smart materials based structural health monitoring (SHM) has attracted extensive research attention in the past decade. Lead zircornate titanate (PZT) impedance transducers, working on the principle of electromechanical impedance (EMI), are among the most widely used smart materials due to their self actuation and sensing capabilities. One single PZT is sensitive enough to detect incipient damage and its propagation [1]. However, it is difficult to identify the location of structural damage by a single PZT. Therefore, in this article, an experimental investigation on damage location using multiple PZTs is firstly presented, followed by the numerical simulation for verification.

EXPERIMENTAL STUDY

The experimental setup comprises of an HP LF 4192A impedance analyzer, a personal computer equipped with data acquisition software and an interface cable, and an aluminum plate specimen of dimension 500mm × 400mm ×10mm. A total of 9 PZTs (designated as PZT1, PZT2 ... PZT9) of dimension 10mm × 10mm × 0.3mm are surface bonded to the plate in the arrangement of a 3 x 3 array, as shown in Figure 1. Two 5mm diameter holes (X1 and Y1) are drilled near PZT6 and PZT2 with a clear distance of 30mm between the hole and PZT.

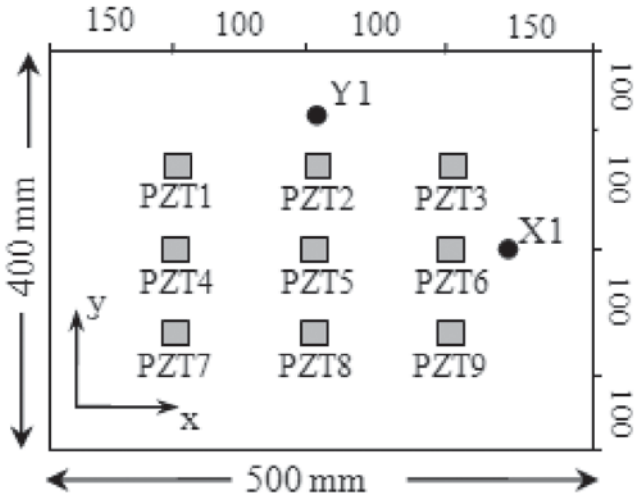

Figure 1. Locations of PZTs and damages on aluminum specimen

Admittance signatures, consisting of real and imaginary parts, are recorded for all 9 PZT patches in the frequency range of 10 to 100 kHz with a scanning step of 0.1 kHz. Signatures obtained before and after damage X1 and Y1 are compared for each PZT.

It has been understood that the real part of admittance signature (conductance) is a better indicator of damage [2] than the imaginary part. Therefore, only conductance signature is analyzed in this study.

Signature acquired after damage shows large deviation from the baseline signature. These variations are significant for all the PZT patches which demonstrate the sensitivity of PZT to structural damage. In order to have a better understanding of the signature change, root mean square deviation (RMSD) will adopted to quantify the variations of conductance signature.

FINITE ELEMENT ANALYSIS (FEA)

A three-dimensional impedance model is employed to predict the PZT conductance signatures. The admittance formulation is:

$$\overline{Y}_c = G + Bj$$

$$= \frac{j\omega LW}{2H}\left[\bar{\varepsilon}_{33} + Y_R\left\{\begin{array}{l} d_{31}\lambda_1\left\{\begin{array}{l}[A_0\sin kL - d_{31}]+\\ R[C_0\sin kW - d_{32}]+\\ R[E_0 k\cos k2H - d_{33}]\end{array}\right\}+ \\ d_{32}\lambda_2\left\{\begin{array}{l}R[A_0\sin kL - d_{31}]+\\ [C_0\sin kW - d_{32}]+\\ R[E_0 k\cos k2H - d_{33}]\end{array}\right\}+ \\ d_{31}\lambda_3\left\{\begin{array}{l}R[A_0\sin kL - d_{31}]+\\ R[C_0\sin kW - d_{32}]+\\ [E_0 k\cos k2H - d_{33}]\end{array}\right\}\end{array}\right\}\right] \quad \ldots (1)$$

where $\overline{Y}_C$ represents the complex admittance of the PZT; G and B are the real and imaginary components of the admittance; j is the imaginary unit; ω is the angular frequency of excitation; L, W and $2H$ are the dimensions of PZT; A_0, C_0 and E_0 are the coefficients along directions X, Y and Z (thickness direction) respectively; $\overline{\varepsilon_{33}}$ is the complex electric permittivity of PZT; d_{31}, d_{32} and d_{33} are the strain displacement coefficients along the X, Y and Z directions in the presence of electric field along the Z direction; λ_1, λ_2 and λ_3 are the response factors along the X, Y and Z directions; $k = \sqrt{\rho / Y_R}$, $Y_R = \overline{E}(1-\nu)/[(1+\nu)(1-2\nu)]$ and

$R = v / (1 - v)$ with ρ, v and $\bar{E}$ being the mass density, Poisson's ratio and complex Young's modulus of the PZT. The coefficients A_0, C_0 and E_0 reflect the mechanical impedance of the structure, which can be calculated by numerical analysis. In this study, FEA using ANSYS is conducted to obtain these coefficients, which are then substituted in Eq. (1) to obtain the admittance signature.

In FEA, the aluminum specimen is discretized into mesh size of 5mm × 5mm × 5mm at the region of nine PZTs while larger mesh size of 20mm × 20mm × 5mm is applied for the remaining part since the region of PZTs is more critical in the analysis (Figure 2).

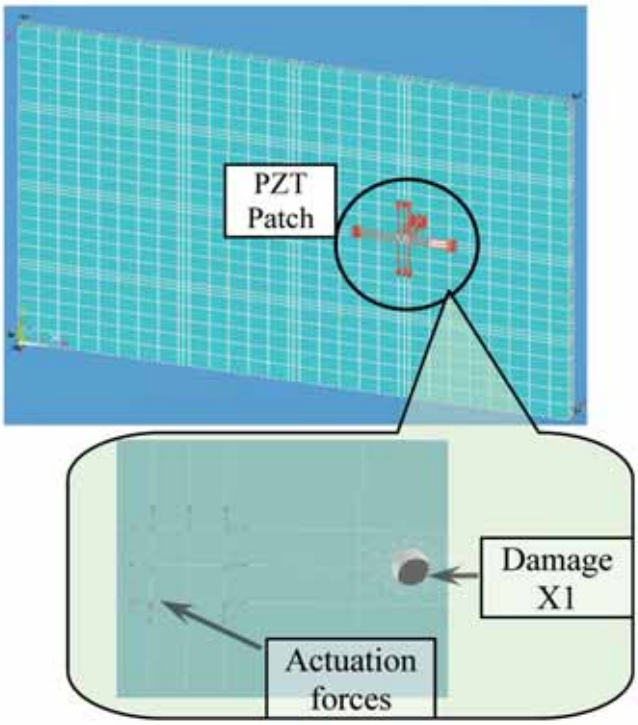

Figure 2. Finite element modelling of specimen with damage X1

Throughout the experiment, the specimen is supported at four corners only. Hence, in the FEA model, displacements along the Z direction at four corners of the plate are restricted (set to zero). The other two constraints are applied at the corner to avoid the rigid body motion of the structure. Overall, these boundary conditions are equivalent to the experimental boundary conditions. Linear harmonic loads are applied to the plate along the edges of PZT to simulate the actuation force of PZT.

After performing the FEA, the coefficients A_0, C_0 and E_0 are obtained by the ratio of applied load to the velocity at the PZT edges. They are then substituted into Eq.(1) to calculate the predicted signatures, which are subsequently analyzed using the RMSD index and compared with the experimental ones.

STATISTICAL ANALYSIS OF EXPERIMENTAL AND NUMERICAL RESULTS

Statistical analysis using RMSD is an effective way to understand the changes in signature due to damage. The equation for calculating the RMSD index is given as

$$\text{RMSD (\%)} = \sqrt{\frac{\sum_{i=1}^{N}\left(y_i - x_i\right)^2}{\sum_{i=1}^{N} x_i^2}} \times 100 \qquad \ldots (2)$$

where y_i (i = 1, 2, 3…N) is the signature obtained from the PZT for certain damage state; and x_i represents the baseline signature. Damage state X1 is compared with the baseline (without damage), while damage state Y1 is compared with damage state X1 since hole Y1 is drilled after hole X1.

Figures 3 and 4 show the plots of experimental and numerical RMSD indices for all the nine PZTs at damage stages X1 (Figure 3 (a) and (b)) and Y1 (Figure 4 (a) and (b)), respectively. The selected frequency range is 10 to 50 kHz since the most major peaks of conductance signature are in the range.

It is observed from the experimental results that the RMSD values of the PZTs close to the damage are significantly larger than those of the remote ones. For example, PZT6 generates the largest RMSD after damage X1 and PZT2 generates the largest after damage Y1. Besides, the RMSD values of the PZTs which are located symmetrically with equal distance to the damage, for example PZT4 and PZT6 at damage state Y1, are considerably close. Comparisons between the experimental and numerical results show good agreement. More importantly, both show the similar pattern of RMSD indices. From the RMSD patterns shown in Figures 3 and 4, it is easy to estimate the damage location. For example, from Figure 3, the damage should be located to the right of PZT6 with approximately equal distance to PZT9 and PZT3. But this method is not able to determine the exact location of the damage. However, in practice, a rough estimation of damage location could provide valuable guideline for inspection and maintenance by saving time and cost for locating the damage. To determine the exact location of damage, further quantitative study is needed to relate the RMSD values to the distance between the damage and the PZTs.

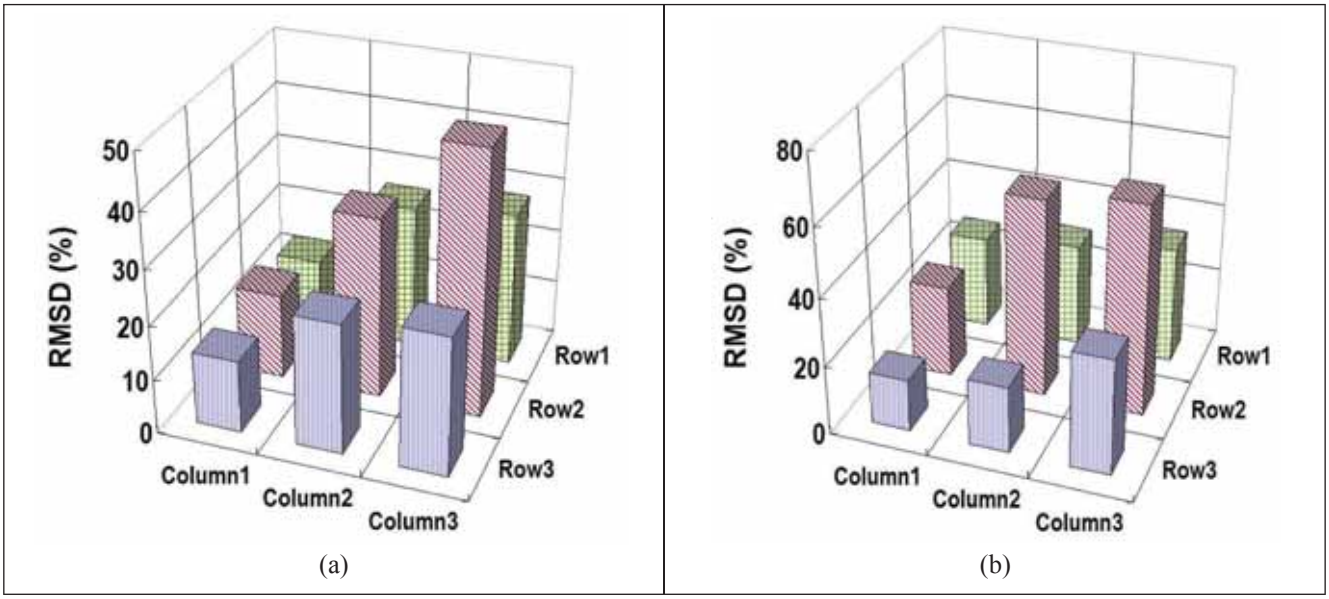

Figure 3. RMSD for damage X1 (a) Experiment (b) FEA simulation

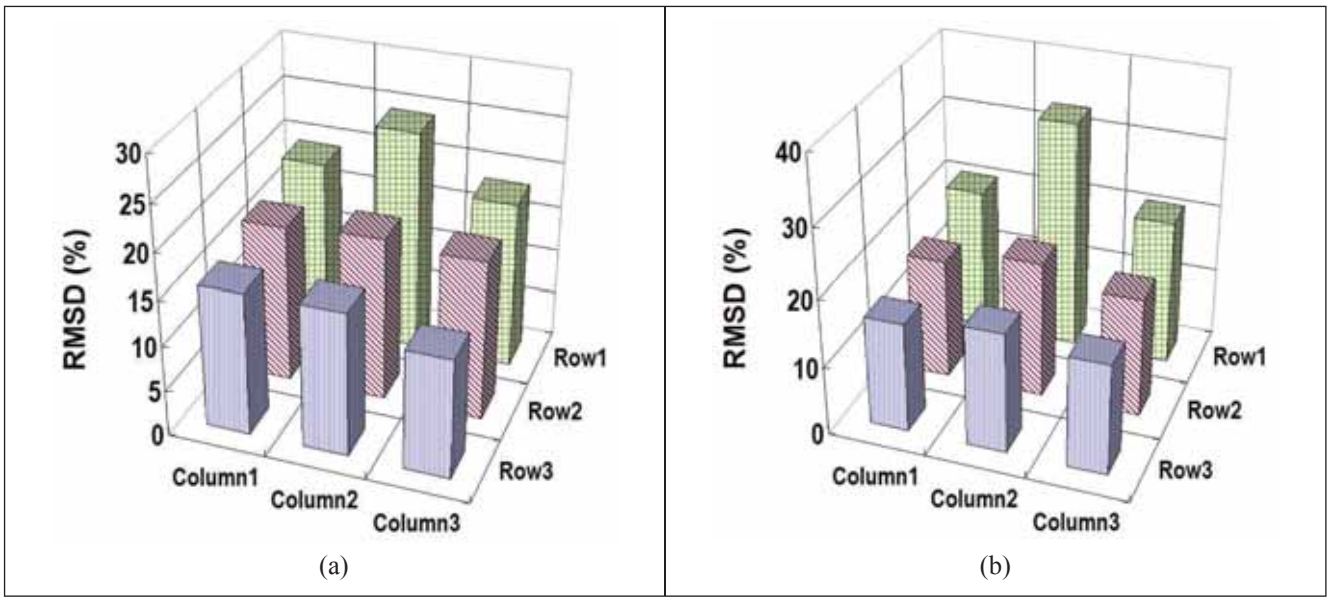

Figure 4. RMSD for damage Y1 (a) Experiment (b) FEA simulation

CONCLUSIONS

This article presents an experimental study of damage localization on an aluminum plate specimen using an array of nine PZT impedance transducers. The RMSD patterns are used to estimate the location of damage. Based on the observation that the PZTs closer to the damage generate larger RMSD values and PZTs with equal distance to the damage generate approximately equal RMSDs, the damage location can be estimated. FEA is also conducted to verify the experimental results. The RMSD values of numerical results show similar patterns to the experimental ones. The results would provide valuable guidelines for estimating damage location in metallic structures.

REFERENCES

[1] Yang, Y.W., Hu, Y.H. and Lu, Y., 2008. "Sensitivity of PZT impedance sensors for damage detection of concrete structures". *Sensors*, Vol. 8, pp. 327-346.

[2] Xu, J.F., Yang, Y.W. and Soh, C.K., 2004. "Electromechanical impedance-based structural health monitoring with evolutionary programming". *Journal of Aerospace Engineering*, *Vol. 17,* No. 4, pp. 182-193.

SCF PREDICTION OF COMPLEX TUBULAR JOINT USING INTERPOLATION APPROACH

Lee Chi King (ccklee@ntu.edu.sg)
Chiew Sing Ping (cspchiew@ntu.edu.sg)
Lie Seng Tjhen (cstlie@ntu.edu.sg)
Sopha Thong (soph0001@ntu.edu.sg)

INTRODUCTION

In the fatigue assessment of tubular joint, the stress concentration factor (SCF) is one of the most important indicators that determine the performance of the joint under cyclic loading. The variation of the SCF with respect to the geometrical and loading parameters is always a critical factor that needed to be considered during tubular joint design. In most design codes for tubular joints, the variations of the SCF with respect to the geometrical and loading parameters are described by some empirical equations. These equations are normally obtained by applying multi-variable regression analysis on the numerical modelling results obtained from parametric studies on a set of identified parameters. For simple joint types under simple loading condition, these empirical equations are often able to provide reasonable predictions. However, for the cases of a more complicated joint or a simple joint under complex loading, such an approach would often result in lengthy equations [1]. Furthermore, due to the complexity of the joint and the presence of many parameters, these lengthy equations would not be able to give good predictions over the whole range of parameters. To overcome this problem, a new approach based on the interpolation method described below was proposed [1-3].

THE INTERPOLATION APPROACH

The main concept of this approach is to combine the results obtained from the numerical parametric studies with the standard interpolation method which is commonly used in finite element (FE) method [4]. Since the responses of the joints for those identified parameters over some selected ranges were pre-computed at some fixed intervals during the parametric study, a logical way to approximate the variation of the responses can be obtained by using the standard Lagrangian interpolation functions that are frequently used in the FE analysis. Figure 1 shows an example where the variation of the response Φ is a function of a certain parameter ξ in the range $[\xi_1, \xi_8]$. Note that Φ could be the SCF of the joint or it could be other key responses such as the stress intensity factor (SIF) at the crack tip for a cracked joint. The values of Φ at the nodes, ξ_i, i = 1,..,8 are already computed during the parametric study and are denoted as Φ_i.

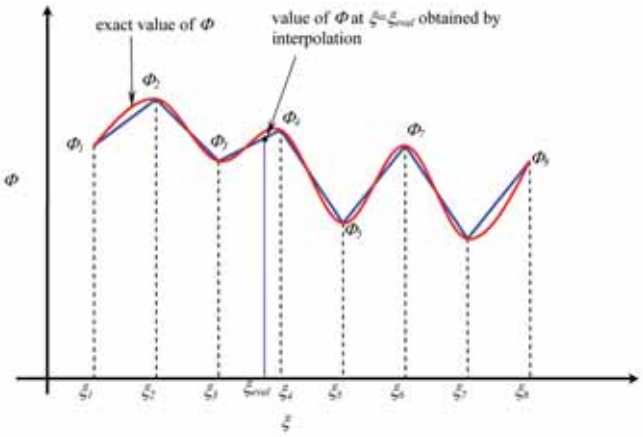

Figure 1. Approximation of Φ for the single parameter (1D) case

If the value of Φ at a given value of $\xi = \xi_{eval}$ is required, the third interval $[\xi_3, \xi_4]$ that contains ξ_{eval} is first identified. The approximated value $\tilde{\Phi}(\xi_{eval})$ is then computed as

$$\tilde{\Phi}(\xi_{eval}) = L_1(\xi_{eval})\Phi_3 + L_2(\xi_{eval})\Phi_4 \quad \ldots (1)$$

In Eqn. (1), $L_j(\xi)$, j=1, 2 are the first order Lagrangian interpolation function defined as

$$L_1(\xi) = \frac{\xi_{i+1} - \xi}{\xi_{i+1} - \xi_i}$$
$$L_2(\xi) = \frac{\xi - \xi_i}{\xi_{i+1} - \xi_i}, i = 3 \quad \ldots (2)$$

For the 2D case, the variation of Φ is a function of two parameters ξ^1 and ξ^2 and the desired point $(\xi^1_{eval}, \xi^2_{eval})$ is enclosed by $2^2=4$ nodal points as shown in Figure 2. The i_1th interval along the ξ^1 axis and the i_2th interval along the ξ^2 axis that enclose $(\xi^1_{eval}, \xi^2_{eval})$ can be easily identified. The approximated value $\tilde{\Phi}(\xi^1_{eval}, \xi^2_{eval})$ at the desired point can be obtained by extending Eqns. (1) and (2) as

$$\tilde{\Phi}(\xi^1_{eval}, \xi^2_{eval}) = \sum_{\alpha_1,\alpha_2=1,2}^{\alpha_1+\alpha_2 \le 4} L^1_{\alpha_1}(\xi^1_{eval}) L^2_{\alpha_2}(\xi^2_{eval}) \Phi_{i_1+\alpha_1-1, i_2+\alpha_2-1} \quad \ldots (3)$$

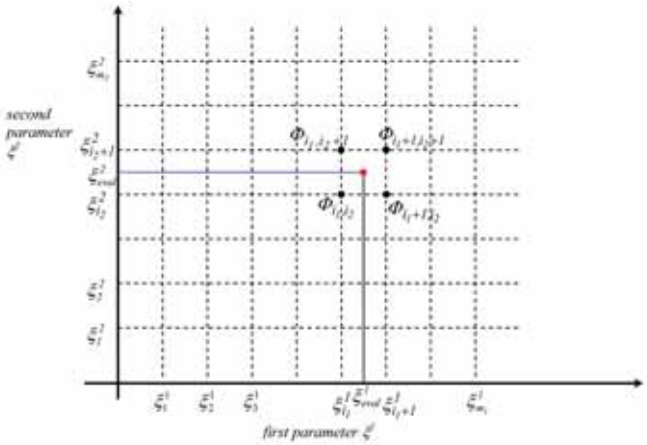

Figure 2. Approximation of Φ for the two parameters (2D) case

where

$$L_1^k\left(\xi^k\right)=\frac{\xi^k_{i_k+1}-\xi^k}{\xi^k_{i_k+1}-\xi^k_{i_k}}$$

$$L_2^k\left(\xi^k\right)=\frac{\xi^k-\xi^k_{i_k+1}}{\xi^k_{i_k+1}-\xi^k_{i_k}},k=1,2 \quad \ldots (4)$$

In general, in order to obtain approximation of Φ with respect to the variation of M selected parameters ξ^k, k = 1, …., M, the above interpolation approach should be extended to the M-dimensional space. In this case, the desired point of evaluation $\xi_{eval} = \xi^1_{eval},\xi^2_{eval},\ldots,\xi^M_{eval}$ is enclosed by a hypercube with 2^M nodes and M intervals $[\xi^k_{i_k},\xi^k_{i_{k+1}}]$ such that $\xi^k_{i_k} \le \xi^k_{eval} \le \xi^k_{i_{k+1}}$ for $k = 1, \ldots, M$. The expression of the approximated value at the point ξ_{eval}, $\tilde{\Phi}\left(\xi_{eval}\right)$, is given by

$$\tilde{\Phi}\left(\boldsymbol{\xi}_{\boldsymbol{eval}}\right)=\sum_{\alpha_k=1,2,k=1,..M}^{\sum\alpha_k\le 2M}\left(\prod_{k=1}^{M}L^k_{\alpha_k}\left(\xi^k_{eval}\right)\right)\Phi_{i_k+\alpha_k-1} \quad \ldots (5)$$

In Eq. (5), $\Phi_{i_k+\alpha_k-1}$ denotes the pre-computed nodal value of Φ at the node $(\xi^1_{i_1+\alpha_1-1},\xi^2_{i_2+\alpha_2-1},\ldots,\xi^k_{i_M+\alpha_M-1})$.

In an extensive numerical study carried out to access the performance of the above interpolation approach for the prediction of the SIF at the deepest point of surface cracks for gap CHS K-joints [1], it was found that this approach could lead to more accurate and reliable response predictions with a lower relative error and a smaller error range. In addition, by using this method, it is possible to estimate the upper error bound of the predicted responses and allow the user to obtain conservative response estimations during design.

EXAMPLES

The above interpolation procedure is applied to the prediction of the SCF of partially overlapped circular hollow section (CHS) K-joints. Figure 3 shows the typical configuration and notations for a partially overlapped CHS K-joint. Due to the complexity of the joint configuration, it was found that for a given loading type, at least six parameters must be specified to describe the variation of the SCF along the three intersection curves of the joint. Hence, the regression approach is deemed to produce lengthy empirical equations which are unlikely to yield accurate results over all the ranges of the selected parameters. In this case, the interpolation method could be used to improve the prediction accuracy. A large scale parametric study contains approximately five thousand partially overlapped CHS K-joint models covering the parametric ranges interested is first conducted. The results obtained (variation of SCF along the intersection curves of the joint) are then processed and organized in a structural manner in order to use with the interpolation method. In order to facilitate the user to compute the predicted value using Eqn. 5, an interactive program which allows user input the dimensional of the joint as well as the loading applied to it was developed. Figure 4 shows the screen shot of the user input interface of the program. The inputs entered by the user are then converted to the corresponding parametric values for SCF estimation. After the requirement SCF estimation is computed. The results are then converted back to hot spot stress values and displayed through the user output interface of the program as shown in Figure 5. In addition, if needed, the user could also save the results into an output file for future reference. Note that this interactive program also allows the user to specify multiple joints and loading configurations through an input file so that the user would able to conduct a fast what-if analysis conveniently.

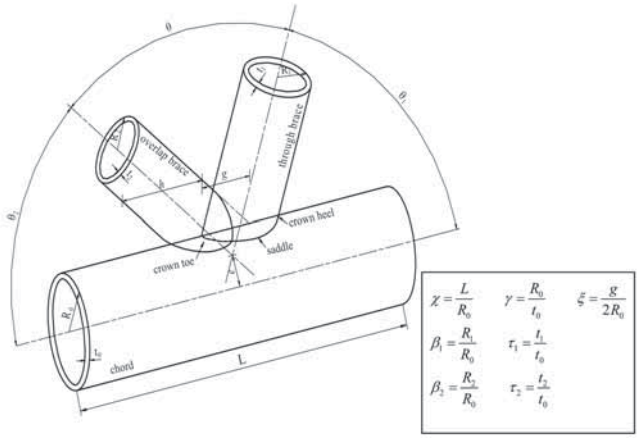

Figure 3. Configuration and notations for a typical partially overlapped CHS K-joint

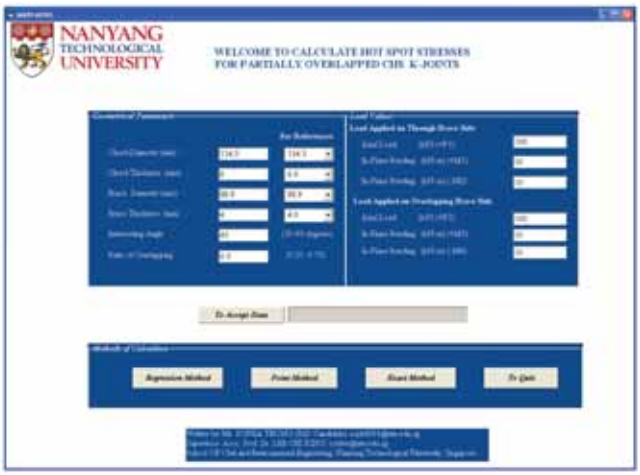

Figure 4. Input screen for the interactive program

Figure 5. Typical output screen for the interactive program

CONCLUSIONS

In this article, a new approach to estimate the SCF values for complex tubular joints is presented. An application example for the SCF estimation of partially overlapped CHS K- joint is presented. In addition, in order to allow the user to compute the estimated SCF value conveniently and convert it back to the corresponding hot spot stress value for design, an interactive programme was created. The total storage size needed to store the program and all the estimate data is approximately 30Mbytes. Therefore, the program and also the data needed could be easily stored and launched from a portable flash drive. Furthermore, the speed of the program is also very fast such that a multiple run involving 30 joint configurations could be completed within one minute on a low end PC.

REFERENCES

[1] Shao, Y.B., 2004. "Fatigue behaviour of uniplanar CHS gap K-joints under axial and in-plane bending loads". *PhD Thesis, School of Civil and Environmental Engineering, Nanyang Technological University, Singapore*.

[2] Lie, S.T., Lee, C.K., Chiew, S.P. and Shao, Y.B., 2005. "Validation of surface crack stress intensity factors of a tubular K-joint". *International Journal of Pressure Vessels and Piping*, Vol. 82, No. 8, pp. 610-617.

[3] Lie, S.T., Shao, Y.B., Lee, C.K. and Chiew, S.P., 2006. "Stress intensity factor solutions for semi-elliptical weld-toe cracks in tubular K-joints". *Advances In Structural Engineering*, Vol. 9, No. 1, pp. 129-139.

[4] Zienkiewicz, O.C., Taylor, R.L. and Zhu, J.Z, 2005. "The Finite Element Method: Its Basis and Fundamentals". *6th Edition, Elsevier Butterworth-Heinemann, UK.*

STATIC ULTIMATE STRENGTH OF CRACKED SQUARE HOLLOW SECTION Y-JOINT

Lie Seng Tjhen (cstlie@ntu.edu.sg)
Yang Zhengmao (ZhengMao.Yang@dnv.com.sg)

INTRODUCTION

To validate the finite element models of a cracked square hollow section (SHS) Y-joint[1], a full-scale specimen was tested under incremental loads up to failure. The Y-joint was first fatigue cracked using the "Orange Frame" test rig available in the Construction Technology Laboratory. The specimen contains a surface crack located at one of the corners as shown in Figure 1. After completion of the fatigue test, the crack dimensions were measured using the Alternating Current Potential Drop (ACPD) technique[2]. The specimen was fabricated from BS4360 structural steel of grade 50D[3]. The weld profile and the specimen preparation were carried out in accordance with the American Welding Society (AWS) Structure Welding Code–Steel D1.1/D.1.1M:2006[4] specifications. The specimen material yield stress is 380.3 MPa.

Figure 1. Crack surface of Y-joint specimen

TEST RIG AND LOADING SYSTEM

A specially designed "Yellow Frame" test rig as shown in Figure 2 was used to test the cracked SHS Y-joint. The ends of the chord were fixed with respect to the test rig. The load was applied on the end of the brace through the spreader

beam which was supported by two hydraulic jacks. Each hydraulic jack can produce load of up to 1000 kN.

Figure 2. "Yellow Frame" test rig set-up of Y-joint specimen

MEASUREMENT OF CRACK MOUTH OPENING DISPLACEMENT (CMOD)

A set of 3 LVDTs with a stroke capacity of 10 mm was used to measure the crack mouth opening displacement (CMOD) along the crack front as shown in Figure 3. One block and one bracket were attached to the chord face and brace face, and in turn three LVDTs were fixed to the bracket. The three LVDTs are in contact with the block so that the vertical displacement of points 1 and 2 and the horizontal displacement of point 3 relative to the brace can be measured accordingly.

In order to transfer the measurements obtained to the crack mouth opening displacement, an extrapolation approach is adopted in the test as shown in Figure 4. If the region between the crack and the measured point is treated as a rigid body, the displacements at the measured points are caused by the displacements and rotations of the crack faces. If the displacement measured by LVDTs 1, 2 and 3 are expressed as d_1, d_2 and l, the following relationships can be found for

$$\gamma = \frac{d_2 - d_1}{L_2}, \text{ rotation of crack} \quad \ldots (1)$$

$$d_c = d_1 - \gamma \cdot L_1, \text{ vertical displacement of crack mouth} \quad \ldots (2)$$

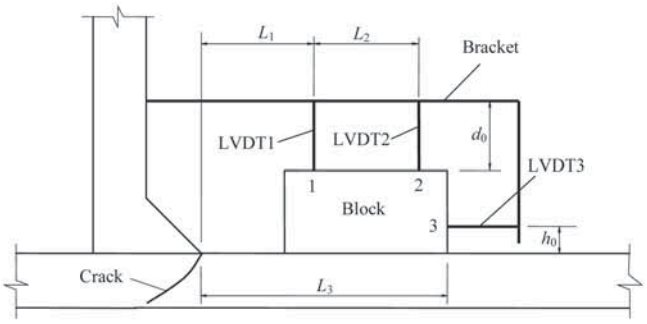

Figure 3. Dimensions of the LVDTs before the test

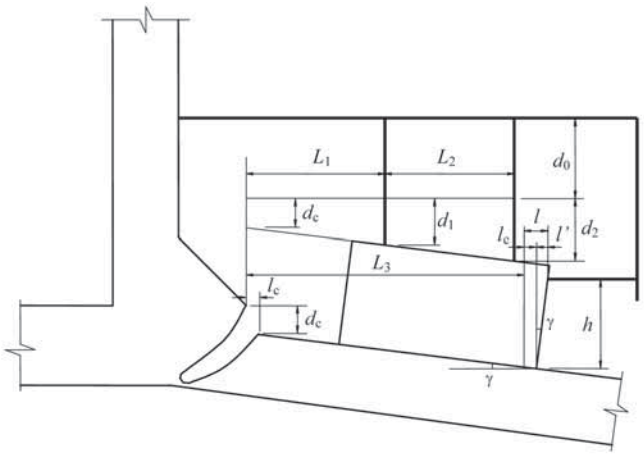

Figure 4. Dimensions of the LVDTs during the test

$l_c = l - l' = l - \gamma \cdot h$, horizontal displacement of crack mouth … (3)

$\delta_{CMOD} = \sqrt{d_c^2 + l_c^2}$, and crack mouth opening displacement (CMOD) … (4)

where L_1, L_2 and L_3 are the respective distances from the LVDTs 1, 2 and 3 to the weld toe, γ is the rotation angle of crack face which is equal to the rotation angle of the chord face, l' is the horizontal displacement caused by the block rotation, h is the vertical distance of the LVDT 3 away from the chord face, and it can be calculated from

$$h = h_0 + d_1 + \gamma \cdot (L_3 - L_1), \text{ vertical distance} \quad \ldots (5)$$

MESUREMENTS OF BRACE END AXIAL LOAD AND DISPLACEMENT

The brace end displacement was obtained from an LVDT with a stroke capacity of 50 mm that was calibrated and attached to the bottom of spreader beam aligned with the centreline of the brace and the two ends of the spreader beam. The load was obtained via load cell, and the load was also measured using the strain gauges attached at the middle of the brace to confirm the load readings.

TEST RESULTS AND COMPARISON WITH NUMERICAL RESULTS

All the numerical analyses are carried using ABAQUS [5], general purpose finite element program. Numerical models for both uncracked and cracked joints are created and the results load-displacement curves are compared for cracked joints and crack mouth opening displacements. Figure 5 shows the load-displacement curve for the Y-joint subjected to brace end axial loads. When the elastic load is up to 520 kN, this curve turn into plastic region. From the ACPD readings, it can be found that the crack shows an obvious ductile tearing, until the load reach 1290 kN, the crack through the chord wall. After this point, the load still can increase slightly to the maximum load of 1311 kN before it drops down.

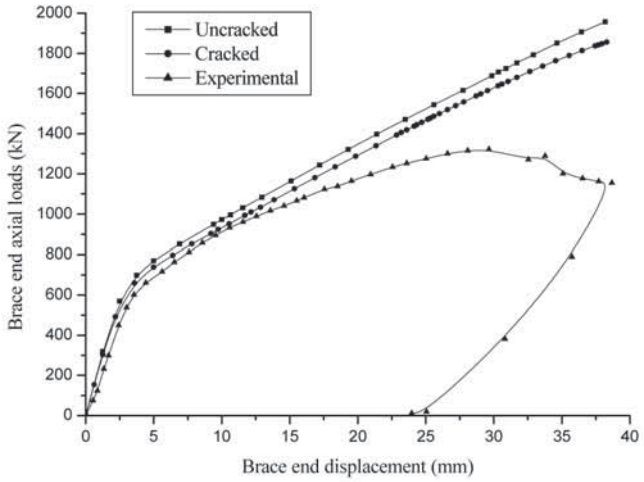

Figure 5. Load-displacement curve for Y-joint specimen

Figure 6 shows the comparison of crack mouth opening displacement (CMOD) versus brace end axial loads. From the results below, it can be seen clearly that a good agreement is obtained between the numerical and the experimental results before the joint had failed.

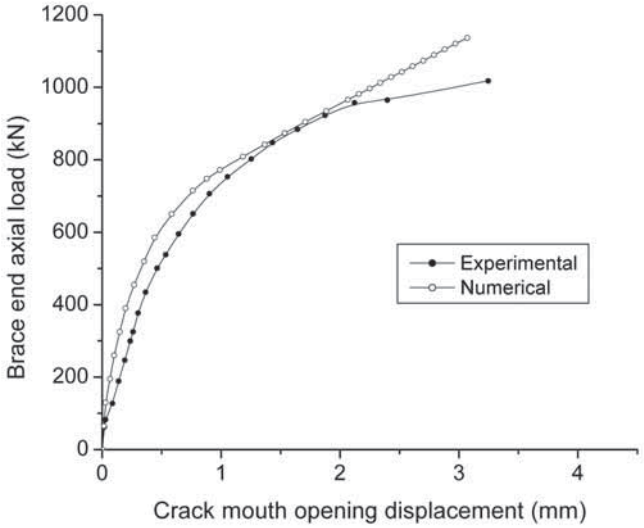

Figure 6. Load-CMOD curves for Y-joint specimen

CONCLUSIONS

It is obvious that the Y-joint specimen has a notable plastic deformation. Compared with the numerical curves which do not model the crack ductile tearing, the experimental loads are lower than the numerical ones. Before the crack propagated significantly, the numerical curve is close to the experimental one. Hence, the proposed numerical model is reliable, and it is suitable to be used for analyzing the plastic collapse behaviour and crack driving force of cracked SHS Y-joints.

REFERENCES

[1] Lie, S.T., Lee, C.K., Chiew, S.P. and Yang, Z.M., 2006. "A Consistent Crack Modelling and Analysis of Rectangular Hollow Section Joints". *Finite Elements in Analysis and Design – An International Journal for Innovations in Computational Methodology and Application*, Vol. 42, No. 8-9, pp. 639-649.

[2] Dover, W.D., Dharmavasan, S., Brennan, F.P. and Marsh, K.J., 1995. *Fatigue Crack Growth in Offshore Structures*. Engineering Materials Advisory Services Ltd., Chameleon Press, London, UK.

[3] American Welding Society (AWS), 2006. *ANSI/AWS D1.1/ D1.1M:2006, Structural Welding Code – Steel*. Miami, USA.

[4] Yang, Z.M., Lie, S.T., and Gho, W.M., 2007. "Failure Assessment of Cracked Square Hollow Section T-Joints". *International Journal of Pressure Vessels and Piping*, Vol. 84, No. 4, pp. 244-255.

[5] ABAQUS, 2006. *Theory Manual*. Version 6.4, Hobbit, Karlsson & Sorensen Inc., USA.

STRAIN TRANSFER MODELS FOR STRAIN ACTUATORS

Yang Yaowen (cywyang@ntu.edu.sg)
Sabet Divsholi Bahador (sabe0002@ntu.edu.sg)

INTRODUCTION

One of the advantages of piezo-composite actuators is to provide low cost and in-situ actuation with high flexibility[1]. Actuators as patches made of bulk lead zirconate titanate (PZT) material are widely used for vibration control of mechanical structures. However, extremely brittle nature of the PZT material requires extra attention during the handling and bonding procedures[2]. Micro fiber composite (MFC) has shown its great potential for vibration and noise control, health monitoring, morphing of structures and energy harvesting[3]. To explore various applications of MFC, a reasonable model accounting for the strain transfer phenomenon between the MFC and the structure is crucial[4]. There have been a few one dimensional (1-D) models on strain transfer[5,6,7], but issues still remain on how accurately these models predict the phenomenon and how effectively they can be extended to two dimensional (2-D) cases to increase the accuracy of prediction.

In this work, the existing 1-D Bernoulli-Euler formulation for bending, coupled bending and extension of isotropic beams/plates with induced strain actuators is extended to 2-D cases. Further, it is improved to account for the reduction in actuation as a result of strain distribution inside the actuator. The improved 1-D and 2-D formulations are compared with the uniform strain model which includes the shear lag effects due to the adhesive layer. A finite element model is also developed to study the strain transfer. Finally, an experimental test is carried out to evaluate the accuracy and limitations of the developed models. Results show that the models are in good agreement with the experiment.

EXISTING STRAIN TRANSFER MODEL

As shown in Figure 1, the existing model is based on a beam with strain actuator bonded to its surface. In this study, MFC type d_{33} is used but the developed models are not limited to this actuator. Besides the dimensions, free induced strain in each direction is needed in modelling. The detailed characteristics of MFC actuators can be found in Smart Materials website[8]. In type d_{33} the electrical potential follows in the longitudinal direction of MFC instead of the thickness direction. The free induced strain of the MFC actuator can be calculated as follows:

$$\Lambda = \varepsilon^E = d\frac{\Delta V}{\Delta X} \qquad \ldots (1)$$

where d is piezoelectric constant; ΔV is the applied voltage; and ΔX is the electrode spacing. For MFC-d_{33}, the free strain is around 0.75 ppm in low electrical field ($|E|<1000\ V\,mm^{-1}$) and 0.9 ppm in high electrical field ($|E|>1000\ V\,mm^{-1}$)[8].

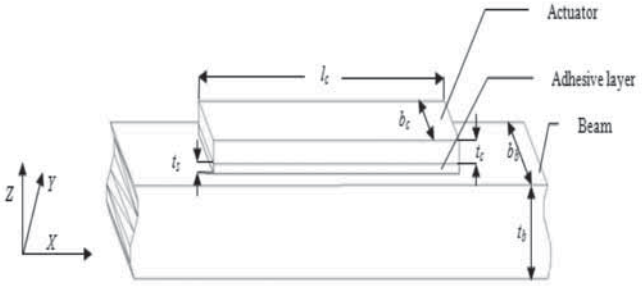

Figure 1. Configuration of beam and actuator

In the 1-D uniform strain method, the solution for the strain transfer with the assumption of finite thickness of the adhesive layer was presented by Park et al.[5]. The strain in the bottom of the beam is

$$\frac{\varepsilon_b^b(\bar{x})}{\Lambda} = -\frac{2}{\psi_b+4} + \frac{2}{(\psi_b+4)\cosh(\Gamma)}\cosh(\Gamma\bar{x}) \qquad \ldots (2)$$

where the non-dimensional shear lag Γ and stiffness ratio ψ are defined as

$$\Gamma^2 = \frac{\psi_s}{\bar{t}_s^2}(1+\frac{4}{\psi_b}),\quad \psi_b = \frac{E_b t_b b_b}{E_c t_c b_c},\quad \psi_s = \frac{E_s t_s b_s}{E_c t_c b_c},\quad \bar{t}_s = \frac{t_s}{l_c/2}$$

where E and G are the shear modulus and Young's modulus, respectively; and the subscripts b, s and c represent the beam, adhesive layer and actuator, respectively. Other geometric dimensions are shown in Figure 1. The bending curvature can be calculated as follows:

$$\frac{\partial^2 w}{\partial x^2} = -\kappa = \frac{2\Lambda}{t_b}\left(\frac{3}{\psi_b+4}\right)\left(1-\frac{\cosh(\Gamma\bar{x})}{\cosh(\Gamma)}\right) \qquad \ldots (3)$$

In the 1-D Bernulli-Euler model proposed by Crawley[7], the strain was assumed to be linear and consistent through the entire cross section. The strain through the thickness of the cross section can be calculated as follows:

$$\varepsilon(z) = \varepsilon_0 - z\kappa \qquad \ldots (4)$$

The induced forces and moments are:

$$P_\Lambda = E_c b_c t_c \Lambda \qquad \ldots (5)$$

$$M_\Lambda = E_c b_c t_c (t_b + t_s + \frac{t_c}{2} - \bar{z})\Lambda \qquad \ldots (6)$$

where

$$\bar{z} = \frac{E_b b_b t_b (\frac{t_b}{2}) + E_s b_c t_s (t_b + \frac{t_s}{2}) + E_c b_c t_c (t_b + t_s + \frac{t_c}{2})}{E_b b_b t_b + E_s b_c t_s + E_c b_c t_c} \quad \ldots (7)$$

If no external forces or moments are present, ε_0 and κ can be calculated as follows:

$$\begin{bmatrix} EA & 0 \\ 0 & EI \end{bmatrix} \begin{bmatrix} \varepsilon_0 \\ -\kappa \end{bmatrix} = \begin{bmatrix} P_\Lambda \\ M_\Lambda \end{bmatrix} \quad \ldots (8)$$

where

$$EA = E_b b_b t_b + E_s b_c t_s + E_c b_c t_c \quad \ldots (9)$$

$$EI = \frac{1}{12} E_b b_b t_b^3 + E_b b_b t_b (\frac{t_b}{2} - \bar{z})^2 + \frac{1}{12} E_s b_c t_s^3 + E_s b_c t_s (t_b + \frac{t_s}{2} - \bar{z})^2 + \frac{1}{12} E_c b_c t_c^3 + E_c b_c t_c (t_b + t_s + \frac{t_c}{2} - \bar{z})^2 \quad \ldots (10)$$

Then by using Eq. (4), the strain at the bottom of the beam can be calculated.

2-D MODEL AND MODIFICATION OF BERNOULLI-EULER FORMULATION

In the 2-D Bernoulli-Euler model, as the modulus of elasticity and the Poisson's ratio of the MFC is different in the X and Y directions, the equivalent section characteristic needs to be calculated for both directions. The average Poisson's ratio for both directions can be calculated by using the rule of mixture. The induced forces and moments can be calculated by extending Eqs. (5) and (6) in the X and Y directions. By using the generalized Hook's law, the internal forces and moments can be obtained. Considering the property of MFC of $\Lambda_{cy} = \frac{-170}{400} \Lambda_{cx}$ [8], the strain and the curvature can be calculated as follows:

$$\frac{\varepsilon_{0x}}{\Lambda_x} = \frac{E_{cx} b_c t_c - (\frac{170}{400}) E_{cy} l_c t_c (\frac{\nu_{21}(1-\nu_{12}^2) E_x A}{(1-\nu_{21}^2) E_y A})}{E_x A (\frac{1-\nu_{21}\nu_{12}}{1-\nu_{21}^2})} \quad \ldots (11)$$

$$\frac{\kappa_x}{\Lambda_x} = -\frac{E_{cx} b_c t_c H - (\frac{170}{400}) E_{cy} l_c t_c H (\frac{\nu_{21}(1-\nu_{12}^2) E_x I}{(1-\nu_{21}^2) E_y I})}{E_x I (\frac{1-\nu_{21}\nu_{12}}{1-\nu_{21}^2})} \quad \ldots (12)$$

where $H = (t_b + t_s + t_c/2 - \bar{z})$. Then by using Eq. (4), the strain at the bottom of the beam can be calculated.

The induced force in the Bernoulli-Euler model[7] is related to the induced strain by Eqs. (5) and (6). However the stress in actuator should be related to difference between the apparent and induced strains as:

$$\sigma_c = E_c(\varepsilon_c - \Lambda) \quad \ldots (13)$$

where E_c is the modulus of elasticity of the actuator; and ε_c is the apparent strain. Therefore the 1-D and 2-D Bernulli-Euler models can be modified as follows. The 1-D modified Bernulli-Euler model is

$$\frac{\varepsilon_0}{\Lambda} = \frac{E_c b_c t_c - \frac{(E_c b_c t_c H)^2}{(EI + E_c b_c t_c H^2)}}{EA + E_c b_c t_c - \frac{(E_c b_c t_c H)^2}{(EI + E_c b_c t_c H^2)}} \quad \ldots (14)$$

$$\frac{\kappa}{\Lambda} = \frac{(EA + E_c b_c t_c)\frac{\varepsilon_0}{\kappa} - E_c b_c t_c}{E_c b_c t_c H}. \quad \ldots (15)$$

The 2-D modified Bernulli-Euler model is

$$\begin{bmatrix} \frac{E_x A}{1-\nu_{12}^2} + E_{cx} b_c t_c & \frac{\nu_{21} E_x A}{1-\nu_{21}^2} & -E_{cx} b_c t_c H & 0 \\ \frac{\nu_{12} E_y A}{1-\nu_{21}^2} & \frac{E_y A}{1-\nu_{12}^2} - E_{cy} l_c t_c & 0 & E_{cy} l_c t_c H \\ E_{cx} b_c t_c H & 0 & -(\frac{E_x A}{1-\nu_{12}^2} + E_{cx} b_c t_c H^2) & -\frac{\nu_{21} E_x I}{1-\nu_{21}^2} \\ 0 & -E_{cy} l_c t_c H & \frac{\nu_{12} E_y A}{1-\nu_{12}^2} & -(\frac{E_y I}{1-\nu_{12}^2} + E_{cy} l_c t_c H^2) \end{bmatrix} \begin{bmatrix} \frac{\varepsilon_{0x}}{\Lambda_x} \\ \frac{\varepsilon_{0y}}{\Lambda_x} \\ \frac{\kappa_x}{\Lambda_x} \\ \frac{\kappa_y}{\Lambda_x} \end{bmatrix}$$

$$= \begin{bmatrix} E_{cx} b_c t_c \\ \frac{170}{400} E_{cy} l_c t_c \\ E_{cx} b_c t_c H \\ \frac{170}{400} E_{cy} l_c t_c H \end{bmatrix}.$$

FINITE ELEMENT MODELING

A finite element model is developed with ABACUS to simulate the actuation of MFC. The piezoelectric elements in ABACUS are used to simulate the d_{31} material. The parameters of the elements need to be changed to simulate the d_{33} material. Figure 2 shows the simulation model of a cantilever beam using ABAQUS.

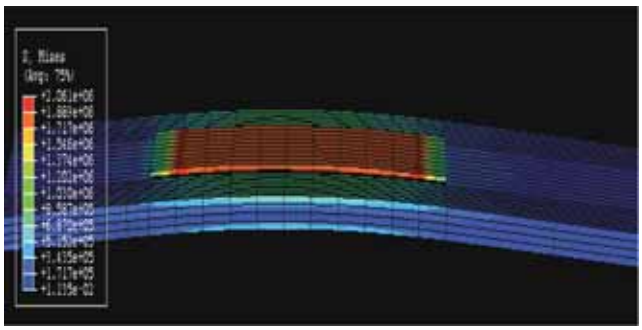

Figure 2. Simulation of cantilever beam and MFC actuator with ABAQUS

EXPERIMENTAL SETUP

In the experiment setup shown in Figures 3 and 4, an MFC actuator is bonded on the top surface of the beam and a strain gauge is bonded on the bottom surface and at the center of MFC. Various beams and MFCs with different sizes are tested to investigate the strain at the bottom of the beam.

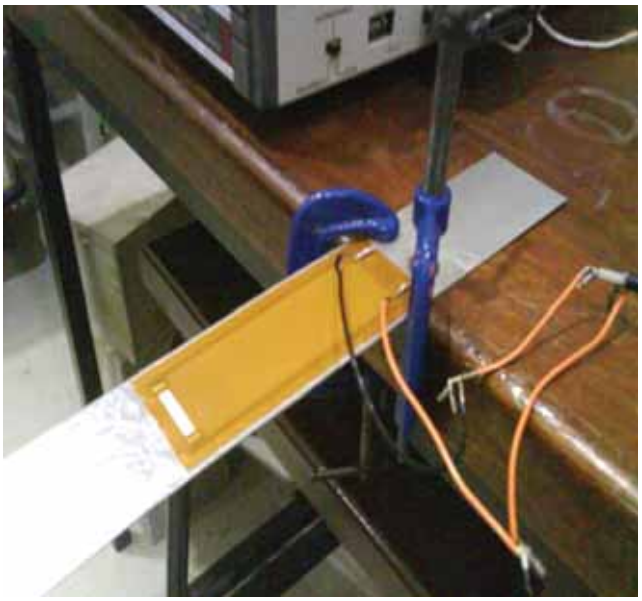

Figure 3. Experimental setup

Figure 4. Strain gauge at bottom of beam

RESULTS AND CONCLUSIONS

Figure 5 shows the theoretical results predicted by different models, with comparison with the numerical and experimental ones. It can be observed that the 2-D Bernoulli-Euler model has better prediction ability compared to its 1-D counterpart, and the modified models improve the accuracy of prediction. The uniform strain model shows a good fit to the experimental data with thickness of epoxy equal to 0.1 mm but the prediction accuracy decreases with increase in the thickness of epoxy. The finite element simulation results are in good agreement with the experimental ones, showing its potential in modelling the MFC-d_{33} material.

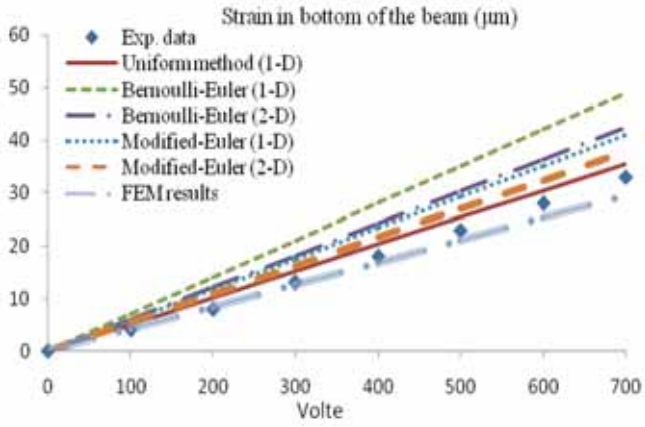

Figure 5: Theoretical, numerical and experimental results

REFERENCES

[1] Werlink, R.J., Bryant, R.G. and Manos, D., 2002. *Macro Fiber Piezocomposite Actuator Poling Study.* NASA/TM-2002-211434.

[2] Sodano Henry A., Park Gyuhae, Inman Daniel J., 2004. *Mechanical systems and signal processing,* Vol. 18, pp. 683-697.

[3] A.J. Schönecker, T. Daue, B. Brückner, C. Freytag, L. Hähne, T. Rödig: *Proceedings of SPIE*, Vol. 6170 (2006), 61701K.

[4] Sabet Divsholi Bahador**,** Yaowen Yang and Lei Zhang, (2008). *Advanced Materials Research*, Vols. 47-50, pp. 254-257.

[5] C. Park, C. Walz, I. Chopra, 1987. *Smart Materials and Structure*, Vol. 5 (1996), p. 98.

[6] E. Crawley, J. de Luis: *AIAA J.*, Vol. 25, p. 1373.

[7] E. Crawley, J. de Luis, 1989. *Proc. 30th AIAA/ASMI/ASCH/AHS/ASC structures, structural dynamics and materials conf.*

[8] http://www.Smatr-material.com

SUMATRAN MEGATHRUST EARTHQUAKES: WHAT HAS HAPPENED, AND WHAT'S NEXT?

Kusnowidjaja Megawati (kusno@ntu.edu.sg)
Kerry Sieh (sieh@ntu.edu.sg)
Tso-Chien Pan (cpan@ntu.edu.sg)

Why does Sumatra keep sending earthquakes our way? And what might be coming next? These are questions that many Singaporeans are asking recently, as the shaking that began in June 2000 continues.

The world's biggest earthquakes and most of its volcanoes occur where giant tectonic plates beneath the oceans are diving down under neighbouring landmasses. Singapore is fortunate to lie several hundred kilometres from the nearest such "subduction" zone, in the middle of a tectonic plate that includes all of its Southeast Asian neighbours. Still, the western edge of that plate, on the other side of Sumatra, generates such big earthquakes that gentle swaying is commonly felt in Singapore.

All of the earthquakes we have felt in the past eight years happened because the upper surface of the downgoing oceanic plate (called the Sunda megathrust) is sticky. As the oceanic plate descends northward at about 60 millimetres per year beneath Sumatra, it clings to Sumatra's underside along the megathrust, until it reaches depths of 50 kilometres or so, where it finally becomes hot and gooey enough to slip steadily into the deep earth.

The great earthquakes of December 2004 (M_w 9.2), March 2005 (M_w 8.6) and September 2007 (M_w 8.4 and 7.9) occurred because very large patches of the megathrust suddenly became unstuck. Imagine a rope tied to an elephant on one end and held by a team of men, some large, some small, some strong, some weak, on the other. The elephant is the dense oceanic plate sinking inexorably into the deep earth. The men are individual patches of the megathrust. The more the elephant pulls on her end of the rope, the more each man has to resist on the other end. Eventually, the weakest man lets go (the first earthquake, in 2000). He is relieved, but his fellows now have to carry his burden, to keep the elephant from winning the tug-of-war. Sometime later another lets go (the 2002 earthquake). He feels much relieved, but those remaining have to resist the elephant with even more force. Finally, half of the team gives up in rapid succession (the giant Aceh earthquake of 2004). And then a neighbouring contingent yields (in 2005). Now the elephant's tug is being resisted by far fewer men.

As of early September 2007, only one major part of the megathrust between Myanmar and Java remained unbroken – that 600-km long section nearest to Singapore. Our GPS instruments in western Sumatra show that the megathrust of this "Mentawai" section continues to resist failure. Ominously, the corals of the Mentawai island reefs show that this section breaks in sequences of great earthquakes about every two centuries and that the last such sequence occurred about two centuries ago, between 1797 and 1833.

And so it appears that even the strong men still holding the rope are, in fact, nearing the end of their rope! For several years now we have been saying that the elephant will win, and probably sometime within the next two or three decades. The large earthquakes of September 2007 were, in fact, our first indication that the Mentawai section has finally begun to fail. On 20 February 2008, a tiny patch between the great 2004 and 2005 ruptures failed in a magnitude 7.4. Curiously, that rupture may have been on the same patch that caused the 2002 foreshock! The more recent small quakes between 22 February and 3 March indicate that the Mentawai section continues to lose its grip. The parts that remain unbroken are large enough to generate a magnitude 9 earthquake, if they all go at once. One might hope that the remaining men will let go one by one (a flurry of smaller earthquakes), so that the elephant doesn't win in one dramatic flash. We consider this piecemeal scenario quite unlikely, since it would entail thousands of such earthquakes. The historical and geological records suggest that within the next couple decades one or two additional great earthquakes will end the contest.

The implications of this are serious for coastal communities of western Sumatra. If the great earthquake were to happen today, strong seismic shaking would likely damage many buildings and other infrastructure. Moreover, scientific estimates of tsunami inundations at Padang and Bengkulu, the two largest cities along the coast, illustrate the urgent need for strong emergency planning and management. Fortunately, some efforts toward these ends are being made by local government and NGOs, including new projects by Singaporean researchers. However, it is too early to tell whether these efforts will lessen losses to levels below those that occurred in Aceh in 2004.

WILL SUMATRAN EARTHQUAKES AFFECT SINGAPORE?

What about the effect of this coming great earthquake on Singapore? It is inevitable that more high-rises will be built in Singapore as its economy grows. High-rise buildings respond to earthquakes, especially shaking from distant earthquakes. The low-frequency seismic waves can travel longer distances than high-frequency waves, just as the bass frequencies of a musical instrument are heard farther than the treble. The low frequency of the earthquake shaking experienced in Singapore from Sumatran earthquakes can be amplified at sites of soft soils. The amplified low frequency shaking may be close to the natural frequencies of high-rise buildings in the city, creating a so-called resonance effect. The high-rise buildings sway back and forth during the earthquake. It is therefore more likely for people living on upper floors of high-rise buildings to sense these earthquakes than those living in low-rise houses.

However, this greater sensitivity to Sumatran earthquakes does not mean that high-rise buildings are more likely to be damaged. The potential of a structure to be damaged is not related to the amplitude of shaking at the top of the building, but rather to the so-called inter-storey drift -- the amount of deformation between one storey and the next. While the inter-storey drift generated by the distant earthquakes may be within the limits of a well-designed building, response of buildings to ground shaking depends on the details of structural configurations, and further research work will be required to better quantify dynamic building responses. It would therefore be prudent to consider the dynamic effects of distant earthquakes in the design of future buildings.

CONCLUDING REMARKS

For scientists, engineers, emergency responders, and urban planners, the ongoing series of Sumatran earthquakes and tsunamis is a rare and fascinating opportunity to observe how Earth's tectonic plates work and to improve the resilience of our engineered structures and our communities to these dynamic natural events. We in Singapore are very well-positioned to learn from the Sumatran activity. As the tectonic motions continue, we and our Indonesian colleagues will also continue to monitor and interpret it with our GPS and seismic networks.

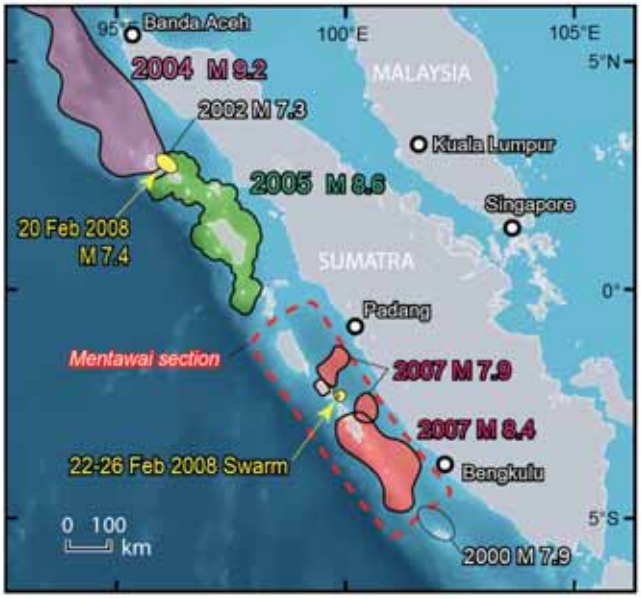

A series of giant earthquakes occurring along Sumatran Megathrust since June 2000

PORE STRUCTURE AND DURABILITY OF CONCRETE CONTAINING GBFS

Sabet Divsholi Bahador (Sabe0001@ntu.edu.sg)
Jong Herman Cahyadi (CHSjong@ntu.edu.sg)

INTRODUCTION

The use of Granulated Blast Furnace Slag (GBFS) as supplementary cementitious material for concrete production is ecologically and economically very important[1]. High quality and durable concrete is required to reduce the rapid deterioration of concrete in severe conditions. It has been proven that GBFS has perfect performance to resist chloride induced corrosion[2]. Replacing Portland Cement (PC) partially by GBFS can improve the fluidity of fresh concrete, reduce its bleeding and postpone the setting[3]. The quality of GBFS depends on the chemical composition, glass phase content and fineness of GBFS[4]. Using mineral admixtures will result in the consumption of calcium hydroxide in concrete. In short curing period, it may increase the carbonation rate of concrete[1]. In this study, the effect of replacing PC with various percentages of GBFS on different characteristics of concrete has been studied. Replacing PC partially with GBFS improved the characteristic of concrete significantly.

EXPERIMENTAL STUDY

In this study over 200 samples with three w/c ratio equal to 0.4, 0.5 and 0.6, and in four cases of 0%, 10%, 30% and 50% GBFS replacements were prepared. The characteristic of GBFS was examined by particle size analyzer, X-ray diffraction test and chemical analysis test. The mean particle size was 9.2 µm in comparison with 14.7 µm for PC, and no crystalline phase was detected in this GBFS[1].

As result of having fine particle size and no crystalline phase, this mineral admixture has high degree of reactivity. The mercury instruction porosimeter (MIP) test was carried out to measure the pore size distribution. The drying rate was observed to study the pore connection, and the chloride penetration test and carbonation test were carried out to study the durability of the concrete containing the GBFS.

RESULTS AND DISCUSSION

As mentioned previously, GBFS can improve fluidity of fresh concrete[3]. The result of slump test for varying amounts of GBFS replacement is presented in Figure 1.

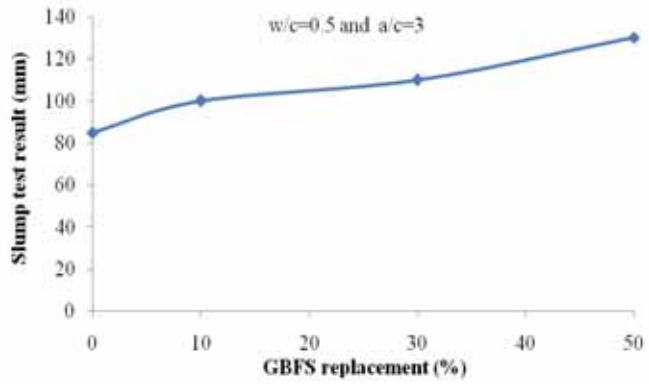

Figure 1. The effect of GBFS replacement on slump test

This GBFS showed to be effective in increasing the compressive strength of concrete even for a short curing period.

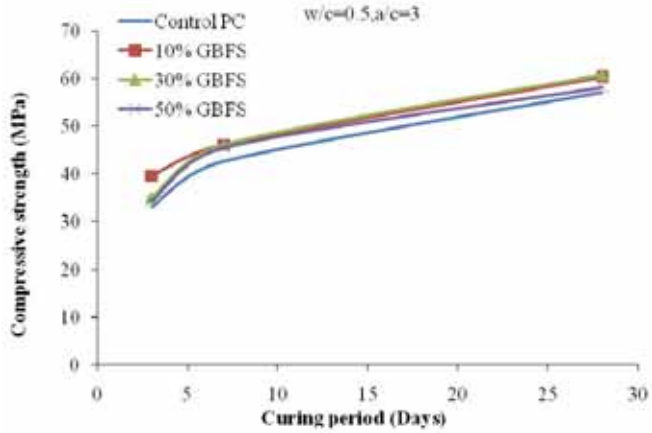

Figure 2: The effect of GBFS replacement on compressive strength of concrete

The result of MIP test shows that although the samples containing the GBFS have same total porosity, the pore size distribution is finer and the average pore size is much smaller compared to PC concrete.

Figures 3 and 4 show the effect of various percentage of GBFS replacement on pore size distribution and average pore diameter respectively.

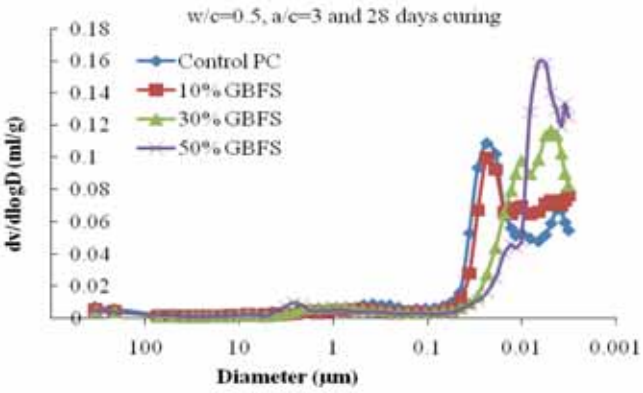

Figure 3. The effect of GBFS replacement on pore size distribution

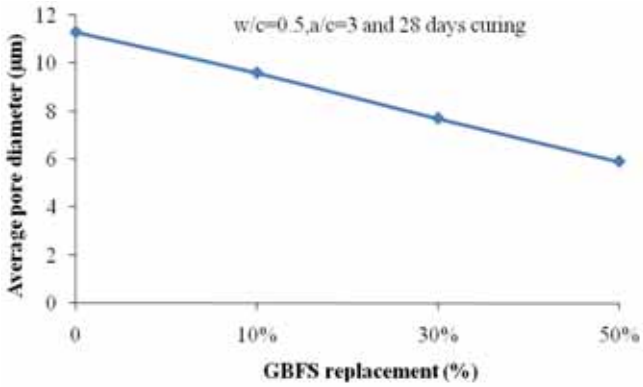

Figure 4. The effect of GBFS replacement on average pore size diameter (µm)

Figure 5 shows the effect of water curing period on average pore diameter of concrete with and without GBFS. As it can be seen the curing period can play a significant role on the pore structure of concrete containing GBFS.

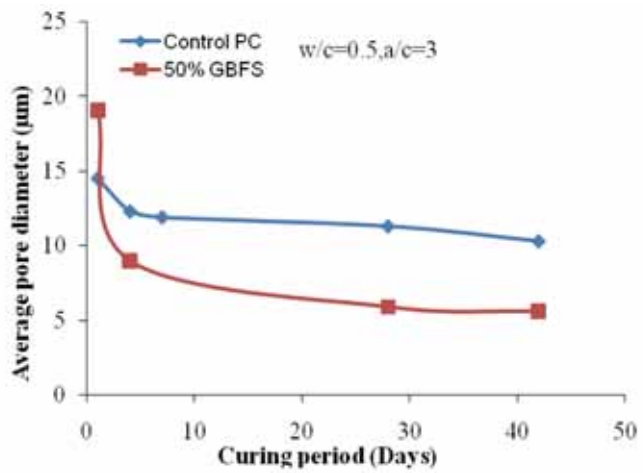

Figure 5. The effect of curing period on average pore diameter of 50% GBFS replacement

The MIP test cannot show the effect of GBFS on the pore connection of concrete. The main contribution of GBFS is to decrease pore connection as well as average pore size. Monitoring the weight loss during the drying process can highlight the effect of GBFS on the reduction of concrete pore connection.

Figure 6 shows the effect of different percentage of GBFS replacement on drying rate of concrete. As shown in Figure 4, the higher GBFS replacement leads to smaller pore size; lower pore connection and lower drying rate, then, is expected.

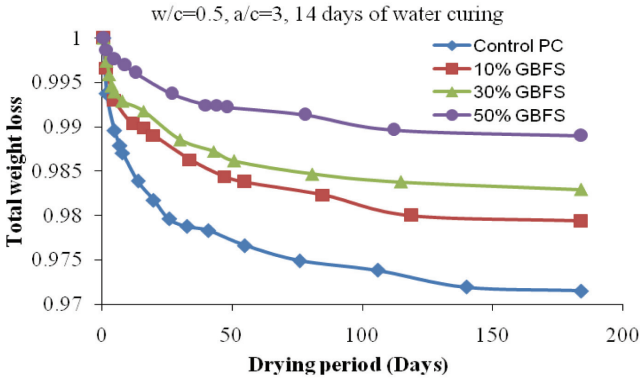

Figure 6. The effect of different percentage of GBFS replacement on drying rate of concrete

Cheng [5] record the total coulomb passed in rapid chloride penetration test (RCPT) in concete reduced by 40% and 70% for 30% and 60% GBFS replacement respectively. Similar results have been proposed by different research studies. Figure 7 shows the effect of GBFS on reduction of total coulomb passed in RCPT test. The result of rapid migration test shows penetration depth of chloride in GBFS concrete samples is very limited and much lower than PC samples.

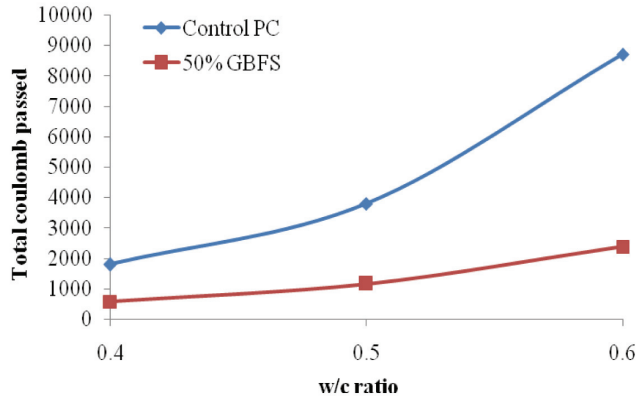

Figure 7. The RCPT results for PC and 50% GBFS replacement with various w/c ratio

Replacing the mineral admixtures will result in consumption of calcium hydroxide in concrete. In short curing period, it may increase the carbonation rate of concrete. Figure 8 shows the effect of various percentage of GBFS replacement on carbonation rate of concrete with 4 days of curing. The results show a considerable amount of increase in carbonation rate especially for higher percentage of GBFS replacement.

However, a longer curing period can eliminate the increase in rate of carbonation significantly. Figure 9 shows the effect of curing period on the reduction of carbonation rate for the case of replacement of 50% of PC with GBFS. As can be seen from Fig. 9, 14 days of curing can eliminate the problem significantly.

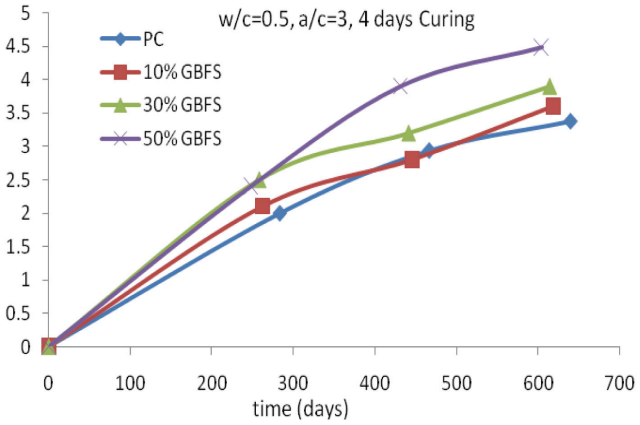

Figure 8. Effect of various percentage GBFS replacement on carbonation rate of concrete

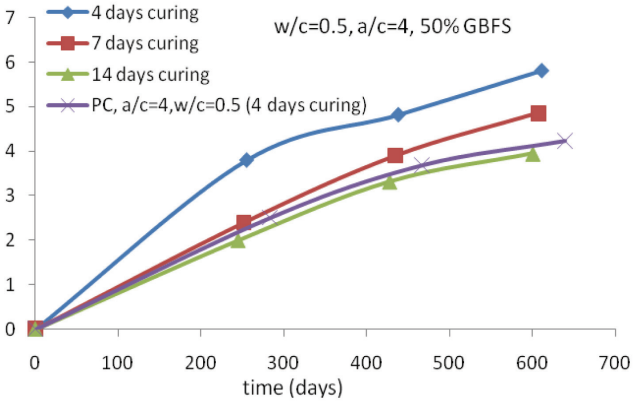

Figure 9. Effect of curing period on carbonation rate of concrete contain GBFS

CONCLUSIONS

Using PC partially replaced by GBFS is not only ecologically and environmentally favourable but the effects on fluidity of fresh concrete, strength, durability and pore structure of hardened concrete is very useful. Especially in marine structures and in hot weather conditions, using PC partially replaced by GBFS is the most economical and safe option. Using the longer curing period (favorably longer than 7 days) can eliminate the problem of increasing the carbonation rate of concrete significantly.

REFERENCES

[1] Sabet Bahador and Jong, H.C., 2007. "Study on properties of the concrete contained Ground Granulated Blast furnace Slag". *1th Conference on Recent Advances in Concrete Technology, USA*, pp. 573-582.

[2] Rui Luo, Yuebo Cai, Changyi Wang and Xiaoming Huang, 2003. "Study of chloride binding and diffusion in GGBS concrete". *Cement and Concrete Research,* Vol. 33, pp. 1-7.

[3] Gao, J.M., Qian, C.X, Liu, H.F., Wang, B. and Li, L., 2005. "ITZ micro structure of concrete containing GGBS". *Cement and Concrete Research,* Vol. 35, pp. 1299-1304.

[4] Ganesh Babu K. and Sree Rama Kumar V., 2000. "Efficiency of GGBS in concrete". *Cement and Concrete Research,* Vol. 30, pp. 1031-1036.

[5] Cheng An, Huang Ran, Kuo Wu Jiann and Hsin Chen Cheng, 2005. "Influence of GGBS on durability and corrosion behavior of reinforced concrete". *Material Chemistry and Physics,* Vol. 93, pp. 404-41.

ABSTRACT OF RESEARCH REPORTS

Database for Dynamic Properties of Singapore Soils

Principal Investigator: **Leong Eng Choon**
Report No: CEE/2008/178

Soil behaviour is highly nonlinear. In the case of dynamic loading (earthquake, explosion etc), the strains experienced by the soils range from very small to very large strains. In order to model such behaviour correctly, it is imperative to obtain the soil stiffnesses over a whole strain range. The very small strain stiffness can be obtained using bender elements. The intermediate strain stiffness can be obtained using cyclic triaxial, cyclic simple shear and torsional shear apparatuses. The large strain stiffness can be obtained using coventional laboratory testing apparatuses. In an earlier project, PTRC-CSE/LEO/99.02, several apparatuses were developed. These include bender elements, P&S wave system, cyclic triaxial apparatus and cyclic simple shear apparatus. Therefore the necessary equipment for the study of dynamic properties of soils are now available. The characterization of the dynamic properties of Singapore soils have been piecemeal so far and a complete database of the dynamic properties of the Singapore soils is not yet available. The research will yield an important database for future applications.

Study of Rainfall - Induced Slope Failures

Principal Investigator: **Harianto Rahardjo**
Report No: CEE/2008/179

The objective of this research is to study the infiltration characteristics of soils and slopes in a one- and two-dimensional laboratory models, respectively, under controlled laboratory conditions.

Mitigation of Progressive Collapse of Tall Buildings

Principal Investigator: **Tan Kang Hai**
Report No: CEE/2008/180

Since the impact of 911, various government bodies are increasingly concerned about a recurrence of the tragic event, brought about by terrorist actions. Thus, this topic of mitigation against progressive collapse of buildings is timely and crucial, particularly more even so, since the targets of terrorists' activities have shifted from military hardened structures to soft civilian buildings. This report gives the background of the problem, setting the scene for the following works. Building fires usually take place after a blast event has occurred. It is well-acknowledged by structural engineers that the twin towers were brought down by ensuing intense fires instead of the initial impact and blast from the aeroplane. Thus, in view of this, the focus of the entire report is on the fire effects on structures, in particular, the connections and composite beams. The scope does not include blast effects on structures.

The mathematical modelling of compartment fires is described through the concept of control volumes, one for the upper hotter layer and one for the lower cooler layer. Fire plume acts as a heat pump driving the convection of the fire dynamics. Pressure difference across the vent opening between the fire compartment interior and exterior drives the ambient air into the compartment through the lower layer and hot air out through the upper layer. The numerical model CFMFAN is then compared with actual compartment fire test results.

The report presents the program FEMFAN3D which is a 3-D finite element program developed at NTU for the analysis of space skeletal steel frame. This forms the kernel of the work for this funded project. The derivations for displacement functions and the stress-strain relations are spelt out explicitly. Virtual work principle is used in the derivations of various terms in the stiffness matrix. The FEM code is followed by numerical validations. A total of 5 case studies are considered, ranging from an academic problem of a sub-frame subjected to fire condition, space frame, semi-rigid connections to experimental validations.

The report also presents the experimental work conducted in NTU through Dr Qian Zhenhai and Dr Ronny Budi Dharma. Dr Qian worked on the steel beam-to-column joint connections. A series of 6 cruciform specimens was tested to failure under elevated temperature conditions under restrained and unrestrained isothermal condition. The work on composite beams was conducted by Dr Ronny Budi Dharma. The ductility of such beams under fire conditions was addressed. Basically, although steel material softens under fire conditions, member ductility does not increase and in fact reduces with increasing temperature. Due to space limitation, only the experimental works for connections and composite beams under fire conditions are presented. Details of their work can be found in their respective PhD thesis.

The report ends with a broad-brush paint of practical design considerations for structural engineers when designing tall buildings against progressive collapse. There is also an attempt to address what is meant by progressive collapse from the design point of view. Two approaches to mitigate against progressive collapse are described, viz. alternate load-path approach and indirect design approach. While one approach is more specific, the other provides a minimum level of protection towards structural resilience and robustness, particularly, with regard to the robustness of connections under catenary action. This has now become the new focus of study in a separate project funded by MHA and administered by DSTA.

Micro-bubble formation by a jet issued from a flow distributor nozzle of a RO unit

Principal Investigator: **Law Wing-Keung, Adrian**
Report No: CEE/2008/181

The study investigates the formation of micro bubbles at the flow distributor to a RO module.

PUB-NTU Joint Collaboration on "Water quality monitoring, modelling and management for catchment and reservoir system."* Project Phase 2

Principal Investigator: **Lo Yat-Man, Edmond**
Report No: CEE/2008/182

To implement a fully operational, real-time system for the Kranji reservoir, comprising integrated monitoring and predictive modeling for the enhanced management of the reservoir water quality for blue-green algae, pathogens and suspended sediments.

Slope instrumentation for the study of rainfall-induced slope failures in Singapore

Principal Investigator: **Harianto Rahardjo**
Report No: CEE/2008/183

Research Collaboration Agreement between NTU and Building Technology Dept, HDB was signed on 21 November 2005. The main objectives of the project are:

1. To study the relationship between soil types and soil properties that display the potential of slope failures in Singapore.
2. To establish the correlation between local climatic conditions (rainfall, infiltration and evaporation) and slope failures in Singapore in terms of soil response such as pore-water pressure changes and deformation.
3. To evaluate the stability of representative slopes in Singapore under typical rainfall and evaporation conditions and establish guidelines for preventive and improvement measures for Singapore slope instability due to rainfall.

Residual strength of blast damaged reinforced concrete columns

Principal Investigator: **Li Bing**
Report No: CEE/2008/184

The basic objectives of this research are to provide a more complete understanding of the dynamic behaviour of RC columns under dynamic loadings, and on this basis develop methods that enable analyses of dynamic behaviour of buildings on pile foundations. A general overview of the main steps are as follows:

- To evaluate and compare the dynamic responses and corresponding damage mechanism for reinforced concrete columns under blast loading from close-in explosion.
- To develop a new procedure to carry out the blast resistant design of reinforced concrete columns based on energy spectra, which could overcome the disadvantages existing in current design procedures.
- To develop a new method of assessing residual strength and stiffness of blast damaged reinforced concrete columns under blast condition. Theoretical predictions will be assessed by experiments conducted in NTU on full-scale specimens.

Jurong Island rock caverns for oil and gas storage

Principal Investigator: **Ashraf Mohamed Hefny**
Report No: CEE/2008/185

The project is part of a feasibility study on the development of oil and gas storage cavern facilities below the Jurong Island. The feasibility study includes site investigation, technical study, system design and cost evaluation. The project is to study the technical issues of cavern construction in the Jurong sedimentary rocks below the Jurong Island. Scope of study includes geological assessment, rock mass characterisation, rock mass properties, design of rock support and reinforcement, and groundwater problems.

Use of recycled rubber tyres in civil engineering applications

Principal Investigator: **Ting Seng Kiong**
Report No: CEE/2008/186

The objective of this project is to explore the use of recycled rubber tyres in civil engineering applications that adopt local materials and construction technology, and are suitable for the aggressive climatic and service conditions in Singapore and the tropical region. Focus is particularly on applications that are technically beneficial, economically viable, and non-hazardous to the environment. The scope of study includes:

a. Review of current state of knowledge to identify the use of recycled rubber tyres in viable civil engineering applications;
b. Laboratory tests to evaluate the basic engineering properties and performance of rubberized material required in each application;
c. Pilot tests and site trials to monitor the performance of the actual completed structure for each application; and
d. Provision of guidelines for the use of recycled rubber tyres in civil engineering applications under severe tropical climates and service conditions.

Development of 3D-GIS (Geographical Information System) for subsurface infrastructure archiving, managing, planning and design

Principal Investigator: **Tor Yam Khoon**
Report No: CEE/2008/187

The current Geographical Information Systems (GIS) in use are mainly developed and used as 2D tools to acquire, manage, process and analyse spatially (geographically) related surface land data. It is not suited for subsurface land data. Developing underground space in land scarce Singapore requires well coordinated subsurface information. *Coordinated* refers not just the salient liaison works amongst the various agencies, but the spatially coordinated subsurface information comprising existing geological features, infrastructure and installations. There is thus a need to develop a 3D-GIS to cater for the third dimension, i.e. the z- or height/depth coordinates. The integration of existing or proposed subsurface infrastructure and installation in such 3D-GIS will require it to possess CAD/AEC capability. Enhancement of 3D-GIS with CAD/AEC capability will enable the integration of CAD/AEC design under a framework of spatially referenced DBMS with 3-D graphical visualisation. Such database is both useful and essential to the development of military, commercial and industrial and other applications in Singapore of subsurface land resources. The 3D-GIS system, when fully developed, will have a wide range of applications for the planning, design, archiving, and maintenance of defence and civilian infrastructures.

ABSTRACT OF PhD THESES

Actuation Characteristics of Piezoelectric Materials and Ionic Polymer-Metal Composites for Biomedical Engineering Applications

Candidate: **Zhang Lei**
Report No.: CEE/PhD/2008/165

This thesis focuses on the actuation characteristics of piezoelectric materials and ionic polymer-metal composites (IPMCs) for biomedical applications. The piezoelectric actuated plates and shells on elastic foundation are investigated. Analytical solutions are obtained to describe the structural responses under the piezoelectric actuation. The optimal placement of a piezoelectric actuator on the plate and shell in terms of maximizing excitation is investigated and solved by proposing a simple and general procedure. The actuation mechanism of the IPMC is also investigated. Explicit bending moment expressions are derived to account for the bending capacity of the IPMC under both the static and dynamic electric potentials. Three IPMC based biomedical prototypes, i.e., an IPMC beam on human tissues, an IPMC ring with elastic medium and an IPMC cylindrical shell with contained flowing fluid are developed based on the bending moment expressions. The output effects, i.e., the pressure on the tissues or organs and the velocity changes in flowing fluid, have been obtained analytically.

Adaptive Analysis of Thin-Walled-Structures using Three Dimensional Solid Element

Candidate: **Xu Qiangxun**
Report No.: CEE/PhD/2008/166

A new adaptive refinement scheme is developed for the analysis of thin-walled structures. They are different from the conventional method where shell elements are used for the analysis of thin-walled structures, as in this thesis, 3D solid elements are used to mesh thin-walled structures. The generated solid mesh will be imported to a commercial software package for the standard finite element analysis. After the FE stress is obtained, stress recovery and error estimation techniques are developed based on the superconvergent patch recovery technique and Z-Z error estimator. Finally, a special designed adaptive refinement scheme is implemented for the whole adaptive analysis procedure for thin-walled structures. Numerical examples are provided to show the validity and efficiency of the developed scheme.

Analysis of the Behaviour of Gravity-load-designed RC Beam-Column Joints Subject to Lateral Loads

Candidate: **Lin Xin**
Report No.: CEE/PhD/2008/167

This dissertation is conducted to model and investigate the behaviour of gravity-load-designed beam-column joints subjected to lateral loads. To study the local behaviour of

the beam-column joint subjected to lateral loads, especially the local strain distribution and local bond slip distribution in the joint, the finite element analysis was carried out. In finite element analysis, a new double-panel element was developed to model both shear and bond behaviour. To study the global overall behaviour of the GLD structures subjected to lateral loads, the frame analysis is usually carried out. In frame analysis, a model of 12-dof joint element was developed to take into account the softening of the beam-column joint under lateral loads. A model with a combination of spring elements was developed to take into account the fixed-end-rotation at interface between the joint and adjacent members. To estimate the shear capacity of beam-column joints, a simple equation is proposed. In the design equation, the joint shear strength estimation is based on the combination of arch and truss mechanisms.

CO-Metabolism of Trichloroethylene by Phenol Grown Aerobic Granules

Candidate: **Zhang Yi**
Report No.: CEE/PhD/2008/168

This thesis focuses on the topic of co-metabolic degradation of trichloroethylene (TCE), a recalcitrant synthetic solvent, by a novel form of biomass-aerobic granules, while phenol was used as the growth substrate. The aim was to explore the feasibility of sustainable TCE degradation operation by aerobic granular sludge and reactor.

Aerobic granulation process was carried out using phenol as the growth substrate. Changes of sludge characteristics and phenol/TCE degradation activity were monitored until stable aerobic granules were formed. The mature granules were characterized for their phenol and TCE degradation activities. Isolation of pure phenol-degrading culture from the granules was further conducted, and a glass reactor was designed and constructed for TCE co-metabolism by aerobic granules, with phenol as the primary substrate.

The aerobic granular sludge could efficiently co-metabolize TCE with phenol as the growth substrate, and showed some interesting characteristics. Aerobic granular sludge reactors could be sustainably operated for TCE co-metabolism operation, and is a promising option for future application.

Creating and Sustaining Competitive Advantage for Small and Medium-sized Enterprises in the Chinese Construction Industry

Candidate: **Yan Shigang**
Report No.: CEE/PhD/2008/169

As the major force in Chinese construction, construction SMEs have played an important role in promoting construction industry growth. However, they are facing a myriad of problems and difficulties which have constrained their further development. The research investigates how construction SMEs in China compete for success via the use of core capability and competitive strategy in a transitional economy in China. Based on industry organization approach and resourced-based view, a theoretical framework is developed to investigate the relationship among core capability, competitive strategy and industry structure factors within Chinese construction SMEs.

Based on the data collected from construction SMEs in China, the empirical findings of the study suggests that core capability, competitive strategy and industry structure related factors have significant impact on the construction SMEs' performance. The pattern among core capability, competitive strategy and industry structure factors are also observed with empirical evidences from case studies of three companies. The case studies illustrate the link between theory and practice as it relates to the relationship among core capability, competitive strategy and industry structure in the construction SMEs and their success.

Despite the significance of the study, it is worth acknowledging the exploratory nature of this study. It is hoped that the framework developed in this study will provide the theoretical foundation for more rigorous research in the future.

Damage-based Seismic Design and Performance Assessment of Reinforced Concrete Structures

Candidate: **Wei Jianwu**
Report No.: CEE/PhD/2008/170

This thesis presents the research work on damage-based seismic design and performance evaluation of RC frame structures. The research involves both analytical and experimental studies. A coherent methodology is developed for damage-based design and evaluation, including the generation of damage-based inelastic spectra and the development of an implementation procedure for actual structural systems. Through a comprehensive investigation on the influences of pertinent parameters, unified empirical formulas are derived for the damage-based inelastic demand spectra. For the implementation in actual structures, two alternative methods, one based on modal pushover analysis and the other based on the characterization with a storey capacity factor, are proposed. A simple method based on a modified storey capacity factor is also developed for the prediction of the inter-storey drift distributions for performance evaluation purpose.

A comparative shake table experiment is conducted on two companion frames of different detailing to investigate the damage and performance of nonseismically designed structures. The importance of evaluating the potential problems with undesired nonseismic details with respect

to realistic seismic demands in low-to-moderate seismicity regions is emphasized. Furthermore, the effectiveness of a commonly used FRP repairing technique in recovering the structural performance is also investigated using shake table tests.

Development of Anaerobic Immobilized-Cell Processes for Biohydrogen Production

Candidate: **Zhang Zhen-Peng**
Report No.: CEE/PhD/2008/171

Two high-rate biohydrogen-producing systems were developed through forming granular sludge in a continuous stirred tank reactor (CSTR) and an anaerobic fluidized bed reactor (AFBR). In such reactors, granules were able to form within 3-5 days after the microbial cultures were subject to an acid incubation for 24 hours by shifting the culture pH from 5.5 to 2.0. Underlying formation mechanisms with respect to physicochemical and biological aspects involved in rapid granulation were investigated. Lowering culture pH resulted in improvement in bacterial surface physicochemical properties favoring microbial agglutination and granulation. It follows from the species composition that *Clostridium pasteurianum*-like bacterium may be the crucial species participating in the granulation. Relative abundance of proteins in the granule centers suggests a possible formation mechanism, this is, microbial aggregation starts as a protein-rich matrix or nucleus has been established.

Development of a 3D GIS Database Model For Geotechnical Analysis Incorporating Geostatistics

Candidate: **Gao Shan**
Report No.: CEE/PhD/2008/172

A new geotechnical database model has been developed in this study to support 3D GIS applications in the geotechnical field. The new geotechnical database model is developed as a hybrid database model inheriting the advantage of existing geotechnical and geological models. It combines the rational worldview of NADM model (North American Geologic-map Data Model), the rigorous data structure of the AGS format, and the flexibility of the XML schema. XML schema for stratigraphy data and variogram data has been developed in this study. The new geotechnical database model also represents an early attempt to manage variography data within a database.

Through two case studies conducted using an application developed based on the new geotechnical database model, the applicability of the database model is affirmed and its advantage is demonstrated. It can be concluded that the identified gap that exists in the data analysis and distribution process could be narrowed or bridged through the new geotechnical database model. The solution provided in this study gives geotechnical engineers a handy tool not only for sharing the geotechnical data but also, and most importantly, sharing their knowledge with each other.

Development of a Fuzzy Knowledge-Based System For Local Traffic Control For Incident Management

Candidate: **Trinh Dinh Toan**
Report No.: CEE/PhD/2008/173

Traffic congestion is a critical and pervasive problem confronting many metropolitan areas worldwide. Congestion can be broadly classified into two types: recurring congestion and non-recurring congestion. Due to the complex, critical and uncertain nature, a traffic control for non-recurring congestion management is characterized by time-critical constraints, by the presence of various types of imprecise data and information, and by the uncertainty in evaluating the state of traffic. Characterised by time-critical constraints, the management of non-recurring congestion on expressways should be remedied by implementing effective control measures to ameliorate traffic conditions on expressways, at the same time to avoid imposing excessive congestion on sub-networks. With the above characteristics, an effective traffic control scheme for incident management often requires techniques that deal efficiently with problems of uncertainty and imprecision.

Fuzzy logic is an advanced technique of approximate reasoning in knowledge-based systems. A key motivation in following the fuzzy logic is that the approach is robust in handling problem of uncertainty and imprecision. Fuzzy logic has been widely applied in control systems to manage complex and ill-structured problems with missing and imprecise information. For this capability, fuzzy logic should be a feasible solution for traffic control in incident management. Nevertheless, while there are a wide variety of applications in traffic control for urban intersections, little is known regarding research effort in applying the fuzzy logic systems for traffic control for incident management.

The goal of this research is the development of a fuzzy knowledge-base system for traffic control in incident management on expressways. The system is designed as an engine for a decision-support system to assist traffic operators in making decisions to ameliorate incident congestion in a systematic and structured way. The primary objectives of this research include the development of a multi-stage fuzzy logic controller (MS-FLC) for local traffic control during incidents on expressways, and the development of a simulation model for the evaluation of the MS-FLC.

The essence of the MS-FLC is the fuzzy rule base. Important issues in the development of the rule base involve determining and calibrating membership

function's parameters. For these purposes, techniques in fuzzy partitioning and fuzzy rule generation including engineering knowledge, grid clustering, and Fuzzy C-Means clustering have been explored. The concept of fuzzy rule generation using the framework of Adaptive Neural Networks has been investigated.

The decision-making logic of the MS-FLC encompasses three stages: the evaluation of the state of traffic under consideration, the prediction of traffic variables and anticipation of incident conditions, and the recommendation of control strategies as well as control actions. The first stage is characterised by a comprehensive appraisal of congestion situation, including congestion level, congestion mobility and congestion status, based on speed and density, being primary measurements of traffic variables. In the evaluation stage, the fuzzy relation is used to establish the degrees of association between elements of fuzzy sets.

In the second stage, the anticipation of traffic conditions, the Support Vector Machine (SVM), an advanced technique in machine learning, has been investigated for short-term prediction of traffic variables. Results from the prediction experiments show that SVM significantly outperforms the base-line predictors in various traffic conditions. In particular, the technique provides pattern recognition capabilities to deal more efficiently with incident conditions at high data resolutions.

The recommendation of control strategies and control actions is the last stage of the MS-FLC. The stage proposes a systematic procedure in decision-making sequence, from general to specific. Rules are designed at both strategic and operational levels, ranging from intervention level and control strategy to control action. The stage receives the current and anticipated traffic conditions from the previous stages to recommend solutions. With these types of information, the MS-FLC seeks to operate on both reactive and proactive control modes.

For the evaluation of the MS-FLC, a traffic simulator and control (TSC) has been developed. The TSC consists of two main components: the car-following model (CFM), and the traffic controller (TC). The CFM has been calibrated and validated using data from Pan-Island Expressway. In the evaluation of the MS-FLC, the local ramp control ALINEA is employed to compare with the MS-FLC in a generic network under various traffic and incident conditions. Results from the evaluation show that the MS-FLC allows significant improvements of travel conditions on the mainline, especially under critical conditions, and substantial reductions of ramp queues. The improvements with MS-FLC show that if properly designed, the MS-FLC will be a robust tool for traffic control under incident conditions.

Dynamic Road Pricing Incorporating Dynamic Traffic Assignment

Candidate: **Zhang Chunrong**
Report No.: CEE/PhD/2008/174

This research aims to design dynamic road pricing incorporating dynamic traffic assignment (DTA). The model is formulated in a framework of Mathematical Programs with Equilibrium Constraints (MPEC). A DTA model from a previous research is revised to represent traffic evolution more appropriately. A new algorithm based on projection method is proposed to solve the DTA model. Numerical example shows that this new algorithm can generate a smoother inflow rate as compared with the "route/time" swapping algorithm suggested in the literature. Differential Evolutionary (DE) algorithm is used to solve the MPEC with a single objective. Numerical examples indicates that DE is superior to some other heuristics algorithm like Pattern Search method. Finally, multi-objective dynamic road pricing model is established for practical consideration. Non-dominated Sorting Genetic Algorithm (NSGA-II) is employed to solve an example which shows the importance of multiple objectives consideration.

Effect of Excavation on Performance of Adjacent Buildings

Candidate: **Darwid Halim**
Report No.: CEE/PhD/2008/175

Deep excavations in urban area can damage surrounding buildings. The current practice in assessing building damage is based on greenfield settlement computed from 2-D finite element analysis. This is less than satisfactory for situations where 3-D effect is prominent. In this case, a 3-D analysis is preferred. Unfortunately, the 3-D finite element analysis is a fairly complex and demanding task. A simple method has been developed to estimate 3-D settlement from 2-D analysis. The conventional method also assumed that the building would settle the same amount as the ground. This assumption is reasonable for buildings supported on individual footings without ground beams. For frame structures and buildings supported on rafts, the differences in building and ground settlements can be significant. A new method has been developed to integrate the soil-structure interaction into the analysis so that the structure stiffness can be taken into consideration. A new chart for damage assessment of frame structures has also been developed. The chart divides the damage into several categories.

This study also investigated the potential causes of post-excavation settlement in deep excavations in soft clay. Results indicate that there are two major causes. The first one is leakage in the retaining wall and the base slab. The second one is under-drainage into a pervious layer that extends into the excavated area and exposed at the formation level.

This research is numerical based with the aid of the computer programs Abaqus and Sage Crisp. The proposed methods and charts have been validated against hypothetical problems and case records.

Enhanced Formation of Microbial Granules Used in Aerobic Wastewater Treatment

Candidate: **Wang Xiaohui**
Report No.: CEE/PhD/2008/176

The aim of this study was to overcome two restrictions in aerobic granulation biotechnology: long start-up period of aerobic granulation process due to long formation time of microbial granules, and potentially high safety risk because aerobically grown microbial granules could be reservoirs harbouring pathogenic bacteria. The goals of this research project were achieved by selection and using environmentally safe granule-forming bacteria as starter culture for aerobic granulation. Microbial strains with high auto-aggregation ability were isolated from fast-aggregated enrichment culture and microbial granules. Afterwards, the strains with aggregation index higher than 50% were identified by 16S rRNA gene sequence analysis for safety assessment. Among nine isolates identified, only one environmentally safe microbial strain, *P. veronii str B*, was selected as starter culture for aerobic granulation in sequencing batch bioreactor. The formation of microbial granules with mean particle size of 600 µm and SVI value of 70 mL g^{-1} from *P. veronii* was shortened to 3 days instead of 3 to 4 weeks when granulation was started from conventional activated sludge. The fate of *P. veronii* and its spatial distribution during granulation start-up period were tracked by denaturing gradient gel electrophoresis and fluorescence *in situ* hybridization. It was shown that the applied *P. veronii str B* remained dominant strain in formed granules throughout the start-up period of aerobic granulation process. These results confirmed that *P. veronii str B* could be sustainable granule-forming bacterial strain. In addition to its granule-structural properties, the other functional properties of *P. veronii str B* were also investigated. It was found that *P. veronii str B* was more effective in estrone and estriol biodegradation, but less effective in 17a-ethynylestradiol biodegradation than that of microbial granules containing nitrifiers. The order of estrogens biodegradation by activated sludge, microbial strain *P. veronii str B*, and microbial granules was as follows: 17ß-estradiol ⇨ estriol ⇨ estrone ⇨ 17a-ethynylestradiol. The biodegradation rate constants of estrogens by microbial strain *P. veronii str B* were 0.87 d^{-1}, 0.39 d^{-1}, and 0.7 d^{-1} for estrone, 17ß-estradiol, and estriol, respectively. Different methods for *P. veronii* preservation were studied and it was found that biomass of *P. veronii str B* could be preserved as dry powder by freeze drying of cell biomass. The viability test indicated that 90% of *P. veronii str B* cells survived after freeze-drying. It can be used for production and storage of dry microbial composition used for enhanced formation of microbial granules in aerobic biological treatment of wastewater.

Fate and Transport of Endocrine Disrupting Chemicals in an Aquifer

Candidate: **Ke Jinxia**
Report No.: CEE/PhD/2008/177

Endocrine disrupting chemicals (EDCs) are of growing concern in recent years, due to their harmful effects on human and wildlife development and reproduction. A wide variety of pollutants have been identified as potential EDCs. Estrogens (estrone, estradiol, estriol and ethylestradiol) are one of the most important groups of EDCs. They are selected as target compounds for this study because of their potential estrogenicity in the environment.

Soil Aquifer Treatment (SAT) is one of the principle technologies for water reuse. Many studies have shown that organic pollutants are significantly reduced during SAT. The reclaimed lands in Singapore have the potential to further polish treated wastewater. If this is the case, it is important to understand the behavior and transformation of selected contaminants which might be present in the water used for recharge.

The objectives of this study are to examine the behavior of the target compounds in the aquifer. A series of laboratory studies, including a batch study and column study has been carried out to achieve the objectives.

A sensitive LC-MS-MS method in conjunction with a single step solid phase extraction pretreatment method was developed for analyzing the estrogens. The single step solid phase extraction pre-treatment method showed good recovery for the ultrapure water when concentrated 1000 times and resulted in a method detection limit of ng/L levels for all the target compounds. However, when the method was applied to natural samples, the matrix effect was very significant and poor recovery was obtained. Therefore, for water with complex matrices a low concentration factor is suggested. In addition, a calibration standard prepared in the same matrix is also suggested for quantifying the water samples.

The sorption and degradation behaviour of estrogens were examined by batch experiments under different redox conditions. In addition, a set of columns packed with aquifer sand was used to simulate the SAT process and assess the attenuation behaviour of these compounds under recharge conditions. The results indicate that the sorption ability of the estrogens were in the following order: E3 < EE2 < E2 < E1 which is inconsistent with their physicochemical properties. Thus, non-hydrophobic portioning may be the dominant sorption mechanism. The degradation study showed that E2 was the most readily degradable compound among these four target compounds. The rapid degradation of E2 was found in all the water matrices under aerobic conditions. Its primary metabolite, E1, was also found to rapidly degrade in all the matrices under aerobic conditions. Under anoxic conditions, E1 and E2 were inter-convertible. In contrast with E2, EE2

was more persistent. It was found to be biodegradable under both aerobic and anoxic conditions at relatively slow degradation rates. Chemical transformation could also be considered as one of the removal mechanisms for this compound.

Three strains of estrogen-degrading bacteria, namely LHJ1, LHJ3 and CYH, were isolated in this study from the aquifer system. LHJ1 and LHJ3 were found to belong to the genus *Acinetobacter* and *Agromyces* respectively, while CYH represents a novel species of the *Sphingobium* genus and was named *Sphingobium estrogenivorans* sp. nov. The three degraders showed the ability to degrade E2 under aerobic conditions. However, only CYH could degrade E1 and only LHJ3 could degrade E3. Under anoxic conditions, CYH and LHJ3 could only degrade E1 and E2 respectively, albeit the degradation rates were much slower than for aerobic conditions. None of the degraders could degrade E3 under anoxic condions. An E3 degradation product was found and hypothesized to be 16-hydroxyl-estrone. With respect to the synthetic estrogen 17 α-ethinylestradiol (EE2), ground water amples from the aquifer site showed the ability to degrade EE2. However, the degrading microorganisms for this compound have not been isolated yet.

Hybrid Submerged Membrane Photocatalytic Process

Candidate: **Chin Sze Sze**
Report No.: CEE/PhD/2008/178

A hybrid system combining low-pressure submerged membrane filtration and photocatalysis in a single module was developed. A comprehensive membrane stability protocol was devised to identify the polymeric membranes that were stable under photocatalytic process. The feasibility of operation of the submerged membrane photocatalytic reactor (SMPR) in the degradation of BPA was investigated. Different methods for controlling membrane fouling during the operation of the SMPR were compared. A new submerged membrane photocatalytic reactor (SMPR) with multiple submerged lamp sources was designed and built. Long-term operation of the SMPR was evaluated and the issues of the lifetime of TiO_2, fouling control and stability of the membrane were systematically addressed. Finally, a modified continuous stirred-tank reactor (CSTR) model was used to predict the degradation of resorcinol in the new SMPR. The adequacy of the modified model in simulating steady-state concentrations for different feed concentrations and residence times was evaluated.

Improved Precise Time-Step Integration Algorithms for Dynamic Problems

Candidate: **Chen Zhen Lin**
Report No.: CEE/PhD/2008/179

The improved precise time-step integration algorithms can reduce the computational cost significantly and maintain the accuracy as well. The precise time-step integration method has been improved by incorporating (1) the extended dimensional expanding method, (2) Duhamel-response matrix, (3) Padé approximation, and (4) Krylov subspace method.

This dimensional expanding method is also extended to solve the second order equations directly. The precise time-step integration method by step-response and impulsive-response matrices is extended by incorporating the Duhamel Integral using the Duhamel-response matrix and is improved to be unconditionally stable using new Padé approximations. The Krylov precise time-step integration algorithm by incorporating Padé series approximations and dimensional expanding methods can reduce the computational effort significantly and improve the stability, especially for solving large-scale systems. The criteria to choose the number of recursive evaluations, the order of Padé approximations and the efficiency range of the order of the Krylov subspace are studied. The proposed algorithms can also be extended to tackle non-linear problems efficiently without difficulty. The efficiency, accuracy and stability of the improved PTI methods are investigated.

Kinetics, Equilibrium Isotherm and Mechanisms of Heavy Metal Biosorption by Aerobic Granules

Candidate: **Xu Hui**
Report No.: CEE/PhD/2008/180

Heavy metals like cadmium, copper and nickel could be successfully removed by aerobic granules from aqueous solution. The biosorption capacity of aerobic granules was in the order of $Cd^{2+} > Cu^{2+} > Ni^{2+}$. The operating parameters, such as initial metal and biomass concentrations, initial pH and temperature would affect the metal biosorption capacity of aerobic granules. The developed reversible first order kinetic model and the equilibrium isotherm based on a thermodynamic approach could satisfactorily predict the experimental data. It seems that the multi-mechanisms, e.g. ion exchange, ECP binding and chemical precipitation, would be involved in the heavy metal biosorption by aerobic granules. The excellent settleability of aerobic granules can ensure a rapid biosolids separation from the treated effluent, which in turn leads to a simple process design. This study showed that aerobic granules could be used as an effective biosorbent for the heavy metal removal from aqueous solution.

Mechanical Properties of Soft Tissue

Candidate: **Yang Wei**
Report No.: CEE/PhD/2008/181

The Esophagus is a neuromuscular tube extending from the pharynx to stomach. Like other soft tissues,

the mechanical properties of the esophageal tissue are nonlinear, anisotropic visco-hyper-elastic. Characterization of the mechanical properties is essential to understand the neuromuscular motion of the esophagus. In this study, firstly, the mechanics of the esophageal tissue was investigated experimentally and theoretically. Under the framework of nonlinear elasticity, a suitable constitutive model was developed to describe the mechanical behaviour of the esophagus. Secondly, a finite element model was established to simulate the process of peristaltic transport. The simulation could successfully capture the main features at each stage of food transport. Lastly, a mathematical model was developed to investigate the mechanism of formation of mucosal folding. The model was shown to be able to predict the buckling mode which was consistent with the experimental observations.

Membrane Bioreactor for Treatment of High Strength Industrial Wastewater

Candidate: **Khor Swee Loong**
Report No.: CEE/PhD/2008/182

This study investigated the sustainability of biological and membrane performance in long SRT (300 days) condition. The experimental results indicated that 300-day SRT MBR provided stable and sustainable treatment efficiency (> 99% COD removal) and low observed sludge yield (0.0228 gVSS.gCOD^{-1}). Supernatant was identified as the crucial factor affecting the filterability and cake resistance. Additionally, the concentration of mixed liquor provided more contribution to cake resistance under the high mixed liquor concentration (> 8,000 mg/L). MF fouling was initiated with a slow fouling stage and followed by a rapid fouling stage. A great change of critical flux and rejection performance occurred at the slow fouling stage which was due to the rapid reduction of effective filtration pore size. A simple perception of membrane fouling steps in MBR was established. Moreover, the integration of cake retarding effect into intermittent permeation operation managed to extend the membrane lifespan.

Microbial Degradation of Phthalic Acid and its Esters by Aerobic Granules in Sequencing Batch Reactor

Candidate: **Zeng Ping**
Report No.: CEE/PhD/2008/183

Phthalates are primarily synthetic compounds have been widely used in industry and consequently became ubiquitous pollutants in natural environment. However, conventional activated sludge process can not effectively treat recalcitrant phthalate wastewater. Therefore, it has been thoroughly realized that bioaugmentation presents significant capability as one of the strategies for enhancement of recalcitrant compound degradation. However, there still exist many factors that may affect the efficiency of bioaugmentation in which the selection of suitable bioseeds is undoubtedly an important parameter. In the current study, it can be concluded that the strategy of bioaugmentation phthalic acid-degrading aerobic granules is successful in enhancing the degradation of high strength of phthalic acid, di-methyl phthalate (DMP) and di-butyl phthalate (DBP) which is one of the recalcitrant phthalates. The enzyme introduced with phthalic acid aerobic granules can change the DMP degradation rate to be $k_3 > k_2 > k_1$, which makes the phthalate degradation proceeded smoothly. Also, the microbial diversity and immigration analyzed by denaturing gradient gel-electrophoresis (DGGE) show that isolate PA-02 also plays an important role in the enhancement of phthalate degradation.

Nano-structured Titanium Dioxide Microsphere For Humic Acid Removal In Water

Candidate: **Lee Pei Fung**
Report No.: CEE/PhD/2008/184

A novel nano-structured TiO_2 microsphere was fabricated for the humic acid removal in water. The prepared nano-structured TiO_2 microsphere had a spherical shape in submicron range (10-50 µm) with 10 nm crystal size, BET surface area of 42 m^2/g, and with mesoporous property. Adsorption studies revealed that the adsorption extent and kinetic were significantly enhanced at low pH value and with the presence of Ca^{2+} in solution. The adsorption kinetic followed a 2-stage process and the adsorption behaviour was well fitted by Langmuir-Freundlich model. Adsorption mechanism of humic acid on TiO_2 microsphere was elaborated in this study. Experimental results indicated that strong adsorption of humic acid on TiO_2 microsphere did not actually enhance the photocatalytic oxidation process. The humic acid was successfully degraded using nano-structured TiO_2 microsphere in photocatalytic oxidation reactor. This novel nano-structured TiO_2 microsphere provides an excellent potential application in removing humic acid from water.

NOM and Contaminant Removal by Ultrafiltration Membranes - Enhancement of Filtration Performance

Candidate: **Wei Xi**
Report No.: CEE/PhD/2008/185

Raw water supplies in Singapore tend to contain high levels of natural organic matter (NOM) and other contaminants. The effective removal of NOM from surface water is a great challenge to the water industry. This work aims to study novel techniques to improve NOM filtration performance of UF membranes with low fouling tendency and high permeability through various approaches, not only from an engineering perspective, but also from the view of UF membrane characteristics.

In this study, tropical NOM (from Singapore) was isolated

and its chemical and filtration characteristics were analyzed comparing to other NOM. A systematic study was carried out using different UF membranes operating over a full spectrum of operating conditions to improve NOM removal. The hybrid membrane process with MIEX and low pressure membranes was another approach. Finally, a novel electrophoresis-UV grafting technique for the surface modification of flat sheet UF membranes was developed in order to reduce their NOM fouling tendency and enhance NOM rejection.

Optimisation of Bus Public Transport Network in Singapore Using Spatial Parameters and Demographic Information

Candidate: **Liu Li**
Report No.: CEE/PhD/2008/186

This project aims to develop a methodology for optimising the design of bus route networks with the help of GIS. Firstly, the locations of bus stops are optimised with the objective of improving accessibility. Two methods are proposed: the first one uses a randomised-sequence improvement algorithm; the second one is developed using a set-cover problem solution. Secondly, bus routes are optimised with the objective of minimising total cost which is the sum of travellers' cost and operation cost. A hybrid simulated annealing (SA) and genetic algorithm (GA) approach is developed to design the bus routes. The proposed method is tested on four theoretical networks and a benchmark network and is also applied to the real transport network in part of Singapore with real demographic data.

Besides looking at transport network design, an evaluation of the current transportation system is done in order to understand the status quo and be able to compare alternative designs.

Optimal Coordination for an Integrated Multimodal and Multi-operator Transit System

Candidate: **Li Shoujie**
Report No.: CEE/PhD/2008/187

With the rapid urbanisation in most parts of the world, modern transit systems have been made more and more convenient, reliable and integrated. This study results from an interest in finding what the situation will be like when multiple operators overlap the service areas partially or fully.

In this optimisation research study, the objective function is formulated as the sum of operator cost and user cost. The formulation of total cost in different coordination scenarios are analyzed under three operator policies, i.e. cooperation, competition and independence respectively. By categorizing different groups of passengers in detail, the passenger flows are estimated by transit path choice model. The optimal results in Stackelberg equilibrium can be obtained by the optimisation procedure. The objective functions in scenarios of no coordination and common headway coordination, which are identified as nonlinear programming problem can be solved by considering the first order and second order conditions; whereas objective function in integer-ratio headway coordination is identified as mixed integer nonlinear programming problem. Evaluation of this model is conducted first, and then extensive sensitivity analysis is carried out to verify the evaluation results. Finally the conclusion can be drawn that integer-ratio headway coordination is an efficient and feasible method when operators adopted cooperation policy, whereas it is not recommended for them to adopt a competition policy, because the coordination benefits are not significant and sometimes they may even get worse.

This research focuses on optimal coordination of public transit operated by multiple operators during off-peak hours. The results would be beneficial to making regulatory policies as references.

Physio-Mechanical Simulation of Human's Left Ventricle Using Finite Element Method

Candidate: **Chen Qiang**
Report No.: CEE/PhD/2008/188

Heart diseases are the leading causes of death worldwide and most of these diseases happen in the left ventricle (LV). So the study on LV's electro-mechanism is very helpful to doctors to make an appropriate diagnosis. In this thesis, based on physiological observation, LV muscle is assumed to be composed of two different materials: myocardium masses (MM) and myocardium fibers (MF). An isotropic Mooney-Rivlin material property is implanted into MM, and a Hill's fiber force model is developed for representing MF which relates the microscopic molecular electricity events to macroscopic LV muscle performance. The fluid-structure interaction between MM and cavity blood (CB) has been considered in using penalty method. The mathematical model has been discretised into numerical model by using finite element method (FEM). MM and MF are meshed by finite element, while CB is meshed by an Arbitrary Lagrangian Eulerian (ALE) finite element. The available FEM package LS-DYNA is used as the solver. The FEM results show good agreements with clinic report and other references. The model can be a powerful tool to diagnose cardiac abnormities in future studies.

Quantifying Qualitative Information on Risks (QQIR) in Structured Finance Transactions

Candidate: **Tillmann Sachs**
Report No.: CEE/PhD/2008/189

Risks can impair the success of business transactions.

Structured finance transactions are exposed to numerous risks.

Some risk factors are well studied and have sufficient historic and numerical data and record to allow for projections and quantifications of the possible impact that these risk factors may have on transactions. Other risk factors may lack such information and projection and quantification become difficult. In some cases, a group of experts may have opinions on such risk factors. For quantifying these perceptions on risk factors, this doctoral research proposes a new methodology for quantifying qualitative information on risks (QQIR) in structured finance transactions. It contributes to the set of risk assessment methods by closing the gap between qualitative and quantitative risk assessment methods and adds value to all transaction participants.

The proposed QQIR method is a fuzzy set approach which allows deriving customized probability density functions based on expert opinion as well as ranking of such aggregated opinions. It is the interface between opinions experts generate based on available information in the market and stochastic cashflow modelling and simulation.

In this research, the QQIR method is derived from theory, validated and tested through a survey, and applied in two case studies. All data in this research is primary data.

The contribution to the sphere of knowledge is the novel development of the QQIR method. The QQIR method is a systematic, comprehensive, and mathematically- thorough approach for translating expert opinions on risk factors into customized probability density functions that can be used for stochastic simulations, rankings, or other applications.

In validating the QQIR method, the QQIR method has been used to quantify the perceived impact of political risks factors on financial decision criteria in project finance. The financial criteria were the expected internal rate of return, the project leverage, the risk premium on project loans, the minimum required debt service coverage ratio, and the insurance premium. The impact was assessed through an international survey across 14 Asian countries and 14 infrastructure sectors. The results of this QQIR survey assessment were then compared with results of an actual value poll, collected in the same survey. The two survey results were validated by triangulation with general country and sector risk perceptions, also collected in the same survey. The validation shows that in 77.5% of all cases, the QQIR method produces mean results that are within 0.85 standard deviations from the absolute value polls. Also the validation shows that with increasing perceived risks, costs of equity and debt finance as well as insurances 4 increase as well.

The application of the QQIR method to two case studies substantiates its validity.

The QQIR method has been applied for assessing the impact of governmental actions on demand and pricing in a power project. The impact was quantified as change in investment return ratios.

In the second case study, the QQIR method has been applied to assess the risk exposure and recovery potential of the involved parties in a guarantee contract in a water project.

Through the validation survey and both case studies, the commercial benefit and 4 contribution of the QQIR method to thorough risk assessment has been demonstrated.

Reverse Osmosis Desalination and Reclamation - Control of Colloidal and Biofouling

Candidate: **Chong Tzyy Haur**
Report No.: CEE/PhD/2008/190

The focus of this thesis work was on the fundamentals of colloidal and biofouling in reverse osmosis (RO) desalination and reclamation. A novel sodium chloride tracer response technique coupled with ultrasonic technique was employed to monitor the progress of fouling by silica colloids, alginic acid and *Pseudomonas fluorescens.* This study provided an insight into the interplay between critical flux, concentration polarization or CP (through the enhanced osmotic pressure effect) and fouling. In colloidal fouling, critical flux determined the deposition of particles on the membrane surface. The build up of deposit layer caused an additional hydraulic resistance as well as the cake enhanced osmotic pressure (CEOP) effect, which could be the predominant contributor in the membrane performance loss. Whereas in biofouling, it was postulated that the role of CP was to control the level of nutrient for the growth of biofilm, which in turn caused the biofilm enhanced osmotic pressure (BEOP) phenomenon.

Shear Capacity of Slab-Column Connections under Gravity and Biaxial Cyclic Lateral Loading

Candidate: **Edward Anggadjaja**
Report No.: CEE/PhD/2008/191

Tests of five large-scale rectangular edge-column slab connections are reported. The objective of the experiments was to investigate the effects of columns rectangularity, magnitudes of gravity loading and cyclic biaxial lateral loading on the connection strength, stiffness, ductility and drift capacity. A new method is presented for calculating the ultimate shear stresses at the critical shear perimeter of interior and exterior slab-column connections. Column rectangularity, connection geometry, influence of reinforcement ratio and gravity shear ratio, and the strength reduction due to cyclic loading are taken into consideration. The proposed equation has been verified for accuracy by

predicting the shear strength of 455 slab-column connections including interior, edge, and corner connections, ranging from symmetrical punching to connections having rectangular columns transferring unbalanced moments due to cyclic lateral loading. The proposed formula gives a very good agreement between the predicted and experimental values, and it also simplifies the design and analysis process.

The Effect of Powdered Activated Carbon Addition and Two-compartment Configuration on Membrane Bioreactor Performance

Candidate: **Ng Choon Aun**
Report No.: CEE/PhD/2008/192

The thesis describes a study that aims to examine the possible mechanisms by which the presence of PAC could improve the filtration performance of the membrane bioreactor (MBR). A protocol had been applied to give a fair comparison of potential mechanisms. The examined mechanisms include:

(i) the effect of PAC on MLSS,
(ii) the effect of PAC on planktonik bacteria,
(iii) the effect of PAC as an adsorbent,
(iv) the effect of PAC as scouring agent, and
(v) the effect of BAC for simultaneous adsorption and biodegradation.

Besides, optimization of the MBR (BAC) in terms of PAC sizes and SRT was carried out. An alternative MBR design was also studied that aimed to separate the supernatant from the MLSS to reduce the contact of biomass flocs with the membrane. Further work is recommended to investigate reusable alternatives to PAC.

Time-Effect and Instability Behaviour of Cohesive Soils

Candidate: **Manish Tiwari**
Report No.: CEE/PhD/2008/193

An experimental study of time-effect on cohesive soils was carried out. Three types of clays, namely undisturbed Singapore marine clay, reconstituted Singapore marine clay and Kaolin were used for the study. The pore water pressure was measured at the top, bottom and mid-height of the specimen for better estimate of effective stress conditions within the soil. A motorized triaxial cell capable of running tests in both load-controlled and deformation-controlled loading modes was used for conducting the tests on normally consolidated specimens of the clay.

The undrained shear strength was found to increase by 6%, 5% and 2% respectively for undisturbed marine clay, reconstituted marine clay and Kaolin due to one log cycle increase in shearing rate. The pore water pressure was found to decrease with the increase in shearing rate irrespective of loading rate or loading mode. Increase in shearing rate resulted in an increase in mean effective stress and corresponding increase in peak deviator stress in a manner such that the effective stress path in faster test reached the failure envelope at a higher deviator stress. Therefore, the rate effect is a result of following different effective stress paths at different rates and is consistent with the failure criteria in terms of effective stresses. The rate effect was found to be related to both permeability and structure of clay.

The undrained shear strength of undisturbed Singapore marine clay was not affected significantly by the loading mode when time taken to reach the peak deviator stress were the same in deformation-controlled and load-controlled tests.

Loading mode significantly affected the behaviour of reconstituted marine clay and Kaolin. The undrained shear strengths in load-controlled tests were higher than the shear strengths in deformation-controlled tests by up to 8% and 5% respectively for reconstituted marine clay and Kaolin.

Drained behaviour of clay is affected by the loading rate and loading mode. Tests conducted at fast shearing rates tests result in up to 15% lower drained shear strength and lower effective friction angles due to an increase of 5 times in strain rate. Large non-uniformity of pore pressure is generated in fast drained tests and such tests are not true representative of drained behaviour of clay. Currently used method of selecting the strain rate for drained test underpredicts the time to failure and result in unrealistically low drained shear strength and friction angle. It was found that the best way to select the shearing rate is to get an estimate from the method recommended by BS1377 (1990) and use mid-height pore pressure measurement to verify the uniformity of pore pressure.

Pre-failure instability, identified by rapid increase in axial strain and axial strain rate, was observed to occur during undrained creep tests in undisturbed marine clay. For undisturbed marine clay, a zone of potential instability may be defined, which is bound by the instability line and the failure envelope of soil, where instability line coincides with the line passing through the peaks of the undrained effective stress paths. If the effective stress state is below the zone of potential instability, instability will not occur even if the stress level is above the threshold deviator stress level. However, if the effective stress state is within this zone, instability will most likely occur. Therefore, instability during undrained creep is governed by the condition of effective stresses with respect to the zone of potential instability. If the problem of undrained creep is foreseen in any field loading condition, use of failure envelope determined from maximum q/p' may result in unconservative design. Pre-failure instability should be taken into account during geotechnical design.

Traffic Safety Estimation at Road Junctions

Candidate: **Aine Kusumawati**
Report No.: CEE/PhD/2008/194

The research was undertaken with the aim of estimating safety at road junctions. Accident prediction models for signalised and unsignalised junctions were developed using a negative binomial regression model which also included a declining power trend. Procedures for developing accident prediction models and safety estimation were established and applied to Singapore road junctions.

Outputs from the accident prediction models were used for safety estimation by means of the original empirical Bayes (EB) method and a modified empirical Bayes (MEB) method. MEB method entails using a generalised Poisson distribution, which was shown to be a better fitting model than Poisson distribution, to model the accident count data of an entity (instead of the Poisson distribution used in the original EB method). A procedure for identification and ranking of hazardous sites based on the MEB method was also established.

The research has shown that use of the MEB method can improve the prediction of safety as compared to the EB method. The MEB method gave relatively more sites (4.4% and 1.3% more, for signalised and unsignalised junctions, respectively) with smaller sum-squares of error between predicted and observed accident frequencies in 2004-2005 than the original EB method.

PUBLICATIONS

*Publications of academic staff in journals and conference proceedings during the period from 1 July 2007 to June 2008. Authors who are not members of the School are marked by *.*

Anggadjaja, E. and Teng, S., 2008. "Edge-column slab connections under gravity and lateral loading." *ACI Structural Journal*, Vol. 105, No. 5, pp. 541-551.

Annamdas, V.G.M., Yang, Y. and Soh, C.K., 2007. "Influence of loading on structures actuated with piezoceramic transducers - art. No. 64140X." *Conference on Smart Structures, Devices and Systems III*, Adelaide, Australia, X4140-X4140.

Annamdas, V.G.M., Yang, Y.W. and Soh, C.K., 2007. "Influence of loading on the electromechanical admittance of piezoceramic transducers." *Smart Materials and Structures*, Vol. 16, No. 5, pp. 1888-1897.

Annamdas, V.G.M. and Soh, C.K., 2008. "Three-dimensional electromechanical impedance model for multiple piezoceffamic transducers - Structure interaction." *Journal of Aerospace Engineering*, Vol. 21, No. 1, pp. 35-44.

Annamdas, V.G.M., Yang, Y.W. and Liu, H., 2008. "Current development in fiber Bragg grating sensors and their applications - art. No. 69320D." *Conference on Sensors and Smart Structures Technologies for Civil, Mechanical, and Aerospace Systems*, San Diego, CA, D9320-D9320.

Arulrajah, A.*, Bo, M.W.*, Chu, J. and Nikraz, H.*, 2008. "Application of prefabricated vertical drains to the Changi land reclamation project, Singapore." *Proceedings of the 4th Asian Regional Conference on Geosynthetics*, 17-18 June, Shanghai, pp. 651-655.

Au, S.K., Ching, J.* and Beck, J.L.*, 2007. "Application of subset simulation methods to reliability benchmark problems." *Structural Safety*, Vol. 29, No. 3, pp. 183-193.

Bahador, S.D., Yang, Y. and Zhang, L., 2008. "Strain transfer models for strain actuators." *International Conference on Multifunctional Materials and Structures*, Hong Kong, Peoples R China, pp. 254-257.

Bansal, A.*, Madhavi, S.*, Tan, T.T.Y. and Lim, T.M.*, 2008. "Effect of silver on the photocatalytic degradation of humic acid." *Proceedings of the 4th Asia-Pacific Congress on Catalysis, Singapore*, Vol. 131, No. 1-4, pp. 250-254.

Blanquez, P.* and Guieysse, B., 2008. "Continuous biodegradation of 17 beta-estradiol and 17 alpha-ethynylestradiol by Trametes versicolor." *Journal of Hazardous Materials*, Vol. 150, No. 2, pp. 459-462.

Bo, M.W.*, Wong, K.S. and Choa, V., 2008. "Constant rate of displacement test on ultra-soft soil." *Proceedings of the Institution of Civil Engineers, Geotechnical Engineering*, Vol. 161, No. 3, pp. 129-135.

Brownjohn, J.M.W.* and Pan, T.-C., 2008. "Identifying loading and response mechanisms from ten years of performance monitoring of a tall building." *Journal of Performance of Constructed Facilities*, Vol. 22, No. 1, pp. 24-34.

Chang, S.*, Yeo, A., Fane, A., Cholewa, M.*, Ping, Y.* and Moser, H.*, 2007. "Observation of flow characteristics in a hollow fiber lumen using non-invasive X-ray micro imaging (XMI)." *Journal of Membrane Science*, Vol. 304, No. 1-2, pp. 181-189.

Chen, M.Y., Lee, D.J. and Tay, J.H., 2007. "Distribution of extracellular polymeric substances in aerobic granules." *Applied Microbiology and Biotechnology*, Vol. 73, No. 6, pp. 1463-1469.

Chen, P.H., 2008. "Integration of cost and schedule using extensive matrix method and spreadsheets." *Automation in Construction*, Vol. 18, No. 1, pp. 32-41.

Chen, P.H. and Shahandashti, S.M., 2008. "Stochastic scheduling with multiple resource constraints using a simulated annealing-based algorithm." *Proceedings of the 25th International Symposium on Automation and Robotics in Construction*, Vilnius, Lithuania, pp. 447-451.

Chen, P.H. and Truc, N.T.L., 2008. "Automatic 3D modeling development and application for hydraulic construction." *Proceedings of the 25th International Symposium on Automation and Robotics in Construction*, Vilnius, Lithuania, pp. 435-439.

Chen, P.H. and Truc, N.T.L., 2008. "Computer-aided visual communication for way-finding in emergency in indoor environment." *Proceedings of the 25th International Symposium on Automation and Robotics in Construction*, Vilnius, Lithuania, pp. 440-446.

Chen, X.L., Zhao, Z.Y. and Liew, K.M., 2008. "Stability of piezoelectric FGM rectangular plates subjected to non-uniformly distributed load, heat and voltage." *Advances in Engineering Software*, Vol. 39, No. 2, pp. 121-131.

Chen, X.W. and Chiew, Y.M., 2007. "Turbulence characteristics of open-channel flow with bed suction." *Journal of Engineering Mechanics, ASCE*, Vol. 133, No. 12, pp. 1388-1393.

Chen, Z., Ren, N., Wang, A., Zhang, Z.P. and Shi, Y., 2008. „A novel application of TPAD-MBR system to the pilot treatment of chemical synthesis-based pharmaceutical wastewater." *Water Research*, Vol. 42, No. 13, pp. 3385-3392.

Cheng, N.S., 2008. "Comparison of settling-velocity-based formulas for threshold of sediment motion." *Journal of Hydraulic Engineering, ASCE, Vol.* 134, No. 8, pp. 1136-1141.

Cheng, N.S., 2008. "Formula for the viscosity of a glycerol-water mixture." *Industrial and Engineering Chemistry Research*, Vol. 47, No. 9, pp. 3285-3288.

Cheng, N.S., 2008. "Formulas for friction factor in transitional regimes." *Journal of Hydraulic Engineering, ASCE*, Vol. 134, No. 9, pp. 1357-1362.

Cheng, N.S., Hao, Z.Y. and Tan, S.K., 2008. "Comparison of quadratic and power law for nonlinear flow through porous media." *Experimental Thermal and Fluid Science*, Vol. 32, No. 8, pp. 1538-1547.

Chiew, S.P., 2007. "Innovative applications of structural hollow sections." *Proceedings of the 3rd IStructE Asia-Pacific Forum on Structural Engineering: - Innovations in Structural Engineering*, Singapore, 2-3 November, pp. 114-127 (ISBN/ISSN: 978-981-05-9267-7).

Chiew, S.P., 2007. "Use of Chinese Steel Materials to BS5950." *Proceedings of the 2nd International Symposium on Advances in Steel and Composite Structures*, Hong Kong, 20 July, pp. 53-74 (ISBN/ISSN: 978-962-367-571-0).

Chiew, S.P., Lee, C.K., Lie, S.T., Nguyen, T.B.N. and Sopha, T., 2007. "Mesh generation for partially overlapped circular hollow section K-joints under fatigue loadings." *Proceedings of the 2nd International Maritime-Port Technology and Development Conference (MTEC-2007)*, Singapore, 26-28 September, pp. 313-318 (ISBN/ISSN: 978-981-05-8949-3).

Chiew, S.P. and Yu, Y., 2007. "Extension of fatigue life of steel flexural members with high strength composite materials." *Proceedings of the 2nd International Maritime, Port Technology and Development Conference (MTEC-2007)*, Singapore, 26-28 September, pp. 286-291 (ISBN/ISSN: 978-981-05-8949-3).

Chiew, S.P., Rush, M.C.*, Nguyen, T.B.N., Lim, S.F. and Lee, Y.F., 2007. "Container handling quay cranes: evolution and fatigue considerations". *Proceedings of the International Symposium on Fatigue and Fracture of Steel Structures*, Singapore, 4 December, pp. 67-85 (ISBN/ISSN: 978-981-05-9644-5).

Chiew, S.P. and Yu, Y., 2007. "Use of fiber reinforced polymer composites in upgrading metallic structures - A State-of-the-Art Review". *Proceedings of the 5th International Conference on Advances in Steel Structures (ICASS-2007)*, Singapore, 5-7 December, pp. 901-907 (ISBN/ISSN: 978-981-05-9365).

Chiew, S.P., Lee, C.K., Lie, S.T. and Ji, H.L., 2007. "Fatigue behaviors of square-to-square hollow section T-joint with corner crack. I: Experimental studies." *Engineering Fracture Mechanics*, Vol. 74, No. 5, pp. 703-720.

Chiew, S.P., Sun, Q. and Yu, Y., 2007. "Flexural strength of RC beams with GFRP laminates." *Journal of Composites for Construction*, Vol. 11, No. 5, pp. 497-506.

Chiew, Y.M., 2008. "Scour and scour countermeasures at bridge sites". *Transactions of Tianjin University*, Vol. 14, No. 4, pp. 289-295.

Chong, T.H.*, Wong, F.S.* and Fane, A.G., 2008. "Implications of critical flux and cake enhanced osmotic pressure (CEOP) on colloidal fouling in reverse osmosis: Experimental observations." *Journal of Membrane Science*, Vol. 314, No. 1-2, pp. 101-111.

Chu, J., Leong W.K., Balasubraniam, A.* and Lo, R.S.*, 2007. "Identification of possible new failure mechanisms for the collapse of tailings." *Proceedings of the 10th Australia New Zealand Conference on Geomechanics*, 21-24 October, Brisbane.

Chu, J., Parashar, S.P.* and Sanmugnathan, D.*, 2007. "Comparison of undrained shear strength of Singapore marine clay determined by laboratory and in-situ tests." *Proceedings of Underground Singapore 2007*, 29-30 November, pp. 123-128.

Chu, J. and Wanatowski, D., 2007. "Deficiencies in the use of post-liquefaction strength." *Proceedings of the 8th Asia Pacific Earthquake Conference*, 5-7 December, Singapore.

Chu, J. and Wardani, S.P.R.*, 2007. "Geotechnical considerations of access road construction for disaster rehabilitation." *Keynote Lecture, Proceedings of the 4th International Conference on Disaster Prevention and Rehabilitation*, 10-11 September, Semarang, pp. II-1-II-8.

Chu, J. and Yan, S.W., 2007. "Innovative ground improvement methods for post-disaster constructions." *Invited Lecture, Proceedings of the UGM-KU-UW Joint Symposium on Disaster Mitigation and Community Based Reconstruction*, 9 August, Yogyakarta, pp. 69-81.

Chu, J. and Lim, T.T., 2008. "Use of sewage sludge and copper slag for land reclamation." *Geotechnics of Waste Management and Remediation, GeoCongress 2008, ASCE Geotechnical Special Publication* No. 177, pp. 352-359.

Chu, J., Yan, S.W. and Indraratna, B.*, 2008. "Vacuum preloading techniques – recent developments and applications." *Geosustainability and Geohazard Mitigation, GeoCongress 2008, ASCE Geotechnical Special Publication* No. 178, pp. 586-595.

Chu, J. and Wanatowski, D., 2008. "Instability conditions of loose sand in plane strain." *Journal of Geotechnical and Geoenvironmental Engineering*, Vol. 134, No. 1, pp. 136-142.

Chua, L.H.C., Lo, E.Y.M., Freyberg, D.L.*, Shuy, E.B., Lim, T.T., Tan, S.K., and Ngonidzashe, M., 2007. "Hydrostratigraphy and geochemistry at a coastal sandfill in Singapore." *Hydrogeology Journal*, Vol. 15, No. 8, pp. 1591-1604.

Chua, L.H.C. and Shuy, E.B., 2008. "Laboratory studies on the coupled oscillations between an internal density interface and a shear layer." *Journal of Engineering Mechanics, ASCE*, Vol. 134, No. 4, pp. 348-352.

Chua, L.H.C., Wong, T.S.W. and Sriramula, L.K., 2008. "Comparison between kinematic wave and artificial neural network models in event-based runoff simulation for an overland plane." *Journal of Hydrology*, Vol. 357, No. 3-4, pp. 337-348.

Dey, S.*, Chiew, Y.M. and Kadam, M.S.*, 2008. "Local scour and riprap stability at an abutment in a degrading bed." *Journal of Hydraulic Engineering, ASCE*, Vol. 134, No. 10, pp. 1496-1502.

Dharma, R.B. and Tan, K.H., 2007. "Proposed design methods for lateral torsional buckling of unrestrained steel beams in fire." *Journal of Constructional Steel Research*, Vol. 63, No. 8, pp. 1066-1076.

Dharma, R.B. and Tan, K.H., 2007. "Rotational capacity of steel I-beams under fire conditions Part I: Experimental study." *Engineering Structures*, Vol. 29, No. 9, pp. 2391-2402.

Dharma, R.B. and Tan, K.H., 2007. "Rotational capacity of steel I-beams under fire conditions Part II: Numerical simulations." *Engineering Structures*, Vol. 29, No. 9, pp. 2403-2418.

Ding, H.B., Liu, X.Y., Stabnikova, O. and Wang, J.Y., 2008. "Effect of protein on biohydrogen production from starch of food waste." *Water Science and Technology*, Vol. 57, No. 7, pp. 1031-1036.

Ding, H.B. and Wang, J.Y., 2008. "Responses of methanogenic reactor to different fractions of fermentative hydrogen production in a 2-phase anaerobic digestion system". *International Journal of Hydrogen Energy*, doi:10.1016/j.ijhydene.2008.09.021.

Duan, H.Q., Yan, R., Koe, L.C.C. and Wang, X.L., 2007. "Combined effect of adsorption and biodegradation of biological activated carbon on H_2S biotrickling filtration." *Chemosphere*, Vol. 66, No. 9, pp. 1684-1691.

Ehrlich, M. and Kong, R.T.L., 2008. „Modelling country reliability in public private partnership infrastructure projects." *Proceedings of the 25th International Symposium on Automation and Robotics in Construction*, Vilnius, Lithuania, pp. 751-758.

Fan, S.C. and Li, S.M., 2008. "Boundary finite-element method coupling finite-element method for steady-state analyses of dam-reservoir systems." *Journal of Engineering Mechanics, ASCE*, Vol. 134, No. 2, pp. 133-142.

Fan, H.S.L., 2008. "Reducing Aircraft Emissions on the Ground". *Invited Paper, Proceedings of the International Forum on Shipping, Ports and Airports 2008*, Hong Kong SAR, May.

Fane, A.G., 2007. "Sustainability and membrane processing of wastewater for reuse." *56th Annual Meeting of the Society for Range Management, Casper, WY*, Vol. 202, Issue No. 1-3, pp. 53-58.

Feng, J., B.W. Zhu, and Lim, T.T., 2008. "Reduction of chlorinated methanes with nano-scale Fe particles: Effects of amphiphiles on the dechlorination reaction and two-parameter regression for kinetic prediction." *Chemosphere*, Vol. 73, No. 11, pp. 1817-1823.

Fung, T.C. and Chen, Z.L., 2008. "Precise time-step integration algorithms using response matrices with Expanded dimension." *AIAA Journal*, Vol. 46, No. 8, pp. 1900-1911.

Gao, F. and Gho, W.M., 2008. "Parametric equations to predict SCF of axially loaded completely overlapped tubular circular hollow section joints." *Journal of Structural Engineering, ASCE*, Vol. 134, No. 3, pp. 412-420.

Gao, F., Shao, Y.B. and Gho, W.M., 2007. "Stress and strain concentration factors of completely overlapped tubular joints under lap brace IPB load." *Journal of Constructional Steel Research*, Vol. 63, No. 3, pp. 305-316.

Gao, L., Yu, S.C.M., Ai, J.J. and Law, A.W.K., 2008. "Circulation and energy of the leading vortex ring in a gravity-driven starting jet." *Physics of Fluids*, Vol. 20, No. 9.

Gho, W.M. and Yang, Y., 2008. "Parametric equation for static strength of tubular circular hollow section joints with complete overlap of braces." *Journal of Structural Engineering, ASCE*, Vol. 134, No. 3, pp. 393-401.

Goh, A.T.C. and Goh, S.H., 2007. "Support vector machines: Their use in geotechnical engineering as illustrated using seismic liquefaction data." *Computers and Geotechnics*, Vol. 34, No. 5, pp. 410-421.

Goh, A.T.C., Kulhawy, F.H.* and Wong, K.S., 2008. "Reliability assessment of basal-heave stability for braced excavations in clay." *Journal of Geotechnical and Geoenvironmental Engineering*, Vol. 134, No. 2, pp. 145-153.

Goh, K.H., Lim, T.T. and Chui, P.C., 2008. "Evaluation of the effect of dosage, pH and contact time on high-dose phosphate inhibition for copper corrosion control using response surface methodology (RSM)." *Corrosion Science*, Vol. 50, No. 4, pp. 918-927.

Goh, K.H., Lim, T.T. and Dong, Z., 2008. "Application of layered double hydroxides for removal of oxyanions: A review." *Water Research*, Vol. 42, No. 6-7, pp. 1343-1368.

Gong, Q.M. and Zhao, J., 2007. "Influence of rock brittleness on TBM penetration rate in Singapore granite." *Tunnelling and Underground Space Technology*, Vol. 22, No. 3, pp. 317-324.

Gong, Q.M., Zhao, J.* and Jiang, Y.S., 2007. "In situ TBM penetration tests and rock mass boreability analysis in hard rock tunnels." *Tunnelling and Underground Space Technology*, Vol. 22, No. 3, pp. 303-316.

Guieysse, B., Hort, C.*, Platel, V.*, Munoz, R.*, Ondarts, M.* and Revah, S.*, 2008. "Biological treatment of indoor air for VOC removal: Potential and challenges." *Biotechnology Advances*, Vol. 26, No. 5, pp. 398-410.

Hao, Z., Cheng, N.S. and Tan, S.K., 2008. "Investigation of inertial effect in simplified porous media flow." *Proceedings of 16th IAHR-APD Congress and 3rd Symposium of IAHR-ISHS*, Tsinghua University Press, Vol. 1, pp. 160-165.

Hao, Z., Zhou, T., Chua, L.P. and Yu, S.C.M., 2008. "Approximations to energy and temperature dissipation rates in the far field of a cylinder wake." *Experimental Thermal and Fluid Science*, Vol. 32, No. 3, pp. 791-799.

Hao, Z., Zhou, T., Zhou, Y. and Mi, J., 2008. "Reynolds number dependence of the inertial range scaling of energy dissipation rate and enstrophy in a cylinder wake." *Experiments in Fluids*, Vol. 44, No. 2, pp. 279-289.

Hu, O.E. and Tan, K.H., 2007. "Large reinforced-concrete deep beams with web openings: test and strut-and-tie results." *Magazine of Concrete Research*, Vol. 59, No. 6, pp. 423-434.

Hu, O.E., Tan, K.H. and Liu, X.H., 2007. "Behaviour and strut-and-tie predictions of high-strength concrete deep beams with trapezoidal web openings." *Magazine of Concrete Research*, Vol. 59, No. 7, pp. 529-541.

Hu, Y.H. and Yang, Y.W., 2007. "Sensing region of PZT transducers bonded to concrete." *Conference on Sensors and Smart Structures Technologies for Civil, Mechanical and Aerospace Systems*, San Diego, CA, pp. U80-U90.

Hu, Y.H., Yang, Y.W., Zhang, L., Lu, Y., 2007. "Identification of structural parameters based on PZT impedance using genetic algorithms." *IEEE Congress on Evolutionary Computation*, Singapore, pp. 4170-4177.

Huang, Z.F. and Tan, K.H., 2007. "Structural response of restrained steel columns at elevated temperatures. Part 2: FE simulation with focus on experimental secondary effects." *Engineering Structures*, Vol. 29, No. 9, pp. 2036-2047.

Huang, Z.F., Tan, K.H. and Phng, G.H., 2007. "Axial restraint effects on the fire resistance of composite columns encasing I-section steel." *Journal of Constructional Steel Research*, Vol. 63, No. 4, pp. 437-447.

Huang, Z.F., Toh, W.S., Tan, K.H. and Phng, G.H., 2007. "Failure process of composite columns with embedded I-section steel under elevated temperature - Load level effects." *International Journal of Steel Structures*, Vol. 7, No. 3, pp. 163-172.

Huang, Z.F., Tan, K.H., Toh, W.S. and Phng, G.H., 2008. "Fire resistance of composite columns with embedded I-section steel - Effects of section size and load level." *Journal of Constructional Steel Research*, Vol. 64, No. 3, pp. 312-325.

Huang, Z.H., 2007. "Reflection and transmission of regular waves at a surface-pitching slotted barrier." *Applied Mathematics and Mechanics, English Edition*, Vol. 28, No. 9, pp. 1153-1162.

Huang, Z.H., 2008. "Wave scattering by double slotted barriers in a steady current: Experiments." *China Ocean Engineering*, Vol. 22, No. 2, pp. 205-214.

Huang, Z.H., Ding, L. and Ghidaoui, M.S.*, 2007. "Scattering of regular waves by irregular porous seabed in the presence of a reflective beach." *Proceedings of the 4th International Conference on Asian and Pacific Coasts*, Nanjing, Peoples R China, pp. 185-188.

Huang, Z.H. and Ghidaoui, M.S.*, 2008. "Experiments on nonlinear wave scattering by a submerged rectangular step in the presence of a current." *Proceedings of the 18th International Offshore and Polar Engineering Conference (ISOPE 2008)*, Vancouver, CANADA, pp. 599-606.

Huang, Z.H. and Liu, C.R., 2008. "A linear theory for wave scattering by double slotted barriers in weak steady currents." *China Ocean Engineering*, Vol. 22, No. 2, pp. 215-226.

Ivanov, V., 2007. "Microbiological monitoring of discharged ballast water." *Proceedings of the International Maritime - Port Technology and Development Conference (MTEC 2007)*, Singapore, 26-28 September 2007.

Ivanov, V., 2007. "The technologies for prevention of bioterrorism attacks in the ports." *Proceedings of the 5th Maritime Security Workshop (Temasek Defence Systems Institute, Naval Postgraduate School, and Lawrence Livermore National Laboratory)*, 4-7 December, Singapore.

Ivanov, V., 2008. "Ecology of suspended microbial aggregates." *IWA Biofilm Technologies Conference*, Singapore, 8-10 January, pp. 9-12.

Ivanov, V. and Chu, J., 2008. "Applications of microorganisms to geotechnical engineering for bioclogging and biocementation of soil in situ". *Reviews in Environmental Science and Biotechnology*, Vol. 7, pp. 139-153.

Ivanov, V., Wang, X.H. and Stabnikova, O., 2008. "Starter culture of Pseudomonas veronii strain B for aerobic granulation." *World Journal of Microbiology and Biotechnology*, Vol. 24, No. 4, pp. 533-539.

Ivanov, V., Wang, X.-H, Liu, Y.-Q. and Stabnikova, O., 2008. "Simultaneous microbial granulation and biodegradation of estrogens in sequencing batch reactor." *Proceedings of the IWA 4th Sequencing Batch Reactor Conference*, Rome, 7-10 April, pp. 365-372.

Ivanov, V., Kuang, S.-L., Guo, C.-H. and Stabnikov, V., 2008. "The removal of phosphorus from reject water in a municipal wastewater treatment plant using iron ore".

Journal of Chemical Technology and Biotechnology, (in press, DOI 10.1002/jctb.2009)

Jiang, H.L., Maszenan, A.M. and Tay, J.H., 2007. «Bioaugmentation and coexistence of two functionally similar bacterial strains in aerobic granules.» *Applied Microbiology and Biotechnology*, Vol. 75, No. 5, pp. 1191-1200.

Jiang, X., Yan, R. and Tay, J.H., 2008. "Reusing H_2S exhausted carbon as packing material for odor biofiltration." *Chemosphere*, Vol. 73, No. 5, pp. 698-704.

Jinadasa, K.*, Tanaka, N.*, Sasikala, S.*, Werellagama, D.*, Mowjood, M.I.M.* and Ng, W.J., 2008. "Impact of harvesting on constructed wetlands performance - a comparison between Scirpus grossus and Typha angustifolia." *Journal of Environmental Science and Health Part A - Toxic/ Hazardous Substances and Environmental Engineering*, Vol. 43, No. 6, pp. 664-671.

Jotisankasa, A.*, Kulsawan, B.*, Toll, D.G.* and Rahardjo, H., 2008. "Studies of Rainfall-induced Landslides in Thailand and Singapore." *Proceedings of the 1st European Conference on Unsaturated Soils.* Durham University, Durham, UK, 30 June – 4 July, pp. 901-907.

Jou, R.C.*, Lam, S.H., Hensher, D.A.*, Chen, C.C.* and Kuo, C.W.*, 2008. "The effect of service quality and price on international airline competition." *Proceedings of the 10th Annual Conference of the Air Transport Research Society, Nagoya, Japan,* Vol. 44, Issue 4, pp. 580-592.

Jou, R.C.*, Lam, S.H., Kuo, C.W.* and Chen, C.C.*, 2008. "The asymmetric effects of service quality on passengers' choice of carriers for international air travel." *Journal of Advanced Transportation*, Vol. 42, No. 2, pp. 179-208.

Jou, R.C.*, Lam, S. H. and Wu, P.H.*, 2007. "Acceptance tendencies and commuters' behavior under different road pricing schemes." *Transportmetrica*, Vol. 3, No. 3, pp. 213-230.

Kao, C.M., Huang, K.D., Wang, J.Y., Chen, T.Y. and Chien, H.Y., 2008. "Application of potassium permanganate as an oxidant for in situ oxidation of trichloroethylene - contaminated groundwater: A laboratory and kinetics study." *Journal of Hazardous Materials*, Vol. 153, No. 3, pp. 919-927.

Kaur, S.*, Gopal, R.*, Ng, W.J., Ramakrishna, S.* and Matsuura, T.*, 2008. "Next generation fibrous media for water treatment." *Mrs Bulletin*, Vol. 33, No. 1, pp. 21-26.

Khoo, J.H. and Li, B., 2007. "Modeling of reinforced concrete sub-frame under cyclic load reversals." *Journal of Earthquake Engineering*, Vol. 11, No. 2, pp. 215-230.

Khor, S.L., Sun, D.D., Liu, Y.J. and Leckie, J.O.*, 2007. "Biofouling development and rejection enhancement in long SRT MF membrane bioreactor." *Process Biochemistry*, Vol. 42, No. 12, pp. 1641-1648.

Khor, S.L., Sun, D.D., Hay, C.T. and Liu, Y., 2008. "Use of biofilm in membrane bioreactor system for water reclamation". *IWA Biofilm Technologies Conference*, 8-10 January, NEC, Singapore.

Kong, D., Tiong, R.L.K., Cheah, C.Y.J., Permana, A. and Ehrlich, M., 2008. "Assessment of credit risk in project finance." *Journal of Construction Engineering and Management, ASCE*, Vol. 134, No. 11, pp. 876-884.

Krisdani, H., Rahardjo, H. and Leong, E.C., 2008. "Measurement of geotextile-water characteristic curve using capillary rise principle." *Geosynthetics International*, Vol. 15, No. 2, pp. 86-94.

Krisdani, H., Rahardjo, H. and Leong, E.C., 2008. "Effects of different drying rates on shrinkage characteristics of a residual soil and soil mixtures". *Journal of Engineering Geology*, Vol. 102, pp. 31-37.

Krisdani, H., Rahardjo, H. and Leong, E.C., 2008. "Measurement of geotextile-water characteristic curve using capillary rise principle". *Geosynthetics International Journal*, Vol. 15, No. 2, pp. 86-94.

Kulkarni, S.A. and Bajoria, K.*, 2007. "Large deformation analysis of piezolaminated smart structures using higher-order shear deformation theory." *Smart Materials and Structures*, Vol. 16, No. 5, pp. 1506-1516.

Kulkarni, S.A., Li, B. and Yip, W.K., 2008. "Finite element analysis of precast hybrid-steel concrete connections under cyclic loading." *Journal of Constructional Steel Research*, Vol. 64, No. 2, pp. 190-201.

Kwon, Y.-N., Tang, C.Y. and Leckie, J.O.*, 2008. "Change of chemical composition and hydrogen bonding behavior due to chlorination of crosslinked polyamide membranes." *Journal of Applied Polymer Science*, Vol. 108, pp. 2061-2066.

Law, A.W.K. and Huang, G.X., 2007. "Observations and measurements of wave-induced drift of surface inextensible film in deep and shallow waters." *Ocean Engineering*, Vol. 34, No. 1, pp. 94-102.

Lee, C.K., Chiew, S.P., Lie, S.T., Sopha, T. and Nguyen, T.B.N., 2007. "Experimental studies on fatigue behaviour of partially overlapped circular hollow section K-Joint". *Proceedings of the 2nd International Maritime, Port Technology and Development Conference (MTEC-2007)*, Singapore, 26-28 September, pp. 280-285 (ISBN/ISSN: 978-981-05-8949-3).

Lee, C.K., Chiew, S.P., Lie, S.T., Sopha, T. and Nguyen, T.B.N., 2007. "Experimental studies on stress concentration factors for partially overlapped circular hollow section K-Joints." *Proceedings of the 5th International Conference on Advances in Steel Structures (ICASS-2007)*, Singapore, 5-7 December, pp. 1015-1020 (ISBN/ISSN: 978-981-05-9365).

Lee C.K., Lie, S.T., Chiew, S.P., Sopha, T. and Nguyen, T.B.N., 2007. "Experimental studies on stress distributions for partially overlapped CHS K-Joints." *Proceedings of the*

9th International Conference on Steel, Space and Composite Structures (SS07), Yantai and Beijing, China, 10-15 October, pp. 389-394 (ISBN/ISSN: 978-981-05-7589-0).

Lee, C.K., Lie, S.T. and Chiew, S.P., 2007. "Finite element modelling of tubular joint structures for fatigue assessment." *Proceedings of the International Symposium on Fatigue and Fracture of Steel Structures, Singapore*, 4 December, pp. 97-117 (ISBN/ISSN: 978-981-05-9644-5).

Lee, C.K. and Shuai, Y.Y., 2007. "An automatic adaptive refinement procedure for the reproducing kernel particle method. Part I: Stress recovery and a posteriori error estimation." *Computational Mechanics*, Vol. 40, No. 3, pp. 399-413.

Lee, C.K. and Shuai, Y.Y., 2007. "An automatic adaptive refinement procedure for the reproducing kernel particle method. Part II: Adaptive refinement." *Computational Mechanics*, Vol. 40, No. 3, pp. 415-427.

Lee, P.F., Zhang, X., Du, A.J., Sun, D.D. and Leckie, J.O.*, 2007. "Ballast water treatment using TiO_2 nano-structured microsphere and nanofiber membrane photocatalytic oxidation reactor: A case study and future application". *International Maritime - Port Technology and Development Conference*, Suntec International Convention and Exhibition Centre, 26-28 September.

Lee, P.F., Zhang, X.W., Sun, D.D., Du, J.H. and Leckie, J.O.*, 2008. "Synthesis of bimodal porous structured TiO_2 microsphere with high photocatalytic activity for water treatment." *Colloids and Surfaces A: Physicochemical and Engineering Aspects*, Vol. 324, No. 1-3, pp. 202-207.

Lei, W.D., Hefny, A.M., Yan, S. and Teng, J., 2007. "A numerical study on 2-D compressive wave propagation in rock masses with a set of joints along the radial direction normal to the joints." *Computers and Geotechnics*, Vol. 34, No. 6, pp. 508-523.

Lei, W.D., Teng, J., Hefny, A., Zhao, J. and Guan, J., 2007. "Experimental study on prediction model for maximum rebound ratio." *Journal of Central South University of Technology*, Vol. 14, No. 1, pp. 115-119.

Leong, E.C., Anand, S., Cheong, H.K.* and Lim, C.H., 2007. "Re-examination of peak stress and scaled distance due to ground shock." *International Journal of Impact Engineering*, Vol. 34, No. 9, 1487-1499.

Li, B. and Pan, T.-C., 2007. "Seismic behavior of non-seismically detailed reinforced concrete structural systems and components - What have we been learning?" *Journal of Earthquake and Tsunami*, Vol. 1, No. 2, pp. 139-159.

Li, B. and Pan, T.-C., 2008. "Lien Institute For the Environment [LIFE]." *I²CTI Newsletter, International Institute for Construction Technology Information*, 11 April, No. 17.

Lim, C.L., Li, B. and Pan, T.-C., 2007. "Shake table tests of masonry walls strengthened by canvas sheets." *Proceedings of the 8th Pacific Conference on Earthquake Engineering*, 5-7 December, Singapore, Paper No. 298.

Li, S.M. and Fan, S.C., 2007. "Parametric analysis of a submerged cylindrical shell subjected to shock waves." *China Ocean Engineering*, Vol. 21, No. 1, pp. 125-136.

Li, X.B., Zhou, Z.L., Lok, T.S., Hong, L. and Yin, T.B., 2008. "Innovative testing technique of rock subjected to coupled static and dynamic loads." *International Journal of Rock Mechanics and Mining Sciences*, Vol. 45, No. 5, pp. 739-748.

Li, Y., Liu, Y., Shen, L. and Chen, F., 2008. "DO diffusion profile in aerobic granule and its microbiological implications." *Enzyme and Microbial Technology*, Vol. 43, No. 4-5, pp. 349-354.

Li, Y., Liu, Y. and Xu, H.L., 2008. "Is sludge retention time a decisive factor for aerobic granulation in SBR?" *Bioresource Technology*, Vol. 99, No. 16, pp. 7672-7677.

Liang, J., Koe, L., Chiaw, C. and Ning, X.G., 2007. "Application of biological activated carbon as a low pH biofilter medium for gas mixture treatment." *Biotechnology and Bioengineering*, Vol. 96, No. 6, pp. 1092-1100.

Lie, S.T. and Yang, Z.M., 2007. "Assessment of fracture strength of cracked offshore tubular joints". *Proceedings of the International Maritime, Port Technology and Development Conference – MTEC 2007*, Singapore, 26-28 September, pp. 235-240.

Lie, S.T. and Yang, Z.M., 2007. "BS7910:2005 Failure Assessment Diagram (FAD) on Cracked Circular Hollow Section (CHS) Welded Joints". *Proceedings of the 5th International Conference on Advances in Steel Structures – ICASS 2007*, Singapore, 5-7 December, pp. 535-540.

Lie, S.T., Yang, Z.M., Chiew, S.P. and Lee, C.K., 2007. "The ultimate behaviour of cracked square hollow section T-joints". *International Journal of Advanced Steel Construction*, Vol. 3, No. 1, pp. 443-458.

Lie, S.T. and Zhang, B.F., 2008. "Failure Assessment of Cracked Circular Hollow Section (CHS) Welded Joints Using BS7910: 2005". *Proceedings of the 12th International Symposium on Tubular Structures, Shanghai, China*, 8-10 October, pp. 367-373.

Shao, Y.B., Lie, S.T. and Chiew, S.P, 2008. "Effect of chord length ratio of tubular joints on stress concentration at welded region". *Proceedings of the 12th International Symposium on Tubular Structures, Shanghai, China, 8-10 October*, pp. 375-379.

Lim, S.H., Ferraris, C., Schreyer, M., Shih, K., Leckie, J.O. and White, T.J., 2007. "The influence of cobalt doping on photocatalytic nano-titania: Crystal chemistry and amorphicity." *Journal of Solid State Chemistry*, Vol. 180, No. 10, pp. 2905-2915.

Lim, T.T. and Zhu, B.W., 2008. "Effects of anions on the kinetics and reactivity of nanoscale Pd/Fe in trichlorobenzene dechlorination." *Chemosphere*, Vol. 73, No. 9, pp. 1471–1477.

Liu, H.B., Zhao, X.L., Al-Mahaidi, R. and Chiew, S.P., 2007. "Experimental Investigations of Advanced Composites Reinforcement of Cracked Steel Structures." *Proceedings of the 2nd International Maritime, Port Technology and Development Conference (MTEC-2007)*, Singapore, 26-28 September, pp. 267-273 (ISBN/ISSN: 978-981-05-8949-3).

Liu, H., Li, X. Z., Leng, Y.J. and Wang, C., 2007. "Kinetic modeling of electro-Fenton reaction in aqueous solution." *Water Research*, Vol. 41, No. 5, pp. 1161-1167.

Liu, H.L., Deng, A. and Chu, J., 2008. (Editors). *Geotechnical Engineering for Disaster Mitigation and Rehabilitation*, Science Press, Beijing and Springer, ISBN: 978-3-504-79845-3.

Liu, T., Tang, H. and Cheng, N.S., 2008. "Longitudinal dispersion of particle motion over inclined rough plane." *Proceedings of 16th IAHR-APD Congress and 3rd Symposium of IAHR-ISHS, Tsinghua University Press*, Vol. 3, pp. 924-927.

Liu, X.J., Yang, J.P. and Yang, Y.W., 2008. "Heat conduction analysis of nano-tip and storage medium in thermal-assisted data storage using molecular dynamics simulation." *Molecular Simulation*, Vol. 34, No. 1, pp. 57-62.

Liu, X.Y., Ding, H.B., Sreeramachandran, S., Stabnikova, O. and Wang, J.Y., 2008. "Enhancement of food waste digestion in the hybrid anaerobic solid-liquid system." *Water Science and Technology*, Vol. 57, No. 9, pp. 1369-1373.

Liu, X.Y., Sreeramachandran, S., Stabnikova, O. and Wang, J.Y., 2008. "Enhancement of food waste digestion in the hybrid anaerobic solid-liquid system". *Water Science and Technology*, Vol. 57, No. 7.

Liu, Y., 2008. "Biosorption isotherms, kinetics and thermodynamics." *Separation and Purification Technology*, Vol. 61, No. 3, pp. 229-242.

Liu, Y., 2008. "New insights into pseudo-second-order kinetic equation for adsorption." *Colloids and Surfaces A: Physicochemical and Engineering Aspects*, Vol. 320, No. 1-3, pp. 275-278.

Liu, Y. and Shen, L., 2008. "From langmuir kinetics to first- and second-order rate equations for adsorption." *Langmuir*, Vol. 24, No. 20, pp. 11625-11630.

Liu, Y. and Shen, L., 2008. "A general rate law equation for biosorption." *Biochemical Engineering Journal*, Vol. 38, No. 3, pp. 390-394.

Liu, Y., Teng, S. and Soh, C.K., 2008. "Three-dimensional damage model for concrete. I: Theory." *Journal of Engineering Mechanics, ASCE*, Vol. 134, No. 1, pp. 72-81.

Liu, Y., Teng, S. and Soh, C.K., 2008. "Three-dimensional damage model for concrete. II: Verification." *Journal of Engineering Mechanics, ASCE*, Vol. 134, No. 1, pp. 82-89.

Liu, Y. and Teng, S.S., 2008. "Nonlinear analysis of reinforced concrete slabs using nonlayered shell element." *Journal of Structural Engineering, ASCE*, Vol. 134, No. 7, pp. 1092-1100.

Liu, Y. and Wang, Z.W., 2008. "Uncertainty of preset-order kinetic equations in description of biosorption data." *Bioresource Technology*, Vol. 99, No. 8, pp. 3309-3312.

Liu, Y.Q., Moy, B.Y.P. and Tay, J.H., 2007. "COD removal and nitrification of low-strength domestic wastewater in aerobic granular sludge sequencing batch reactors." *Enzyme and Microbial Technology*, Vol. 42, No. 1, pp. 23-28.

Liu, Y.Q. and Tay, J.H., 2007. "Characteristics and stability of aerobic granules cultivated with different starvation time." *Applied Microbiology and Biotechnology*, Vol. 75, No. 1, pp. 205-210.

Liu, Y.Q. and Tay, J.H., 2007. "Cultivation of aerobic granules in a bubble column and an airlift reactor with divided draft tubes at low aeration rate." *Biochemical Engineering Journal*, Vol. 34, No. 1, pp. 1-7.

Liu, Y.Q. and Tay, J.H., 2007. "Influence of cycle time on kinetic behaviors of steady-state aerobic granules in sequencing batch reactors." *Enzyme and Microbial Technology*, Vol. 41, No. 4, pp. 516-522.

Liu, Y.Q. and Tay, J.H., 2008. "Influence of starvation time on formation and stability of aerobic granules in sequencing batch reactors." *Bioresource Technology*, Vol. 99, No. 5, pp. 980-985.

Liu, Y.Q., Wu, W.W., Tay, J.H. and Wang, J.L., 2007. "Starvation is not a prerequisite for the formation of aerobic granules." *Applied Microbiology and Biotechnology*, Vol. 76, No. 1, pp. 211-216.

Low, B.K., Lacasse, S.* and Nadim, F.*, 2007. "Slope reliability analysis accounting for spatial variation". *Georisk: Assessment and Management of Risk for Engineered Systems and Geohazards, Taylor & Francis*, London, Vol. 1, No. 4, pp. 177-189.

Low, B.K. and Tang, W.H.*, 2007. "Efficient spreadsheet algorithm for first-order reliability method." *Journal of Engineering Mechanics, ASCE*, Vol. 133, No. 12, pp. 1378-1387.

Low, B.K., 2008. "Efficient probabilistic algorithm illustrated for a rock slope". *Rock Mechanics and Rock Engineering, Springer-Verlag*, Vol. 41, No. 5, pp. 715-734.

Low, B.K. and Wilson H. Tang,* 2008. "New FORM Algorithm with example applications". *Proceedings of the Fourth Asian-Pacific Symposium on Structural Reliability and its Applications (APSSRA'08)*, Hong Kong, 19-20 June, pp. 221-226.

Low, Y.M., 2008. "Prediction of extreme responses of floating structures using a hybrid time/frequency domain coupled analysis approach." *Ocean Engineering*, Vol. 35, No. 14-15, pp. 1416-1428.

Low, Y.M. and Langley, R.S.*, 2008. "A hybrid time/frequency domain approach for efficient coupled analysis of vessel/mooring/riser dynamics." *Ocean Engineering*, Vol. 35, No. 5-6, pp. 433-446.

Low, Y.M. and Langley, R.S.*, 2008. "Understanding the dynamic coupling effects in deep water floating structures using a simplified model." *Journal of Offshore Mechanics and Arctic Engineering, Transactions of the ASME*, Vol. 130, No. 3.

Lu, Y. and Chiew, Y.M., 2007. "Suction effects on turbulence flows over a dune bed." *Journal of Hydraulic Research*, Vol. 45, No. 5, pp. 691-700.

Lu, Y., Chiew, Y.M. and Cheng, N.S., 2008. "Review of seepage effects on turbulent open-channel flow and sediment entrainment." *Journal of Hydraulic Research*, Vol. 46, No. 4, pp. 476-488.

Lu, Y. and Gong, S.F., 2007. "An analytical model for dynamic response of beam-column frames to impulsive ground excitations." *International Journal of Solids and Structures*, Vol. 44, No. 3-4, pp. 779-798.

Lu, Y. and Wei, J.W., 2008. „Damage-based inelastic response spectra for seismic design incorporating performance considerations." *Soil Dynamics and Earthquake Engineering*, Vol. 28, No. 7, pp. 536-549.

Lu, Y. and Xu, K., 2007. "Prediction of debris launch velocity of vented concrete structures under internal blast." *International Journal of Impact Engineering*, Vol. 34, No. 11, pp. 1753-1767.

Luo, J., Shu, D.W., Shi, B.J. and Gu, B., 2007. "The pulse width effect on the shock response of the hard disk drive." *International Journal of Impact Engineering*, Vol. 34, No. 8, pp. 1342-1349.

Ma, G.W. and An, X.M., 2008. "Numerical simulation of blasting-induced rock fractures." *International Journal of Rock Mechanics and Mining Sciences*, Vol. 45, No. 6, pp. 966-975.

Ma, G.W., Shi, H.J. and Shu, D.W., 2007. "P-I diagram method for combined failure modes of rigid-plastic beams." *International Journal of Impact Engineering*, Vol. 34, No. 6, pp. 1081-1094.

Ma, G.W. and Ye, Z.Q., 2007. "Analysis of foam claddings for blast alleviation." *Proceedings of the International Conference on Impact Loading of Lightweight Structures, Florianopolis, France*, Vol. 34, Issue 1, pp. 60-70.

Madhav, A.V.G. and Soh, C.K., 2008. "Uniplexing and multiplexing of PZT transducers for structural health monitoring." *Journal of Intelligent Material Systems and Structures*, Vol. 19, No. 4, pp. 457-467.

Mak, C.L. and Fan, H.S.L., 2007. "Development of dual-station automated expressway incident detection algorithms." *IEEE Transactions on Intelligent Transportation Systems*, Vol. 8, No. 3, pp. 480-490.

Mao, T.H. and Show, K.Y., 2007. "Influence of ultrasonication on anaerobic bioconversion of sludge." *Water Environment Research*, Vol. 79, No. 4, pp. 436-441.

Massih, D.*, Soubra, A.H.* and Low, B.K., 2008. "Reliability-based analysis and design of strip footings against bearing capacity failure." *Journal of Geotechnical and Geoenvironmental Engineering*, Vol. 134, No. 7, pp. 917-928.

Maszenan, A.M., Jiang, H.L., Tay, J.H., Schumann, P.*, Kroppenstedt, R.M.* and Tay, S.T.L.*, 2007. "Granulicoccus phenolivorans gen nov, sp nov, a Gram-positive, phenol-degrading coccus isolated from phenol-degrading aerobic granules." *International Journal of Systematic and Evolutionary Microbiology*, Vol. 57, pp. 730-737.

Megawati, K., Shaw, F., Lin, N., Sieh, K. and Pan, T.-C., 2007. "Future rupture scenarios of the Manila trench." *South China Sea Tsunami Workshop*, 5-7 December, Taipei, Taiwan.

Mei, C.C., Chiew, S.P. and Toh, S.L., 2007. "Full-scale proof load test of ultralite cold-formed steel roof truss". *Proceedings of the 9th International Conference on Steel, Space and Composite Structures (SS07)*, Yantai and Beijing, China, 10-15 October, pp. 285-292 (ISBN/ISSN: 978-981-05-7589-0).

Miao, A.W. and Yang, Y.W., 2008. "Monitoring vibrating structures using PZT impedance transducers." *International Conference on Multifunctional Materials and Structures*, Hong Kong, Peoples R China, pp. 85-88.

Narasimhan, S.*, Suresh, S., Nagarajaiah, S.* and Sundararajan, N., 2008. "On-line learning failure-tolerant neural-aided controller for earthquake excited structures." *Journal of Engineering Mechanics, ASCE*, Vol. 134, No. 3, pp. 258-268.

Ohno, T.*, Krauthammer, T.* and Pan, T.-C., 2007. "Design and analysis of protective structures against impact/impulsive/shock loads (DAPSIL) - Preface." *International Journal of Impact Engineering*, Vol. 34, No. 9, pp. 1486-1486.

Olszewski, P.S., 2007. "Singapore motorisation restraint and its implications on travel behaviour and urban sustainability." *Transportation*, Vol. 34, No. 3, pp. 319-335.

Pan, J.H., Zhang, X.W., Du, A.J., Sun, D.D. and Leckie, J.O.*, 2008. "Self-etching reconstruction of hierarchically mesoporous F-TiO_2 hollow microspherical photocatalyst for concurrent membrane water purifications." *Journal of the American Chemical Society*, Vol. 130, No. 34, pp. 11256-+.

Pan, T.-C., 2007. "Seismic hazard and risk in Singapore from an engineering perspective." *Managing the Changing*

Landscape of Catastrophe Risk, 10th Aon Re Australia Biennial Hazards Conference, 16-18 September, Gold Coast, Queensland, Australia, pp. 137-156.

Pan, T.-C, Megawati, K. and Lim, C.L., 2008. "Effect of long-distance Sumatra earthquakes on high-rise buildings in Singapore." *Proceedings of the 5th International Conference on Urban Earthquake Engineering*, 4-5 March, Tokyo, Japan, pp. 55-60.

Pan, T.-C., You, X.T. and Lim, C.L., 2008. "Evaluation of floor vibration in a biotechnology laboratory caused by human walking." *Journal of Performance of Constructed Facilities*, Vol. 22, No. 3, pp. 122-130.

Parashar, S.P., Chu, J. and Sanmugnathan, D., 2008. "Characterization of the undrained shear strength of marine clay at the Changi water reclamation plant project, Singapore", *Geotechnical and Geophysical Site Characterization*, Eds. Huang & Mayne, Taylor and Francis Group, pp. 505-510.

Peng, S., and Fan, H.S.L., 2007. "A New Computational Model for the Design of an Urban Inter-modal Public Transit Network." *Journal of Computer-aided Civil and Infrastructure Engineering*, USA, Vol. 22, No. 7, pp 499-510.

Phattaranawik, J.*, Fane, A.G., Pasquier, A.C.S.* and Bing, W.*, 2008. "A novel membrane bioreactor based on membrane distillation." *Conference of the European Desalination Society and Center for Research and Technology Hellas, Halkidiki, Greece*, Vol. 223, Issue 1-3, pp. 386-395.

Phattaranawik, J.*, Fane, A.G. and Wong, F.S., 2008. "Novel membrane-based sensor for online membrane integrity monitoring." *Journal of Membrane Science*, Vol. 323, No. 1, pp. 113-124.

Qian, G.R., Shi, J., Cao, Y.L., Xu, Y.F. and Chui, P.C., 2008. "Properties of MSW fly ash - calcium sulfoaluminate cement matrix and stabilization/solidification on heavy metals." *Journal of Hazardous Materials*, Vol. 152, No. 1, pp. 196-203.

Qian, Z.H., Tan, K.H. and Burgess, I.W.*, 2008. "Behavior of steel beam to column joints at elevated temperature: Experimental investigation." *Journal of Structural Engineering, ASCE*, Vol. 134, No. 5, pp. 713-726.

Rahardjo, H., Leong, E.C. and Rezaur, R.B., 2008. "Effect of antecedent rainfall on pore-water pressure distribution characteristics in residual soil slopes under tropical rainfall." *Hydrological Processes*, Vol. 22, No. 4, pp. 506-523.

Rahardjo, H., Ong, T.H., Rezaur, R.B. and Leong, E.C., 2007. "Factors controlling instability of homogeneous soil slopes under rainfall." *Journal of Geotechnical and Geoenvironmental Engineering*, Vol. 133, No. 12, pp. 1532-1543.

Rahardjo, H., Indrawan, I.G.B., Leong, E.C. and Yong, W.K., 2008. "Effects of coarse-grained material on hydraulic properties and shear strength of top soil". *Journal of Engineering Geology*, Vol. 101, pp. 165-173.

Rahardjo, H., Leong, E.C. and Rezaur, R.B., 2008. "Effect of antecedent rainfall on pore-water pressure distribution characteristics in residual soil slopes under tropical rainfall". *Hydrological Processes, Special Issue on Rainfall Induced Landslides and Debris Flow*, Vol. 22, pp. 506-523.

Rahardjo, H., Ong, T.H., Rezaur, R.B. and Leong, E.C., 2007. "Factors controlling instability of homogeneous soil slopes under rainfall loading". *ASCE Journal of Geotechnical and Geoenvironmental Engineering*, December, Vol. 133, No. 12, pp. 1532-1543.

Rahardjo, H., Rezaur, R.B., Leong, E.C., Alonso, E.E., Lloret, A. and Gens, A., 2008. "Monitoring and modeling of slope response to climate changes". Keynote Lecture. *Proceedings of the 10th International Symposium on Landslides and Engineered Slopes. Chinese Institution of Soil Mechanics and Geotechnical Engineering – China Civil Engineering Society, Chinese National Commission on Engineering Geology, Chinese Society of Rock Mechanics and Engineering, Geotechnical Division of the Hong Kong Institution of Engineers*, Xi'an, China, 30 June – 4 July, Vol. 1, pp. 67-84.

Rahardjo, H., Satyanaga, A. and Leong, E.C., 2008. "Role of real time monitoring in slope stability". Keynote Lecture. *Proceedings of the International Seminar on Civil and Infrastructure Engineering 2008 for Environmental Sustainability.* Shah Alam, Malaysia, 11-12 June, pp. 1-20.

Rahardjo, H., Rezaur, R.B. and Leong, E.C., 2008. "Role of antecedent rainfall in slope stability." Keynote Lecture. *Proceedings of the GEOTROPIKA 2008.* Kuala Lumpur, Malaysia, 26-27 May, pp. 1-19.

Rahardjo, H., Krisdani, H., Leong, E.C., Ng, Y.S., Foo, M.D. and Wang, C.L., 2007. "Unsaturated soil mechanics for solving seepage and slope stability problems." Keynote Lecture. *Proceedings of the 12th International Colloquium on Structural and Geotechnical Engineering.* Ain Shams University, Cairo, Egypt, 10-12 December, pp. 1-38.

Rahardjo, H., Krisdani, H., Leong, E.C., Ng, Y.S., Foo, M.D. and Wang, C.L., 2007. "Capillary barrier as slope cover." *Proceedings of the 10th Australia New Zealand Conference on Geomechanics "Common Ground"*. Brisbane, Australia, 21-24 October, Vol. 2, pp. 698 - 703.

Rahardjo, H., Satyanaga, A., Leong, E.C., Ng, Y.S., Foo, M.D. and Wang, C.L., 2007. "Slope failures in Singapore due to rainfall." *Proceedings of the 10th Australia New Zealand Conference on Geomechanics "Common Ground"*. Brisbane, Australia, 21-24 October, Vol. 2, pp. 704-709.

Rahardjo, H., Satyanaga, A. and Leong, E.C., 2007. "Unsaturated soil mechanics for slope stability." Invited Lecture. *Proceedings of 2007 National Conference of Korean Geotechnical Society (KGS)*, Busan, Korea, 14-15 September, pp. 1-21.

Remesh, K. and Tan, K. H., 2007. "Performance comparison of zone models with compartment fire tests." *Journal of Fire Sciences*, Vol. 25, No. 4, pp. 321-353.

Rong, H.C. and Li, B., 2008. "Deformation-controlled design of reinforced concrete flexural members subjected to blast loadings." *Journal of Structural Engineering, ASCE*, Vol. 134, No. 10, pp. 1598-1610.

Ruan, D., Lu, G., Ong, L.S. and Wang, B., 2007. "Triaxial compression of aluminium foams." *Composites Science and Technology*, Vol. 67, No. 6, pp. 1218-1234.

Rujikiatkamjorn, C.*, Indraratna, B.* and Chu, J., 2008. "2D and 3D numerical modeling of combined surcharge and vacuum preloading with vertical drains." *International Journal of Geomechanics, ASCE*, Vol. 8, No. 2, pp. 144-156.

Shao, Z.S. and Ma, G.W., 2007. "Free vibration analysis of laminated cylindrical shells by using Fourier series expansion method." *Journal of Thermoplastic Composite Materials*, Vol. 20, No. 6, pp. 551-573.

Shao, Z.S. and Ma, G.W., 2008. "Thermo-mechanical stresses in functionally graded circular hollow cylinder with linearly increasing boundary temperature." *Composite Structures*, Vol. 83, No. 3, pp. 259-265.

Shaw, F., Liu, X., Megawati, K., Sieh, K. and Pan, T.-C., 2007. "Modelling tsunami hazards from the manila trench subduction megathrust." *Proceedings of the 8th Pacific Conference on Earthquake Engineering*, 5-7 December, Singapore, Paper No. 319.

Shaw, F., Liu, X., Megawati, K., Sieh, K., Tan, S.K., Huang, Z. and Pan, T.-C., 2008. "Tsunami hazard from the potential rupture of the Manila trench." *Bulletin of Civil Engineering Research*, School of Civil and Environmental Engineering, Nanyang Technological University, Singapore, Issue 21, pp. 64-67.

Shi, B.J., Shu, D.W., Luo, J., Gu, B., Ma, G.W., Ng, Q.Y. and Gan, S., 2007. "Operational shock, simulation of the head-disk assembly of a small-form factor drive." *IEEE Transactions on Magnetics*, Vol. 43, No. 11, pp. 4042-4047.

Show, K.Y., Mao, T.H. and Lee, D.J., 2007. "Optimisation of sludge disruption by sonication." *Water Research*, Vol. 41, No. 20, pp. 4741-4747.

Show, K.Y., Zhang, Z.P., Tay, J.H., Liang, D.T., Lee, D.J. and Jiang, W.J., 2007. "Production of hydrogen in a granular sludge-based anaerobic continuous stirred tank reactor." *International Journal of Hydrogen Energy*, Vol. 32, No. 18, pp. 4744-4753.

Si, W.J., Li, C.X., Gong, S.W. and Yong, L.K., 2008. "Spline-discretization-based free vibration analysis for orthotropic plates." *Journal of Engineering Mechanics, ASCE*, Vol. 134, No. 5, pp. 405-416.

Sieh, K., Megawati, K. and Pan, T.-C., 2008. "The elephant and the tectonic plate." The Sunday Times, *The Straits Times*, Singapore, 9 March, pg. 37.

Sivadas, V., Heitor, M.V.* and Fernandes, R.*, 2007. „A functional correlation for the primary breakup processes of liquid sheets emerging from air-assist atomizers." *Journal of Fluids Engineering, Transactions of the ASME*, Vol. 129, No. 2, pp. 188-193.

Soares, A.*, Guieysse, B., Jefferson, B.*, Cartmell, E.* and Lester, J.N.*, 2008. "Nonylphenol in the environment: A critical review on occurrence, fate, toxicity and treatment in wastewaters." *Environment International*, Vol. 34, No. 7, pp. 1033-1049.

Sopha, T., Nguyen, T.B.N., Chiew, S.P., Lee, C.K. and Lie, S.T., 2008. "Stress analysis and fatigue test on partially overlapped CHS K-Joints". *International Journal of Advanced Steel Construction*, Vol. 4, No. 2, June, pp. 134-146 (ISBN/ISSN: 1816-112X).

Stabnikova, O., Ivanov, V., Larionova, I.*, Stabnikov, V.*, Bryszewska, M.A.* and Lewis, J.*, 2008. "Ukrainian dietary bakery product with selenium-enriched yeast." *LWT-Food Science and Technology*, Vol. 41, No. 5, pp. 890-895.

Stabnikova, O., Liu, X.Y. and Wang, J.Y., 2008. "Anaerobic digestion of food waste in a hybrid anaerobic solid-liquid system with leachate recirculation in an acidogenic reactor." *Biochemical Engineering Journal*, Vol. 41, No. 2, pp. 198-201.

Stabnikova O., Liu X.Y. and Wang J.Y., 2008. "Anaerobic digestion of food waste in a hybrid anaerobic solid-liquid system with leachate recirculation in an acidogenic reactor". *Waste Management*, Vol. 28, No. 9, pp. 1654-1659.

Stabnikova, O., Liu, X.Y. and Wang, J.Y., 2008. "Digestion of frozen/thawed food waste in the hybrid anaerobic solid-liquid system." *Waste Management*, Vol. 28, No. 9, pp. 1654-1659.

Sun, D.D., 2007. "Nanomaterial can reduce filter residue". *Filtration and Separation*, July/August, Vol. 44, No. 6, page 11.

Sun, D.D., 2007. "Membrane technology: removing contaminants in wastewater". *Filtration and Separation*, September, Vol. 44, No. 7, page 14.

Suresh, S., Narasimhan, S.* and Sundararajan, N., 2008. "Adaptive control of nonlinear smart base - isolated buildings using Gaussian kernel functions." *Structural Control and Health Monitoring*, Vol. 15, No. 4, pp. 585-603.

Swamee, P.K.*, Rathie, P.N.* and Wong, T.S.W., 2007. "Exact solutions for normal depth problem." *Journal of Hydraulic Research*, Vol. 45, No. 4, pp. 567-571.

Tan, K.H. and Qian, Z.H., 2008. "Experimental behaviour of a thermally restrained plate girder loaded in shear at elevated temperature." *Journal of Constructional Steel Research*, Vol. 64, No. 5, pp. 596-606.

Tan, K.H., Toh, W.S., Huang, Z.F. and Phng, G.H., 2007. "Structural responses of restrained steel columns at elevated temperatures. Part 1: Experiments." *Engineering Structures*, Vol. 29, No. 8, pp. 1641-1652.

Tan, K.H. and Yuan, W.F., 2008. "Buckling of elastically restrained steel columns under longitudinal non-uniform temperature distribution." *Journal of Constructional Steel Research*, Vol. 64, No. 1, pp. 51-61.

Tan, S.B.K., Chua, L.H.C., Shuy, E.B., Lo, E.Y.M. and Lim, L.W., 2008. "Performances of rainfall-runoff models calibrated over single and continuous storm flow events." *Journal of Hydrologic Engineering*, Vol. 13, No. 7, pp. 597-607.

Tan, S.B.K., Shuy, E.B. and Chua, L.H.C., 2007. "Effects of meteorological and hydrogeological factors on gross recharge percentage at unconfined sandy aquifers with an equatorial climate." *Hydrological Processes*, Vol. 21, No. 18, pp. 2493-2503.

Tan, S.B.K., Shuy, E.B. and Chua, L.H.C., 2007. "Modelling hourly and daily open-water evaporation rates in areas with an equatorial climate." *Hydrological Processes*, Vol. 21, No. 4, pp. 486-499.

Tan, S.B.K., Shuy, E.B. and Chua, L.H.C., 2007. "Regression method for estimating rainfall recharge at unconfined sandy aquifers with an equatorial climate." *Hydrological Processes*, Vol. 21, No. 25, pp. 3514-3526.

Tan, S.B.K., Shuy, E.B., Chua, L.H.C. and Yee, W.K., 2007. "Studies on groundwater recharge characteristics at a reclaimed land site with an equatorial climate using time-series and spectral analyses." *Hydrological Processes*, Vol. 21, No. 7, pp. 939-948.

Tang, L., Tang, H., Chen, H. and Cheng, N.S., 2008. "Statistical analysis of collision between saltation particle and bed surface." *Proceedings of the 16th IAHR-APD Congress and 3rd Symposium of IAHR-ISHS, Tsinghua University Press*, Vol. 3, pp. 849-853.

Tay, J.H., Yang, P., Zhuang, W.Q., Tay, S.T.L. and Pan, Z.H., 2007. "Reactor performance and membrane filtration in aerobic granular sludge membrane bioreactor." *Journal of Membrane Science*, Vol. 304, No. 1-2, pp. 24-32.

Tay, J.-H., Tay, S.T.-L., Ivanov, V., Stabnikova, O. and Wang, J.-Y., 2008. "Compositions and methods for the treatment of wastewater and other waste". US Patent 7,393,452, Date of grant July 1, 2008, Date of filing 1 April 11, 2003.

Tay, J.H., Tay, T.L.S., Ivanov, V., 2008. "Methods and kits for quantitative simultaneous detection of specific microorganisms and nucleic acid sequences". Singapore Patent No.111927, date of filing 28 December 2001, date of grant 30 April 2008.

Thu, T.M., Rahardjo, H. and Leong, E.C., 2007. "Critical state behavior of a compacted silt specimen." *Soils and Foundations*, Vol. 47, No. 4, pp. 749-755.

Thu, T.M., Rahardjo, H. and Leong, E.C., 2007. "Elastoplastic model for unsaturated soil with incorporation of the soil-water characteristic curve." *Canadian Geotechnical Journal*, Vol. 44, No. 1, pp. 67-77.

Thu, T.M., Rahardjo, H. and Leong, E.C., 2007. "Soil-water characteristic curve and consolidation behavior for a compacted silt." *Canadian Geotechnical Journal*, Vol. 44, No. 3, pp. 266-275.

Tiwari, M. and Chu, J., 2007. "Undrained creep behavior of Singapore marine clay." *Proceedings of the 13th Regional Conference on Soil Mechanics. and Geotechnical Engineering*, Kolkata, 10-14 December, Vol. 1, pp. 79-84.

To, P.C.*, Marinas, B.J.* Snoeyink, V.L.* and Ng, W.J., 2008. "Effect of strongly competing background compounds on the kinetics of trace organic contaminant desorption from activated carbon." *Environmental Science and Technology*, Vol. 42, No. 7, pp. 2606-2611.

Tran, C.T.N., Li, B. and Pan, T.-C., 2007. "Effect of axial compression load on seismic behavior of non-seismically detailed interior beam-wide column joints." *Proceedings of the 8th Pacific Conference on Earthquake Engineering*, 5-7 December, SINGAPORE, Paper No. 289.

Trinh, M.T., Rahardjo, H. and Leong, E.C., 2007. "Critical state behaviour of a compacted silt". *Soils and Foundations*, August, Vol. 47, No. 4, pp. 749 -755.

Vimonsatit, V., Tan, K.H. and Ting, S.K., 2007. "Shear strength of plate girder web panel at elevated temperature." *Journal of Constructional Steel Research*, Vol. 63, No. 11, pp. 1442-1451.

Wanatowski, D. and Chu, J., 2007. "K-0 of sand measured by a plane-strain apparatus." *Canadian Geotechnical Journal*, Vol. 44, No. 8, pp. 1006-1012.

Wanatowski, D. and Chu, J., 2007. "Static liquefaction of sand in plane-strain." *Canadian Geotechnical Journal*, Vol. 44, No. 3, pp. 299-313. Or 311 (in CER 2007)

Wanatowski, D. and Chu, J., 2008. "Effect of specimen preparation method on the stress - strain behavior of sand in plane-strain compression tests." *Geotechnical Testing Journal*, Vol. 31, No. 4, pp. 308-320.

Wanatowski, D. and Chu, J., 2008. "Undrained behaviour of Changi sand in triaxial and plane-strain compression." *Geomechanics and Geoengineering: An International Journal*, Vol. 3, No. 2, pp. 85-96.

Wanatowski, D., Chu, J. and Lo, S-C.R., 2008. "Strain softening behaviour of sand in strain path testing under plane-strain conditions". *Acta Geotechnica*, Springer, Published online on 2 April.

Wanatowski, D., Chu, J. and Lo, R.S.-C., 2008. "Types of flowslide failures and possible failure mechanisms." *Invited Paper, Proceedings of the 2nd International Conference on Geotechnical Engineering for Disaster Mitigation and Rehabilitation*, 30 May – 2 June, Nanjing, pp. 242-251.

Wang, D., Hassan, O.*, Morgan, K.* and Weatherill, N.*, 2007. "Enhanced remeshing from STL files with applications to surface grid generation." *Communications in Numerical Methods in Engineering*, Vol. 23, No. 3, pp. 227-239.

Wang, W.Y. and Teng, S., 2007. "Modeling cracking in shell-type reinforced concrete structures." *Journal of Engineering Mechanics, ASCE*, Vol. 133, No. 6, pp. 677-687.

Wang, X.K. and Tan, S.K., 2007. "Experimental investigation of the interaction between a plane wall jet and a parallel offset jet." *Experiments in Fluids*, Vol. 42, No. 4, pp. 551-562.

Wang, X.H. and Huang, X.Y., 2008. "A simple modeling and experiment on dynamic stability of a disk rotating in air." *International Journal of Structural Stability and Dynamics*, Vol. 8, No. 1, pp. 41-60.

Wang, X.K. and Tan, S.K., 2008. "Comparison of flow patterns in the near wake of a circular cylinder and a square cylinder placed near a plane wall." *Ocean Engineering*, Vol. 35, No. 5-6, pp. 458-472.

Wang, X.K. and Tan, S.K., 2008. "Near-wake flow characteristics of a circular cylinder close to a wall." *Journal of Fluids and Structures*, Vol. 24, No. 5, pp. 605-627.

Wang, X.K., Hao, Z. and Tan, S.K., 2008. "Visualization of the vortical structures behind a normal plate near a plane wall." *Proceedings of ISFV13/FLUVISU12 (13th International Symposium on Flow Visualization and 12th French Congress on Visualization in Fluid Mechanics)*, 1-4 July, Nice, France, Paper #358.

Wang, X.L. and Day, A.H., 2007. "Numerical instability in linearized planning problems." *International Journal for Numerical Methods in Engineering*, Vol. 70, No. 7, pp. 840-875.

Wang, Z.H. and Tan, K.H., 2007. "Temperature prediction for contour-insulated concrete-filled CHS subjected to fire using large time Green's function solutions." *Journal of Constructional Steel Research*, Vol. 63, No. 7, pp. 997-1007.

Wang, Z.H. and Tan, K.H., 2007. "Temperature prediction for multi-dimensional domains in standard fire." *Communications in Numerical Methods in Engineering*, Vol. 23, No. 11, pp. 1035-1055.

Wang, Z.H. and Tan, K.H., 2008. "Radiative heat transfer for structural members exposed to fire: An analytical approach." *Journal of Fire Sciences*, Vol. 26, No. 2.

Wang, Z.Q., Tan, S.K., Cheng, N.S. and Goh, K.W., 2008. "A simple relationship for crenulate-shaped bay in static equilibrium." *Coastal Engineering*, Vol. 55, No. 1, pp. 73-78.

Wang, Z.Q. and Cheng, N.S., 2008. "Influence of secondary flows on distribution of suspended sediment concentration." *Journal of Hydraulic Research, IAHR*, Vol. 46, No. 4, pp. 548-552.

Wong, T.S.W., 2008. "ANN and fuzzy logic models for simulating event-based rainfall-runoff" by Gokmen Tayfur and Vijay P. Singh - Discussion." *Journal of Hydraulic Engineering, ASCE*, Vol. 134, No. 9, pp. 1400-1400.

Wong, T.S.W., 2008. "Discussion of "Storm-Water Predictions by Dimensionless Unit Hydrograph" by James C. Y. Guo." *Journal of Irrigation and Drainage Engineering, ASCE*, Vol. 134, No. 2, pp. 269-269.

Wong, T.S.W., 2008. "Effect of channel shape on time of travel and equilibrium detention storage in channel." *Journal of Hydrologic Engineering*, Vol. 13, No. 3, pp. 189-196.

Wong, T.S.W., 2008. "How to review or not to review a paper." *Journal of Professional Issues in Engineering Education and Practice*, Vol. 134, No. 4, pp. 327-328.

Wong, T.S.W., 2008. "How to write an award-winning paper." *Journal of Professional Issues in Engineering Education and Practice*, Vol. 134, No. 1, pp. 11-11.

Wong, T.S.W., 2008. "Optimum rainfall interval and Manning's roughness coefficient for runoff simulation." *Journal of Hydrologic Engineering*, Vol. 13, No. 11, pp. 1097-1102.

Xu, G., Zhou, T. and Rajagopalan, S., 2007. "Similarity of intermittency characteristics of temperature and transverse velocity." *Physical Review E*, Vol. 76, No. 4.

Xu, H. and Liu, Y., 2008. "Mechanisms of Cd2+, Cu2+ and Ni2+ biosorption by aerobic granules." *Separation and Purification Technology*, Vol. 58, No. 3, pp. 400-411.

Yan, J., Cheng, N.S., Tang, H.W. and Tan, S.K., 2007. "Oscillating-grid turbulence and its applications: a review." *Journal of Hydraulic Research*, Vol. 45, No. 1, pp. 26-32.

Yan, S. W. and Chu, J., 2008. "Geo-bag method for levee construction and rehabilitation." *Geosustainability and Geohazard Mitigation, GeoCongress 2008, ASCE Geotechnical Special Publication No. 177*, pp. 694-699.

Yan, S. W., Wang, C. and Chu, J., 2008. "Analysis and rehabilitation of a failed submarine slope cut in soft clay." *Geosustainability and Geohazard Mitigation, GeoCongress 2008, ASCE Geotechnical Special Publication No. 177*, pp. 483-490.

Yang, G.C. and Lok, T.S., 2007. "Analysis of RC structures subjected to air-blast loading accounting for strain rate effect of steel reinforcement." *International Journal of Impact Engineering*, Vol. 34, No. 12, pp. 1924-1935.

Yang, S.Q. and Tan, S.K., 2008. "Flow resistance over mobile bed in an open-channel mobile flow." *Journal of Hydraulic Engineering, ASCE*, Vol. 134, No. 7, pp. 937-947.

Yang, Y.W., Annamdas, V.G.M., Wang, C. and Zhou, Y.X., 2008. "Application of multiplexed FBG and PZT impedance sensors for health monitoring of rocks." *Sensors*, Vol. 8, No. 1, pp. 271-289.

Yang, Y.W. and Hu, Y.H., 2008. "Electromechanical impedance modeling of PZT transducers for health monitoring of cylindrical shell structures." *Smart Materials and Structures*, Vol. 17, No. 1.

Yang, Y.W., Hu, Y.H. and Lu, Y., 2008. "Sensitivity of PZT impedance sensors for damage detection of concrete structures." *Sensors*, Vol. 8, No. 1, pp. 327-346.

Yang, Y.W., Lim, Y.Y. and Soh, C.K., 2008. "Practical issues related to the application of the electromechanical impedance technique in the structural health monitoring of civil structures: I. Experiment." *Smart Materials and Structures*, Vol. 17, No. 3.

Yang, Y.W., Lim, Y.Y. and Soh, C.K., 2008. "Practical issues related to the application of the electromechanical impedance technique in the structural health monitoring of civil structures: II. Numerical verification." *Smart Materials and Structures*, Vol. 17, No. 3.

Yang, Y.W., Liu, H., and Annamdas, V.G.M., 2008. "Monitoring damage propagation using PZT impedance transducers - Art. No. 693410." *Conference on Nondestructive Characterization for Composite Materials, Aerospace Engineering, Civil Infrastructure, and Homeland Security 2008*, San Diego, CA, pp. 93410-93410.

Yang, Y.W., Liu, X.J. and Yang, J.P., 2008. "Nonequilibrium molecular dynamics simulation for size effects on thermal conductivity of Si nanostructures." *Molecular Simulation*, Vol. 34, No. 1, pp. 51-55.

Yang, Y.W. and Zhang, L., 2008. "Modeling of an ionic polymer-metal composite ring." *Smart Materials and Structures*, Vol. 17, No. 1.

Yeo, A.P.S., Law, A.W.K. and Fane, A.G., 2007. "The relationship between performance of submerged hollow fibers and bubble-induced phenomena examined by particle image velocimetry." *Journal of Membrane Science*, Vol. 304, No. 1-2, pp. 125-137.

Yu, G. and Tan, S.K., 2007. "Estimation of boundary shear stress distribution in open channels using flownet." *Journal of Hydraulic Research*, Vol. 45, No. 4, pp. 486-496.

Yu, L., 2007. "Overview of some theoretical approaches for derivation of the Monod equation." *Applied Microbiology and Biotechnology*, Vol. 73, No. 6, pp. 1241-1250.

Yu, S.C.M., Ai, J.J., Gao, L. and Law, A.W.K., 2008. "Vortex formation process of a starting square jet." *AIAA Journal*, Vol. 46, No. 1, pp. 223-231.

Yu, Y. and Chiew, S.P., 2007. "Numerical study of FRP bonded steel beams with different strengthening parameters". *Proceedings of the 9th International Conference on Steel, Space and Composite Structures (SS07)*, Yantai and Beijing, China, 10-15 October, pp. 323-328 (ISBN/ISSN: 978-981-05-7589-0).

Yu, Y. and Chiew, S.P., 2007. "Fatigue behavior of CFRP bonded steel plates". *Proceedings of the 5th International Conference on Advances in Steel Structures (ICASS-2007)*, Singapore, 5-7 December, pp. 863-868 (ISBN/ISSN: 978-981-05-9365).

Yuan, W.F. and Tan, K.H., 2007. "An advanced model of evacuation using cellular automata." *Proceedings of the 4th International Conference on Structural Engineering and Construction*, Melbourne, Australia, pp. 1253-1258.

Yuan, W.F. and Tan, K.H., 2007. "An algorithm for simulation of multi-velocity in cellular automata model incorporating tenability analysis." *Proceedings of the 4th International Conference on Structural Engineering and Construction*, Melbourne, Australia, pp. 1259-1264.

Zeng, P., Zhuang, W.Q., Tiong-Lee, S., and Tay, J.H., 2007. "The influence of storage on the morphology and physiology of phthalic acid-degrading aerobic granules." *Chemosphere*, Vol. 69, No. 11, pp. 1751-1757.

Zhai, X.F., Tiong, R.L.K., Bjornsson, H.C., Chua, D.K.H., 2007. "Simulation based planning for precast production with two critical resources." *2007 Winter Simulation Conference*, Washington, DC, pp. 2083-2090.

Zhang, H.Y., Wang, R., Liang, D.T. and Tay, J.H., 2008. "Theoretical and experimental studies of membrane wetting in the membrane gas-liquid contacting process for CO_2 absorption." *Journal of Membrane Science*, Vol. 308, No. 1-2, pp. 162-170.

Zhang, L. and Yang, Y.W., 2007. "Modeling of a fluid-filled ionic polymer-metal composite cylindrical shell - art. No. 64140E." *Conference on Smart Structures, Devices, and Systems III*, Adelaide, Australia, pp. E4140-E4140.

Zhang, L. and Yang, Y.W., 2007. "Charge redistribution under dynamic actuation of ionic polymer-metal composites - art. No. 65240C." *Conference on Electroactive Polymer Actuators and Devices (EAPAD) 2007*, San Diego, CA, pp. C5240-C5240.

Zhang, L. and Yang, Y.W., 2007. "Modeling of an ionic polymer-metal composite beam on human tissue." *Smart Materials and Structures*, Vol. 16, No. 2, pp. S197-S206.

Zhang, L. and Yang, Y.W., 2007. "Optimal excitation of a cylindrical shell by piezoelectric actuators - art. No. 65251Q." *Conference on Active and Passive Smart Structures and Integrated Systems*, San Diego, CA, pp. Q5251-Q5251.

Zhang, L. and Yang, Y.W., 2008. "Three-dimensional charge redistribution of ionic polymer-metal composites with uncertainty in surface conductivity." *Proceedings of the International Conference on Multifunctional Materials and Structures*, Hong Kong, Peoples R China, pp. 379-382.

Zhang, N. and Tan, K.H., 2007. "Direct strut-and-tie model for single span and continuous deep beams." *Engineering Structures*, Vol. 29, No. 11, pp. 2987-3001.

Zhang, N. and Tan, K.H., 2007. "Size effect in RC deep beams: Experimental investigation and STM verification." *Engineering Structures*, Vol. 29, No. 12, pp. 3241-3254.

Zhang, X.W., Du, A.J., Lee, P.F., Sun, D.D. and Leckie, J.O.*, 2008. "TiO_2 nanowire membrane for concurrent filtration and photocatalytic oxidation of humic acid in water." *Journal of Membrane Science*, Vol. 313, No. 1-2, pp. 44-51. *available online doi:10.1016/j.memsci.2007.12.045*

Zhang, X.W., Pan, J. H., Du, A.J., Wang, Y., Sun, D.D. and Leckie, J.O.*, 2008. *"TiO_2 nanowire free-standing membrane for water treatment by concurrent filtration and photocatalytic oxidation." America Chemical Society Spring meeting 2008*, 6-10 April, New Orleans, LA USA.

Zhang, X.W., Du, A.J., Wang, Z., Tan, H.M., Wang, H. and Sun, D.D., 2008. "TiO_2 nanotubes photocatalytic oxidation for drinking water treatment." *IWA Singapore International Water Week, Singapore*, June.

Zhang, X.W., Du, A.J., Sun, D.D. and Leckie, J.O.*, 2008. "Multifunction TiO_2 nanowire membrane for removal of humic acid in water without fouling." *IWA Singapore International Water Week, Singapore*, June.

Zhang, X.W., Pan, J.H., Du, A.J., Lee, P.F., Sun, D.D. and Lee, J.O., 2008. "Aggregating TiO_2 (B) nanowires to porous basketry-like microspheres and their photocatalytic properties." *Chemistry Letters*, Vol. 37, No. 4, pp. 424-425.

Zhang, X.W., Sun, D.D., Li, G.T. and Wang, Y.Z., 2008. "Investigation of the roles of active oxygen species in photodegradation of azo dye AO7 in TiO_2 photocatalysis illuminated by microwave electrodeless lamp." *Journal of Photochemistry and Photobiology A - Chemistry*, Vol. 199, No. 2-3, pp. 311-315.

Zhang, Y.Q., Lu, Y. and Ma, G.W., 2008. „Effect of compressive axial load on forced transverse vibrations of a double-beam system." *International Journal of Mechanical Sciences*, Vol. 50, No. 2, pp. 299-305.

Zhang, Z.P., Show, K.Y., Tay, J.H., Liang, D.T. and Lee, D.J., 2008. "Biohydrogen production with anaerobic fluidized bed reactors - A comparison of biofilm-based and granule-based systems." *Asian Biohydrogen Symposium, Taichung, Taiwan*, Vol. 33, Issue 5, pp. 1559-1564.

Zhang, Z.P., Show, K.Y.*, Tay, J.H., Liang, D.T. and Lee, D.J., 2008. "Enhanced continuous biohydrogen production by immobilized anaerobic microflora." *Proceedings of the International Conference on Bioenergy Outlook, Singapore*, January-February, Vol. 22, Issue 1, pp. 87-92.

Zhang, Z.P., Show, K.Y., Tay, J.H., Liang, D.T., Lee, D.J. and Jiang, W.J., 2007. "Rapid formation of hydrogen-producing granules in an anaerobic continuous stirred tank reactor induced by acid incubation." *Biotechnology and Bioengineering*, Vol. 96, No. 6, pp. 1040-1050.

Zhang, Z.P., Tay, J.H., Show, K.Y., Yan, R., Liang, D.T., Lee, D.J. and Jiang, W.J., 2007. "Biohydrogen production in a granular activated carbon anaerobic fluidized bed reactor." *International Journal of Hydrogen Energy*, Vol. 32, No. 2, pp. 185-191.

Zhao, J., Gong, Q.M. and Eisensten, Z.*, 2007. "Tunnelling through a frequently changing and mixed ground: A case history in Singapore." *Tunnelling and Underground Space Technology*, Vol. 22, No. 4, pp. 388-400.

Zhao, X.B., Zhao, J., Cai, J.G. and Hefny, A.M.*, 2008. "UDEC modelling on wave propagation across fractured rock masses." *Computers and Geotechnics*, Vol. 35, No. 1, pp. 97-104.

Zhou, J.Z., Qian, G.R., Cao, Y.L., Chui, P.C., Xu, Y.F. and Liu, Q., 2008. "Transition of Friedel phase to chromate-AFm phase." *Advances in Cement Research*, Vol. 20, No. 4, pp. 167-173.

Zhou, Q. and Cheng, N.S., 2007. "Particle settling behavior in turbulent flow generated by oscillating grid." *Proceedings of the 5th International Conference on Fluid Mechanics*, Shanghai, Peoples R China, pp. 142-145.

Zhou, Q. and Cheng, N.S., 2008. "Simultaneous measurements of particle settling velocity and oscillating-grid turbulence." *Proceedings of 16th IAHR-APD Congress and 3rd Symposium of IAHR-ISHS*, Tsinghua University Press, Vol. 3, pp. 913-918.

Zhou, Z.L., Li, D.Y., Ma, G.W. and Li, J.C., 2008. "Failure of rock under dynamic compressive loading." *Journal of Central South University of Technology*, Vol. 15, No. 3, pp. 339-343.

Zhu, B.W. and Lim, T.T., 2007. "Catalytic reduction of Chlorobenzenes with Pd/Fe nanoparticles: reactive sites, catalyst stability, particle aging, and regeneration." *Environmental Science and Technology*, Vol. 41, No. 21, pp. 7523-7529.

Zhu, B.W., Lim, T.T. and Feng, J., 2008. "Influences of amphiphiles on dechlorination of a trichlorobenzene by nanoscale Pd/Fe: Adsorption, reaction kinetics, and interfacial interactions." *Environmental Science and Technology*, Vol. 42, No. 12, pp. 4513-4519.

Zilouei, H.*, Guieysse, B. and Mattiasson, B.*, 2008. "Two-phase partitioning bioreactor for the biodegradation of high concentrations of pentachlorophenol using Sphingobium chlorophenolicum DSM 8671." *Chemosphere*, Vol. 72, No. 11, pp. 1788-1794.

CONTENTS

ADDITIONAL COPIES AND ENQUIRIES

For general enquiries about this publication and request for additional copies, please write to:

Chair
School of Civil and Environmental Engineering
Nanyang Technological University
50 Nanyang Avenue
Singapore 639798
Tel: 65-67905264
Fax: 65-67910676
Email: D-CEE@ntu.edu.sg

Published by School of Civil and Environmental Engineering, Nanyang Technological University, Singapore

Printed by PHOTOPLATES PTE LTD